CHEMISTRY & CHEMICAL TECHNOLOGY

CONFERENCE 2023 VILNIUS

CONFERENCE BOOK

March 10, 2023
VILNIUS

THE CONFERENCE IS DEDICATED TO PROF. EDVARDAS RAMANAUSKAS 100TH ANNIVERSARY

CHEMISTRY & CHEMICAL TECHNOLOGY

CONFERENCE 2023 VILNIUS

Conference Book
International Conference
Chemistry and Chemical technology

CCT-2023

The conference is dedicated to prof. Edvardas Ramanauskas 100th anniversary

https://doi.org/10.15388/CCT.2023

ISBN 978-609-07-0833-0 (Leidinio forma: Elektroninis - PDF)

Vilnius, Lithuania 2023

Prof. habil. dr. Edvardas Ramanauskas 100th anniversary

Prof. habil. dr. Edvardas Ramanauskas was a Lithuanian scientist, born in 1923 on March 11, in Panevėžys. In 1945, he enrolled to Vilnius University, where he studied chemistry, and worked as a laboratory assistant at the Department of Organic Chemistry. After graduating from the university in 1950 started working as an assistant in the Department of Inorganic and Analytical Chemistry, with which he connected his entire life and activities. In 1959 E. Ramanauskas defended his doctoral thesis "Physicochemical and microelemental characteristics of groundwater in Vilnius". in 1982 E. Ramanauskas defended his habilitation doctor's thesis at the Ukrainian Academy of Sciences.

In his scientific career, professor examined and summarized the possibilities of using the three-component systems consisting of triphenylmethane, xanthene, monoazo, oxazine, triazine and rhodamine-type dyes, oxidant, halogen and sulfur-containing complex anions in the analysis. Proposed more than 150 spectrophotometric, extractive, fluorimetric, kinetic and potentiometric methods for the determination of halogens, sulfur-containing anions, some oxidants and reductants. In his later works, prof. E. Ramanauskas examined the methods of mathematical experiment planning and quantum chemical calculation, the possibilities of determining the surface activity of materials, the application of the obtained results in the production of selective ion electrodes. In 1986, 3 inventions were registered under prof. habil. dr. E. Ramanauskas name. He published more than 200 scientific articles on mathematical experiment planning and quantum chemical calculation methods, determination of surface activity of materials and their application in the production of selective electrodes. He was co-author of two books: "General Chemistry" (1967), and "Inorganic Synthesis" (1970). Prof. habil. dr. E. Ramanauskas was the dean of the Faculty of Chemistry (from 1964 to 1977), gave various lecture cycles.

The professor was a simple, kind-hearted, unobtrusive head of department and dean. E. Ramanauskas, who did scientific work intensively and did not shy away from public duties, is recognized as the leader of Lithuanian chemical analysts. By nature, extremely patient and taciturn prof. E. Ramanauskas proved to colleagues and students not by words, but by deeds and example, that work can be not only a duty, but also the greatest pleasure of life, that even the busiest person must be sensitive, punctual, keep promises and trust others.

SCIENTIFIC COMMITTEE

Chair
Assoc. prof. dr. ***Lina Mikoliūnaitė***
Vilnius University

Assoc. prof. dr. ***Živilė Stankevičiūtė***
Vilnius University

Assoc. prof. dr. ***Justina Gaidukevič***
Vilnius University

Prof. dr. ***Rasa Pauliukaitė***
Centre for Physical Sciences and Technology

Prof. (HP) dr. ***Almira Ramanavičienė***
Vilnius University

Prof. dr. ***Kęstutis Baltakys***
Kaunas University of Technology

Prof. (HP) dr. ***Jurgis Barkauskas***
Vilnius University

Prof. habil. dr. ***Aivaras Kareiva***
Vilnius University

Prof. habil. dr. ***Rimantas Ramanauskas***
Centre for Physical Sciences and Technology

Prof. habil. dr. ***Audrius Padarauskas***
Vilnius University

ORGANIZING COMMITTEE

Chairperson
Assoc. prof. dr. ***Lina Mikoliūnaitė***
Vilnius University

Assoc. prof. dr. ***Živilė Stankevičiūtė***
Vilnius University

Dr. ***Jolanta Raudonienė***
Vilnius University

Assist. prof. dr. ***Medeina Steponavičiūtė***
Vilnius University

Assist. prof. dr. ***Inga Gabriūnaitė***
Vilnius University

J. assist. prof. ***Julija Grigorjevaitė***
Vilnius University

Scientific secretary
PhD student ***Greta Inkrataitė***
Vilnius University

PhD student ***Justinas Januškevičius***
Vilnius University

PhD student ***Gintarė Rimkutė***
Vilnius University

PhD student ***Paulina Kaziukonytė***
Vilnius University

Conference organized by

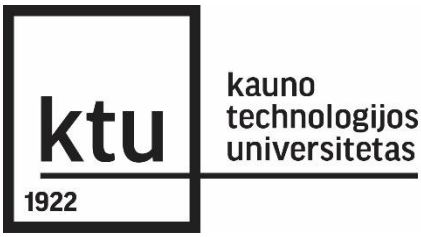

CENTER
FOR PHYSICAL SCIENCES
AND TECHNOLOGY

LIETUVOS CHEMIKŲ
DRAUGIJA
Lithuanian Chemical Society

SPONSORS

INVITED SPEAKERS

Prof. (HP) dr. **Jurgis Barkauskas**
Vilnius University, Lithuania

Prisiminimai mokinio akimis
Memories through the Eyes of a Student

Prof. dr. **Rimantas Ramanauskas**
Center for Physical Sciences and Technology, Lithuania

Prisiminimai apie tėvą
Memories of Father

Prof. dr. **Ingrida Ancutienė**
Kaunas University of Technology, Lithuania

Analizinė chemija Kauno technologijos universitete: nuo ištakų iki dabar
Analytical Chemistry at Kaunas University of Technology: from the Beginning to the Present

Prof. dr. **Vladas Algirdas Bumelis**
Lithuanian Academy of Sciences, Lithuania

Analizinės chemijos katedros alumno prisiminimai
Memories of an Alumnus of the Department of Analytical Chemistry

Antanas Marcinonis
Company "Grota", Lithuania

Analizinės chemijos svarba hidrogeologijoje
Importance of Analytical Chemistry in Hydrogeology

Dr. **Olga Kizinievič**
Vilnius Tech, Lithuania

Komunalinių kietųjų atliekų deginimo lakiųjų pelenų poveikis deginto molio medžiagų struktūrai
Effect of Municipal Solid Waste Incincration Fly Ash on the Structure of Fired Clay Materials

Prof. dr. **Ivo Leito**
University of Tartu, Estonia

Unified pH – What, Why and How?

Prof. dr. **Markku Leskelä**
University of Helsinki, Finland

Area Selective Deposition – the New Challenge in Atomic Layer Deposition

Prof. dr. **Edvinas Orentas**
Vilnius University, Lithuania

Supramolecular Chemistry of Hydrogen-Bonded Tubular Assemblies

Prof. dr. **Donats Erts**
University of Latvia, Latvia

Bi_2Se_3 Thin Films and Bi_2Se_3/SWCNT Heterostructures as a Perspective Anode for Lithium-Ion Batteries

Prof. dr. **Juozas Gražulevičius**
Kaunas University of Technology, Lithuania

Organic Semiconductors for Optoelectronic Devices and Sensors

Dr. **Mariana Emilia Ghica**
University of Coimbra, Portugal

Electrochemistry: a Powerful Tool for Synthesis and Characterization of Nanomaterials

Prof. dr. **Daumantas Matulis**
Vilnius University, Lithuania

Searching for Principles of Protein-Ligand Recognition by Varying Protein or Compound Structure

Dr. **Anna Wrona-Piotrowicz**
University of Lodz, Poland

Essential Oils and Their Use in the Cosmetics Industry

Prof. dr. **Torben René Jensen**
Aarhus University, Denmark

Chemistry – the Key to Novel Solid State Batteries

Dr. **Ieva Uogintė**
Center for Physical Sciences and Technology, Lithuania

Micro/Nano Plastics as a New Emerging Concern: from the Environment to Human Health

Prof. dr. **Gintaras Denafas**
Kaunas University of Technology, Lithuania

Microplastics in the Products of Waste Biological Treatment

Dr. **Andris Anspoks**
Institute of Solid State Physics, Latvia

X-ray Absorption Spectroscopy in Physics, Material Science and Chemistry

Conference Program
March 10th, 2023

Time	Presenter	Institution	Title of the Lecture
8:00 – 9:00	Participant registration		
9:00 – 9:10	Opening of the conference. Welcome speech from the Vicerector of Vilnius University Prof. Edita Sužiedėlienė		
9:10 – 9:20	Welcome speech from the Dean of Faculty of Chemistry and Geosciences Prof. Aivaras Kareiva		
Part I (in Lithuanian). Let's Remember the Professor Edvardas Ramanauskas Chairperson Assoc. Prof. Lina Mikoliūnaitė			
9:20 – 9:40	Prof. Jurgis Barkauskas	Vilnius University, Lithuania	Prisiminimai mokinio akimis *Memories through the Eyes of a Student*
9:40 – 10:00	Prof. Rimantas Ramanauskas	Center for Physical Sciences and Technology, Lithuania	Prisiminimai apie tėvą *Memories of Father*
10:00 – 10:20	Prof. Ingrida Ancutienė	Kaunas University of Technology, Lithuania	Analizinė chemija Kauno technologijos universitete: nuo ištakų iki dabar *Analytical chemistry at Kaunas University of Technology: from the Beginning to the Present*
10:20 – 10:40	Prof. Vladas Algirdas Bumelis	Lithuanian Academy of Sciences, Lithuania	Analizinės chemijos katedros alumno prisiminimai *Memories of an Alumnus of the Department of Analytical Chemistry*
10:40 – 11:00	Antanas Marcinonis	Company "Grota", Lithuania	Analizinės chemijos svarba hidrogeologijoje *Importance of Analytical Chemistry in Hydrogeology*
11:00 – 11:20	Dr. Olga Kizinievič	Vilnius Tech, Lithuania	Komunalinių kietųjų atliekų deginimo lakiųjų pelenų poveikis deginto molio medžiagų struktūrai *Effect of Municipal Solid Waste Incineration Fly Ash on the Structure of Fired Clay Materials*
11:20 – 11:40	**Coffee Break**		

Part II. Oral Presentations (in English) Chairperson Dr. Jurga Juodkazytė			
11:40 – 12:00	Prof. Ivo Leito	University of Tartu, Estonia	Unified pH – What, Why and How?
12:00 – 12:20	Prof. Markku Leskelä	University of Helsinki, Finland	Area Selective Deposition – The New Challenge in Atomic Layer Deposition
12:20 – 12:40	Prof. Edvinas Orentas	Vilnius University, Lithuania	Supramolecular Chemistry of Hydrogen-Bonded Tubular Assemblies
12:40 – 13:00	Prof. Donats Erts	University of Latvia, Latvia	Bi_2Se_3 Thin Films and Bi_2Se_3/SWCNT Heterostructures as a Perspective Anode for Lithium-Ion Batteries
13:00 – 13:20	Prof. Juozas Gražulevičius	Kaunas University of Technology, Lithuania	Organic Semiconductors for Optoelectronic Devices and Sensors
13:20 – 14:20	**Lunch Break**		
Chairperson Prof. Artūras Katelnikovas			
14:20 – 14:40	Dr. Mariana Emilia Ghica	University of Coimbra, Portugal	Electrochemistry: a Powerful Tool for Synthesis and Characterization of Nanomaterials
14:40 – 15:00	Prof. Daumantas Matulis	Vilnius University, Lithuania	Searching for Principles of Protein-Ligand Recognition by Varying Protein or Compound Structure
15:00 – 15:20	Dr. Anna Wrona-Piotrowicz	University of Lodz, Poland	Essential Oils and Their Use in the Cosmetics Industry
15:20 – 15:40	Prof. Torben René Jensen	Aarhus University, Denmark	Chemistry – the Key to Novel Solid State Batteries
15:40 – 16:00	Dr. Ieva Uogintė	Center for Physical Sciences and Technology, Lithuania	Micro/Nano Plastics as a New Emerging Concern: from the Environment to Human Health
16:00 – 16:20	Prof. Gintaras Denafas	Kaunas University of Technology, Lithuania	Microplastics in the Products of Waste Biological Treatment
16:20 – 16:40	Dr. Andris Anspoks	University of Latvia, Latvia	X-ray Absorption Spectroscopy in Physics, Material Science and Chemistry
16:40 – 17:40	**Coffee Break and Poster Session (Chairperson Assoc. Prof. Živilė Stankevičiūtė)**		
18:00	**Conference Gala Dinner (Universiteto St. 3)**		

INVITED TALKS

Analizinė chemija Kauno technologijos universitete: nuo ištakų iki dabar

I. Ancutienė
Kauno technologijos universitetas, Radvilėnų pl. 19, LT-50254 Kaunas, Lietuva
e-paštas: ingrida.ancutiene@ktu.lt

Analizinė chemija Kaune dėstoma nuo 1922 metų, kai Lietuvos universiteto Matematikos-gamtos fakultete buvo įkurta Neorganinės ir analizinės chemijos katedra. Tuomet dabartinių Kauno technologijos universiteto (KTU) pirmųjų rūmų rūsyje 6 kambariai buvo priskirti Neorganinės ir analizinės chemijos laboratorijai. Katedros organizatorius ir pirmasis vedėjas buvo ekstraordinarinis profesorius Filypas Butkevičius. Jis pirmasis įvedė lietuviškuosius neorganinės ir analizinės chemijos terminus ir 1929 metais paskelbė juos žurnale „Kosmos“. Parašė ir išleido tris analizinės chemijos vadovėlius: „Elementinis kokybinis analizis“ (1929), „Retųjų elementų kokybinis analizis“ (1931), „Įvadas į analitinę chemiją (1932). Pradžioje eksperimentiniams mokslams trūko būtinų mokymosi priemonių. F. Butkevičius daug ką pirko už skolintus pinigus, chemikalus iš pradžių laikė savo bute, iš ten nešdavosi į paskaitas [1]. Darbo sąlygos pagerėjo 1931 metais pastačius Fizikos-chemijos instituto rūmus, kuriuose katedrai skirta 260 m^2 salė, kurioje vienu metu galėjo dirbti 120 studentų. Ši laboratorija buvo 7 m aukščio, per visą ją ėjo dvi eilės kolonų, prie kurių stovėjo nedidelės, bet geros traukos spintos [2]. Katedrai dar priklausė sulfidų laboratorija, svarstyklių kambarys ir kt. patalpos. Kokybinės analizės darbų programa chemikams numatė 22 privalomas užduotis. Buvo nustatomi visi dažniau pasitaikantys metalai, kai kurie nemetalai, rūgštys ir mokslo bei technikos požiūriu svarbesni retieji elementai. Kiekybinės analizės programoje chemikams numatyti 47 darbai buvo suskirstyti į 6 grupes: svorio analizė, tūrio analizė – alkalimetrija, acidimetrija, jodometrija, oksidimetrija, nusodinimas, kolorimetrija, dujų analizė, elektrolizė, potenciometrinė analizė [2].

1944 metais atkūrus universitetą Technologijos fakulteto Chemijos skyrius įsikūrė buvusiuose Krašto apsaugos ministerijos Ginklavimo valdybos tyrimų laboratorijos komplekse (dabar Cheminės technologijos fakulteto A, B ir D korpusai). Katedrai praktikos darbams buvo skirta dalis A korpuso trečio aukšto: dvi nedidelės mokomosios laboratorijos, sulfidų kambarys (atskiras bokštelis ant stogo). 1971 metais pastačius Cheminės technologijos fakulteto C korpusą, analizinės chemijos darbams atlikti buvo skirtos 2 mokomosios laboratorijos ir sulfidų kambarys [1]. Sisteminė katijonų analizė sulfidiniu metodu yra tikslesnė, tačiau dėl nemalonaus divandenilio sulfido kvapo ir jo nuodingumo 1988 metais sulfidinis metodas buvo pakeistas rūgščių ir bazių metodu. Analizuojant šiuo metodu, katijonai grupuojami pagal jų reakcijas su rūgštimis ir bazėmis ir jie suskirstomi į 6 analizines grupes. Kokybinės analizės programoje numatyta ir anijonų analizė, o šie taip pat skirstomi į analizines grupes, atsižvelgiant į bario ir sidabro druskų tirpumą bei oksidacines ir redukcines savybes. Praktinių darbų metu ne tik atliekamos katijonų ir anijonų atpažinimo reakcijos, tačiau ir analizuojami kontroliniai tirpalai. Kiekybinės analizės kurse pagrindinis dėmesys skirtas svorio ir tūrio (neutralizacijos, oksidimetrijos, kompleksonometrijos, nusodinamojo titravimo) analizės metodams.

Laikui bėgant buvo keičiamas dalyko pavadinimas: 1996 metais „Analizinė chemija 1“ ir „Analizinė chemija 2“ buvo pervadinta į „Kokybinę cheminę analizę“ ir „Kiekybinę cheminę analizę, o 1999 metais abu moduliai buvo sujungti į vieną „Cheminės analizės“ modulį. Ženkliai buvo mažinamos ir laboratorinių darbų apimtys, būtent buvusios 96 laboratorinių darbų valandos 1999 metais sumažintos iki 64 val., o 2014 metais – iki 48 val. Dabar atliekamos I-VI analizinių grupių katijonų ir I-III analizinių grupių anijonų identifikavimo reakcijos, I-III analizinių grupių katijonų mišinio analizė, sausos medžiagos identifikavimas rūgščių ir bazių metodu. Studentai atlieka tris kiekybinės analizės darbus: silpnos rūgšties kiekybinė analizė, Cu^{2+} arba Fe^{2+} jonų kiekybinė analizė ir Mg^{2+} jonų kiekybinė analizė arba vandens kietumo nustatymas.

KTU analizinę chemiją dėstė ir studentus mokė chemiškai mąstyti doc. L. Bernatonienė, doc. Z. Martynaitienė, doc. A. Degutienė, doc. S. Grevys, doc. A. Žarnauskas, doc. G. Paulauskas, doc. N. Kreivėnienė ir doc. V. Krylova. Buvo išleistas „Cheminės analizės“ vadovėlis, daugybė mokomųjų knygų ir metodinių priemonių.

Naudota literatūra

1. V. Zelionkaitė, E. Rinkevičienė, Neorganinės chemijos katedra 1922-1997. Kaunas, 1997.
2. Z. Mačionis. Iš chemijos mokslo istorijos Lietuvoje. Kaunas, Šviesa, 1991.

Analizinės chemijos svarba hidrogeologijoje

A. Marcinonis[1,*], Aleksandra Babičeva[1], Arnas Adomavičius[1]
[1]UAB „GROTA“, Eišiškių pl. 26, 02184 Vilnius, Lietuva
**el. paštas: antanas@grota.lt*

Pranešime bus aptariamos požeminio vandens ir uolienų užterštumo laboratorinio tyrimo galimybės, rezultatų patikimumas ir jų palyginamumas su teisės aktais nustatytomis normatyvinėmis vertėmis.

● Laboratoriniais metodais vandenyje ir ypač uolienoje nustatoma teršiančių medžiagų koncentracija priklauso nuo laboratorinio tyrimo metodikos. Teisės aktuose, nustatančiuose vandens ar uolienos terpėje leistinas teršiančių medžiagų koncentracijos ribines vertes, nurodoma ir kokiais laboratoriniais metodais tos vertės turi būti nustatytos. Tačiau metodų aprašuose dažnai nurodoma, kad analizė gali būti atliekama pasirenkant skirtingus tiriamos medžiagos ekstrahavimo iš mėginio būdus. Skirtingai ekstrahuojant neišvengiamai gaunami skirtingi rezultatai, kurie apsunkina jų vertinimą ir palyginamumą su ribinėmis vertėmis. Savo ruožtu, praktikoje kyla grėsmė neadekvačiai įvertinti tam tikro objekto geologinės aplinkos užterštumo lygį ir patirti iš to išplaukiančias negatyvias pasekmes – nepastebėti viršnormatyvinio, pavojingo aplinkai vandens ar uolienų užterštumo, imtis perteklinių geologinės aplinkos valymo priemonių ir t.t.

● Tiriant geologinės aplinkos elementų, ypač uolienų užterštumą sunkiaisiais metalais susiduriama su realų užterštumą reprezentuojančios koncentracijos identifikavimu. Sunkieji metalai yra sudėtinė uolienas sudarančių elementų dalis, todėl atliekant laboratorinius jų koncentracijos tyrimus kyla grėsmė natūraliai uolienoje esantį sunkųjį metalą ar jo dalį priskirti teršalui. Savo ruožtu ir šiuo atveju kyla užterštumo lygio adekvataus įvertinimo problema. Reikalingas išsamesnis teisės aktais nustatytų ribinių užterštumo verčių ir jų nustatymo laboratorinių metodų pagrįstumas ir suderinamumas.

● Valant naftos produktais užterštą geologinę aplinką, o taip natūralios savivalos metu vyksta taršos metamorfozė. Naftos angliavandeniliai yra, susidaro tarpinės, už pačius angliavandenilius pavojingesnės ir geologinėje aplinkoje judresnės medžiagos. Vertinant tokių teritorijų pavojingumą aplinkai ir jų tvarkymo priemonių poreikį labai svarbu šias medžiagas ištirti požeminiame vandenyje tiek kiekybiškai, tiek kokybiškai ir tyrimo rezultatų pagrindu optimizuoti naftos produktais užterštų teritorijų valymo reikalavimus.

Effect of Municipal Solid Waste Incineration Fly Ash on the Structure of Fired Clay Materials

O. Kizinievič[1*], V. Voišienė[1], V. Kizinievič[1]
[1]Vilnius Gediminas Technical University, Linkmenų g. 28, LT-08217 Vilnius, Lithuania
**Corresponding author, e-mail: olga.kizinievic@vilniustech.lt*

Increase in the residues from Municipal Solid Waste Incineration (MSWI) residues has become a major concern in many countries. The bottom ash and fly ash generate require appropriate management in order to minimize their effect on the environment. The bottom ash is classified as non-hazardous waste by the European Waste Catalogue [1] and fly ash is classified as hazardous waste owing to its high contents of heavy metals and soluble salts [2]. The studied fly ash (cogeneration power plant UAB "Fortum Klaipėda") was found to contain a high content of of CaO, which was 45.17%, chlorides (mainly KCl, NaCl, $MgCl_2$) – 19.01%, sulphate – 7.32%, Na_2O, K_2O, MgO, Al_2O_3, Fe_2O_3, TiO_2, and heavy metals: lead, cadmium, chromium, copper, mercury, molybdenum, tin, wolfram, strontium, etc. At present, fly ash (FA) from municipal incineration waste are practically not utilized in Lithuania. However, we believe that fly ash or washed fly ash (additional treatment with water) can be used in fired clay building materials production fired at 1000°C. The microstructure of clay materials and identification of minerals presented in Fig.1

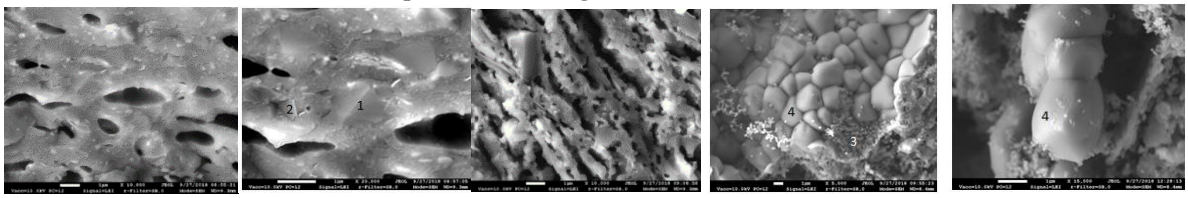

a) b) c) d) e)

Fig. 1. The microstructure of clay materials and identification of minerals: a), b) – control clay materials, c), d) – clay materials +2.5% FA; identified minerals: 1 – quartz (SiO_2), 2 – hematite (Fe_2O_3), 3 – diopside ($MgCaSi_2O_6$), 4 – calcium sulfate ($CaSO_4$)

Minerals of quartz, hematite, albite-anorthite, spinel, diopside are identified in the control clay samples clay brick. Isomorphic minerals, plagioclases – albite-anorthite, hematite, spinel, diopside, as well as calcium sulphate were identified in clay materials with FA [3]. It should be emphasized that the formation of minerals may be affected by the presence of heavy metals in the FA [4-5]. Heavy metals such as Cu, Zn, Ni, etc. can interfere with the structure of the spinel or/and diopside and thus affect their identification and intensity. The formation of calcium sulphate mineral is influenced by a sufficiently high content of calcium and sulphates in FA. Calcium sulphate mineral is not a preferred mineral in the building ceramics industry, as it can negatively affect the structure of clay materials by increasing porosity due to its properties – sufficiently large volume and the possibility of formation in pores. It was determined that, the chemical composition of fly ash influences the formation of a different structure in the clay body. With the formation of calcium sulphate mineral, evaporation of chlorides, decomposition of $CaCO_3$, more long, large and open pores are formed in the structure (Fig.1 c). Summarizing the obtained results of the study, it is recommended to utilize up to 2.5% fly ash in the production of fired clay bricks. The obtained clay bricks would have the following characteristics: shrinkage after combustion – up to 9.5%, bulk density is not less than 1.7 g/cm^3, compressive strength is not less than 25 MPa, water absorption is not higher than 15%, total porosity is not higher than 31%, frost resistance by one-side freeze-thaw method 100–115 cycles.

References

3. Europe Waste Catalog. Guidance on using the European Waste Catalogue (EWC) to code waste November 2015.
4. J.R. Pan, C. Huang, J.-J. Kuo, S.-H. Lin. Waste Manag., 28(7) (2008) 1113-1118.
5. V. Voišnienė. Doctoral dissertation. Vilnius, Lithiania, 2021, 2021-040-M.
6. L. Mao, H. Cui, H. An, B. Wang, J. Zhai, Y. Zhao, Q. Li. Chemosphere, 117 (2016) 745–752.
7. Y. Tang, K. Shih, K. Chan., Chemosphere, 117 (2014) 575–581.

Unified pH – What, Why and How?

I. Leito[1,*] A. Heering[1]
[1]*University of Tartu, Institute of Chemistry, Ravila 14a, 50411 Tartu, Estonia*
**Corresponding author, e-mail: ivo.leito@ut.ee*

Acidity is one of the most important characteristics of liquids/solutions, and its measurement is crucial to understanding and controlling essential processes in fundamental chemistry, industry and living organisms, such as catalysis, extraction, chromatography, processes in micelles/bilayers, etc. Acidity refers to the activity of the solvated proton and is typically expressed as pH. However, the conventional pH scale is well established only in dilute aqueous solutions at medium pH values. It has serious limitations at extreme values, in other solvents or more complex media where most of the real-life chemistry takes place. Most importantly, comparison of the conventional pH values between different media (solvents) is impossible, because every solvent has its own pH scale. Example: pH 7 in water is neural but pH 7 in acetonitrile is strongly acidic.

In view of the above, a decade ago, the concept of "unified pH scale" was put forward, defining unified pH (pH_{abs}) via the absolute chemical potential of the solvated proton [1]. For easier comparability the pH_{abs} scale was subsequently "aligned" with the aqueous pH scale, termed as pH_{abs}^{H2O} [2], so that any medium/solution with pH_{abs}^{H2O} 7.00 has the same thermodynamic activity of the solvated proton as an aqueous solution with pH 7.00. The merits of this approach are a strict thermodynamic foundation and direct comparability of pH_{abs}^{H2O} values between any solvents/media.

Initially, the pH_{abs}^{H2O} scale was a theoretical concept with no practical implementation. However, in the recent years, to a large part thanks to the European Union UnipHied (17FUN09, www.uniphied.eu) project, the pH_{abs}^{H2O} measurement possibilities for have been developed [2,3] and the concept has now been published as an IUPAC technical report [4].

The presentation will give an overview of the pH_{abs}^{H2O} concept, the principles of its current experimental realization and exemplary applications.

References

1. D. Himmel, S. K. Goll, I. Leito, I. Krossing, Angewandte Chemie International Edition, **49** (2010) 6885–6888.
2. A. Suu, L. Jalukse, J. Liigand, A. Kruve, D. Himmel, I. Krossing, M. Rosés, I. Leito, Analytical Chemistry **87** (2015) 2623–2630.
3. A. Heering, D. Stoica, F. Camões, B. Anes, D. Nagy, Z. Nagyné Szilágyi, R. Quendera, L. Ribeiro, F. Bastkowski, R. Born, J. Nerut, J. Saame, S. Lainela, L. Liv, E. Uysal, M. Roziková, M. Vičarová, A. Snedden, L. Deleebeeck, V. Radtke, I. Krossing, I. Leito, Symmetry **12** (2020) 1150.
4. V. Radtke, D. Stoica, I. Leito, F. Camões, I. Krossing, B. Anes, M. Roziková, L. Deleebeeck, S. Veltzé, T. Näykki, F. Bastkowski, A. Heering, N. Dániel, R. Quendera, L. Liv, E. Uysal, N. Lawrence, Pure and Applied Chemistry **93** (2021) 1049–1060.

Area Selective Deposition – The New Challenge in Atomic Layer Deposition

M. Leskelä

Department of Chemistry, PO Box 55, University of Helsinki, FI-00014 Helsinki, Finland
e-mail: markku.leskela@helsinki.fi

Microelectronics is the most important application of Atomic Layer Deposition (ALD) because of the many benefits the technology enables. ALD is a chemical gas-phase thin film deposition technique, where the precursor gases are alternatively introduced onto the substrate. The film is growing in saturative manner and enables the growth of conformal and very thin films needed in 3D structures in microelectronic devices.

Area selective deposition is coming extremely important when the feature sizes in microelectronics are shrinking beyond 10 nm. Patterned surfaces contain chemically different areas and area selective ALD (AS-ALD) utilizes these differences to get growth only on the desired areas. Several approaches have been developed for AS-ASD, the most common method being the use of self-assembled monolayers (SAM) to block the growth on unwanted areas. The same principle is applied in small molecule inhibition (SMI) where small molecules inhibit the growth on undesired areas. The most attractive AS-ALD process would be inherent selective growth. In that process the precursor molecule selectively adsorbs on the desired areas leaving the other areas bare. One important reason for this phenomenon is the Lewis acidity difference between the areas and the proton transfer from the surface hydroxyl groups [1,2]. The inherent selectivity is possible also in case of two different metals and two different dielectrics as well as in growth of low-k polymer films [3].

In processing of small microelectronic devices, selective atomic layer etching is as important as AS-ALD. Etching is often made by plasma but thermal processes that may contain several process steps can be found in literature. We have focused on catalytic selective etching of polymers using thin metal or metal oxide film below the polymer film as catalyst for oxidative remove of the polymers [4].

References

1. Y. Li, Y. Lan, K, Cao, J. Zhang, Y. Wen, B. Shan, R. Chen, Chem. Mater., **34** (2022) 9013-9022.
2. C. Zhang, E. Tois, M. Leskelä, M. Ritala, Chem. Mater. **34** (2022) 8379-8388.
3. C. Zhang, M. Vehkamäki, M. Pietikäinen, M. Leskelä, M. Ritala, Chem. Mater., **32** (2020) 5073-5083.
4. C. Zhang, M. Leskelä, M. Ritala, Coatings **11** (2021) 1124.

Supramolecular Chemistry of Hydrogen-Bonded Tubular Assemblies

E. Orentas

[1]*Department of Organic Chemistry, Faculty of Chemistry and Geosciences, Vilnius University, Naugarduko 24, LT-03225, Vilnius, Lithuania*
Corresponding author, e-mail:edvinas.orentas@chf.vu.lt

The examples of the iconic DNA double helix and protein tertiary structures highlight the importance of hydrogen bonds (H-bonds) for structure, function and stability of the fundamental units of biosystems and serve as an inspiration for chemist in designing artificial non-covalent constructs. Indeed, among various non-covalent interactions used in supramolecular chemistry, the H-bond is perhaps the most versatile one due to its strength and directionality. Based on reversible nature of H-bonds, the design and synthesis of new stimuli-responsive H-bonding monomers that display a diversity of self-assembly pathways and structural features became possible by clever use of rigid molecular scaffolds and tautomeric equilibrium. In this presentation, several unique methods to obtain new types of dynamic supramolecular tubular aggregates and polymers, assembled from very small and thus easily modifiable chiral H-bonding bicyclic building blocks will be discussed.

Bi_2Se_3 Thin Films and Bi_2Se_3/SWCNT Heterostructures as a Perspective Anode for Lithium-Ion Batteries

D. Erts[1,2*], V. Lazarenko[1], J. Rublova[1], R. Meija[1], J. Andzane[1], V. Voikiva[1], D. Salnajs[1], A. Viksna[2], I. Olyshevets[1]

[1]Institute of Chemical Physics, [2]Faculty of Chemistry, University of Latvia, Raina blvd. 19, LV-1586, Riga, Latvia
**Donats Erts, e-mail: donats.erts@lu.lv*

In the last decades, lithium-ion batteries (LIBs) have dominated the field of energy storage and portable energy sources. Organic solvents-based lithium-ion batteries have been used in a variety of portable devices (phones, tablets, smartwatches, etc.). Also, LIBs have played a crucial role in the automotive industry, as well as being used in large-scale storage units for intermittent energy, which is usually produced by solar and wind power plants. However, organic solvents-based LIBs have three major drawbacks: high cost, sensitivity to high temperatures, and risk of ignition. The further development of LIBs, addressing these issues, is essential to sustain and facilitate the aforementioned energy consumption and storage technology. Aqueous electrolyte is a promising alternative to toxic and potentially flammable organic solvents. However, aqueous electrolyte-based LIBs suffer from disadvantages such as low voltage windows, poor cycling characteristics, formation of dendritic structures, resulting in a short connection between the battery electrodes, etc.

The main components of a battery are cathode, anode and electrolyte. Among these components, the anode is of great importance for the reliable and effective performance of the battery. One of the promising anode materials for application in LIBs is bismuth selenide (Bi_2Se_3). It has already shown good perspectives as an anode material for conventional organic electrolyte-based LIBs, and thus can be a promising candidate for use in aqueous rechargeable lithium-ion batteries (ARLIBs).

Here we present application of Bi_2Se_3 nanostructured films and Bi_2Se_3 deposited on single wall carbon nanotubes (SWCNT) for application as anodes in ARLIBs [1] and LIBs respectively. Bi_2Se_3 nanostructured thin films used as anodes were synthesized by physical vapor deposition on glass substrates or pre-fabricated SWCNT networks [2]. Deposition of Bi_2Se_3 on SWCNTs ensures direct mechanical and electrical contact between Bi_2Se_3 and SWCNTs, which can improve the performance of the anode material in battery applications.

The electrochemical behavior of Bi_2Se_3 nanostructured thin films in aqueous 5 M $LiNO_3$ electrolyte with two different interface layers on the electrode surface—the solid electrolyte interphase (SEI) and the Bi_2O_3 layer—were investigated. The results of this work showed that the formation of the SEI layer on the surface of Bi_2Se_3 thin films ensures high diffusivity of Li^+, high electrochemical stability, and high capacity up to 100 cycles. Bi_2Se_3 nanostructured thin films showed the highest capacity among reported state-of-the-art anode electrodes for aqueous electrolyte-based LIBs.

Bi_2Se_3/SWCNT heterostructures with different Bi_2Se_3:SWCNT mass ratios were investigated for application as anodes in organic solvent-based LIBs. It was found that the chalcogenide chemical composition, and consequently, the anode performance may be altered by the presence of copper back-electrode during the Bi_2Se_3 deposition. The novel Bi_2Se_3/SWCNT electrodes demonstrated high capacity up to 500 cycles.

References

1. V. Lazarenko, Y. Rublova, R. Meija, J. Andzane, V. Voikiva, A. Kons, A. Sarakovskis, A. Viksna, D. Erts, Batteries. 8 (2022) 144.
2. K. Buks, J. Andzane, K. Smits, J. Zicans, J. Bitenieks, A. Zarins, D. Erts, Mater. Today Energy (2020) 18, 100526.

Organic Semiconductors for Optoelectronic Devices and Sensors

J.V. Gražulevičius

Department of Polymer Chemistry and Technology, Kaunas University of Technology, K. Barsausko g. 59, 51423 Kaunas, Lithuania
e-mail: juozas.grazulevicius@ktu.lt

Growing interest has been in recent decades focused on organic glass-forming semiconductors. They are used as emitters and hosts in organic light emitting diodes, as charge transporting materials (HTMs) in rapidly developing organic and hybrid sol cells. Organic emitters exhibiting long-living emission such as thermally activated delayed fluorescence or room-temperature phosphorescence are recently widely studied as active materials of the different sensors. The examples of organic semiconductors recently synthesized, studied in the laboratories of the author are reviewed.

Asymmetric multiple donor-acceptor type derivatives of *tert*-butyl carbazole and trifluoromethyl benzene were designed and synthesized exploiting different electron-accepting anchoring groups [1]. Sky blue emitting OLED with the emitting layer of one compound dispersed in host 1,3-bis(N-carbazolyl)benzene displayed emission peak at 477 nm, brightness over 39 000 cd/m2, and external quantum efficiency (EQE) up to 15.9%.

Compounds containing triphenylamine or 9-phenylcarbazole as donor moieties and pyrimidine-5-carbonitrile as electron-withdrawing unit were synthesized and studied [2]. Pure blue and greenish-blue fluorescent OLEDs with EQE reaching 7% and 6%, correspondingly, were obtained using the newly synthesized compounds as emitters. EQE of more than 20% and the operation time exceeding 20000 h were recorded for electroluminescent devices with pyrimidine-5-carbonitriles as the hosts.

Sky-blue emitting derivatives of pyrimidine-5-carbonitrile and electron-donating carbazole, tert-butylcarbazole or methoxy carbazole showed good performance both as emitters of OLEDs and as active materials of oxygen sensors [3]. Sky-blue OLED with EQE of 12.8% was fabricated using the newly synthesized emitter. The emitters were also used as xygen probes with fast response, high sensitivity and good stability.

Derivatives of thianthrene and phenothiazine were synthesized as emitters for oxygen sensing [4]. Room temperature phosphorescence (RTP) of the different intensity was detected for the compounds being in crystalline or amorphous phase and for their dispersions in different polymeric matrices. Fast oxygen response (ca. 0.1 s) of RTP was observed for only 1 wt.% of the dispersions in polymeric host.

Very sensitive probes for quantitative and organoleptic detection of oxygen based on conformer-induced RTP enhancement of the derivative of triazatruxene and phenothiazine were developed [5]. For 1% solid solution of the compound in Zeonex, the ratio of intensity of RTP observed under vacuum and fluorescence intensity recorded in air reached the value of 19.

Derivatives of dibenzothiophene with methoxyphenyl, trimethoxyphenyl, and carbazole moieties were synthesized as HTMs for perovskite solar cells (PSCs) [6]. Using the synthesized derivative of dibenzothiophene as HTM, power conversion efficiency (PCE) of 20.9% was achives for additive-free PSC, which is among the state-of-the-art values for devices with undoped HTM.

Indolo[3,2-b]carbazole-based HTMs also showed very good performance in dopant-free PSCs [7]. The devices demonstrated considerably higher stability and comparable efficiency as additives-containing reference PSCs with conventional hole-transporting material spiro-OMeTAD.

Acknowledgment. This project has received funding from the Research Council of Lithuania (LMTLT), agreement No S-MIP-22-78

References

1. M. Mahmoudi, D.Gudeika, J. Simokaitiene, et. al., ACS Appl. Mater. Interfaces, **14** (2022) 40158−40172.
2. U. Tsiko, D. Volyniuk, V. Andruleviciene, et al., Mater. Today Chem., **25** (2022) 100955.
3. U. Tsiko, O. Bezvikonnyi, G.. Sych, J. Adv. Res **33** (2021) 41–51.
4. K Leitonas, A.Tomkeviciene, G. Baratte, et al., Sens. Actuators B Chem.,**345** (2021) 130369.
5. E. Skuodis, K. Leitonas, A. Panchenko, et al., Sens. Actuators B Chem., **373** (2022) 132727.
6. R. Durgaryan, J. Simokaitiene, D. Volyniuk, et. al., Sol. RRL, (2022), 2200128.
7. E. Jatautiene, J. Simokaitiene, R. Durgaryan, et al., Nano Energy **101** (2022) 107618.

Electrochemistry: a Powerful Tool for Synthesis and Characterization of Nanomaterials

M. E. Ghica[1,2*], W. da Silva[2,3], Ch. M.A. Brett[2]

[1]University of Coimbra, CIEPQPF, Department of Chemical Engineering, 3030-790, Coimbra, Portugal
[2]University of Coimbra, CEMMPRE, Faculty of Sciences and Technology, Department of Chemistry, 3004-535 Coimbra, Portugal
[3]Instituto Federal de Educação, Ciências e Tecnologia de Alagoas (IFAL)-Campus São Miguel dos Campos, Hélio Jatobá III, Quadra B6, 57246-615, São Miguel dos Campos-AL, Brazil
**meghica@eq.uc.pt*

Nanomaterials, e.g., carbon-based, metal nanoparticles, conducting polymers, represent excellent candidates for a wide range of applications, including catalysis, imaging, biotechnology, and sensing. For sensing applications, nanomaterial-modified electrodes present numerous benefits [1], such as: high electroactive area, fast electrochemical reaction (electrocatalysis), low trace level of quantification, high selectivity, among others.

Electrosynthesis is a simple and rapid method to prepare nanomaterial-modified electrodes with desired properties. In this sense, cyclic voltammetry (CV) is the most used electrochemical technique. CV offers fast location of redox potentials of the electroactive species and permits the convenient evaluation of the influence of the media upon the redox process [2,3]. CV can be coupled with electrochemical quartz crystal microbalance (EQCM) to offer additional information during electrosynthesis. The EQCM can monitor the changes in the mass of the electrode, that can be associated with the nanomaterial film deposited [4].

For the characterization of the nanomaterial-modified electrodes, CV is also the election technique, because has the ability to rapidly furnish crucial information on the thermodynamics of redox processes, the kinetics of heterogeneous electron-transfer reactions, and coupled chemical reactions or adsorption processes [5,6]. Additional to CV, differential pulse voltammetry (DPV) can be used, since provides improved selectivity and resolution for observing different redox processes [7]. Electrochemical impedance spectroscopy (EIS) has been also shown to be a valuable tool for characterization of nanomaterials-modified electrodes. EIS has demonstrated its ability for investigating the architecture of sensing platforms, as well as for quantitative impedimetric sensing of key analytes [8].

The synthesis and characterization of different nanomaterial-modified electrodes will be presented and the benefits of using electrochemical techniques for these purposes will be discussed.

References

1. N. Baig, M. Sajid, T.A. Saleh, TrAC-Trends Anal. Chem. **111** (2019) 47–61.
2. J. Wang, Analytical Electrochemistry, John Wiley & Sons Ltd, New York, 2014.
3. C.M.A. Brett, A.M.O. Brett, Electrochemistry: Principles, Methods and Applications, Oxford University Press, Oxford, 1998.
4. W. da Silva, C.M.A. Brett, J. Electroanal Chem., **896** (2021) 115188.
5. W. da Silva, M.E. Ghica, C.M.A. Brett, Electrochim. Acta, **317** (2019) 766-777.
6. W. da Silva, M.E. Ghica, R.A. Ajayi, E.I.Iuwoha, C.M.A. Brett, Food Chem., **282** (2019) 18-26.
7. V. S. Bagotsky, Fundamentals of electrochemistry, Jonh Wiley Sons, Hoboken, 2006
8. W. da Silva, M.E. Ghica, R.A. Ajayi, E.I.Iuwoha, C.M.A. Brett, Talanta, **195** (2019) 604-612.

Searching for Principles of Protein-Ligand Recognition by Varying Protein or Compound Structure

V. Dudutienė, J. Smirnovienė, A. Zubrienė, V. Kairys [2], A. Smirnov, L. Baranauskienė, A. Zakšauskas, V. Petrauskas, A. Mickevičiūtė, V. Michailovienė, E. Čapkauskaitė, E. Manakova[3], S. Gražulis[3], J. Leitans[4], A. Kazaks[4], K. Tars [4], and D. Matulis*

[1]Department of Biothermodynamics and Drug Design, Institute of Biotechnology, Life Sciences Center, Vilnius University, Vilnius, Lithuania

[2]Department of Bioinformatics, Institute of Biotechnology, Life Sciences Center, Vilnius University, Vilnius, Lithuania

[3]Department of Protein-DNA Interactions, Institute of Biotechnology, Life Sciences Center, Vilnius University, Vilnius, Lithuania

[4] Latvian Biomedical Research and Study Centre, Riga, Latvia, Street and number, zip code City, Country

**Corresponding author, daumantas.matulis@bti.vu.lt*

Pharmaceutical drug design depends on the success to build small a molecule that specifically and tightly binds to a target protein participating in disease progression. However, the principles of protein – ligand recognition are poorly understood and most new drugs are discovered by screening rather than by rational design. In the design of high-affinity and selective inhibitors, we applied an approach of augmenting the chemical structure of compounds. The increased size of the substituents determined the spatial limitations of the active sites of the 12 catalytically active human carbonic anhydrase (CA) isoforms until no binding observed because of the inability of the compounds to fit in the active site. This approach led to the discovery of high-affinity and -selectivity compounds for the anticancer target CA IX. The X-ray crystallographic structures of compounds bound to CA IX showed the positions of the bound compounds, whereas computational modeling confirmed that steric clashes prevent the binding of these compounds to other isozymes.

We also used a reverse engineering approach where mutation of the key six amino acids in the active site of human CAXII into the CAII isozyme performed to provide a protein chimera (chCA XII). The compounds that bound CA XII more strongly than CAII, switched their preference and bound more strongly to the engineered chimera, chCA XII, based on CA II, but containing the 6 key amino acids from CA XII. The structures of the compounds in the chimeric active site resembled those determined for complexes with CAXII. Both the compound augmentation and protein engineering provided information on the recognition mechanism based on the Lock-and-Key principle and validated both approaches in the development of new enzyme-specific drug candidate compounds.

References

1. Linkuvienė, V., A. Zubrienė, E. Manakova, V. Petrauskas, L. Baranauskienė, A. Zakšauskas, A. Smirnov, S. Gražulis, J.E. Ladbury, and D. Matulis. 2018. Thermodynamic, kinetic, and structural parameterization of human carbonic anhydrase interactions toward enhanced inhibitor design. Q. Rev. Biophys. 51:1–48.
2. Matulis (Ed.), D. 2019. Carbonic anhydrase as drug target: thermodynamics and structure of inhibitor binding. SPRINGER NATURE.
3. Dudutienė, V., A. Zubrienė, V. Kairys, A. Smirnov, J. Smirnovienė, J. Leitans, A. Kazaks, K. Tars, L. Manakova, S. Gražulis, and D. Matulis. 2020. Isoform-Selective Enzyme Inhibitors by Exploring Pocket Size According to the Lock-and-Key Principle. Biophys. J. 119:1513–1524.
4. Smirnovienė, J., A. Smirnov, A. Zakšauskas, A. Zubrienė, V. Petrauskas, A. Mickevičiūtė, V. Michailovienė, E. Čapkauskaitė, E. Manakova, S. Gražulis, L. Baranauskienė, W.-Y. Chen, J.E. Ladbury, and D. Matulis. 2021. Switching the Inhibitor-Enzyme Recognition Profile via Chimeric Carbonic Anhydrase XII. ChemistryOpen. 10:567–580.

Essential Oils and Their Use in the Cosmetics Industry

A. Wrona-Piotrowicz[1*]

[1]University of Lodz, Faculty of Chemistry, Department of Organic Chemistry, Tamka 12, 91-403 Lodz
**Corresponding author, e-mail:anna.wrona@chemia.uni.lodz.pl*

Essential oils found in plants are mixtures of volatile substances of different chemical nature, characterized by a strong, generally pleasant smell. The basis for qualifying to this group is not the chemical structure, but the physicochemical properties and the method of their isolation from the plant material. Essential oils are mainly obtained by steam distillation but can also be obtained by pressing, adsorption, extraction with organic solvents or supercritical carbon dioxide [1]. In chemical terms, essential oils are multi-component mixtures of mono-, sesqui- and (rarely) diterpene compounds (terpene oils) or phenylpropane derivatives (non-terpene oils). In their composition, the presence of compounds belonging to hydrocarbons, alcohols, aldehydes, ketones, esters and ethers was found. In addition to the listed terpene compounds and phenylpropane derivatives, there are also sulfur substances (mustard oils), nitrogenous substances, acetylene derivatives, tropolones, coumarins, organic acids and others. One oil can contain several dozen different compounds, but most of them contain a dominant ingredient, e.g. (-)-menthol in *Oleum Menthae pipertae* peppermint oil, which gives the oil its fragrance. The percentage of individual ingredients in the oil is variable and depends on many factors, both genetic (species, chemical breed of the plant) and environmental (e.g. climate, sunlight in the place where the plant grows). For this reason, oils are usually classified and evaluated based on the content of the main ingredient, e.g. menthol or thymol. In total, more than 1,500 have been discovered so far components of various essential oils.

The history of perfumery begins with essential oils, where alchemists and perfumers have been perfecting the methods of obtaining fragrances from various parts of plants for decades. Currently, they are used not only in the production of perfumes, but also in air aromatization, massage, care and hygiene products. In addition, essential oils containing terpene compounds have, among others, anti-inflammatory, antiseptic, antimicrobial, relaxing and warming properties [2]. They can be used in various forms of cosmetics: emulsions (creams, lotions, milks), simple single-phase systems (tonics, oil serums, massage oils), detergent products (shower gels, shampoos, soaps, micellar liquids), solid forms (peelings sugar-salt, soaps, shampoos and conditioners) [3]. However, there are some formulation limitations to be aware of. A big problem and challenge for technologists is the neutralization or escape of the smell, which manifests itself in a significant weakening of the olfactory sensation, especially in the case of citrus scents. For example, to perfume shampoos and shower gels with essential oils is particularly difficult because surfactants effectively bind and neutralize them. As a result, the expected smell will be distorted, weakened, and over time it may become completely imperceptible. In addition, some oils can cause an imbalance in the emulsion (e.g. vetiver), which leads to its stratification. This shows how important in design of cosmetics containing essential oils, apart from sensory sensations, is the knowledge of their physical and chemical properties [4].

References

1. V. N. Padole, S. Sarade, S. Rathod, S. More, S. Mendhi, Int. J. Pharm. Sci. Rev. Res., **73** (2022) 97-105.
2. W. Dhifi, S. Bellili, S. Jazi, N. Bahloul, W. Mnif, Medicines, **3** (2016) 25.
3. A. Sarkic, I. Stappen, Cosmetics, **5** (2018) 11.
4. Handbook of Essential Oils Science, Technology, and Applications, Ed K. H. C. Baser, G. Buchbauer, CRC Press, Taylor & Francis Group, Boca Raton, FL, 2010

Chemistry – the Key to Novel Solid State Batteries

T. R. Jensen

Interdisciplinary Nanoscience Center (iNANO) and Department of Chemistry
Aarhus University, Langelandsgade 140, 8000 Aarhus C, Denmark.
**Corresponding author, e-mail: trj@chem.au.dk*

Hydrogen has an extremely interesting chemistry and form compounds with most elements in the periodic table and with a variety of different types of bonds. Metal hydrides has recently become very interesting as new classes of energy materials for batteries and hydrogen storage [1]. Synthesis and characterisation of novel battery materials is the fundament for our research and we have discovered a range of new solid state electrolytes with fast cationic conductivity [2].

Recently, we synthesised a new metal borohydride, $Mg(BH_4)_2{\cdot}NH_3$, with high Mg^{2+} ionic conductivity. Density functional theory calculations (DFT) reveal that the neutral molecule (NH_3) is exchanged between the lattice and interstitial Mg^{2+} facilitated by a highly flexible structure, mainly owing to a network of di-hydrogen bonds, $N–H^{\delta+}\cdots{}^{-\delta}H–B$, and the versatile coordination of the BH_4^- ligand [3]. Di-hydrogen bonds in inorganic matter is a new tool for materials design and have similar bond strengths and bond lengths as hydrogen bonds in biological materials. A composite material consisting of two crystalline compounds, $Mg(BH_4)_2{\cdot}NH_3–Mg(BH_4)_2{\cdot}2NH_3$, is eutectic melting (~55 °C) and the melt can be stabilised to form a functional solid material with $\sigma(Mg^{2+}) \sim 10^{-3}$ S cm^{-1} at T = 70 °C using inert, insulating MgO nanoparticles as an additive. Solid state NMR reveal that the properties of the eutectic molten state is stabilised to form a solid with high thermal stability up to 200 °C [4]. An analogue lithium compound, $LiBH_4{\cdot}0.5NH_3$ have a similar Li^+ conductivity mechanism [5], and $MgCl_2{\cdot}2NH_3$, which lack dihydrogen bonds is an insulator.

These new phenomena is generally applicable for rational design of new electrolytes for multivalent solid state batteries. This is demonstrated by design and synthesis of series of novel cationic conductors, e.g. $Mg(BH_4)_2{\cdot}R$, R = NH_3, CH_3NH_2, $(CH_3)_2CHNH_2$, $(CH_2)_4O$ (THF), with extreme cationic conductivities, etc. [3,6-8]. Recently, we created the first inorganic magnesium battery that was charged and discharged for ten cycles, $Mg|Mg(BH_4)_2{\cdot}1.5THF–MgO(75\ wt\%)|TiS_2$ [8]. A new type of a solid state lithium battery, $Li|LiBH_4{\cdot}CH_3NH_2|TiS_2$ was also made based on hydride materials from our laboratory.

We conclude, that the chemistry of hydrides is very divers, towards rational design of multi-functional materials, including new electrolytes for future all-solid-state multi-valent batteries created completely from inorganic materials.

References

1. **Metal Borohydrides and derivatives - synthesis, structure and properties**, M. Paskevicius, L. Jepsen, P. Schouwink, R. Ĉerný, D. B. Ravnsbæk, Y. Filinchuk, M. Dornheim, T. R. Jensen, *Chem. Soc. Rev*. 2017, **46**, 1565, DOI: 10.1039/c6cs00705h
2. **New Perspectives of Functional Metal Borohydrides**, J. Grinderslev, M. Amdisen, L. Skov, K. Møller, M. Polanski, M. Heere, T.R. Jensen,* *J. Alloys Comp*., 2022, **896**, 163014, 1-19. https://doi.org/10.1016/j.jallcom.2021.163014
3. **The mechanism of Mg^{2+} conduction in ammine magnesium borohydride promoted by a neutral molecule**, Y. Yan, W. Dononelli, M. Jørgensen, J. B. Grinderslev, Y.-S. Lee, Y. Whan Cho, R. Černý, B. Hammer, T. R. Jensen, *Phys. Chem. Chem. Phys*., 2020, **22**, 9204-9209. DOI: 10.1039/D0CP00158A.
4. **Ammine Magnesium Borohydride Nanocomposites for All-Solid-State Magnesium Batteries**, Y. Yan, J. Grinderslev, L. Skov, T. R. Jensen*, *ACS Applied Energy Materials*, 2020, **3**, 9264−9270. https://dx.doi.org/10.1021/acsaem.0c01599
5. **Ammonia-assisted fast Li-ion conductivity in a new hemiammine lithium borohydride**, **$LiBH_4{\cdot}½NH_3$**, Y. Yan, J. Grinderslev, Y.-S. Lee, R. Cerný, T. Jensen, *Chem. Commun*., 2020, **56**, 3971-3974. DOI: 10.1039/c9cc09990e.
6. **Methylamine Magnesium Borohydrides as Electrolytes for All-Solid-State Magnesium Batteries,** M. Amdisen, J. Grinderslev, L. Skov, T. Jensen*, *Chem. Mater*., 2022 submitted
7. **Fast magnesium ion conducting isopropylamine magnesium borohydride enhanced by nanoparticles,** L. Kristensen, M. Amdisen, T. R. Jensen, *Phys. Chem. Chem. Phys.*, 2022, , **24**, 18185–18197, DOI: 10.1039/D1CP05063J
8. **Towards Solid-State Magnesium Batteries: Ligand-Assisted Superionic Conductivity**, L. Skov, J. Grinderslev, A. Rosenkranz, Y.-S. Lee, T. R. Jensen*, *Batteries & Supercaps* 2022, e202200163. doi.org/10.1002/batt.202200163
9. **Methylamine Lithium Borohydride as Electrolyte for All-Solid-State Batteries**, J. Grinderslev, L. Skov, J. Andreasen, T. R. Jensen*, *Angew. Chem. Int. Ed*. 2022, e202203484. doi.org/10.1002/anie.202203484. VIP - very important paper

Micro/Nano Plastics as a New Emerging Concern: from the Environment to Human Health

I. Uogintė

Center for physical sciences and technology, LT-02300, Lithuania
**I.Uogintė, e-mail: ieva.uoginte@ftmc.lt*

According to Europe plastic organization data, in 2016 world plastic production reached 380 million tons, in 2018 – 359 million tones. Globally, only 18% of plastics waste are recycled, and 24% are incinerated, and the remaining 58% enter the natural environment where plastics accumulate and persist for hundreds or even thousands of year [1]. Small plastic fragments are known as microplastic. The size of microplastic is less than 5 mm in diameter. They have been already detected in varies environmental systems such as: water, soil, air and sediments, moreover in water animals, and even in food products (for instance salts, sea food) [2]. Because smaller particles penetrate human tissues more easily, the adverse effects of MP /NPs on human health increase as particle size decreases. Since humans are at the top of the food chain, they may be the organism most at risk. Airborne MP /NPs are not only a source of toxicity, but also a highly adsorbent transport vector for polycyclic aromatic hydrocarbons (PAHs), heavy metals, furans, dioxins, and other air pollutants, especially in urban environments where 99% of the world's population is exposed to particulate matter levels above the updated WHO clean air guidelines. MP /NPs can accumulate in human tissues and cause local cytotoxicity and promote host immunological responses and carcinogenesis. MP /NPs, depending on the concentration, can also potentially cause tissue damage in the human respiratory system [3]. The rapid increase in plastic pollution and its impact on nature and human health urgently require new technologies and mechanisms for the identification and degradation of microplastics. The current methods for degradation of microplastics can be divided into photothermal degradation, ozone-induced degradation, catalytic degradation, and biodegradation [4]. However, finding efficient methods for microplastic fragmentation remains a major challenge.

References

1. Chamas A., Moon H., Zheng J., Qiu Y., Tabassym T., Jang J.H. Abu-Omar M., Scott S.L., Suh S. 2020. *ACS Sustainable Chemistry and Engineering* **8** (9) 3494-3511.
2. Iñiguez M.E., Conesa J.A., Fullana A. 2017. *Scientific Reports* **7**(1) 1–7
3. Prata JC. Airborne microplastics: Consequences to human health? Environ Pollut. 2018.
4. L. Zhenyan, T. Jin, T. Zou, L. Xu, B. Xi, J. He, L. Xiong, C. Tang, J. Peng, Y. Zhou, J. Fei. 2022. *Environmental Pollution*, 304 (July): 119159.

Microplastics in the Products of Waste Biological Treatment

A. Sholokhova G. Denafas

Department of Environmental Technology, Faculty of Chemical Technology, Kaunas University of Technology, Radvilėnų pl. 19, LT-50254, Kaunas, Lithuania
gintaras.denafas@ktu.lt

From the 20th centure evenly increasing production of plastic and subsequently increasing plastic waste generation cause not only the use of natural resources, greenhouse gas emissions and visually observed environmental contamination with plastic. They also contribute to the formation of microplastics, spreading in nature and effects on living organisms. This encourage research, both in the evaluation of the sources of microplastics and in the search for effective and accessible microplastics analysis in environmental components.

As our research objects the biological stabilate from mechanical-biological processing of mixed municipal waste, the compost obtained from food and green waste, and landfills fine fraction have been chosen. Each biological treatment residues contains larger or smaller amounts of plastic waste.

The samples of the aforementioned substances were sifted into three granulometric fractions: > 5 mm, 1 mm ÷ 5mm and <1 mm. The largest fraction was rejected. The 1 mm ÷ 5mm faction was investigated visually, and further microplastics were separated using saline solutions of different density. The chemical structure of the separated microplastics was determined by the FTIR method.

The <1 mm fraction was treated by a Fenton reagent, thus removing the organic admixtures. Further microplastics were distinguished by the above density method, affected by the Nile red and analyzed by fluorescent microscopy.

The results of the study confirmed the abundance of microplastic particles in waste biological treatment products, assuming that this is the presence of macroplastics, mechanical effect during waste processing and biological oxidation. The effect of the latter was further investigated in green waste composting pillow by placing various types of plastics and holding it there for 8 months. Increase in the amount of microplastics and by the SEM method evaluated erosion of PE, PP and PS samples was obvious. The biodegradable sample of PLA was practically fully destroyed.

In this way, it becomes evident that plastic waste separate collection and recycling, as well as replacement of conventional plastic with biodegradable plastic significantly reduces the formation of microplastics and its impact to environment and human health.

References

1. Sholokhova, G. Denafas, V. Mykhaylenko. Waste Management and Research. **39** (2021), 652-663.
2. Sholokhova, J. Čeponkus, V. Šablinskas, G. Denafas. Environmental Science and Pollution Research International. **29(14)** (2022), 20665–20674.
3. Sholokhova, G. Denafas, V. Mykhaylenko. Environmental Research. **214** (2022), 113825.
4. Sholokhova, G. Denafas, J. Čeponkus, R. Kriulienė. Sustainability. **15** (2023), 1-11.

X-ray Absorption Spectroscopy in Physics, Material Science and Chemistry

A. Anspoks*[1], A. Kuzmins[1], I. Pudža[1]
[1]*Institute of Solid State Physics, University of Latvia*
**Corresponding author, e-mail: andris.anspoks@cfi.lu.lv*

X-ray absorption spectroscopy (XAS) is a powerful tool to study local electronic and atomic structure of solids, liquids, and gases in a wide range of external conditions defined by temperature, pressure, etc. The information on the local electronic structure can be extracted from x-ray absorption spectrum in the vicinity of an absorption edge of an atom, whereas structural information can be determined from the extended X-ray absorption fine structure (EXAFS), having an oscillating character, and located beyond the absorption edge.

XAS can be used to determine very small atomic movements [2], atom distribution functions and local environment of particular chemical element [1, 3] as well to test molecular dynamic models [4]. Since early days XAS is used to study catalysts and chemical reactions [6]. Modern X-ray free electron lasers bring a fs resolution to the structure analysis [5]. Special advantage this method is in determining atomic structure around dopants [7].

In this talk I will give and overview of the modern methods using XAS for various analysis of solids, dopant structure analysis and reactions. Methods will include data analysis and modelling approach developed by our team [4, 8].

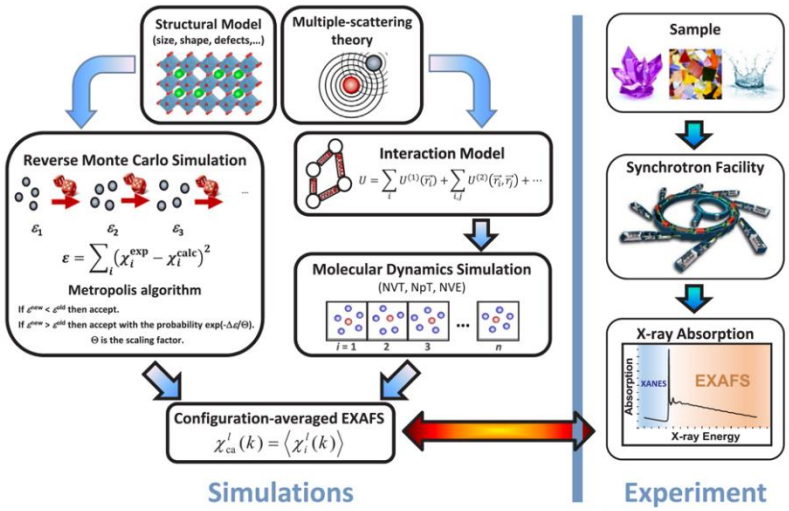

References

1. Pudza, A. Anspoks, G. Aquilanti, A. Kuzmin, Revealing the local structure of $CuMo_{1-x}W_xO_4$ solid solutions by multi-edge X-ray absorption spectroscopy, Mater. Res. Bull. 153 (2022) 111910. Doi: 10.1016/j.materresbull.2022.111910
2. S. Kato, N. Nakajima, S. Yasui, S. Yasuhara, D. Fu, J. Adachi, H. Nitani, Y. Takeichi, A. Anspoks, Dielectric response of $BaTiO_3$ electronic states under AC fields via microsecond time-resolved X-ray absorption spectroscopy,Acta Mater. 207 (2021) 116681. Doi: 10.1016/j.actamat.2021.116681
3. Pudza, A. Anspoks, A. Cintins, A. Kalinko, E. Welter, A. Kuzmin, The influence of Zn^{2+} ions on the local structure and thermochromic properties of $Cu_{1-x}Zn_xMoO_4$ solid solutions, Mater. Today Commun. 28 (2021) 102607. Doi: 10.1016/j.mtcomm.2021.102607
4. Kuzmin, J. Timoshenko, A. Kalinko, I. Jonane, A. Anspoks, Treatment of disorder effects in X-ray absorption spectra beyond the conventional approach, Rad. Phys. Chem. 175 (2020) 108112. [Review] Doi: 10.1016/j.radphyschem.2018.12.032
5. Suga, M., Akita, F., Hirata, K. et al. Native structure of photosystem II at 1.95 Å resolution viewed by femtosecond X-ray pulses. Nature 517, 99–103 (2015). Doi: 10.1038/nature13991
6. S. Mukerjee, S. Srinivasan, M. P. Soriaga, J. McBreen, Role of Structural and Electronic Properties of Pt and Pt Alloys on Electrocatalysis of Oxygen Reduction: An In Situ XANES and EXAFS Investigation, 1995 J. Electrochem. Soc. 142 1409. Doi: 10.1149/1.2048590
7. J.M. Ribeiro, F.C. Correia, A. Kuzmin, I. Jonane, M. Kong, A.R. Goni, J.S. Reparaz, A. Kalinko, E. Welter, C.J. Tavares, Influence of Nb-doping on the local structure and thermoelectric properties of transparent TiO2:Nb thin films, J. Alloys Compd. 838 (2020) 155561. Doi: 10.1016/j.jallcom.2020.155561
8. http://www.dragon.lv/exafs/xas.htm

POSTER SESSION

POSTER SESSION

Chairperson Assoc. Prof. Živilė Stankevičiūtė
Friday (10th March)
16:40 – 17:40

P 001	A. Afonina, G. Antanaitis, A. Kareiva, I. Grigoraviciute	Low-Temperature Synthesis of Magnesium Whitlockite Nanopowder Under Static and Rotating Conditions
P 002	V. Špiliauskas, K. Anusevičius, B. Grybaitė, I. Jonuškienė, B. Sapijanskaitė-Banevič, R. Vaickelionienė, V. Mickevičius	Synthesis of N-[3-(Hydrazinecarbonyl)-4-hydroxyphenyl]acetamide Derivatives
P 003	R. Aukštakojytė, J. Gaidukevič, J. Barkauskas	Effect of B- and N-Codoping on the Structural and Morphological Properties of Reduced Graphene Oxide
P 004	M. Babelyte, R. Rutkaite, D. Liudvinaviciute, L. Peciulyte, V. Samaryk	Thermoresponsive Properties of Chitosan-graft-poly(N-isopropylacylamide) Copolymers
P 005	R. Baranauskienė, P. R. Venskutonis	Aroma Profile and Total Phenolics of Hop Cones and Pellets
P 006	S. Barysaitė, A. Gelzinis, J. Chmeliov, L. Valkunas	Electronic Excited States of Chlorophylls in Photosynthetic Complex CP29
P 007	M. R. Bartkus, G. Varvuolytė, A. Žukauskaitė, V. Martynaitis, R. Tamulienė, A. Šačkus, N. Kleizienė	Synthesis and Evaluation of Optical Properties of New Conjugated 3H-Indole Moiety Possessing Systems
P 008	M. Baublytė, D. Sokol, R. Skaudžius	Multifunctional Wood – Properties of $GdPO_4 \cdot H_2O:Eu^{3+}$ Doped Wood
P 009	R. Beresneviciute, H. Bi, J. Liu, G. Kapil, D. Tavgeniene, Z. Zhang, L. Wang, C. Ding, S. R. Sahamir, Y. Sanehira, A. K. Baranwal, K Takeshi, D. Wang, Y. Wei, Y. Yang, D. W. Kang, S. Grigalevicius, Q. Shen, S. Hayase	Wide Bandgap Lead Perovskite Solar Cells with Monomolecular Layer from Viewpoint of PTAA Band Bending

P 010	R. Beresneviciute, D. Tavgeniene, D. Blazevicius, G. Krucaite, B. Achramovic, S. S. Swayamprabha, J.-H. Jou, S. Grigalevicius	3-(N,N-Diphenylamino)carbazole Acceptor Containing Bipolar Derivatives as TADF Emitters for OLED Devices
P 011	D. Blaževičius, R. Beresnevičiūtė, G. Kručaite, D. Tavgenienė, S. Grigalevičius, M. R. Nagar, C. T. Hao, J.-H. Jou, K. Kumar, S. Banik	Central Benzophenone Fragment Having Solution Processable Derivatives as Bipolar Hosts for Green TADF OLEDs
P 012	R. Boguzaite, V. Ratautaite, G. Pilvenyte, E. Brazys, A. Ramanavicius	Polypyrrole Modifications with Methylene Blue
P 013	E. Brazys, V. Ratautaitė, R. Bogužaitė, A. Ramanavičius	Evaluation of the Interaction Between SARS-CoV-2 Spike Glycoproteins and the Molecularly Imprinted Polypyrrole
P 014	D. Budrevičius, A. Pakalniškis, A. Kareiva, R. Skaudžius	Improvement of Luminescent Properties of $GdPO_4$ Doped with Europium
P 015	C. Zhu, I. Pundienė, J. Pranckevičienė, M. Kligys	Biomass Fly Ash-Based Alkali-Activated Materials
P 016	U. Cigane, A. Palevicius, G. Janusas	Vibration Application for Porous AAO Membrane Synthesis
P 017	Š. Daškevičiūtė-Gegužienė, Y. Zhang, K. Rakštys, M. Daškevičienė, V. Jankauskas, M. K. Nazeeruddin, V. Getautis	Passivating Defects of Perovskite Solar Cells with Functional Donor-Acceptor-Donor Type Hole Transporting Materials
P 018	E. Didžiulytė, R. Šlinkšienė, R. Paleckienė	Analysis and Usage Perspectives of Solid Digestate
P 019	K. Dzedulionytė, N. Fuxreiter, E. Schreiber-Brynzak, A. Žukauskaitė, V. Pichler, E. Arbačiauskienė	From Natural Products to Synthetic Analogues: Pyrrole-Pyrazole Exchange in Lamellarin O
P 020	M. Dzvinka, M. Misevičius	Analysis of Europium-Doped Sodium Aluminum Germanate
P 021	E. Ezerskyte, A. Morkvenas, Z. Jurgelene, V. Karabanovas, V. Klimkevicius	Well-Defined $GdPO_4:Eu^{3+}$ Nanophosphors for Assessment of Environmental Toxicity
P 022	J. Gaidukevič, R. Trusovas, R. Pauliukaitė, J. Barkauskas	A Dopamine Electrochemical Sensor Based on Reduced Graphene Oxide Obtained by the Laser-Induced Reduction Method

P 023	R. Gelminauskaitė, B. Grybaitė, E. Mickevičiūtė	Synthesis of Novel N-(4-Hydroxyphenyl)-β-alanine Derivatives
P 024	B. Golcienė, A. Voskienė, V. Mickevičius	Synthesis of Novel N-(4-Acetylphenyl)imidazole and Dihydropyrimidine Derivatives
P 025	R. Grabauskaitė, L. Jūrienė, R. Kazernavičiūtė, R. Maždžierienė, P. R. Venskutonis	Isolation of Hydrophilic Fractions from Defatted Strawberry, Blackberry and Elderberry Seeds and Rowanberry Pomace by Pressurized Liquid Extraction
P 026	K. Naruševičiūtė, B. Grybaitė, B. Sapijanskaitė-Banevič, R. Vaickelionienė, K. Anusevičius, V. Mickevičius	Synthesis of Novel Functionalized N,N-Disubstituted Aminothiazoles
P 027	R. Gruškienė, T. Kavleiskaja, R. Stanevičienė, E. Servienė, J. Sereikaitė	Iron Oxide Magnetic Nanoparticles Functionalized by Nisin
P 028	G. Gudinskaitė, R. Paleckienė, R. Šlinkšienė	Possibilities of Using Non-Traditional Raw Materials for Fertilizer Production
P 029	G. Inkrataitė, J. N. Keil, T. Jüstel, R. Skaudžius	Effect of Different Amounts of Cr^{3+} and B^{3+} Ions on the Luminescence Properties of LuAG
P 030	G. Janusauskaite, M. Misevicius	Synthesis and Luminescent Properties of Eu^{3+}, Dy^{3+}, Bi^{3+}-Doped Sodium Aluminum Germanate $NaAlGeO_4$ Phosphors
P 031	K. Čeplinskas, A. Jaskūnas	Catalytic Activity of Mixed Cu, Co and Cr Oxide Catalysts
P 032	L. Jūrienė, A. Pukalskas, P. R. Venskutonis	Fractionation of Lipophilic Components of Chokeberry Pomace by Innovative Extraction Technique
P 033	E. Juzeliūnas, P. Kalinauskas, L. Staišiūnas, A. Grigucevičienė, K. Leinartas, D. Bučinskienė, A. Šilėnas	Catalytic Hydrogen Evolution Reaction on a Composite p-Si/Al_2O_3/Ni Photoelectrode
P 034	L.-M. Kaljusmaa, O. Järvik	Finding Potential Phase Change Materials Among Ionic Liquids with The Aid of Machine Learning Model
P 035	A. Nurpeissov, D. Vistorskaja, S. Pazylbek, D. Karoblis, A. Lukowiak, W. Strek, A. Laurikenas, T. Nurakhmetov, T. Raudonis, A. Zarkov, A. Kareiva	On the Synthesis of New $Y_{3-x-y-z}Ca_xLi_y Ce_zGa_5O_{12}$ Garnets

P 036	D. Karoblis, A. Zarkov, A. Kareiva	Molten Salt Synthesis of $REMnO_3$ (RE – Y, Er, Tm, Yb) Manganites
P 037	V. Kavaliauskas, V. Olšauskaitė, A. Padarauskas	Investigation of Hexafluoroisopropanol-Based Aqueous Biphasic System
P 038	P. Kaziukonytė, V. Petraška, A. Brukštus	Synthesis of 5-(2,4-Dihydroxyphenyl)imidazole Derivatives as Potential Hsp90 Inhibitors
P 039	G. Klydžiūtė, E. Raudonytė-Svirbutavičienė, A. Žarkov, A. Kareiva, A. Beganskienė	Influence of Hydrothermal Synthesis Parameters on the Properties of Calcium Hydroxyapatites
P 040	V. Klimavičius, G. Inkrataitė, V. Kalendra, A. Kareiva, G. Buntkowsky	Garnets as Systems for Endogenous Dynamic Nuclear Polarization (DNP)
P 041	K. Krasauskaitė, R. Šlinkšienė	The Interaction of Monoammonium Phosphate with Zinc Sulphate and Starch Solutions
P 042	G. Krucaite, D. Tavgeniene, S. Grigalevicius, Bi. Huan, Z. Zhen, G. Kapil, S. Qing, S. Hayase, E. Zaleckas	3,6-Diarylcarbazoles for Hole Transporting Layers of SOLAR Cells
P 043	E. Kvietkauskas, S. Budrienė	Synthesis and Characterization of Unsaturated Polyesters Modified with Malic Acid and PDMS for Tissue Engineering Applications
P 044	D. Liudvinavičiūtė, R. Grabauskaitė, R. Rutkaitė	Investigation and Properties of Complexes of Anthocyanins and Cross-Linked Pectin or Sodium Alginate
P 045	M. Liudžiūtė, S. Žalenkienė, I. Ancutienė	Quantitative Analysis of Cadmium Telluride-Cadmium Sulphide Layers on Polyamide 6
P 046	J. Luneckas, L. Peciulyte, J. Bendoraitiene, R. Rutkaite	Properties of Starch Modified with Dodecenylsuccinic Anhydride and Acetic Anhydride
P 047	S. Macionis, J. Simokaitiene, J. V. Grazulevicius, J. H. Lee, C. H. Chen, B. Y. Lin, T. L. Chiu	Modified 1,2-Diphenylbenzoimidazole Materials for Green and Sky-Blue Emission OLEDs
P 048	G. Mačiuitytė, V. Petkevičius	Synthesis of Substrates for the Investigation of PmlABCDEF Monooxygenase Selectivity
P 049	G. Masione, D. Ciuzas, E. Krugly, M. Tichonovas, D. Martuzevicius	Optimisation of Factors Affecting the Electrospinning for Prediction of the Morphology of Biobased Poly(butylene succinate) Nanofibrous Mats
P 050	Š. Masys, V. Jonauskas	The Surfaces of Nanodiamonds: A Modeling Perspective

P 051	T. Matijošius, G. Bikulčius, S. Asadauskas	Antifrictional Effect on Dyeing of Anodic Coatings Impregnated with Fillers
P 052	U. Milerytė, A. Brukštus, I. Žutautė	Introduction of Benzyl Substituents to Resorcinol Moiety in Search for N-Domain HSP90 Inhibitors
P 053	T. Mumladze, A. Šleiniūtė, G. Denafas	Current Challenges in the Solvent-Based Multilayer Composite Waste Recycling
P 054	M. Navickas, E. Skliutas, M. Malinauskas, M. Vengris	Transient Absorption Spectroscopy of Photochemical Reactions in Different Photoinitiators
P 055	V. Navikaite-Snipaitiene, A. Kairyte, M. Babelyte, L. Peciulyte, R. Rutkaite, V. Samaryk	Synthesis of Chitosan-graft-poly(N-isopropylacrylamide) Copolymers
P 056	E. Onokwai, I. Stasiulaitiene	Life-Cycle Assessment of CO_2 Mineralization Product: Comparing Magnesia Cement and Portland Cement
P 057	M.-A. Onoriode-Afunezie, A. Sulciute, V. Abromaitis	Synthesis and Application of TiO_2 Nanotube Arrays for Treatment of Pharmaceuticals in Model Wastewater
P 058	A. Pakalniškis, G. Niaura, D. Karpinsky, G. Rogez, P. Rabu, S. Chen, T. C-K Yang, R. Skaudžius, A. Kareiva	Effects of Sol-Gel Synthesis Procedure Conditions on The Stability of Polar Active Hexagonal Phase in $LuFeO_3$-$LuMnO_3$ System
P 059	M. Gilić, R. Alaburdaitė, E. Paluckienė, N. Petrašauskienė	Effect of Deposition Cycles on the Properties of Copper Sulfide Thin Films Deposited by CBD
P 060	G. Poceviciute, G. Masione, D. Ciuzas, E. Krugly, M. Tichonovas, D. Martuzevicius, V. Kauneliene	Application of Capillary Flow Porometry to Predict the Filtration Efficiency of Nanofibrous Polymer Membranes
P 061	O. Pocienė, E. Griškaitis, R. Šlinkšienė	Polyvinyl Acetate as Binder in the Formation of Granules of Buckwheat Husk Ash
P 062	E. Potapov, L. Pastarnokienė, T. Kochanė, R. Makuška	Synthesis of Microcapsules Containing Polyaspartic Acid Ester within UV Curable Shell
P 063	G. Pranaitytė, B. Grybaitė, E. Mickevičiūtė	Synthesis of Novel 1-(2,4-Difluorophenyl)-5-oxopyrrolidine-3-carboxylic Acid Derivatives
P 064	V. Pudžaitis, M. Talaikis, G. Niaura	Electrochemical SEIRAS Analysis of Imidazole Ring Functionalized Self-Assembled Monolayers

P 065	A. Pupiute, D. Ciuzas, D. Martuzevicius, E. Krugly	Fibrous Polycaprolactone-Based 3D Scaffolds for In Vitro Cell Models
P 066	R. Raiseliene, G. Linkaite, A. Kareiva, I. Grigoraviciute	Synthesis and Investigation of Biphasic Calcium Phosphate Granules
P 067	S. Ramanavičius, A. Popov, S Adomavičiūtė-Grabusovė, M. Talaikis, V. Šablinskas, G. Niaura, A. Ramanavičius	Tunable Properties of $Ti_3C_2T_x$ MXenes 2D Structures for Applications in a Surface Enhanced Raman Spectroscopy
P 068	G. Rankelytė, J. Chmeliov, A. Gelzinis, L. Valkunas	Excited States of Chlorophyll Molecules in Light-Harvesting Antenna of PSI
P 069	P. Rivera, M. Petrulevičienė, I. Savickaja, K. Turuta, J. Juodkazytė, A. Ramanavičius	Effect of Mn^{+2} Doping on the Formation and Properties of $BiVO_4$ Coatings
P 070	D. Rubinaite, T. Dambrauskas, A. Eisinas	Role of Water Vapour Pressure in the Carbonation Process of Calcium Monosulfoaluminate 12-Hydrate
P 071	E. Mieliauskaitė, B. Sapijanskaitė-Banevič, R. Vaickelionienė, B. Grybaitė, K. Anusevičius	Synthesis of New 1-(9-Ethylcarbazol-3-yl)-5-oxopyrrolidine-3-carbohydrazide Derivatives
P 072	E. Skuodaitė, V. Krylova	Investigation of the Changes in Structural and Optical Properties of Ag-O/PET/PVC Composites after Aging
P 073	I. Stebryte, K. Baltakys	Effect of Titanium Oxide on the Formation of Hydroxyapatite under Microwave Synthesis Conditions
P 074	S. Barua, A. Balčiūnaitė, J. Vaičiūnienė, L. Tamašauskaitė-Tamašiūnaitė, E. Norkus	Bimetallic Nickel-Manganese/Titanium Electrocatalyst for Efficient Hydrogen Evolution Reaction
P 075	I. Sulym, O. Goncharuk, K. Terpiłowski, Z. Valdez-Nava	Structural Properties of MWCNTs@PDMS-1000 Nanocomposites
P 076	R. Surblyte, K. Baltakys	Microwave Synthesis of Hydroxyapatite Substituted with Zn^{2+} Ions in the Temperature Range of 80 - 200°C
P 077	E. Švedaitė, K. Baltakys, T. Dambrauskas	Adsorption of Phosphate Ions by CSH (CaO/SiO_2=1.5) Adsorbent
P 078	A. Šermukšnytė, V. Petrikaitė, K. Kantminienė, I. Jonuškienė, I. Tumosienė	Design of 5-Substituted 2-Oxindole-hydrazone Derivatives Bearing 1,2,4-Triazole-3-thiol Moiety as Anticancer Agents
P 079	A. Šleiniūtė, T. Mumladze, G. Denafas	Delamination of Multilayer Composite Packaging Waste by HNO_3 and Its Analysis with MODDE Software

P 080	D. Tavgenienė, B. Zhang, B. Achramovič, S. Grigalevicius	Di(arylcarbazole) Substituted Oxetanes as Efficient Hole Transporting Materials with High Thermal and Morphological Stability for OLEDs
P 081	D. Tavgenienė, H. Bi, Y. Fujiwara, Ch. Ding, S. R. Sahamir, Y. Sanehira, A. K. Baranwal, K. Takeshi, G. Shi, G. Kapil, Z. Zhang, L. Wang, T. Bessho, H. Segawa, B. Achramovič, S. Grigalevicius, Q. Shen, S. Hayase	Perovskite Solar Cells with Monolayer Modified PTAA and Its Application to All-Perovskite Tandem Solar Cells
P 082	D.Tediashvili, L. Vilčiauskas	Chemical and Electrochemical Stability of Vanadium-Based Cathodes for Aqueous Na-Ion Batteries
P 083	E. Ūsovienė, E. Griškonis	Copper Sulfide-Based Anode Materials for Sodium-Ion Batteries
P 084	K. Vaičiukynaitė, S. Žalenkienė, R. Ivanauskas	Study of the Quantitative Composition of the Cobalt Sulfide Layers on the Polyamide 6 Surface
P 085	R. Vaitkus, I. Jonuškienė, K. Kantminienė, Z. J. Beresnevičius, I. Tumosienė	Synthesis and Antioxidant Activity of 4-Amino-5-(2-((2-methylquinolin-6-yl)amino)ethyl)-2,4-dihydro-3H-1,2,4-triazole-3-thione
P 086	J. Urbonavičius, A. Zagorskis, D. Vasiliauskienė, V. Valentinas	Screening and Identification of Microorganisms that Degrade Oil Products
P 087	M. Veikšaitė, K. Dzedulionytė, V. Moravek, A. Žukauskaitė, E. Arbačiauskienė, A. Šačkus	Synthesis of N-Heterocycle-Fused Tetrahydro-1,4-diazepinones
P 088	K. Venskūnaitė, A. Brukštus	4-(Cycloalkyl)-6-(1-(4-substituted)-1H-imidazol-5-yl)benzene-1,3-diols and 4-(Cycloalkyl)-6-(5-(4-methoxyphenyl)-1,2,3-thiadiazol-4-yl)benzene-1,3-diols Synthesis
P 089	P. Virbickas, G. Ziziunaite, A. Valiūnienė	Glucose Oxidase Inhibition-Based Hg^{2+} Ion Biosensor
P 090	D. Vištorskaja, A. Kareiva	Sol-Gel Synthesis and Characterization of Novel Garnets with Various Stoichiometric Compositions
P 091	E. Zubrytė, A. Gefenienė, S. Jankauskas, R. Ragauskas, R. Ramanauskas	Wastewater Treatment of Spent Dyeing Bath Using Ion Exchange and Activated Carbon Adsorbents

P 092	A. Žilinskas, S. Višniakova, M. Lobanovas	Application of Crude Animal Origin Extracts in the Aldol Reactions for the Synthesis of Chiral Bicyclic Compounds
P 093	V. Žutautas, R. Trusovas, A. Sartanavičius, K. Ratautas, T. Rakickas, R. Pauliukaite	Conducting Polymer Modified Laser-Induced Graphene Usage For pH Sensing
P 094	M. Žvirblis, A. Sakalauskas, V. Dudutienė, V. Smirnovas, D. Matulis	Amyloid Aggregation Suppression and Carbonic Anhydrase Inhibition with Fluorinated Benzenesulfonamides
P 095	R. Šiaučiūnas, E. Prichockienė, Z. Valančius	Carbonated rankinite binder from JSC Akmenes cementas raw materials

P 001

Low-Temperature Synthesis of Magnesium Whitlockite Nanopowder Under Static and Rotating Conditions

A. Afonina[1,*], G. Antanaitis[2], A. Kareiva[1], I. Grigoraviciute[1]

[1]Faculty of Chemistry and Geosciences, Vilnius University, Naugarduko 24, LT-03225 Vilnius, Lithuania

[2]GA Medical Pty Ltd, P.O. Box 243, North Balwyn, 3104, Victoria, Austalia

**Corresponding author, e-mail: anastasija.afonina@chgf.vu.lt*

Synthetic calcium phosphates are widely considered as a kind of excellent bone regenerative materials due to their similarity to the bone mineral composition, good biocompatibility and bioactivity [1]. Recently, magnesium whitlockite ($Ca_{18}Mg_2(HPO_4)_2(PO_4)_{12}$, WH) was recognized as the second most abundant mineral of bone in the human body [2]. In our work we prepared nanopowder of WH from calcium sulphate dehydrate (gypsum, $CaSO_4 \cdot 2H_2O$). A dissolution-precipitation synthesis of WH samples was performed at 80 °C in the presence of Mg^{2+} ions. To verify the formation WH phase under static and rotating conditions in time, we gradually increased reaction time keeping the synthesis temperature constant.

References

1. H.-Y. Lin, Y.-K. Huang, P.-Y. Hsu, W.-H. Tuan, M. Naito, Ceram. Int., **47** (2021) 21714-21720.
2. H. Cheng, R. Chabok, X. Guan, A. Chawla, Y. Li, A. Khademhosseini, H. L. Jang, Act. Bio., **69** (2018) 342-351.

P 002

Synthesis of *N*-[3-(Hydrazinecarbonyl)-4-hydroxyphenyl]acetamide Derivatives

V. Špiliauskas, K. Anusevičius*, B. Grybaitė, I. Jonuškienė, B. Sapijanskaitė-Banevič, R. Vaickelionienė, V. Mickevičius

Kauno technologijos universitetas K. Donelaičio g. 73, LT-44249 Kaunas, Lietuva

Corresponding authors emails: kazimieras.anusevičius@ktu.lt:

Mesalazine is also known as 5-aminosalicylic acid and used to treat inflammatory bowel disease. However, 5-aminosalicylic carbohydrazyde was studied as a promising scaffold with antibacterial properties [1]. In this work *N*-[3-(hydrazinecarbonyl)-4-hydroxyphenyl]acetamide (**1**) was synthesized by the method described in article [2]. Developing of compounds with antibacterial properties are involved to synthesis of 1,3,4-oxadiazole [3], 4-amino-1,2,4-triazole [4], triazolothiadiazine [5] or certain Schiff base [6] moiety. Bearing in mind these properties, we proceeded with modification of the 5-aminosalicylic carbohydrazide **1** following **scheme 1**.

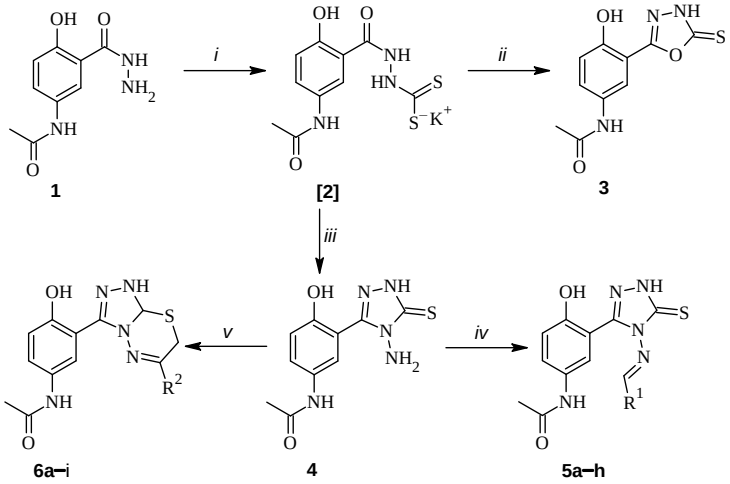

R^1 = **a)** C_6H_5; **b)** 4-Cl-C_6H_4; **c)** 4-Br-C_6H_4; **d)** 4-NO_2-C_6H_4; **e)** 2-furanyl; **f)** 5-nitrofuran-2-yl; **g)** 2-thiophenyl; **h)** 5-nitrothiophen-2-yl; **i)** 3-indolyl;
R^2 = **a)** H; **b)** CH_3; **c)** C_6H_5; **d)** 4-F-C_6H_4; **e)** 4-Cl-C_6H_4; **f)** 4-Br-C_6H_4; **g)** 4-NO_2-C_6H_4; **h)** 2-naphthyl.

i) CS_2, KOH, MeOH, RT, 24 h; ***ii)*** AcOH, heated to reflux; ***iii)*** $H_2NNH_2 \cdot H_2O$, 2-PrOH, reflux 24 h; ***iv)*** corresp. aldehyde, MeOH, HCl, reflux, 4 h; ***v)*** corresp. α-haloketone, 1,4-dioxane, TEA, reflux, 8 h.

Scheme 1. Synthesis and transformation of azole **3, 4**.

Potassium dithiocarbazide **2** was obtained by the reaction of hydrazide **1** with carbon disulfide in presence of excess amount of potassium hydroxide. Compound **2** was used in the next step without further purification. 1,3,4-Oksadiazol-5-thione **3** was synthesized by adding acetic acid to the solution containing compound **2** and heating it to reflux. Further, reaction of potassium dithiocarbazide **2** with hydrazine hydrate was performed in propan-2-ol to synthesis 4-amino-1,2,4-triazol-5-thione **4**. Schiff bases **5a–h** were synthesized by reactions of 4-amino-1,2,4-triazol-5-thione **4** with according to aromatic or heterocyclic aldehydes in presence of few drops of hydrochloric acid. By the reactions of 4-amino-1,2,4-triazol-5-thione **4** with different α-halogen ketones were obtained 3,6-disubstituted 1,2,4-triazole[3,4-*b*][1,3,4]thiodiazides **6a–i**. The structure of synthesized compounds was confirmed by the elemental analysis, ^{1}H, ^{13}C NMR, IR spectroscopy and mass spectrometry.

References

1. H. Sabir, S. Jyoti, A. Mohd, *e-J. Org. Chem*., **5** (2008) 963–968.
2. O. Tapanyiğit, O. Demirkol, E. Güler, *Arab. J. Chem.*, **13** (2020) 9105–9117.
3. A.A. Othman, M. Kihel, S. Amara, *Arab. J. Chem.*, **12** (2019) 1660–1675.
4. S. Kooi-Mow; T. Kah-Cheng, *Lett. Drug Des. Discov*., **15** (2018) 733–743.
5. B.S. Holla, B.K. Sarojini, B.S. Rao, P.M. Akberali, N.S. Kumari, V. Shetty, *Il Farmaco*, **56** (2001) 565–570.
6. C.M. Silva, D.L. Silva, L V. Modolo, R.B. Alves, M.A. Resende, C.V.B. Martins, Â. Fátima, *J. Adv. Res.*, **2** (2011) 1–8.

P 003

Effect of B- and N-Codoping on the Structural and Morphological Properties of Reduced Graphene Oxide

R. Aukštakojytė[1*], J. Gaidukevič[1], J. Barkauskas[1]

[1]Vilnius University, Naugarduko Str. 24, LT-03225, Vilnius, Lithuania

**Corresponding author, e-mail: ruta.aukstakojyte@chgf.vu.lt*

In recent years, graphene-based materials such as graphene oxide (GO) and reduced graphene oxide (rGO) have attracted worldwide attention in the areas of supercapacitors, (bio)sensors, fuel or solar cells. The successful application of rGO in sensing devices and catalysts strongly depends on its physicochemical properties. Present studies have demonstrated that doping with foreign heteroatoms (B, N, P, and S) could be a key strategy to alter the electrochemical, electronic, and structural characteristics of rGO [1, 2]. Nitrogen and boron are ideal dopants for graphene-based materials, since they exhibit an atomic radius similar to that of carbon. It is well known that the nitrogen-rich sites in rGO can effectively improve electrochemical activity, especially, in the presence of pyrrolic-N and pyridinic-N bonding configurations. N-doping also increases the electrical conductivity of graphene-based materials due to the formation of N-graphitic atoms in the lattice and enhances the specific surface area by larger defect sizes and a more porous structure [2]. In the case of B-doping, the incorporation of B atoms can lead to extra sites grafted onto the carbon surface, enabling both enhanced hydrophilicity and durability for the carbon materials [3]. Therefore, the boron and nitrogen-codoped rGO (BN-rGO) samples synthesized with improved structural and electrochemical properties may be promising candidates as metal-free and non-expensive electrode materials for the development of supercapacitors or (bio)sensors.

This study focusses on the synthesis procedure as well as the structural and morphological characterisation of B- and N-codoped reduced graphene oxide (BN-rGO) nanostructures. BN-rGO samples are prepared by a two-stage synthesis method. In the first step, a homogenous suspension of GO (2 mg/mL) mixed with different amounts of NH_4BF_4 is hydrothermally treated in a Teflon-lined stainless-steel autoclave at a temperature of 180 °C for 20 hours. In the second step, the resulting materials are thermally annealed in a tube furnace at 850 °C temperature for 30 min under Ar atmosphere. The impact of B- and N-codoping on the morphology and structure of rGO is analysed by scanning electron microscopy (SEM), energy dispersive X-ray (EDX), and Raman spectroscopies. The BN-rGO materials obtained are also studied by measuring nitrogen adsorption-desorption isotherms at 77 K. The Brunauer-Emmett-Teller method is used to calculate the specific surface area of the samples, while the pore size distributions are derived by the Barrett-Joyner-Halenda model.

References

1. S. Kaushal, M. Kaur, N. Kaur, V. Kumari, P. P. Singh, RSC Adv, **10** (2020) 28608.
2. D. Li, X. Duan, H. Sun, J. Kang, H. Zhang, M. O. Tade, S. Wang, Carbon, **115** (2017) 649–658.
3. Gul, M. Yar, A. Ahmed, M. A. Hashmi, K. Ayub, RSC Adv, **12(7)** (2022) 3883–3891.

P 004

Thermoresponsive Properties of Ghitosan-*graft*-poly(N-isopropylacylamide) Copolymers

M. Babelyte[1,*], R. Rutkaite[1], D. Liudvinaviciute[1], L. Peciulyte[1], V. Samaryk[2]
[1]*Department of Polymer Chemistry and Technology, Kaunas University of Technology, Lithuania*
[2]*Department of Organic Chemistry, Lviv Polytechnic National University, Ukraine*
**Corresponding author, e-mail: migle.babelyte@ktu.edu*

One of the most perspective biopolymers is chitosan (CS), because it is biodegradable, biocompatible, inexpensive and also antimicrobial. Moreover, due to the structure and reactive groups its macromolecules can be easily modified *via* grafting reactions. N-isopropylacrylamide (NIPAAm) is one of the most perspective acrylic monomers that can be grafted on chitosan backbone, perhaps due to its thermoresponsive behavior and promising applications in the area of advanced materials, especially in the biomedical field including drug delivery systems [1] and tissue engineering [2].

The aim of the present work was to investigate thermoresponsive behavior of chitosan-*graft*-poly(N-isopropylacrylamide) (CS-*g*-PNIPAAm) copolymers in aqueous solutions. By changing the molar ratio of CS:NIPAAm from 1:0.25 to 1:10 the copolymers with different composition were prepared. Preparation of CS-g-PNIPAAm has been achieved by using initiator potassium persulfate (PPS).

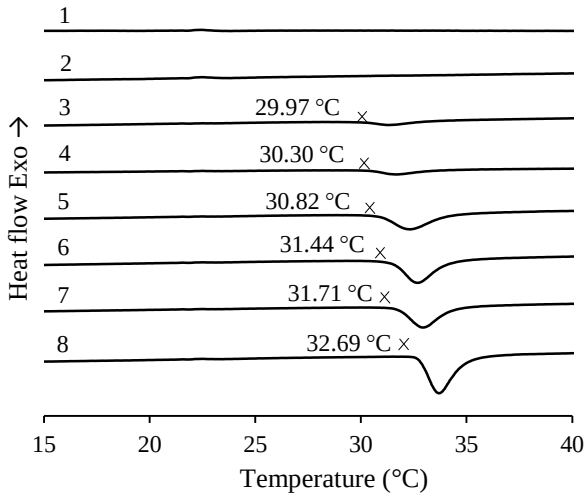

Fig. 1. DSC thermograms showing LCST of the PNIPAAm and synthesized copolymers in aqueous solution: 1 – CS-*g*-PNIPAAm-1; 2 – CS-*g*-PNIPAAm-2; 3 – CS-*g*-PNIPAAm-3; 4 – CS-*g*-PNIPAAm-4; 5 – CS-*g*-PNIPAAm-5; 6 – CS-*g*-PNIPAAm-6; 7 – CS-*g*-PNIPAAm-7; 8 – PNIPAAm

The obtained CS-g-PNIPAAm copolymers were characterized by X-ray, FT-IR, ^{1}H-NMR spectroscopy and other techniques. Moreover, the lower critical solution temperature (LCST) behavior of synthesized copolymers was assessed by cloud point, different scanning calorimetry (DSC) (see Fig. 1.), particle size and fluorescence spectroscopy analysis.

Acknowledgment. The financial support of the Research Council of Lithuania for the project No. S-LU-22-11 in the frame of Lithuanian–Ukrainian Cooperation Programme in the Fields of Research and Technologies is highly acknowledged.

References

1. H., Zhang, H., Zhong, L., Zhang, S., Chen, Y., Zhao and Y., Zhu. Carbohydr. Polym., **77** (2009) 785-790.
2. D., Lu, Z., Liu, M., Zhang, X., Wang, Z., Liu. Biochem. Eng. J., **27** (2006) 336-343.

P 005

Aroma Profile and Total Phenolics of Hop Cones and Pellets

R. Baranauskienė*, P. R. Venskutonis
[1]*Kaunas University of Technology, Radvilėnų rd. 19, 50254 Kaunas, Lithuania*
**Corresponding author, e-mail: renata.baranauskiene@ktu.lt*

Hops are the flowers (cones) of hop plant *Humulus lupulus* L., a member of the Cannabaceae family of flowering plants. Hops are used primarily as a bittering, flavouring, and stabilizing agent in beer; they also valued in herbal medicine for their sedative, anti-inflammatory, antioxidant, antimicrobial, neuroprotective, antitumor, anticarcinogenic and other properties. The mentioned health-beneficial effects are attributed to the structural diversity of secondary metabolites present in hops [1-4].

The aim of this study was to compare chemical composition and aroma profile of hop cones (Lithuanian origin) and commercial pellets (German origin), and determine the total phenolic content (TPC) in EOs (essential oils) and WEs (water extracts). Before analysis cones (C) and pellets (P) were ground by an ultra-centrifugal mill ZM 200 using a 0.5 mm hole size sieve. The aroma compounds of hops C and P were collected by headspace solid phase microextraction and analysed by gas chromatography time-of-flight mass spectrometry (HS-SPME-GC-TOFMS). The EOs were hydrodistilled (HD) in Clevenger type apparatus and further analysed by GC-TOFMS. Proximate composition was determined by the standard AOAC methods, total amount of phenolic compounds (TPC) was determined by Folin–Ciocalteu method.

It was determined that C were characterized by higher moisture and lipid content, while P were of higher ash and dry matter content: C and P consist of moisture (9.9 and 8.2%), ash (6.6 and 7.7%), lipid (13.9 and 10.4%) and vitamin C (9.9 mg%), respectively. The yields of EO varied from 0.18 (C) to 0.41% (P). The residues after HD were separated to liquid and solid fractions by filtration. The liquid fractions were lyophilized resulting in WEs, yielding from 24.9% (C-WE) to 30.8% (P-WE), respectively. Solid residues yielded from 57.5% (P) to 59.8% (C) of the initial hop raw material subjected to HD.

In total, 63 and 54 volatile compounds were released and quantified in C and P headspaces by HS-SPME-GC-TOFMS, accounting up to 75.8% and 83.7% of the total integrated peak area (TIPA), respectively. 2-Methyl-3-buten-2-ol (26.8% and 39.6%) possessing „oily, earthy, herbaceous“ odour notes, 4-methyl-2-pentanone (15.3% and 18.6%) with „fruity, spicy, ethereal“ odour and 3-methyl-2-butanone (9.3% and 16.0%) of „camphor“ odour were the major compounds in C and P, respectively. In the EOs of C and P 92 and 73 volatile components were identified, constituting 78.7% and 69.6% of the TIPA. The main volatile organic compounds identified in C-EO were 2-methylbutyl 2-methyl propionate (13.7%), α-humulene (4.1%), 2-undecanone (3.7%), 2-methylpropyl 2-methyl propionate (3.6%), following by 3-methylbutyl propionate, methyl 4-decanoate, methylgeranate, humulene epoxide II, 6-methyl-5-hepten-2-one, γ-murolene and myrcene. For instance, α-humulene provides "woody" aroma, while 2-undecanone may impart "green", "iris" and "citrus" odour character; humulene epoxides are responsible for „sharp“ and „bitter“ aroma notes in beer. 2-Undecanone (13.8%), 2-tridecanone (7.7%), α-selinene (3.7%), β-eudesmol (3.6%), 6-methyl-5-hepten-2-one (2.1%) were quantitatively major constituents in P-EO.

It was found that TPC was statistically different ($p<0.05$) in all tested fractions and were as follows: P-WE (82.1 ± 0.3 mg GAE/g) > C-WE > P-EO > C-EO (33.0 ± 3.5 mg GAE/g). . In general, the TPC in P were ~1.6 fold higher than in C and constituted 2764.8 ± 109.2 mg GAE/100 g pdw and 1764.7 ± 53.6 mg GAE/100 g pdw, respectively.

This study revealed that hops (both cones, and pellets form) are a good source of bioactive secondary metabolites, including volatile essential oil and non-volatile phenolic compounds, and could be used not only as natural flavourings and antioxidants in food and beverage, but could find applications in pharmaceutical, nutraceutical and cosmetics industries.

References

1. M. Lin, D. Xiang, X. Chen, H. Huo. J. Agric. Food Chem., **67** (2019) 8291-8302.
2. T. Nuutinen. Eur. J. Med. Chem., **157** (2018) 198-228.
   A. Aberl, M. Coelhan. J. Agric. Food Chem., **60** (2012) 2785-2792.
3. M.K. Hrnčič, E. Španinger, I.J. Košir, Ž. Knez, U. Bren. Nutrients, 11 (2019) 257.

P 006

Electronic Excited States of Chlorophylls in Photosynthetic Complex CP29

S. Barysaitė[1,2*], A. Gelzinis[1,2], J. Chmeliov[1,2], L. Valkunas[1,2]
[1]Faculty of Physics, Vilnius University, Sauletekio al. 9, LT-10222 Vilnius, Lithuania
[2]Department of Molecular Compound Physics, Centre for Physical Sciences and Technology, Sauletekio al. 3, LT-10257 Vilnius, Lithuania
**sandra.barysaite@ff.stud.vu.lt*

Light harvesting – the first step of photosynthesis – is carried out by photosystems I and II (PSI and PSII) that are located in the thylakoid membrane of chloroplasts. PSII oxidizes water and produces oxygen molecules that can react with the excited triplet state of chlorophyll and generate singlet oxygen which can cause photo-oxidative damage to PSII. For this reason, plants have developed protective mechanisms such as non-photochemical quenching (NPQ) [1]. Quenching sites have been identified in LHCII and CP29 antenna complexes of PSII. NPQ in LHCII is thought to be correlated with Chl–Chl charge-transfer (CT) states [2]; this could also be the case for CP29 because it is positioned between the outer antenna complexes and the reaction center.

In this work, the high resolution crystal structure of spinach photosynthetic complex CP29 [3] was chosen for the identification of Chl–Chl CT states in CP29. CT states can form between strongly interacting chlorophylls, so only those chlorophyll dimers with distances less than 10 Å between chlorophylls were used in calculations. The geometries of chlorophylls forming the dimers were optimized in vacuum using density functional theory (DFT). In all calculations performed in this work, the phytyl group in chlorophyll structure was changed to methyl group. The excited state energy spectra and related parameter values for each dimer were calculated using time-dependent density functional theory (TD-DFT).

Nine CT states were identified in five of the six analysed chlorophyll dimers and are presented in Table 1 together with the energy values. CT states with the lowest energies could possibly be related to NPQ and other processes in PSII; the lowest energy CT state was identified in dimer *b*614–*a*613. The results were compared to the experimental data in Ref. [4], where time-resolved fluorescence was measured in CP29 and its knock-out mutants, i.e. CP29 lacking either chlorophyll *a*612 or *a*603; these chlorophylls form strongly coupled dimers *a*611–*a*612 and *a*603–*a*609 that were analyzed in this work.

Table 1. Excited states S_n corresponding to the identified CT states in dimers and their energies in ascending order.

Chl–Chl dimer	S_n	Energy, cm^{-1}
*b*614–*a*613	S_5	22565
*b*606–*a*604	S_5	22780
*a*611–*a*612	S_5	23070
*a*611–*a*615	S_5	24276
*a*603–*a*609	S_5	24417
*a*603–*a*609	S_6	24672
*a*611–*a*612	S_6	25330
*a*611–*a*615	S_6	25394
*b*606–*a*604	S_6	25459

References

1. P. Müller, X.-P. Li, K. K. Niyogi, Plant Physiology **125**, 1558–1566 (2001)
2. Y. Miloslavina, et al., FEBS Letters **582**, 3625–3631 (2008)
3. X. Pan, et al., Nature Structural & Molecular Biology **18**, 309–315 (2011)
4. V. Mascoli, et al., Chemical Science **11**, 5697–5709 (2020)

P 007

Synthesis and Evaluation of Optical Properties of New Conjugated 3*H*-Indole Moiety Possessing Systems

M. R. Bartkus[1*], G. Varvuolytė[2], A. Žukauskaitė[3], V. Martynaitis[2], R. Tamulienė[1], A. Šačkus[1,2], N. Kleizienė[1,2]

[1]*Institute of Synthetic Chemistry, Kaunas University of Technology, K. Baršausko g. 59, Kaunas LT-51423, Lithuania*

[2]*Department of Organic Chemistry, Kaunas University of Technology, Radvilėnų pl. 19, Kaunas LT-50254, Lithuania*

[3]*Department of Chemical Biology, Palacký University, Šlechtitelů 27, CZ-78371, Olomouc, Czech Republic*

**martynas.bartkus@ktu.lt*

3*H*-Indole derivatives are important in medicinal chemistry because they can have a wide range of properties: biological activity (e.g. antimitotic agent) [1], fluorescence (e.g. fluorescent probes for cell imaging) [2], photodynamic activity (e.g. photosensitizers for photodynamic therapy) [3] and other. A wide array of suitable optical and biological properties possessing photosensitizers are based on cyanine dye structure containing 3*H*-indole moiety [4]. Although many studies have been performed with these compounds, their number in clinical use is scarce. Therefore, synthesis of new 3*H*-indole derivatives remains of high interest.

In this work, a series of new conjugated 3*H*-indole moiety possessing compounds were synthesized employing Suzuki cross-coupling and Knoevenagel condensation reactions. Subsequent alkylation of the final compounds afforded 3*H*-indolium iodide salts. Structures of new compounds were confirmed by 1D, 2D NMR, HRMS and FT-IR spectroscopic data and their optical properties were thoroughly investigated.

Upon investigation of optical properties of newly prepared compounds in aqueous solutions, it was observed that the compounds had weak fluorescence, however the values of their absorption and emission peaks were observed in the visible part of electromagnetic spectrum. Absorption peaks were in the range of 383–477 nm, whereas emission peaks were in the range of 504–616 nm. In addition, the Stokes shifts of the tested compounds were quite large (71–233 nm). Interestingly, 3*H*-indolium salts did not produced fluorescence under excitation with UV light.

Overall, presented results show, that conjugated 3*H*-indole moiety possessing systems are easily obtainable and could be used for further investigation of their biological activity and applicability as fluorescent probes.

References

1. J. Zheng, et al. Eur. J. Med. Chem. **65** (2013), 158–167.
2. C. Benitez-Martin, et al. ACS Sens. **5** (2020), 1068–1074.
3. X. Tan, et al. Biomaterials. **33** (2012), 2230–2239.
4. N. Lange, et al. Pharmaceutics. **13** (2021), 818.

P 008

Multifunctional Wood – Properties of $GdPO_4 \cdot H_2O:Eu^{3+}$ Doped Wood

M. Baublytė[1*], D. Sokol[1], R. Skaudžius[1]

[1]*Department of Inorganic Chemistry, Faculty of Chemistry, Vilnius University, Naugarduko St. 24, 03225 Vilnius, Lithuania*

**Corresponding author, e-mail:monika.baublyte@mb.vu.lt*

Wood is one of the essential construction materials humankind has ever come across, owing to its versatility, abundance in nature, and environmental friendliness. It has various types and a remarkably diverse range of modifications and applications. In recent years inorganic materials doped wood became an attractive solution to challenge wood's multifunctionality and acquire new functions that could modernize wood exploitation [1,2]. Thus, this work characterizes wood doped with $GdPO_4 \cdot H_2O:Eu^{3+}$ nanoparticles and discus application perspectives.

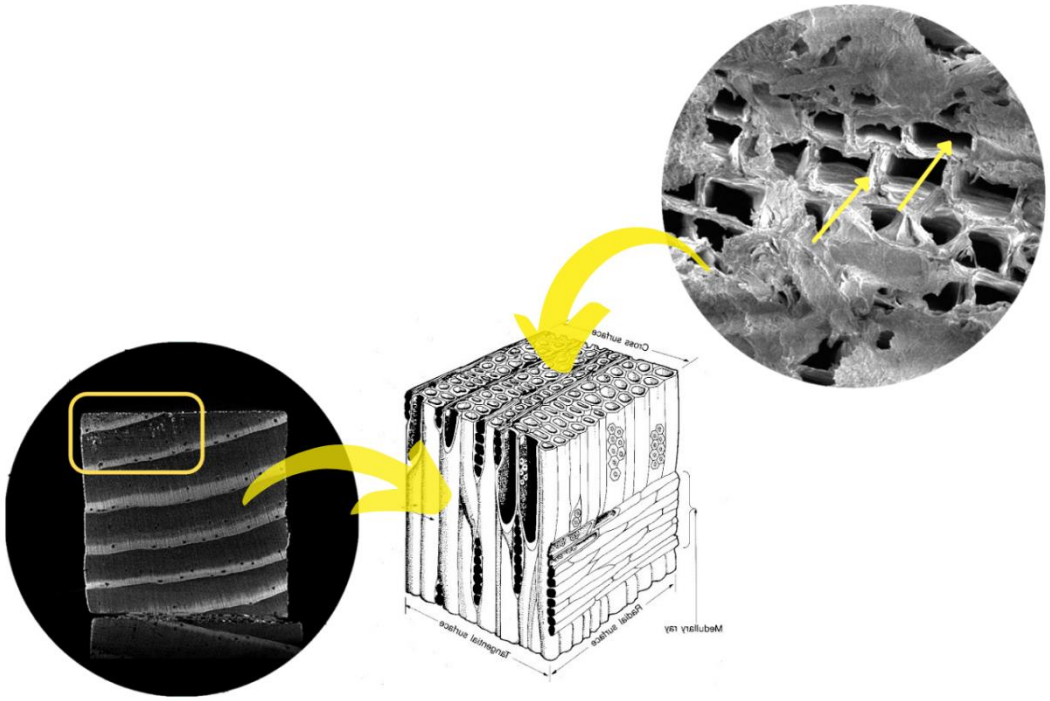

Fig. 1. Wood modification

References

1. H. Khajuria, J. Ladol, S. Khajuria, M. S. Shah, and H. N. Sheikh, Surfactant mediated hydrothermal synthesis, characterization and luminescent properties of GdPO4: Ce3+/Tb3+ @ GdPO4 core shell nanorods, Mater. Res. Bull., 80 (2016) 150–158.
2. K. M. Heffernan, N. L. Ross, E. C. Spencer, and L. A. Boatner, The structural response of gadolinium phosphate to pressure, J. Solid State Chem., 241 (2016) 180–186.A.A. Autor, B. Autor, The Chemical Synthesis. Wiley & Sons, New York, 1999.

P 009

Wide Bandgap Lead Perovskite Solar Cells with Monomolecular Layer from Viewpoint of PTAA Band Bending

R. Beresneviciute[1*], H. Bi[2], J. Liu[2], G. Kapil[2], D. Tavgeniene[1], Z. Zhang[2], L. Wang[2], C. Ding[2], S. R. Sahamir[2], Y. Sanehira[2], A. K. Baranwal[2], K. Takeshi[2], D. Wang[2], Y. Wei[2], Y. Yang[2], D. W. Kang[3], S. Grigalevicius[1], Q. Shen[2], S. Hayase[2]

[1]Department of Polymers Chemistry and Technology, Kaunas University of Technology, Radvilenu Plentas 19, LT-50254, Lithuania

[2]i-Powered Energy System Research Center, The University of Electro-Communications, 1-5-1 Chofugaoka, Chofu, Tokyo, 182-8585, Japan

[3]School of Energy Systems Engineering, Chung-Ang University, Seoul, 06974, Republic of Corea

**raminta.beresneviciute@ktu.lt*

Recent years have reached intense research and development efforts of perovskite solar cells (PSCs), due to their growing efficiency [1]. Self-assembled mono-molecular layers have been proven to be useful as the HTL for high-efficiency Pb-PVK PSCs.[2] The molecules for these monolayers have p-type group/linker group/anchor groups. The molecules with phosphonic acids as the anchor group (PACz) are widely used in PSCs.

Poly[bis(4-phenyl) (2,4,6-trimethylphenyl) amine] (PTAA) is commonly employed as a hole transporting layer for $FA_{0.8}Cs_{0.2}PbI_{1.8}Br_{1.2}$. However, since the hydrophobic surface sometimes suppressed the crystal growth of the $FA_{0.8}Cs_{0.2}PbI_{1.8}Br_{1.2}$ layer and the Fermi level of PTAA is not well matched with that of perovskite film, the efficiency of the WBG Pb-PVK PSCs consisting of PTAA was not high.

In this study, a series of PACz-based SAMs with different functional groups (**I-3PACz, 9p-3PACz, 2M3P-3PACz**) were synthesized to modify the interface between PTAA and perovskite film. The structures of compounds are shown in Figure 1.

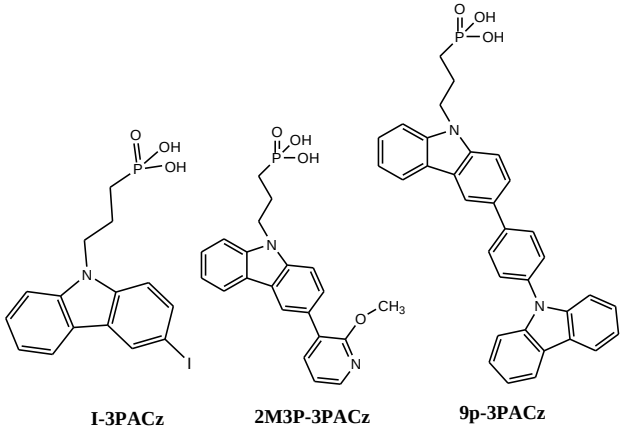

Fig. 1. Structures of compounds **I-3PACz, 9p-3PACz** and **2M3P-3PACz**

The experimental results showed that molecules with more bulky substituted groups (**9p-3PACz**) achieved the best results. After the **9p-3PACz** modification, not only the crystallization of the perovskite thin film improved but also the defect density of the perovskite film reduced. The energy-band bending due to SAMs molecular polarity also reduces the carrier transport and extraction resistance. Also, PTAA/9p-3PACz-based PSCs achieved a high PCE of 16.52 % with a bandgap of 1.77 eV.

Acknowledgements. This research was conducted in the frame of the project with support grant S-LJB-22-2 from Research Council of Lithuania

References

1. P. Yan, D. Yang, H. Wang, S. Yang, Z. Ge. Energy Environ. Sci., **15**, (2022), 3630-3669.
2. F. Ali, C. Roldan-Carmona, M. Sohail, M.K. Nazeeruddin.. Advanced Energy Materials, 2020.

P 010

3-(N,N-Diphenylamino)carbazole Acceptor Containing Bipolar Derivatives as TADF Emitters for OLED Devices

R. Beresneviciute[1*], D. Tavgeniene[2], D. Blazevicius[1], G. Krucaite[1], B. Achramovic[1], S. S. Swayamprabha[2], J.-H. Jou[2], S. Grigalevicius[1]

[1]*Department of Polymer Chemistry and Technology, Kaunas University of Technology, Radvilenu plentas 19, LT 50254, Kaunas, Lithuania*

[2] *Department of Materials Science and Engineering, National Tsing-Hua University, No. 101, Kaunghu Rd. Hsin-Chu, 30013, Taiwan*

**raminta.beresneviciute@ktu.lt*

Nowadays, there has been a lot of interest in third-generation organic light-emitting diodes characterized by thermally activated delayed fluorescence (TADF) [1]. Aromatic amine-based molecular glasses belong to the group of charge-transporting and light emitting layer derivatives and are well known in OLEDs field applications [2]. The main advantages of the electroactive low molar mass compounds against polymers are their low melt viscosity, possibility of purification by chromatographic methods and large variety of synthesis methods [3].

In this study, electroactive bipolar derivatives containing 3-(N,N-diphenylamino)-9H-carbazole as donor and (bis)phenylsulfone or benzophenone as acceptor fragments were synthesized and characterized. The structures of materials **1-3** are shown in Figure 1.

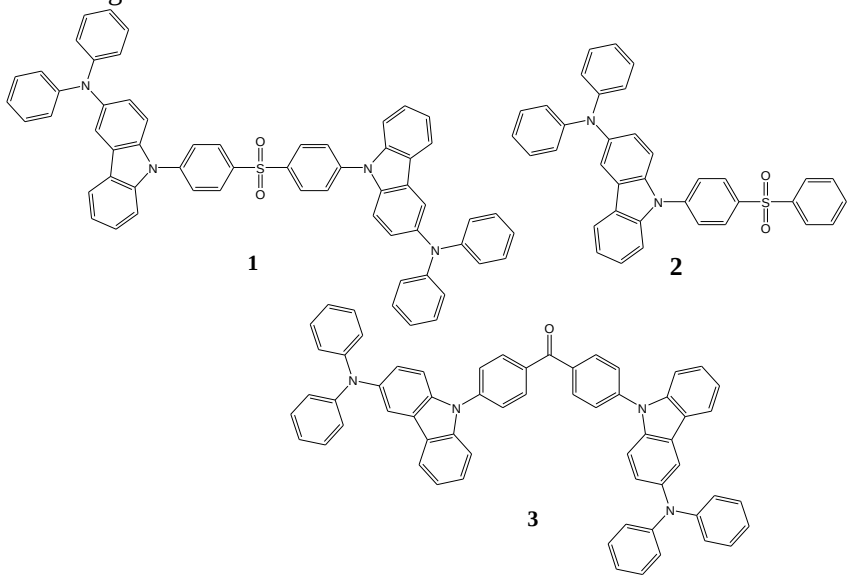

Fig. 1. Structures of compounds **1-3**

The compounds, which were well soluble in common organic solvents, were tested as emitting materials dispersed in CBP host. The OLED using the emitter **1** demonstrated low turn-on voltage 3 V, maximum brightness exceeding 2630 cd/m^2, current efficiency of 3,2 cd/A, power efficiency of 2,2 lm/W and EQE exceeding 1,7 % at 100 cd/m^2.

Acknowledgements. This research was conducted in the frame of the project with support from the Research Council of Lithuania (grant No. S-LLT-19-2).

References

1. T. Huang, W. Jang, L. Duan. J. Mater. C. **6** (2018) 5577-5596.
2. M. Korzec et al., J. Mater. C. **55** (2020) 3812-3832.
3. V. Vaitkeviciene et al., European Polymer Journal, 42 (2006) 2254-2260.

P 011

Central Benzophenone Fragment Having Solution Processable Derivatives as Bipolar Hosts for Green TADF OLEDs

D. Blaževičius[1*], R. Beresnevičiūtė[1], G. Kručaite[1], D. Tavgenienė[1], S. Grigalevičius[1], M. R. Nagar[2], C. T. Hao[2], J.-H. Jou[2], K. Kumar[3], S. Banik[4]

[1]Department of Polymer Chemistry and Technology, Kaunas University of Technology, Radvilenu Plentas 19, LT50254, Kaunas, Lithuania

[2]Department of Materials Science and Engineering, National Tsing Hua University, Taiwan

[3]School of Chemical Sciences, Indian Institute of Technology, Mandi, HP, India

[4]Department of Chemistry, School of Chemical and Biotechnology, SASTRA Deemed University, Thanjavur 613401, Tamil Nadu, India.

**Corresponding author, e-mail: dovydas.blazevicius@ktu.lt*

Solution processable bipolar materials have been reported as emitters and host materials in organic light emitting diodes (OLEDs) [1]. These materials exhibited a thermally activated delayed fluorescence nature and have the capability of harvesting triplet excitons from excited triplet to singlet states by reverse intersystem crossing [2]. Thus, the TADF materials based organic LEDs have reached an internal quantum efficiency of nearly 100%. Herein, we have successfully designed and synthesized solution-processable bipolar carbazole-benzophenone derivatives as host materials, i.e. 4,4'-di(3-phenylcarbazol-9-yl)benzophenone (BPBCzO) and 4,4'-di[3-[4-(carbazol-9-yl)phenyl] carbazol-9-y] benzophenone (BCzBCzO). Structures of objective materials are shown in Figure 1.

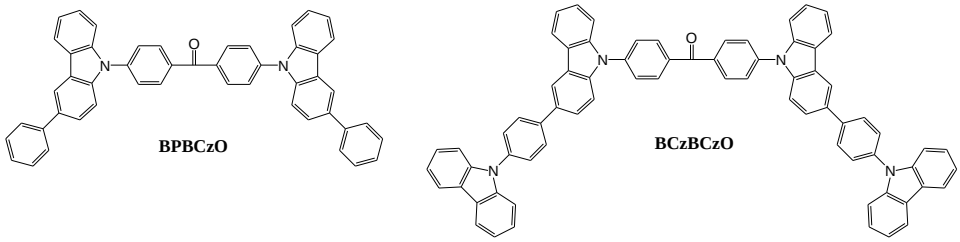

Fig. 1. Synthesis of objective benzophenone-based materials

These newly synthesized hosts exhibited high-triplet energies, balanced charge-transporting properties, suitable molecular orbital energy levels, good thermal stability, and good solubility, which are required to realize green TADF based organic LEDs. Initially, we fabricated two different types of TADF organic LEDs using these hosts and commercially available guest 4CzIPN as a green dopant and compared their device characteristics. A green TADF based organic LED employing BPBCzO host displayed excellent performance with a maximum external quantum efficiency (EQE, current efficacy (CE), and power efficacy (PE) as high as 23.2 %, 70.7 cd/A, and 55.6 lm/W, respectively. In particular, over 90% of EQE was reserved (EQE of 21.3%) at the practical luminance of 1,000 cd/m^2, which is advantageous for display technology. At last, green OLED was also fabricated with a cross-linkable hole transport material 3,6-bis(4-vinylphenyl)-9-ethylcarbazole and realized PE of 63.6 lm/W with EQE of 25.3%, which could be very effective for lighting and display devices. These excellent outcomes demonstrate the big potential of the carbazole-benzophenone derivatives as host materials for next-generation solution-processable display and lighting technologies.

Aknowledgements

We acknowledge support from the Research Council of Lithuania (grant No. S-MIP-22-84).

References

1. M. Godumala, J. Hwang, H. Kang, J.-E. Jeong, A. K. Harit, M. J. Cho, H. Y. Woo, S. Park, D. H. Choi, ACS Appl. Mater. Interfaces **12** (2020) 35300-35310.
2. N. Ikeda, S. Oda, R. Matsumoto, M. Yoshioka, D. Fukushima, K. Yoshiura, N. Yasuda, T. Hatakeyama, Adv. Mater. **32** (2020) 2004072.

P 012

Polypyrrole Modifications with Methylene Blue

R. Boguzaite*[1], V. Ratautaite[1], G. Pilvenyte[1], E. Brazys[2], A. Ramanavicius[1,2]

[1]Center for Physical Sciences and Technology, Department of Nanotechnology, Sauletekio av. 3, Vilnius LT-10257, Lithuania
[2]Vilnius University, Faculty of Chemistry and Geosciences, Institute of Chemistry, Naugarduko str. 24, Vilnius LT 03225, Lithuania
raimonda.boguzaite@ftmc.lt

Polypyrrole (Ppy) is one of the conducting polymers that has been studied the most and is used to create various kinds of sensors [1]. Conjugated polymers can exhibit electrochromic properties due to changes in the π-π conjugated electronic system and the ability to participate in electrochemical oxidation and reduction [2,3].

Ppy and MB may be combined to provide electrochromic coatings with superior characteristics [4,5]. Furthermore, dopants can significantly alter the conductivity of Ppy. [6] Saccharides may be one of those dopants that will have a beneficial effect on surface modification. [7]

This study aimed to investigate the effects of various saccharides on the electrochromic characteristics while simultaneously co-depositing the Ppy-PMB layer on the ITO electrode in the presence of three saccharides (lactose, sucrose, and heparin). A solution comprising 50 mM pyrrole, 10 mM methylene blue, and one of the doping substances (lactose, sucrose, or heparin) was used for the electrochemical deposition (by using cyclic voltammetry) of the polymer layer.

AFM and SEM techniques were used to analyse the surface morphology. The surface roughness of Ppy-PMB layers was moderately affected by the saccharides utilized in this work. By adjusting the potential and pH of the BRB solution, the Ppy-PMB layers were investigated.

The best conductivity characteristics and quickest bleaching and colouration times were found in the $(Ppy\text{-}PMB)_{Suc}$ layer.

References

1. R. Celiesiute, A. Ramanaviciene, M. Gicevicius, A. Ramanavicius, Electrochromic Sensors Based on Conducting Polymers, Metal Oxides, and Coordination Complexes, Critical Reviews in Analytical Chemistry, Vol. 49, Issue 3, 195-208, 2019.
2. A.A. Argun, P.-H. Aubert, B.C. Thompson, I. Schwendeman, C.L. Gaupp, J. Hwang, N.J. Pinto, D.B. Tanner, A.G. MacDiarmid, J.R. Reynolds, Multicolored electrochromism in polymers: structures and devices, Chem. Mater. 16, 4401–4412, 2004.
3. V. Ratautaite, R. Boguzaite, M.B. Mickeviciute, L. Mikoliunaite, U. Samukaite-Bubniene, A. Ramanavicius, A. Ramanaviciene, Evaluation of Electrochromic Properties of Polypyrrole/Poly(Methylene Blue) Layer Doped by Polysaccharides. Sensors, 22, 232, 2022.
4. P. Moarref, M. Pishvaei, A. Soleimani-Gorgani, F. Najafi, Synthesis of polypyrrole/indium tin oxide nanocomposites via miniemulsion polymerization, Des. Monomers Polym. 19, 138–144, 2016.
5. R. Boguzaite, V. Ratautaite, L. Mikoliunaite, V. Pudzaitis, A. Ramanaviciene, A. Ramanavicius, Towards analytical application of electrochromic polypyrrole layers modified by phenothiazine derivatives. J. Electroanal. Chem., 886, 115132, 2021.
6. J.M. Fonner, C.E. Schmidt, P. Ren, A combined molecular dynamics and experimental study of doped polypyrrole. Polymer, 51, 4985–4993, 2010.
7. J. Serra Moreno, S. Panero, S. Materazzi, A. Martinelli, M.G. Sabbieti, D. Agas, G. Materazzi, Polypyrrole-polysaccharide thin films characteristics: Electrosynthesis and biological properties. J. Biomed. Mater. Res. A, 88A, 832–840, 2009

P 013

Evaluation of the Interaction Between SARS-CoV-2 Spike Glycoproteins and the Molecularly Imprinted Polypyrrole

E. Brazys[1*], V. Ratautaitė[2], R. Bogužaitė[2], A. Ramanavičius[1,2]

[1]Department of Physical Chemistry, Institute of Chemistry, Faculty of Chemistry and Geosciences, Vilnius University, Naugarduko str. 24, Vilnius LT-03225, Lithuania

[2]Department of Nanotechnology, State Research Institute Center for Physical Sciences and Technology, Sauletekio av. 3, Vilnius LT-10257, Lithuania

**Corresponding author, e-mail: ernestas.brazys@chgf.stud.vu.lt*

Severe acute respiratory syndrome coronavirus 2 (SARS-CoV-2) is a virus that causes COVID-19 disease. The COVID-19 pandemic began in late 2019. This pandemic brought a lot of changes to the scientific world too. The extremely rapid spread of the disease in the communities demanded new analytical tools for the identification of the virus. In this study, SARS-CoV-2 spike glycoprotein was chosen as a template for the developed sensor. The electrochemical SARS-CoV-2 virus protein sensor based on the molecular imprinting technique was developed in this research.

Generally, molecular imprinting is carried out by chemical or electrochemical polymerization from a mixture of functional monomers and template molecules. The removal of the template is then performed, which creates the binding sites in the structure of the polymer, which are specific or complementary to the template molecules [1]. This property can be applied in developing sensors for detecting biological and chemical molecules [2].

In this research, the SARS-CoV-2 spike glycoprotein imprinted polypyrrole-based (MIP-Ppy) sensor was developed [3]. The pre-polymeric mixture consisted of 0.5 M pyrrole as a monomer and 50 µg/mL of SARS-CoV-2 spike glycoprotein as a template in PBS solution, pH 7.4. The polymeric film was deposited electrochemically onto the surface of a platinum electrode by a sequence of potential pulses. The template molecules were removed by washing the polymer in 0.05 M H_2SO_4 solution for 10 min. In comparison, an electrode was modified with a non-imprinted polypyrrole layer (NIP-Ppy). The characteristics of both MIP-Ppy and NIP-Ppy were assessed by pulsed amperometric detection. The interaction between SARS-CoV-2 spike glycoproteins and MIP-Ppy was evaluated by the Anson plot-based calculations.

The obtained results display that SARS-CoV-2 glycoprotein interaction is stronger with MIP-Ppy film than with NIP-Ppy film.

Acknowledgement: This project has received funding from the Research Council of Lithuania (LMTLT), GILIBERT 2021 program agreement No S-LZ-21–4 and was co-founded by Campus France grant No. 46593RA (PHC GILIBERT 2021).

References

1. S. A. Piletsky, A. P. F. Turner. Electrochemical Sensors based on Molecularly Imprinted Polymers. *Electroanalysis*, **14**(5), 317–323 (2002).
2. L. Uzun, A. P. F. Turner. Molecularly-imprinted polymer sensors: realising their potential. *Biosensors and Bioelectronics*, **76**(1), 131–144 (2016).
3. V. Ratautaite, R. Boguzaite, E. Brazys, D. Plausinaitis, S. Ramanvicius, U. Samukaite-Bubniene, M. Bechelany, A. Ramanavicius. Evaluation of the interaction between SARS-CoV-2 spike glycoproteins and the molecularly imprinted polypyrrole. Talanta, **253** (2023).

P 014

Improvement of Luminescent Properties of $GdPO_4$ Doped with Europium

D. Budrevičius*, A. Pakalniškis, A. Kareiva, R. Skaudžius

Institute of Chemistry, Faculty of Chemistry and Geosciences, Vilnius University, Naugarduko 24, LT-03225 Vilnius, Lithuania

**Corresponding author, e-mail:Darrius.budrevicius@chgf.vu.lt*

Due to the strong paramagnetic nature of gadolinium, Gd-based materials are commonly used in medicine as a magnetic resonance contrast agents and in other areas [1,2]. While MRI is a powerful technique used for medical diagnosis, still new ways of improving the imaging are needed. To improve the quality of the MRI, materials are being developed and are already being used to obtain T1 and T2 MRI together, as single mode MRI does not always provide sufficient image quality. Multimodal materials suitable for bioimaging and MRI are also being developed. One such way is to combine the MRI with luminescence measurements. Europium is quite commonly used as a dopant in the preparation of various compounds as it exhibits excellent luminescence properties, even when it is introduced even at small concentrations. Additionally, europium is suitable for the doping of $GdPO_4$ nanoparticles because it results in emission at ~577 nm, ~590 nm, ~615 nm, ~650 and ~700 nm wavelengths and when considering the interest of the compounds for bioimaging it is quite desirable, since part of the emission, in this case exist in a so-called first biological window, and is absorbed by the tissue to a much lesser extent [3]. Thus, Eu-doped $GdPO_4$ nanoparticles attract a lot of attention as an efficient single-phase multimodal nanoprobe with both luminescent and magnetic properties [4]. However, the Europium concentration further optimization and investigation is required. This is due to the fact that if the concentration of light emitting dopant introduced into the crystal structure is too large concentration quenching is often observed. In the case of europium, this boundary can change drastically depending on the initial host matrix. Furthermore, irrespective of the crystalline environment, the Eu^{3+} ion usually emits red light under UV excitation, however, there have been reports that in certain situations weak emission bands can also be obtained in the green and sometimes blue range [5-8].

Hexagonal gadolinium phosphate hydrate doped with different europium amounts ($Gd_{1-x}PO_4:Eu_x \cdot H_2O$; x = 0.01, 0.05, 0.10, 0.15 and 0.20) was synthesized by the hydrothermal synthesis method and the obtained samples were analyzed giving the optimal dopant concentration. All of the synthesized compounds were analyzed by X-ray diffraction in order to investigate their crystal structure. SEM analysis was used to characterize the morphology of synthesized particles. The luminescence properties were also characterized and discussed in detail.

References

1. Y. Huang, P.O. Boamah, J. Gong, Q. Zhang, M. Hua, Y. Ye, Gd (III) complex conjugate of low-molecular-weight chitosan as a contrast agent for magnetic resonance/fluorescence dual-modal imaging, Carbohydr. Polym. 143 (2016) 288–295.
2. T. Jahanbin, H. Sauriat-Dorizon, P. Spearman, S. Benderbous, H. Korri-Youssoufi, Development of Gd(III) porphyrin-conjugated chitosan nanoparticles as contrast agents for magnetic resonance imaging, Mater. Sci. Eng. C. 52 (2015) 325–332A.A. Autor, B. Autor, The Chemical Synthesis. Wiley & Sons, New York, 1999.
3. S. Golovynskyi, I. Golovynska, L.I. Stepanova, O.I. Datsenko, L. Liu, J. Qu, T.Y. Ohulchanskyy, Optical windows for head tissues in near-infrared and short-wave infrared regions: Approaching transcranial light applications, J. Biophotonics. 11 (2018).
4. W. Ren, G. Tian, L. Zhou, W. Yin, L. Yan, S. Jin, Y. Zu, S. Li, Z. Gu, Y. Zhao, Lanthanide ion-doped $GdPO_4$ nanorods with dual-modal bio-optical and magnetic resonance imaging properties, Nanoscale. 4 (2012) 3754–3760.
5. X.Q. Guo, Y. Yan, H.C. Zhang, Y. Han, J.J. Song, GdPO4:Er3+/Yb3+ nanorods: Hydrothermal synthesis and sensitivity of green emission to Yb3+ concentration, Ceram. Int. 42 (2016) 8738–8743.
6. D. Chen, Y. Yu, P. Huang, H. Lin, Z. Shan, Y. Wang, Color-tunable luminescence of Eu3+ in LaF3 embedded nanocomposite for light emitting diode, Acta Mater. 58 (2010) 3035–3041.
7. H. Lin, S. Tanabe, L. Lin, D.L. Yang, K. Liu, W.H. Wong, J.Y. Yu, E.Y.B. Pun, Infrequent blue and green emission transitions from Eu3+ in heavy metal tellurite glasses with low phonon energy, Phys. Lett. Sect. A Gen. At. Solid State Phys. 358 (2006) 474–477.
8. M. Dejneka, E. Snitzer, R.E. Riman, Blue, green and red fluorescence and energy transfer of Eu3+ in fluoride glasses, J. Lumin. 65 (1995) 227–245.

P 015

Biomass Fly Ash-Based Alkali-Activated Materials

C. Zhu[1,2,*], I. Pundienė[1], J. Pranckevičienė[1], M. Kligys[1]

[1]Institute of Building Materials, Vilnius Gediminas Technical University, Linkmenu st. 28, 08217 Vilnius, Lithuania

[2] College of Civil Engineering, Yancheng Institute of Technology, Xiwang ave. 1, 224051 Yancheng, China

**Corresponding author, e-mail: chengjie.zhu@vilniustech.lt*

Abstract: Biomass fly ash (BFA), a by-product of wood biomass energy production, is difficult to utilize due to its low inorganic content. This study explored the possibility of using untreated BFA in alkali-activated materials (AAM). The used alkaline activator solution (AAS) is a mixture of Na_2CO_3 solution and Na_2SiO_3 solution with less alkalinity. This article systematically examined how the Na_2CO_3/Na_2SiO_3 (SC/SS) ratio of the AAS affected the structure formation, product synthesis, and physical-mechanical properties of BFA-based AAM pastes cured at 40 °C. Increasing the SC/SS ratio of the AAS from 0.40 to 1.20 increased the density (28 d, from 1287 to 1359 kg/m^3) and compressive strength (28 d, from 2.36 to 3.97 MPa) of the AAM samples. The AAM sample with the lowest SC/SS ratio has the longest setting time and the highest water absorption. As the SC/SS ratio rose, gaylussite and C-S-H were synthesized in the samples, contributing to the compressive strength of the AAM pastes with higher SC/SS ratio, according to XRD analyses. The results of this study can help the development of eco-friendly BFA-based AAM.

Keywords: biomass fly ash; alkali-activated materials; Na_2CO_3/Na_2SiO_3 ratio; structure formation; compressive strength

P 016

Vibration Application for Porous AAO Membrane Synthesis

U. Cigane, A. Palevicius, G. Janusas
Faculty of Mechanical Engineering and Design, Kaunas University of Technology, Studentu str. 56, LT-51424 Kaunas, Lithuania
**Corresponding author, e-mail: urte.cigane@ktu.lt*

Researchers have made many achievements in the field of porous AAO membranes, making it an interesting research topic due to its high versatility and applications in various fields, such as filtration [1], sensors [2], tissue engineering [3], etc. Also, various anodization conditions were established using different anodization parameters to obtain nanopores with different geometries. For example, anodization has been performed using different types of acidic electrolytes, by varying experimental conditions such as anodization temperature, applied anodization potential, current, etc. According to these parameters, the pore size, the distance between the pores and the thickness of the AAO membranes were determined. However, the effect of vibration on the pore geometry has not been analyzed yet. Therefore, a well-known two-step anodization process (using 0.3 M oxalic acid at a constant temperature of 5 °C and a constant voltage of 60 V), in which vibrations are applied to investigate the effect of vibration on the pore geometry of AAO is presented in this paper.

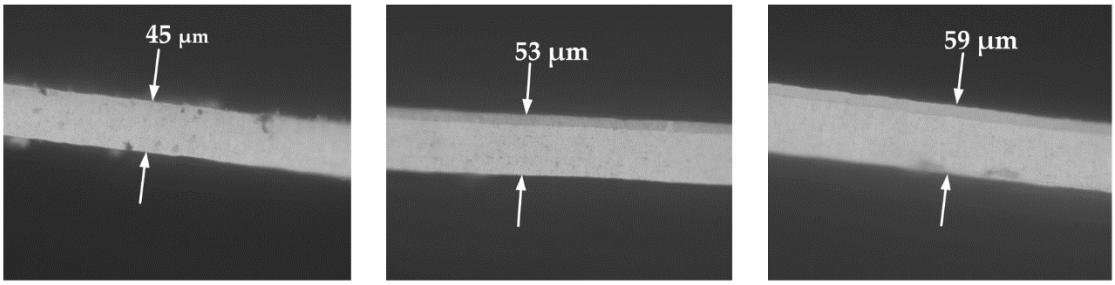

(a) (b) (c)

Fig. 1. Images of the AAO membrane thickness when the membranes were fabricated under different anodization conditions: (a) no frequency excitation, (b) excitation at 20 kHz, (c) excitation at 40 kHz.

Parameter	Pore diameter (nm)	Interpore distance (nm)	Thickness (μm)
No excitation	104 ± 10	143 ± 10	45 ± 0.5
Excitation frequency 20 kHz	103 ± 10	140 ± 10	53 ± 0.5
Excitation frequency 40 kHz	105 ± 10	140 ± 10	59 ± 0.5

Table 1. Pore diameter, interpore distance, and thickness of AAO nanoporous membranes.

Scanning electron microscopy (SEM) and energy dispersive spectroscopy (EDS) were used to determine the nanopore morphology and surface chemical composition of AAO membranes after two-step anodization process in which vibrations were applied. EDS analysis showed that aluminum and oxygen elements predominate. This confirmed the formation of Al_2O_3. After EDS analysis, it can be concluded that the frequency did not affect the chemical composition of the membrane. On the other hand, the thickness of the membrane increased by 17.8% at 20 kHz, and 31.1% at 40 kHz. Besides, the pore diameter and distance between pores remained unchanged.

References

1. C.W. Hun, Y.J. Chiu, Z. Luo, C.C. Chen, S.H. Chen, Appl. Sci., **8** (2018) 1055.
2. S. Mondal, S.J. Kim, C.G. Choi, ACS Appl. Mater. Interfaces **12** (2020) 17029–17038.
3. E. Davoodi, M. Zhianmanesh, H. Montazerian, A.S. Milani, M. Hoorfar, J Mater Sci: Mater Med **31** (2020) 60.

P 017

Passivating Defects of Perovskite Solar Cells with Functional Donor-Acceptor-Donor Type Hole Transporting Materials

Š. Daškevičiūtė-Gegužienė[1*], Y. Zhang[2], K. Rakštys[1], M. Daškevičienė[1], V. Jankauskas[3], M. K. Nazeeruddin[2], V. Getautis[1]

[1]Department of Organic Chemistry, Kaunas University of Technology, Lithuania
[2]Group for Molecular Engineering of Functional Material, École Polytechnique Fédérale de Lausanne, Switzerland
[3]Institute of Chemical Physics, Vilnius University, Lithuania
**Corresponding author, e-mail: sarune.daskeviciute@ktu.lt*

Over the recent years, organic-inorganic hybrid perovskite solar cells (PSCs) have been attracting a massive worldwide attention due to their low cost and facile fabrication. HTM is one of the quintessential components required for the efficient and stable PSC devices. The hunt is now on for new organic semiconductors that are prepared by simple, cost-effective, and green chemistry without sacrificing the efficiency [1].

In this study, a series of donor–acceptor–donor (D-A-D) type small molecules based on the fluorene and diphenylethenyl enamine units, which are distinguished by different acceptors, as hole transporting materials (HTMs) for perovskite solar cells is presented. The incorporation of the malononitrile acceptor units is found to be beneficial for not only carrier transportation but also defects passivation via Pb–N interactions.

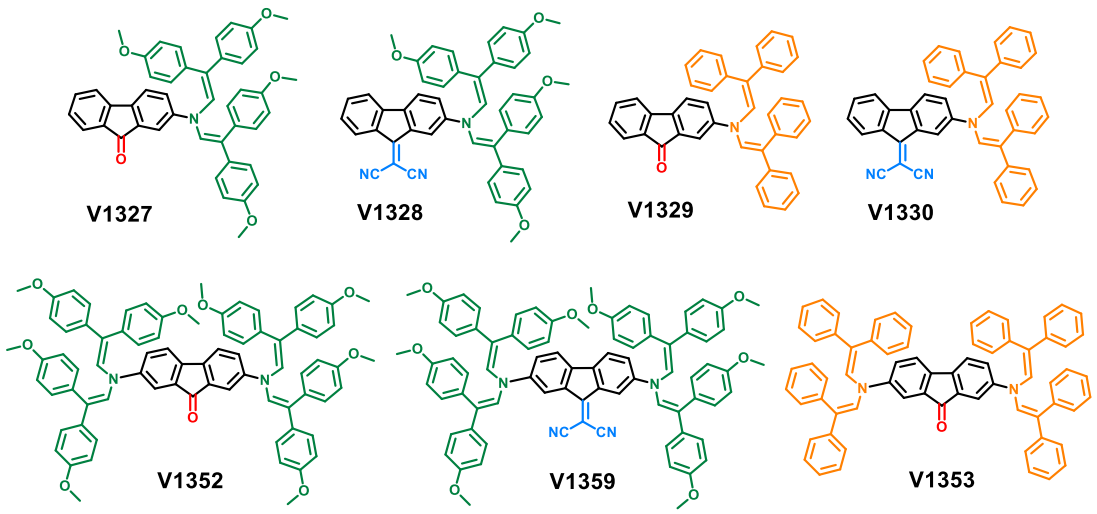

Fig. 1. Reaction scheme of fluorenone/dicianofluorenylidene enamine HTMs and their molecular structures.

The highest power conversion efficiency of over 22% is achieved on cells based on V1359, which is higher than that of spiro-OMeTAD under identical conditions. In addition, we fabricated perovskite solar mini-modules (6.5 × 7 cm) exhibiting efficiency of 18.6%. This shows that HTMs prepared via simplified synthetic routes are not only a low-cost alternative to spiro-OMeTAD but also outperform in efficiency and stability state-of-art materials obtained via expensive cross-coupling methods.

References

1. M. L. Petrus, A. Music, A. C. Closs, J. C. Bijleveld, M. T. Sirtl, Y. Hu, T. J. Dingemans, T. Bein and P. Docampo, J. Mater. Chem. A, **5** (2017) 25200–25210.

P 018

Analysis and Usage Perspectives of Solid Digestate

E. Didžiulytė*, R. Šlinkšienė, R. Paleckienė
Kaunas University of Technology, Radvilenu st.19, 50254 Kaunas, Lithuania
**Corresponding author, e-mail: egle.didziulyte@ktu.lt:*

About 180 million tons of digestate is produced in the 28 EU countries, and almost half of it is produced in Germany. Most of the digestate (about 120 million tons) is agricultural digestate (a mixture of manure and plants). The rest is obtained by mechanical biological treatment from municipal solid waste, separated biological waste or sewage sludge, and the agricultural/food industry. In the past, this anaerobically degradable biological waste (digestate) was extracted from manure and/or sewage sludge. However, renewable energy policies and subsidies for electricity, gas, and heat production from biomass have improved the economic conditions for the anaerobic digestion of biological waste or food waste in various EU countries. In this way, in addition to energy production from biogas power plants, biogas digestate/fallow is also produced. In 2000, scientific research on digestate was started and it revealed a quite wide field of usage of this product. According to various studies, the fallow of biogas is a product that can be used for plant fertilization, animal feed, extracting water for irrigation, etc. However, it was also noted that a lot of detailed scientific research should be done on risk factors, environmental effects, fertilizer treatment methods, and enrichment during long-term use [1-3].

The aim of this work was to analyze and evaluate the chemical composition of the thick digestate (remaining after separation) in detail and to predict its areas of usage. Digestate obtained from three companies was used for the research (Fig. 1): *Agaro riešutas* (Biržai), *Tvari energija* (Vievis), and *Kurana* (Pasvalys). The concentration of nitrogen, phosphorus, potassium, calcium, magnesium, carbon, trace elements, and heavy metals was determined. Moisture content, pH, and granulometric composition in the initial raw material were also determined.

Fig.1. Different types of digestate: 1 –*Agaro riešutas*, 2 – *Tvari energija*, 3 – *Kurana*

Summarizing the obtained results, it can be stated that all types of digestate can be used to fertilize plants, but the concentration of nutrients in it varies in a very wide range. Water-soluble total nitrogen has been found to range from 0.81% to 10.78%; water-soluble phosphorus (P_2O_5) 0.69-1.60%, water-soluble potassium (K_2O) 0.69-0.75%. The concentrations of CaO, MgO, trace elements, and heavy metals were even lower. Therefore, in order to produce high-quality fertilizers, the digestate has to be enriched with other substances. The digestate pH values were very similar in all cases at 7.3-7.6 and the moisture content range from 73.68% to 79.39%.

References

1. D. Kovacic, Z. Loncaric, Applied sciences, **12** (2022) 9216.
2. N. Cheffins, D. Stainton, Final project report for OMK006-06. WRAP, Banbury UK, 2015.
3. Regulation (EU) 2019/1009 of the European Parliament and of the Council of 5 June 2019 laying down rules on the making available on the market of EU fertilising products and amending.

P 019

From Natural Products to Synthetic Analogues: Pyrrole-Pyrazole Exchange in Lamellarin O

K. Dzedulionytė[1*], N. Fuxreiter[2], E. Schreiber-Brynzak[2], A. Žukauskaitė[3], V. Pichler[2], E. Arbačiauskienė[1]

[1]Department of Organic Chemistry, Faculty of Chemical Technology, Kaunas University of Technology, Radvilėnų pl. 19, LT-50254 Kaunas, Lithuania

[2]Department of Pharmaceutical Sciences, Division of Pharmaceutical Chemistry, Faculty of Life Sciences, University of Vienna, Althanstraße 14, 1090 Vienna, Austria

[3]Department of Chemical Biology, Faculty of Science, Palacký University, Šlechtitelů 27, CZ-78371 Olomouc, Czech Republic

**Corresponding author, e-mail: karolina.dzedulionyte@ktu.lt*

Lamellarins are a group of natural marine-derived alkaloids with a characteristic central pyrrole moiety and widely reported biological activity. Since their discovery in 1985, more than 50 compounds of this family have been isolated from various marine organisms, such as sponges or ascidians [1].

The biological spectrum of lamellarins is manifold, with pronounced cytotoxic activity [2],[3]. For example, lamellarin D, a leading compound in the family, induces its anticancer activity through topoisomerase I inhibition and mitochondrial targeting that triggers cell death [4]. Whereas lamellarin O was reported to exhibit moderate cytotoxicity against colorectal cancer SW620 and its multi-drug resistant daughter cell line SW620/Ad300 [5].

The structure of lamellarin O is easily accessible for replacement of the central pyrrole ring to design new derivatives with structural similarities like shape and electronic configuration by other five membered ring systems. Pyrazole is a versatile moiety taking place in various biologically active compounds as well as in-use pharmaceuticals [6]. Replacement of the central pyrrole to pyrazole is expected to change e.g., the energy of the highest occupied molecular orbital which is associated with increased metabolic stability [7].

In this study it was ought to synthesize and investigate various functionalized pyrazole derivatives of lamellarin O. The goal was based on the scaffold hopping of the pyrrole ring in natural lamellarin O to its pyrazole counterpart. Obtained compounds were evaluated for their physicochemical properties and further investigated as potent agents against human colon cancer cell lines HCT116, HT29 and SW480. Moreover, after structure-activity relationship determination, the most cytotoxic compounds were used to investigate their mode of action in the beforementioned cell lines.

References

1. J. Bracegirdle et al. *Journal of Natural Products*, **2019**, 82, 2000–2008. DOI: 10.1021/acs.jnatprod.9b00493.
2. C. Bailly. *Marine Drugs*, **2015**, 13, 1105–1123. DOI: 10.3390/md13031105.
3. P. Sopha et al. *Toxicology*, **2021**, 462, 152963. DOI: 10.1016/j.tox.2021.152963.
4. C. Ballot et al. *Marine Drugs*, **2014**, 12, 779–798. DOI: 10.3390/md12020779.
5. X. C. Huang et al. *Marine Drugs*, **2014**, 12, 3818–3837. DOI: 10.3390/md12073818.
6. P. K. Mykhailiuk. *Chemical Reviews*, **2021**, 121, 1670–1715. DOI: 10.1021/acs.chemrev.0c01015.
7. P. R. Lazzara and T. W. Moore. *RSC Medicinal Chemistry*, **2020**, 11, 18–29. DOI: 10.1039/C9MD00396G.

P 020

Analysis of Europium-Doped Sodium Aluminum Germanate

M. Dzvinka*, M. Misevičius
Institute of Chemistry, Vilnius University, Naugarduko st. 24 LT-03225 Vilnius, Lithuania
marius.dzvinka@chgf.stud.vu.lt

Luminescent materials nowadays find use among a variety of different applications, thus attracting a lot of attention for studying such compounds. Many such materials can be obtained by doping a certain matrix with lanthanide ions. This work concentrates on $NaAlGeO_4$ doped with europium (III) ions, as properties of such compound are relatively unknown.

Samples ($Na_{1-x}AlGe_{1-0.5x}O_4Eu_x$) were obtained using solid-state synthesis. Stoichiometric amounts of sodium carbonate, aluminum oxide, germanium (IV) oxide and europium (III) oxide were weighed, mixed in agate mortar and sintered in 1000 ^{0}C for 6 hours.

The samples were firstly analyzed by X-ray diffractometer. Using the obtained X-ray diffraction results, it was concluded that all of the samples are single-phased. The aforementioned data was also used to refine the existing $NaAlGeO_4$ unit cell using the Rietveld method. It was determined that the occupancy of europium sites in the crystal cell directly correlates to the bulk concentration of europium during the solid-state synthesis. Also, samples with more europium tended to have a bigger unit cell.

The luminescent properties of the specimens were investigated by photoluminescence spectroscopy. Samples with higher europium concentrations showed strongest emission when excited by light wavelength of 392.5 nm. The highest emission peaks observed were at 610 nm and 702.5 nm.

P 021

Well-Defined $GdPO_4:Eu^{3+}$ Nanophosphors for Assessment of Environmental Toxicity

E. Ezerskyte[1*], A. Morkvenas[2,4], Z. Jurgelene[3], V. Karabanovas[2,4], and V. Klimkevicius[1]

[1]Institute of Chemistry, Vilnius University, Naugarduko str. 24, LT-03225, Vilnius, Lithuania

[2]Biomedical Physics Laboratory, National Cancer Institute, Santariskiu str. 1, LT-08660, Vilnius, Lithuania

[3]Nature Research Centre, Akademijos str. 2, LT-08412, Vilnius, Lithuania

[4]Department of Chemistry and Bioengineering, Vilnius Gediminas Technical University, Sauletekio av. 11, LT-10223, Vilnius, Lithuania

**Corresponding author, e-mail: egle.ezerskyte@chgf.stud.vu.lt*

Inorganic luminescent nanoparticles doped with various lanthanide ions are in high demand, especially for use in fields such as energetics, biomedicine, and anti-counterfeiting. However, the synthesis of these materials often ignores the principles of green chemistry, and relies on environmentally harmful precursors and solvents, which usually yield nanoparticles with hydrophobic surface, and, therefore, limits potential applicability, particularly in bio-related fields [1, 2].

This study focuses on hydrothermal $GdPO_4:Eu^{3+}$ nanoparticle synthesis route, which is considered to comply with the principles of green chemistry. In addition, nanoparticles synthesized using this method are hydrophilic meaning they are easily redispersed in aqueous media and have a high potential to be applied in bio-related fields [3]. Since these nanoparticles possess magnetically active Gd^{3+} and optically active Eu^{3+} ions, they may be considered as promising bioimaging agents. In this study, a detailed analysis of $GdPO_4:Eu^{3+}$ nanoparticles' structural, optical, and magnetic properties was performed, and the initial bioaccumulation and toxicological studies on zooplankton *Daphnia magna* (Fig. 1) were conducted.

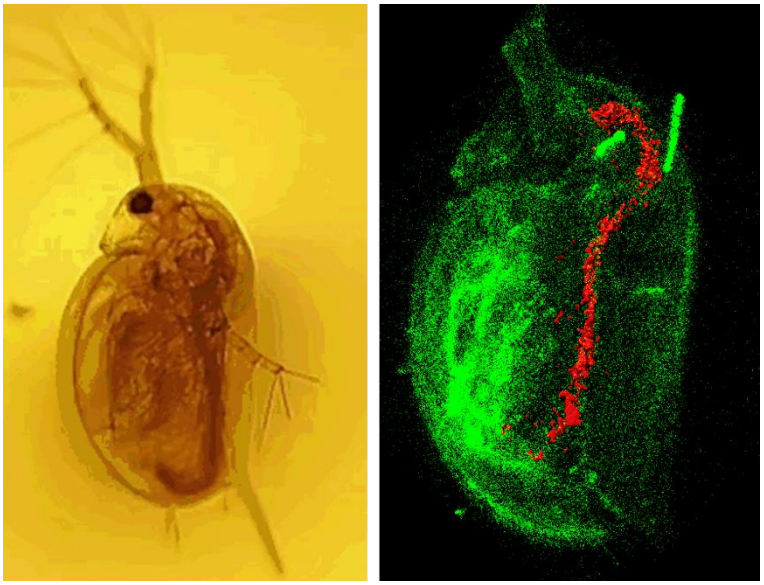

Fig. 1. Optical microscopy image of a *Daphnia magna* (left) and representative confocal microscopy image of a *Daphnia magna* with $GdPO_4$:15%Eu^{3+} nanorods visible in its digestive tract (right).

References

1. Wang, G., Q. Peng, and Y. Li, Lanthanide-doped nanocrystals: synthesis, optical-magnetic properties, and applications. Accounts of chemical research, 2011. 44(5): p. 322-332.
2. Zhou, J., et al., Upconversion luminescent materials: advances and applications. Chemical reviews, 2015. 115(1): p. 395-465.
3. Janulevicius, M., et al., Controlled hydrothermal synthesis, morphological design and colloidal stability of $GdPO_4 \cdot nH_2O$ particles. Materials Today Communications, 2020. 23: p. 100934.

P 022

A Dopamine Electrochemical Sensor Based on Reduced Graphene Oxide Obtained by the Laser-Induced Reduction Method

J. Gaidukevič[1,3*], R. Trusovas[2], R. Pauliukaitė[3], J. Barkauskas[1]

[1]*Institute of Chemistry, Faculty of Chemistry and Geosciences, Vilnius University, Naugarduko str. 24, LT – 03225, Vilnius, Lithuania.*

[2] *Department of Laser Technologies, Center for Physical Sciences and Technology, Savanoriu Ave. 231, LT-02300 Vilnius, Lithuania*

[3] *Department of Nanoengineering, Center for Physical Sciences and Technology, Savanoriu Ave. 231, LT-02300 Vilnius, Lithuania*

justina.gaidukevic@chf.vu.lt

Reduced graphene oxide (rGO) is conquering space in graphene-based sensors due to some similarities to graphene, such as a high specific surface area, mechanical, and thermal properties, compatibility with other materials, and its low-cost production [1]. Various methods including chemical reaction, thermal treatment, photochemical reaction, and laser reduction techniques have been applied to remove oxygen species for the reduction of GO [2]. The laser-induced reduction of graphene oxide (GO) has been actively investigated because it has several technical advantages over other chemical or thermal methods. Laser-induced GO treatment is a highly effective and simple one-step method for producing rGO. In addition, during this reduction method, the costly processes of product separation and purification are avoided. This is a further advantage in comparison with the methods described above. However, because of the small diameter of the focused beam, large-scale laser reduction of GO may require significant processing time. Moreover, systematic investigations considering the effect of laser scanning parameters on the electrochemical performance of rGO are lacking [3]. Factors such as the laser wavelength and laser-exposure duration can affect the structural morphology and the chemical composition of the rGO. Therefore, the aim of this work is to develop a laser-induced reduction approach for the preparation of reduced graphene oxide (GO) and to investigate the electrochemical performance of the final products for dopamine detection.

GO was prepared from natural graphite using the synthesis protocol proposed in our research group [4]. In a typical experiment, graphite powder was treated with concentrated H_2SO_4, H_3BO_3, and CrO_3. The obtained pre-oxidized graphite was subjected to oxidation by Hummers' method using $NaNO_3$, H_2SO_4, and $KMnO_4$ [5]. Then, GO reduction was performed using the laser ablation in a liquid environment technique. Picosecond laser ablation experiments were performed employing two different lasers with a wavelength of 532 nm and 355 nm, a repetition rate of 100 kHz, and GO suspensions were ablated at different times 15, 30, and 45 minutes. The experiments were carried out at a laser power of 1 W. In our experimental setup, a fixed volume of GO ($5 \cdot 10^{-5}$ mg L^{-1}) suspension was placed in a beaker and the laser ablation was performed from the top in order to avoid laser reflections through the glass walls. Before and after the laser irradiation with different processing parameters, the materials obtained were characterized by different methods (XPS, UV-Vis, and Raman spectroscopy). Electrochemical measurements, in particular, cyclic voltammetry and differential pulse voltammetry were used to evaluate the sensitivity of the obtained samples to dopamine detection.

The results demonstrated that after the laser-induced reduction of GO, the oxygen content of the rGO powders decreased with increasing the irradiance time. The most effective reduction was achieved using a laser of 355 nm wavelength and an ablation time of 45 min. Moreover, it was observed that two types of nitrogen species including pyrrolic-N and quaternary-N were detected in the rGO samples. Finally, the electrochemical measurements conducted highlighted that rGO obtained using laser ablation in a liquid environment technique could be a promising electrode material for the detection of dopamine.

References

1. Balandin, Nature Mater. **10** (2011) 569–581.
2. Y. C. Guan, Y. W. Fang, G. C. Lim, H. Y. Zheng, M. H. Hong, Sci. Rep. **6** (2016) 28913.
3. T. X. Tran, H. Choi, C. H. Che, J. H. Sul, I. G. Kim, S. M. Lee, J. H. Kim, J. B. In, ACS Appl. Mater. Interfaces **10** (2018) 39777-39784.
4. J. Gaidukevic, R. Aukstakojyte, T. Navickas, R. Pauliukaite, J. Barkauskas, Appl. Surf. Sci. **567** (2021) 150883.
5. W. S. Hummers, R. E. Offeman, J. Am. Chem. Soc. **80** (1958) 1339.

P 023

Synthesis of Novel *N*-(4-Hydroxyphenyl)-*β*-alanine Derivatives

R. Gelminauskaitė[1*], B. Grybaitė[1], E. Mickevičiūtė[2]

[1]Kaunas University of Technology, Department of Organic Chemistry, Radvilėnų pl. 19, Kaunas, Lithuania
[2]Department of Information Systems, Kaunas University of Technology, Studentų g. 50, Kaunas, Lithuania
**Corresponding author, e-mail: roberta.gelminauskaite@ktu.edu*

β-Amino acids are promising intermediates in organic, bioorganic, medicinal, and peptide chemistry. Great number of natural and synthetic compounds, containing b-alanine moiety, are biologically active and find application in pharmacy. A large number of chemotherapeutics are developed for medicinal use nowadays but the increasing resistance of pathogens to available pharmaceuticals has created an essential demand for new efficient classes of antimicrobial agents.

Given the promising pharmacological potential of highly functionalized carbocyclic β-amino acids bearing hydroxy, azido, amino, or fluoro groups can be as building blocks in the synthesis of novel bioactive compounds. The aim of this work was to synthesize compounds containing the above-mentioned two fragments and to determine the biological properties of the obtained compounds. [1-3]

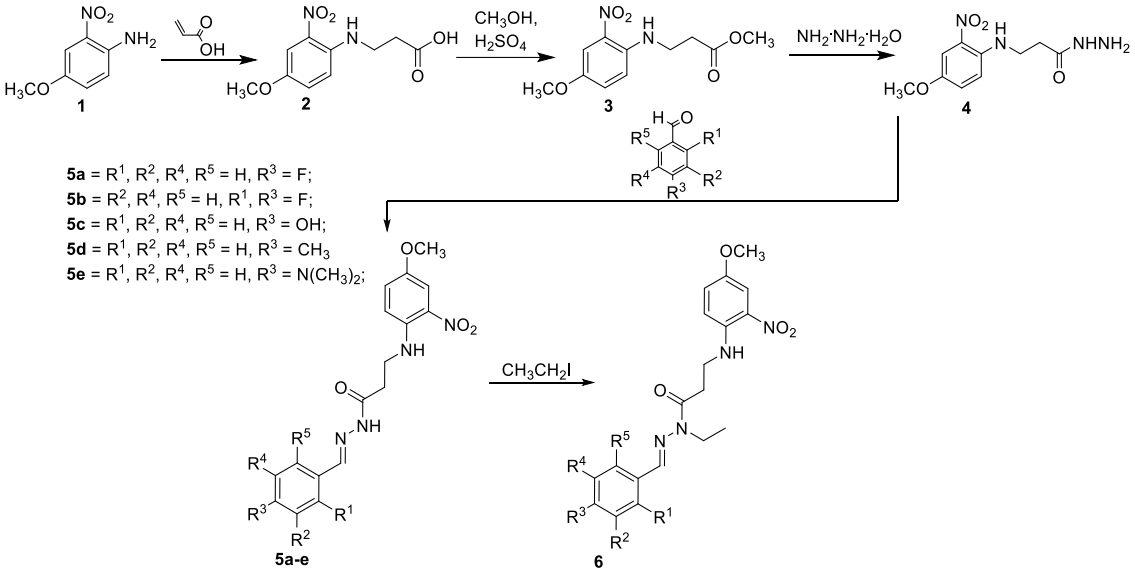

Fig. 1. Synthesis of novel *N*-(4-hydroxyphenyl)-*β*-alanine derivatives

The reaction of 4-methoxy-2-nitroaniline **(1)** with acrylic acid in water at reflux afforded intermediates 3-((4-methoxy-2-nitrophenyl)amino)propanoic acid **(2)**. Acid **2** were esterified with methanol for 3 hours in the presence of a catalytic amount of sulfur acid in the reaction mixture (Fig. 1). The obtained methyl esters **3** reacted with hydrazine monohydrate in 2-propanol at reflux, and the corresponding hydrazide **4** were synthesized. Hydrazones **5a-e** were prepared by the reaction of hydrazide **4** and aromatic aldehydes in 2-propanol. Alkylation of hydrazone **5e** was carried out in the dimethylformamide in the presence of a catalytic amount of potassium hydroxide and potassium carbonate in the reaction mixture. The structures of the obtained compounds were confirmed by the data of the ^{1}H, ^{13}C NMR and FT-IR spectra and elemental analysis.

References

1. J. M. Otero, A. M. Estévez, J. C. Estévez et al., Highly functionalized cyclic and bicyclic β-amino acids from sugar β-nitroesters, Tetrahedron 76, 130837 (2020).
2. L. Kiss, I. M. Mándity, F. Fülöp, Highly functionalized cyclic β-amino acid moieties as promising scaffolds in peptide research and drug design, Amino Acids 49, 1441-1455 (2017).
3. M. Risseeuw, M. Overhand, G. W. J. Fleet et al., A compendium of cyclic sugar amino acids and their carbocyclic and heterocyclic nitrogen analogues, Amino Acids 45, 613-689 (2013).

P 024

Synthesis of Novel N-(4-Acetylphenyl)Imidazole and Dihydropyrimidine Derivatives

B. Golcienė[1,*], A. Voskienė[2], V. Mickevičius[3]

[1]*Kaunas University of Technology, Radvilėnų pl. 19, LT-50254 Kaunas, Lithuania*
[2]*UAB "Contract Pharma Solutions", Bijūnų str. 30 Garliava, LT-53267, Lithuania*
[3]*Kaunas University of Technology, Radvilėnų pl. 19, LT-50254 Kaunas, Lithuania*
**Corresponding author, e-mail: bozena.sovkovaja@ktu.edu*

A well-known fact is that a variety of microorganisms have become resistant to a number of available drugs, what leads scientist to discover and develop new biologically active compounds.

Reportedly azole or azine fragments containing compounds display a number of positive effects, such as antitubercular [1], antimalarial [2], anticancer [3,4], antibacterial and antifungal activity [5]. Therefore, synthesis of potentially biologically active azole or azine fragments baring compounds was chosen for this study.

In most cases, reaction of N-aryl-β-amino acids with carbamide or thiocyanates of alkali metals in acidic medium results in formation of corresponding 1-substituted dihydro-2,4-(1*H*,3*H*)-pyrimidinediones or their 2-thio analogues. Condensation of N-(4-acetylphenyl)-β-alanine (**2**) with carbamide as well as with potassium thiocyanate was carried out in acetic acid under reflux (*Fig. 1*). Firstly, the corresponding ureido acids **3**,**5** were formed. They were cyclized in situ on treatment with hydrochloric acid to more stable dihydropyrimidinedione **4** and its 2-thio analogue **6**.

The preparation of imidazoles from α-amino ketones and cyanates or thiocyanates of alkali metals is a common method for the synthesis of imidazoles. Reactions of amino ketones **7,8** with potassium cyanate or thiocyanate were carried out in acetic acid at reflux and gave imidazoles **9-12** (*Fig. 1*).

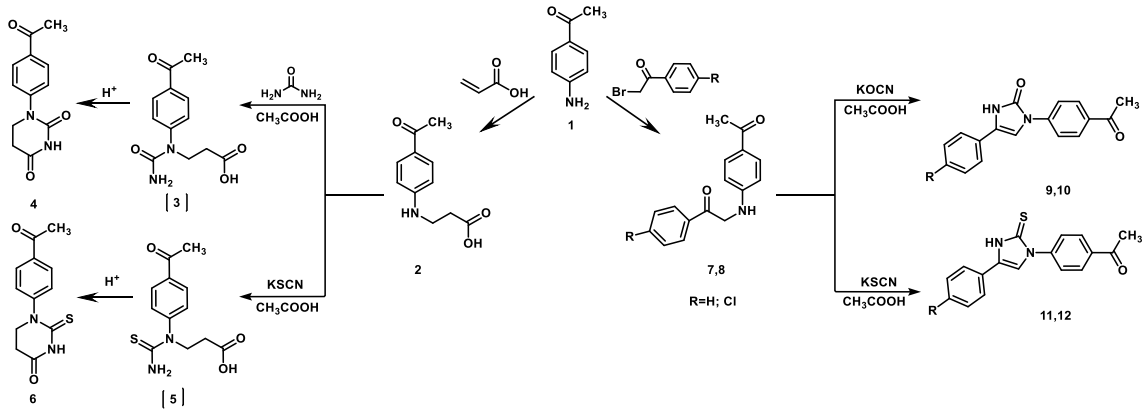

Fig. 1. Synthesis of dihydropyrimidinone and imidazole derivatives

The structure of the compounds has been proven by ^{1}H NMR, ^{13}C NMR, FT-IR spectroscopy and elemental analysis. Further studies on biological activity of newly synthesized compounds are planned.

References

1. J. Liu, Z. Ren, et al., Bioorganic & Medicinal Chemistry, 27(**1**), (2019), 175-187.
2. C. Gao, L. Chang, et al., European Journal of Medicinal Chemistry, 163(**1**) (2019), 404-412.
3. Sh. Bommagani, N. R. Penthala, et al., Bioorganic & Medicinal Chemistry Letters, 29(**2**), (2019), 172-178.
4. B. Balandis,V. Mickevičius, V. Petrikaitė, Pharmaceuticals, 14(**11**) 2021, 1158.
5. E. Abdel-Galil, A. M. Arab, E. M. Afsah, Synthetic Communications, 51 (**9**), 2021.

P 025

Isolation of Hydrophilic Fractions from Defatted Strawberry, Blackberry and Elderberry Seeds and Rowanberry Pomace by Pressurized Liquid Extraction

R. Grabauskaitė*, L. Jūrienė, R. Kazernavičiūtė, R. Maždžierienė, P. R. Venskutonis
Kaunas University of Technology, Department of Food Science and Technology, Radvilėnų pl. 19, Kaunas, LT-50254, Lithuania
**rugile.grabauskaite@ktu.edu*

Significant part of berry processing is juice production which generates huge amounts of pomace including skin, seeds and residue of fruit pulp. Often discarded as a waste, berry press cake contains valuable bioactive compounds having health-promoting effects and various possible applications. Berry seeds are known as an excellent source of phenolic compounds, fatty acids and tocopherols providing such properties as antioxidant, anti-inflammatory and anti-proliferative. Extraction of these water or oil-soluble components is of great interest in regards of developing functional value-added products [1].

In this study, pressurized liquid extraction (PLE) is used for polar fraction recovery from the residue of berry seeds and pomace obtained after lipophilic fraction isolation by supercritical carbon dioxide extraction. The materials for this study were strawberry (*Fragaria* × *ananassa*), blackberry (*Rubus fruticosus* L.*)* and elderberry seeds (*Sambucus nigra* L.) as well as rowanberry pomace (*Sorbus aucuparia* L.). Chemical composition of raw material is given in Table 1. Elderberry seeds had the highest moisture, lipid and fiber content, while strawberry seeds were rich in proteins and ash.

Table 1. Chemical composition of strawberry, blackberry and elderberry seeds and rowanberry pomace

Material	Moisture content (%)	Lipid content (%)	Protein content (%)	Ash content (%)	Fibre (g/100 g)
Strawberry seeds	2.30 ± 0.17	15.75 ± 0.35	12.27 ± 0.38	3.03 ± 0.08	29.84 ± 1.91
Blackberry seeds	2.77 ± 0.06	15.43 ± 0.64	8.86 ± 0.69	2.18 ± 0.05	24.13 ± 0.69
Elderberry seeds	3.55 ± 0.003	16.04 ± 0.52	8.69 ± 0.19	2.81 ± 0.01	40.28 ± 0.14
Rowanberry pomace	3.44 ± 0.18	9.45 ± 1.37	9.59 ± 0.39	2.81 ± 0.004	7.81 ± 0.40

PLE was performed in an accelerated solvent extractor Dionex ASE 350 with ethanol and water mixture (70:30) as a solvent at 100 °C and 10 MPa. The extraction yielded 20,61-47,29 % hydrophilic extracts while the highest yield resulted from rowanberry pomace (47.29 ± 2.27 %) (Table 2). Antioxidant capacity of PLE extracts was determined by total phenolic content (TPC) according to Folin-Ciocalteu method and $ABTS^{\bullet+}$ radical scavenging and reducing antioxidant capacity (CUPRAC) assays. Strawberry seed extract had the most phenolic compounds (92.18 ± 3.90 mg GAE/g extract). Slightly lower TPC was found in blackberry seed extract (87.77 ± 1.75 mg GAE/g extract) which also had the highest ABTS and CUPRAC values compared to other extracts, 419.56 ± 15.52 mg TE/g extract and 314.42 ± 2.52 mg TE/g extract respectively.

Table 2. Comparison of PLE extracts from berry seeds and pomace yields and antioxidant (TPC, ABTS and CUPRAC) capacity

PLE extract	Yield (%)	TPC (mg GAE/g extract)	$ABTS^{\bullet+}$ (mg TE/g extract)	CUPRAC (mg TE/g extract)
Strawberry seeds	20.61 ± 2.26	92.18 ± 3.90	370.41 ± 36.94	288.18 ± 0.46
Blackberry seeds	31.84 ± 1.95	87.77 ± 1.75	419.56 ± 15.52	314.42 ± 2.52
Elderberry seeds	20.81 ± 0.41	47.41 ± 2.09	148.44 ± 10.06	110.45 ± 2.16
Rowanberry pomace	47.29 ± 2.27	27.26 ± 1.11	88.28 ± 4.11	94.43 ± 0.7

References

1. M. Fidelis, et al. Fruit seeds as sources of bioactive compounds: Sustainable production of high value-added ingredients from by-products within circular economy. Molecules, 2019, 24(21), p. 3854.

P 026

Synthesis of Novel Functionalized *N*,*N*-Disubstituted Aminothiazoles

K. Naruševičiūtė[1], B. Grybaitė[1,*], B. Sapijanskaitė-Banevič[1], R. Vaickelionienė[1], K. Anusevičius[1], V. Mickevičius[1]

[1]*Kaunas University of Technology, Department of Organic Chemistry, Radvilėnų pl. 19, 50254 Kaunas, Lithuania*
**Corresponding author, e-mail: birute.grybaite@ktu.lt*

A large number of chemotherapeutics are developed for medicinal use in nowadays but the increasing resistance of pathogens to available pharmaceuticals has created an essential demand for new efficient classes of antimicrobial agents. A unique small-ring heterocycle – thiazole containing nitrogen and sulphur atoms, play an important role in medicinal chemistry and is widely used in the development of bioactive compounds, drugs, as well as industrial products [1, 2]. Pharmaceuticals based on thiazole and its derivatives are used in medical practice for the treatment of hypertension, Alzheimer's disease, diabetes, schizophrenia, allergies they act as anti-cancer, antimicrobial, antifungal agents [3].

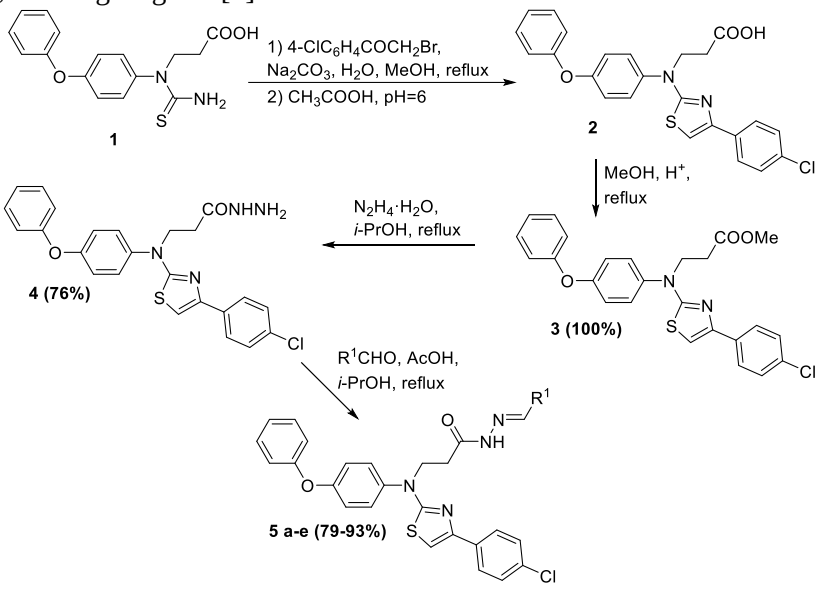

5a R^1= C_6H_5; **5b** R^1= 4-ClC_6H_4; **5c** R^1= 4-BrC_6H_4; **5d** R^1= 4-$O_2NC_6H_4$; **5d** R^1= 2-thienyl

Fig. 1. Synthesis of novel functionalized *N*,*N*-disubstituted aminothiazoles.

In this study, the prepared compound **1** was used as a precursor for the preparation of thiazole **2** by the *Hantsch* method by combining thioureido acid **1** with the corresponding acetophenones (**Fig 1**). Using the reactivity of carboxylic group, the esterification of compound **2** and subsequent hydrazinolysis of the resulting ester **3** was performed. Acid **2** was esterified with methanol at reflux for 4 hours in the presence of a catalytic amount of sulfuric acid in the reaction mixture. The obtained methyl ester **3** was reacted with hydrazine monohydrate in 2-propanol and the corresponding hydrazide **4** was synthesized. Condensation of compound **4** with aromatic aldehydes in propan-2-ol and using a catalytic amount of glacial acetic acid led to the formation of *N*'-benzylidene hydrazides **5a**–**e**. The structures of the obtained compounds were confirmed by the data of the ^{1}H, ^{13}C NMR and FT-IR spectroscopy, and elemental analysis.

References

1. M. V. J. Nora de Souza, J. Sulphur Chem., **26** (2005) 429-449.
2. P. K. Sasmal, S. Sridhar, J. Idbal, Tetrahedron Lett., **47** (2006) 8661-8665.
3. V. Kojić, M. Popsavin, S. Spaić, D. Jakimov, I. Kovačević, M. Svirčev, L. Aleksić, B. S. Zelenović, V. Popsavin, Eur. J. Med. Chem., **183** (2019) 111712.

P 027

Iron Oxide Magnetic Nanoparticles Functionalized by Nisin

R. Gruškienė[1,*], T. Kavleiskaja[2], R. Stanevičienė[3], E. Servienė[1,3], J. Sereikaitė[1]

[1]*Department of Chemistry and Bioengineering, Vilnius Gediminas Technical University, Saulėtekio 11, 10223 Vilnius, Lithuania*

[2]*Institute of Chemistry, Vilnius University, Naugarduko 24, 03225 Vilnius, Lithuania*

[3] *Laboratory of Genetics, Institute of Botany, Nature Research Centre, Akademijos g. 2, 08412 Vilnius, Lithuania*

**Corresponding author, e-mail: ruta.gruskiene@vilniustech.lt*

Over the last decades iron oxide magnetic nanoparticles, mostly magnetite (Fe_3O_4) and maghemite (γ–Fe_2O_3), have increasingly attracted attention as an efficient tool in various fields of application [1]. Here, we present the preparation and characterization of iron oxide magnetic nanoparticles functionalized by nisin. Nisin is naturally produced by *Lactococcus lactis* subsp. l*actis* as a small cationic peptide composed of 34 amino acid residues and is a well-known bacteriocin approved as a food additive for food preservation [2]. Iron oxide magnetic nanoparticles were prepared by the co-precipitation method and characterized by X-ray diffraction method. Magnetic nanoparticles were stabilized by citric, ascorbic, gallic, or glucuronic acid coating and were functionalized by nisin using a simple and low-cost adsorption method (Fig. 1). Nisin loading was confirmed by FT-IR spectra, thermogravimetric analysis, and dynamic light scattering methods. Nisin-loaded iron oxide magnetic nanoparticles were stable for at least six weeks as judged by zeta-potential and hydrodynamic diameter measurements. The functionality of nisin-loaded iron oxide magnetic nanoparticles was demonstrated on Gram-positive bacteria. Functionalized nanoparticles could find their application in innovative and emerging technologies as antimicrobials.

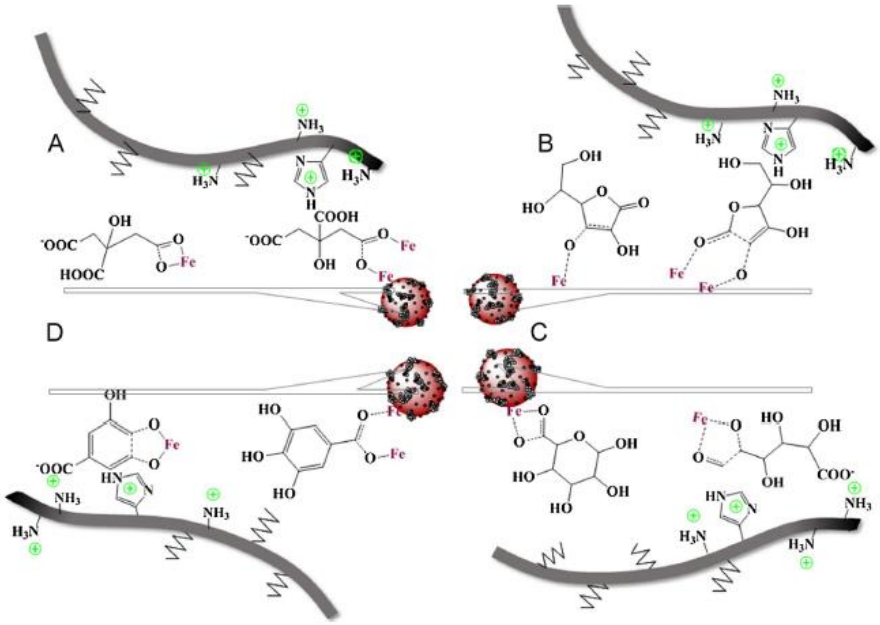

Fig. 1. Simplified scheme of iron oxide nanoparticles stabilized with citric (A), ascorbic (B), glucuronic (C) and gallic (D) acids and coated with nisin by hydrophobic ( ) and electrostatic interactions ( ).

References

1. W. Wu, Z. Wu, T. Yu, Ch. Jiang, W.S. Kim, Sci. Technol. Adv. Mater., **16** (2015) 023501.
2. A. Bahrami, R. Delshadi, S. M. Jafari, L. Williams, Trends in Food Sci. Technol., **94**, (2019) 20.

P 028

Possibilities of Using Non-Traditional Raw Materials for Fertilizer Production

G. Gudinskaitė*, R. Paleckienė, R. Šlinkšienė
KTU Faculty of Chemical Technology, Kaunas, Lithuania
goda.gudinskaite@ktu.edu

The aim of this research is to respond to the provisions of the Green Course by selecting and applying methods and technologies for processing of various non-traditional raw materials, by-products of agricultural, food industries and their production waste. Various kinds of organic waste, obtained from natural sources (e.g. animal and bird droppings, insect remains (frass), plant residues, biogas residues and agricultural by-products) can be used as alternative raw materials [1]. Insect farming waste (frass) is potentially valuable as a bioactive resource for plant nutrients [2]. The possibility of creating fertilizing products from the waste generated during the cultivation of Mealworm was analyzed. Several different batches of frass (DF1, DF2) from UAB "Divaks" were evaluated for their suitability for fertilizer production, i.e. chemical and instrumental analysis. The concentration of macro elements and microelements in the waste was determined, and the thermal stability of the raw material was analyzed. Crystallographic studies of the Frass samples were carried out using the X-ray diffraction (XRD) method, the XRD curve of the DF1 sample is presented in Figure 1.

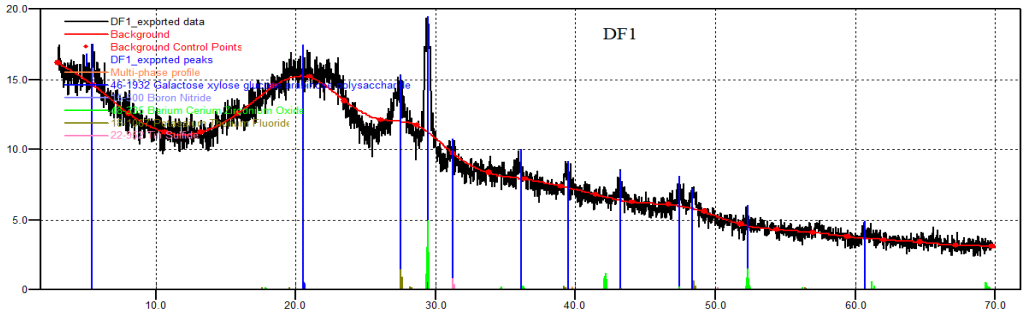

Fig. 1. XRD curve of DF1 Frass sample

It can be seen from the XRD curve that its characteristic are that of the amorphous material structure. And due to the amorphous structure, it is not possible to identify specific salts, but according to the location of the characteristic peaks, using the data in the databases, the corresponding substances were identified. A hump is observed in the curve, the maximum of which is at a value of 2θ of ~21°. It can be attributed to chitosan, which is a linear polysaccharide composed of D-glucosamine and N-acetyl-D-glucosamine randomly linked through β-(1-4). And a small but brighter peak at 2θ value ~27° can be attributed to silicon oxide (SiO_2). Additional peaks are visible in the XRD curve of the sample, which partly correspond to the interlamellar distances of different polysaccharides, boron and potassium compounds. To analyze more detailed composition, FTIR analysis was performed, and chemical bonds (C=C, C–H) and bonds of other functional groups (Si–O, O–H, O–C=O) characteristic of substances of organic origin were determined. Considering that frass contains a lot of mineral substances necessary for plants, there are no harmful impurities, it can be used as a component for the production of fertilizing products.

References:

1. CHOJNACKA, Katarzyna; MOUSTAKAS, Konstantinos; WITEK-KROWIAK, Anna. Bio-based fertilizers: A practical approach towards circular economy. *Bioresource Technology*, 2020, 295: 122223.
2. BARRAGÁN-FONSECA, Katherine Y., et al. Insects for peace. Current opinion in insect science, 2020, 40: 85-93

P 029

Effect of Different Amounts of Cr^{3+} and B^{3+} Ions on the Luminescence Properties of LuAG

G. Inkrataitė[1*], J.N. Keil[2], T. Jüstel[2], R. Skaudžius[1]

[1]Institute of Chemistry, Faculty of Chemistry and Geosciences, Vilnius University, Naugardukas st. 24 LT-03225 Vilnius, Lithuania

[2]Department of Chemical Engineering, Münster University of Applied Sciences, Stegerwaldstraße 39, 48565 Steinfurt, Germany

**Corresponding author, e-mail: greta.inkrataite@chgf.vu.lt*

In order to convert high-energy radiation, such as gamma or X-rays, into visible light, special converter materials are needed. Such compounds are usually referred to as scintillators. Over the years many different candidates to fit the requirements were examined. However, compounds with garnet structures have attracted a particularly large amount of attention. Cerium or chromium doped lutetium and aluminum garnets have high density, high thermal stability, rather efficient luminescence processes, and thus high quantum efficiency which are needed for a good scintillator [1]. However, further optimization and improvement are still required especially w.r.t. a reduced decay time. The duration of the luminescence decay is important because if it is very short then the more signals can be measured within a defined timeframe, resulting in a better resolved and higher quality image, for example in CT devices. One way to improve materials properties is to doping the aforementioned compounds with different elements. As such, by doping we could potentially be able to improve key aforementioned parameters: emission intensity, quantum efficiency and decay times [2,3]. One of these elements is boron. Primarily, it can be used as a flux, and also B^{3+} ion has a suitable neutron capture cross section and can also help absorb gamma radiation [4]. However, garnets can be doped with larger amounts of other elements. In this case, we replaced some of the aluminium with scandium. Lutetium aluminium scandium garnets doped with Cr^{3+} / B^{3+} were obtained as a result. These garnets are synthesized and studied for the first time.

In the present work, the effect of boron and scandium co-doping on the various characteristic of the LuAG doped by chromium is investigated. Garnets doped with different amounts of boron and scandium were synthesized by the aqueous sol-gel method. The phase purity of the samples was analyzed by means of X-ray diffraction. The morphology of the compounds was evaluated by using scanning electron microscopy. Photoluminescence properties such as emission and excitation spectra, decay curves and quantum efficiency have been investigated. Radioluminescence was also measured in order to determine the scintillation properties of the samples. The positive impact of boron addition into the garnet structure on the luminescence properties will be discussed in detail.

ACKNOWLEDGEMENTS:

This research was funded by German Academic Exchange Service (DAAD) scholarship.

References

1. Machado I.P., Teixeira V.C., Pedroso C.C.S., et. al. J. Alloys Compd. **777** (2019) 638-645.
2. Foster C., Wu Y., Koschan M., et. al. J. Cryst. Growth **486** (2018) 126-129.
3. McGregor D.S. Annu. Rev. Mater. Res. **48** (2018) 254-277.
4. Inkrataite G., Kemere M., Sarakovskis A., Skaudzius R. J. Alloys Compd. **875** (2021) 160002.

P 030

Synthesis and Luminescent Properties of Eu^{3+}, Dy^{3+}, Bi^{3+}-Doped Sodium Aluminum Germanate $NaAlGeO_4$ Phosphors

G. Janusauskaite[1,*], M. Misevicius[1]

[1]Institute of Chemistry, Faculty of Chemistry and Geosciences, Vilnius University, Naugarduko street 24, LT-03225 Vilnius, Lithuania

**Corresponding author, e-mail: gabija.janusauskaite@chgf.stud.vu.lt*

Aluminum germanates are a class of materials that exhibit persistent luminescence and have been the subject of extensive research in recent years. Aluminum germanates can be synthesized using a variety of methods, including solid-state reactions, hydrothermal and sol-gel methods. The persistent luminescence of these materials is caused by the presence of rare-earth ions in their structure, which act as activators for the luminescence. Afterglow duration of more than 100 h achieved in high-albite $Na(Al,Ga)Ge_3O_8$ [1] nanocrystals via controlled thermal annealing from supercooled melt. Persistent luminescence has numerous applications including emergency lighting, decoration, data storage, temperature sensors, and structural failure detection [2,3]. Recently, new interest in biomedical sensing and imaging has been directed due to the limited availability of materials with useful phosphorescence properties, particularly with various emission colors [3].

Sodium aluminum germanate $NaAlGeO_4$ is a crystalline material with a calcium ferrite structure and belongs to the Pnma space group. Its cell parameters are a=8.87 Å, b=2.84 Å, c=10.40 Å and its density is 4.73 g/cm^3 [4]. It has unique optical and electronic properties, including high thermal stability, strong photoluminescence, and high transparency in the visible and near-infrared range. Additionally, its composition and crystal structure make it suitable for use in a wide range of applications, including as a host material for rare earth ions in solid-state lighting and as a dielectric material for capacitors.

During this work, compositions with different charge compensation of Eu^{3+}-doped $NaAlGeO_4$ were synthesized using solid-state synthesis method $Na_{1-x}AlGe_{1-0,5x}O_4$, $Na_{1-x}AlGeO_4$, $Na_{1-3x}AlGeO_4$ and $NaAl_{1-x}GeO_4$. X-ray diffraction (XRD), excitation and emission spectra showed that $Na_{1-x}AlGe_{1-0,5x}O_4$ is the purest compound with the highest intensities. A series of $Na_{1-x}AlGe_{1-0,5x}O_4$ samples activated with varying concentrations of trivalent Eu, Dy, and Bi ions were synthesized. The samples were then characterized using XRD and photoluminescence (PL) measurements, including examination of the excitation and emission spectra, luminescence decay times, and quantum efficiencies. Results from the XRD analysis showed that all the samples consist of pure $NaAlGeO_4$ phase. The PL measurements showed that the Eu^{3+}-doped samples exhibited red emission at 611 nm, while the Dy^{3+}-doped samples showed yellow emission at 573.5 nm and the Bi^{3+}-doped samples demonstrated emission at 420 nm.

References

1. P. Li, M. Peng, L. Wondrazek et al., Red to near infrared ultralong lasting luminescence from Mn2+-doped sodium gallium aluminum germanate glasses and (Al,Ga)-albite glass-ceramics, Journal of Materials Chemistry C, Issue 14 (2015).
2. P. F. Smet, D. Poelman and M. P. Hehlen, Focus issue introduction: persistent phosphors, Optical Materials Express, Volume 2, 452–454 (2012).
3. M. Peng, J. Qiu and Q. Zhang, An introduction to the 2nd International Workshop on Persistent and Photostimulable Phosphors (IWPPP 2013), Optical Materials, Volume 36, 1769–1770 (2014).
4. A. F. Reid, A. D. Wadsley, A. E. Ringwood, High pressure $NaAlGeO_4$, a calcium ferrite isotype and model structure of silicates at depth in the earth's mantle, Acta Crystallographica, 23, 736–739 (1967).

P 031

Catalytic Activity of Mixed Cu, Co and Cr Oxide Catalysts

K. Čeplinskas, A. Jaskūnas*
Department of Physical and Inorganic Chemistry,
Kaunas University of Technology
Radvilėnų rd. 19, LT-50254 Kaunas, Lithuania E-mail address: andrius.jaskunas@ktu.lt

Supported catalysts used to oxidate volatile organic compounds (VOCs) are usually prepared by wet impregnation method and one of the most active components in this area is CuO [1]. Active sites are formed through the process of adsorption of thermally destructible salts on the selected support and their subsequent calcination. Mixed metal oxides catalysts have great potential in the field of VOCs oxidation because of many kinds of fundamental structures and numerous possibilities of various compositions [2]. In this study the influence of various additions of Co and Cr oxides on catalytic activity of CuO was investigated.

According to the previous research of Cu, Co and Cr adsorption on aluminum oxide, it was decided to investigate 5 different mixed oxide catalysts: $Cu50/Al_2O_3$; $Cu50\text{-}Co10/Al_2O_3$; $Cu50\text{-}Co50/Al_2O_3$; $Cu50\text{-}Cr10/Al_2O_3$; $Cu50\text{-}Cr50/Al_2O_3$ (numbers indicate corresponding concentrations of metal ions in sorption solution, g/l). Catalysts' composition was determined using atomic absorption spectrometry. Catalysts with Co additives had the largest total amount of active components on the surface of support – up to ~14 % total catalyst's mass. Formation of Cu and Cr oxide mixtures on the surface of support caused the decrease of CuO content. This indicates competitive simultaneous adsorption of active components. The maximum amount of active components in Cu-Cr oxide catalyst reached ~11,5 %, when compared to single CuO catalyst it was ~9 %.

Measurements of catalytic activity and selectivity was made by complete oxidation of propyl acetate in the air in fixed catalyst bed tubular reactor. Amounts of propyl acetate and intermediate compounds were determined using gas chromatography and mass spectroscopy methods. CO, CO_2 quantities were measured by gas composition analyzer. Oxidation experiments were carried out in temperature range from 150 to 300 °C with the step of 25 °C. Gas flow to the reactor was maintained constant at 1 l/min with initial concentration of propyl acetate ~1 g/m^3 (±0,05 g/m^3).

During experiments synergetic effect of adsorption and catalytic oxidation reaction were observed. Obtained conversion curves had two conversion maximums at two different temperatures. First maximum was reached at temperature of 200 °C and apparent conversion of contaminated gas depending on catalyst composition was: 9,15 % CuO – 76,8 %; 8,91 % CuO and 1,12 % Co_3O_4 – 83 %; 9 % CuO and 5,44 % Co_3O_4 – 90 %; 7,62 % CuO and 2,08 % Cr_2O_3 – 78,6 %; 5,88 % CuO and 5,80 % Cr_2O_3 – 79,7 %. However, the lack of CO and CO_2 in the outgoing flow indicated, that this is not because of oxidation reaction, but because of adsorption. Overall, catalyst with 9 % CuO and 5,44 % Co_3O_4 was defined as the most catalytically active and with the highest adsorptive influence. It was also determined that Cr_2O_3 additive increases selectivity of CuO/Al_2O_3 catalyst. In this case just two intermediate compounds were captured. Small amounts of pentane were measured in the outgoing flow after reaction on Cu-Co oxide catalysts – up to 0,15 mmol/(1 g propyl acetate) on $Cu50\text{-}Co10/Al_2O_3$ and ~0,01 mmol/(1 g of propyl acetate) on $Cu50\text{-}Co50/Al_2O_3$. Another intermediate compound was 1-propanol, which was found in all analyzed gaseous streams. 1-Propanol maximum content reached ~0,6 mmol/(1 g of propyl acetate) for $Cu50/Al_2O_3$; $Cu50\text{-}Co10/Al_2O_3$; $Cu50\text{-}Co50/Al_2O_3$ catalysts while for $Cu50\text{-}Cr10/Al_2O_3$ and $Cu50\text{-}Cr50/Al_2O_3$ samples this concentration was more than two times smaller – 0,27 and 0,21 mmol/(1 g of propyl acetate) respectively. Also, the positive effect of increased selectivity because of addition of Cr was confirmed by measurements of CO concentration. It was determined that using Cu-Cr oxide catalysts the CO maximum concentration decreased by more than two times when compared to CuO catalyst and by around 30 % when compared to Cu-Co oxide catalysts.

References

1. W Y. Jung, S. S. Hong. J. Nanosci. Nanotechnol. **5** (2016) 4576-4579.
2. M. B. Gawande, R. K. Pandey R., V. Jayaram. Catal. Sci. Technol. **2.6** (2012) 1113-1125.

P 032

Fractionation of Lipophilic Components of Chokeberry Pomace by Innovative Extraction Technique

L. Jūrienė[1*], A. Pukalskas[1], P. R. Venskutonis[1]
[1]Kaunas University of Technology, Radvilėnų pl. 19, LT-50254 Kaunas, Lithuania
**Corresponding author, e-mail:laura.juriene@ktu.lt*

Black chokeberries have a strong mouth-drying effect, for this reason, most of times these berries are used to make jams, juices, purées, jellies, syrups, teas or wines [1]. Pressing juices of these berries generates large amounts of pomace, which usually is discarded or used very inefficiently. For this reason, is very urgent to find a way how to recover high added value bioactives. It is well known that chokeberries are characterized by strong antioxidant properties due to high content of polyphenolic compounds, whereas its pomace is also rich in bioactives, especially anthocyanins, procyanidins, flavonols and phenolic acids; although these pomaces are a good source of lipophilic compounds such as fatty acids, triacylglycerols, tocopherols etc [2]. The aim of this study was to evaluate the possibilities of fractionation of the chokeberry pomace lipophilic fraction during supercritical fluid extraction with carbon dioxide (SFE-CO_2) with or without co-solvent ethanol (5%) in two post-extraction separators by changing the temperature in the range of subcritical CO_2 level at a constant pressure and to characterize the composition of the obtained fractions. SFE with pure CO_2 gave a 14% lower yield, while the addition of 5% co-solvent EtOH increased the yield. In the case of SFE with pure supercritical CO_2 the highest amount of the total extract was collected in first separator (1S), the remaining in second separator (2S). In the case of SFE with supercritical CO_2 and 5% EtOH, the effects of separation were not so negligible; although almost in all cases higher yields were detected in second separator. The antioxidant capacity of extracts and fractions was measured by using an L-ORAC assay which measures the peroxyl radical scavenging capacity of antioxidants which may donate a hydrogen atom. First of all, it may be noted that the ORAC values of lipophilic extracts obtained in first separator by pure supercritical CO_2 and 5% co-solvent EtOH were 2 folds higher than those of extracts obtained by supercritical CO_2. While in second separator antioxidant capacity was quite similar in both cases. Highly unsaturated TAGs were majorly found in the extracts and fractions. The LLLn constituted 23.26–24.18%, OLnL 20.35–22.10%, LLnLn 13.20–15.10% and OLL 10.02–12.06%. Four tocopherols (sometimes also called E-vitamers) and 4 phytosterols were preliminarily quantified by their peak areas in the extracts and fractions. It may be observed that, in the case of pure supercritical CO_2, the concentration of tocopherols was higher in second separator, while the content of phytosterols was slightly higher in first. The addition of co-solvent 5% EtOH increased the concentration of these compounds in second separator. It might be concluded that, by modifying the supercritical extraction solvent and changing the parameters of the system separators, it is possible to produce fractions of lipophilic substances of various compositions.

References

1. V. Kitryte, V. Kraujaliene, V. Sulniute, A. Pukalskas, P.R. Venskutonis, Chokeberry pomace valorization into food ingredients by enzyme-assisted extraction: Process optimization and product characterization. Food and Bioproducts Processing 105, 36-50 (2017).
2. A. Sidor and A. Gramza-Michałowska, Black chokeberry Aronia Melanocarpa L.—A qualitative composition, phenolic profile and antioxidant potential, Molecules 24(20), 3710 (2019).

P 033

Catalytic Hydrogen Evolution Reaction on a Composite p-Si/Al_2O_3/Ni Photoelectrode

E. Juzeliūnas[1]*, P. Kalinauskas[1], L. Staišiūnas[1], A. Grigucevičienė[1], K. Leinartas[1], D. Bučinskienė[1], A. Šilėnas[1]

[1]Centre for Physical Sciences and Technology, Saulėtekio av. 3, LT-10257, Vilnius, Lithuania
**Corresponding author, e-mail: eimutis.juzeliunas@ftmc.lt*

Hydrogen generation from water by its photoelectrochemical splitting offers a great opportunity for solar energy accumulation and transmitting with a very low carbon footprint. There is, therefore, permanent demand in efficient and low-cost photoelectrodes for hydrogen evolution reaction (HER). Silicon-based photoelectrodes are most promising due to its narrow band gap, which seamlessly matches solar spectrum and efficiency absorbs photons. Silicon is likely to dominate the solar energy market for the next few decades [1].

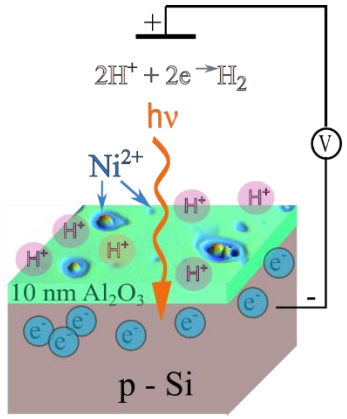

Fig. 1. Schematic representation of hydrogen reduction at Ni microcatalyst formations by the photoelectrons induced in p-Si/Al_2O_3 electrode.

We developed a photoelectrode for HER, which is based on p-type silicon (p-Si) passivated with ultrathin (10 nm) Al_2O_3 layer and modified with microformations of Ni catalyst (Fig. 1). The alumina layer has been formed by the atomic layer deposition (ALD), while nickel microcatalyst was deposited photoelectrochemically (PEC). The alumina film improves the electronic properties of silicon and, at the same time, protects the substrate from corrosion and enables PEC deposition of Ni microformations. The Ni catalyst increased the HER rate up to one order of magnitude. Such rate was comparable with the rate measured on a coating-free hydrogen-terminated electrode.

Properties of the alumina film have comprehensively been studied using various techniques: grazing incidence X-ray diffraction (GIXRD), optical profilometry, spectroscopic ellipsometry (SE), quartz crystal nanogravimetry (QCN), resistivity measurements, and photoelectrochemistry. Considerable attention was paid to postdeposition annealing, which substantially reduces Si surface recombination velocities. It was determined that annealing at 400 °C increases the electric resistance of Al_2O_3 layer as well as its resistance against electrolyte penetration, thereby enhancing the electrode stability in the electrolyte.

References

1. E. Juzeliūnas, Silicon. Electrochemistry, production, purification and applications. Wiley-VCH, 2023.

P 034

Finding Potential Phase Change Materials Among Ionic Liquids with The Aid of Machine Learning Model

L.-M. Kaljusmaa[1,*], O. Järvik[1]
[1]*Tallinn University of Technology, Ehitajate tee 5, 19086 Tallinn, Estonia*
**Corresponding author, e-mail: liisamaria.kaljusmaa@taltech.ee*

Ionic liquids (IL) can be potential phase change materials (PCM) for thermal energy storage [1]. To find the best PCM candidates among these materials with high enthalpy of fusion values the application of machine learning (ML) could be beneficial. The results as root mean square error (RMSE) of implementing extreme gradient boosting (XGBoost) ML algorithm on enthalpies of fusion of ILs found from NIST Ionic Liquids Database (SRD 147) v2.0 [2] are shown in Table 1. Data distribution is illustrated on Fig. 1.

Dataset	$RMSE_{training}$	$RMSE_{test}$
390 IL	33.72	45.00
386 IL	21.74	38.93
127 ammonium cation IL	21.59	42.61
111 imidazolium cation IL	22.29	26.92

Table 1. ML results for 4 datasets, test dataset formed 25% of each dataset

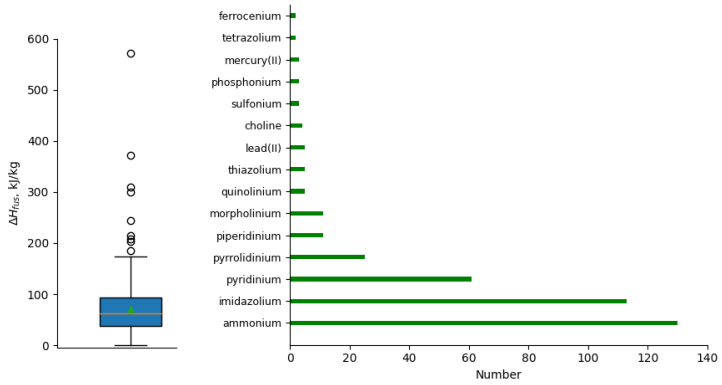

Fig. 1. Data distribution of 390 ILs with their experimental enthalpy of fusion values (ΔH_{fus}, kJ/kg)

The smaller difference between test and training RMSE was gained with imidazolium cation ILs when test dataset contained more ILs with a similar structure and enthalpy of fusion values as ILs in the training dataset. As the quality and the quantity of current available data on ILs thermal properties is questionable then it is important to be critical about the reported ML results gained with smaller datasets and to highlight the need for trustworthy experimental data on ILs thermal properties. In addition, it would be useful to focus on certain cation and anion types to gain further knowledge about the thermal behavior of ILs and a ML model with molecule design capability to find PCMs with desirable properties.

References

1. S. L. Piper, M. Kar, D. R. MacFarlane, K. Matuszek, and J. M. Pringle, "Ionic liquids for renewable thermal energy storage – a perspective," *Green Chemistry*, vol. 24, no. 1, pp. 102–117, Jan. 2022, doi: 10.1039/D1GC03420K.
2. Dong, Q.; Muzny, C.D.; Kazakov, A.; Diky, V.; Magee, J.W.; Widegren, J.A.; Chirico, R.D.; Marsh, K.N.; Frenkel, M., "ILThermo: A Free-Access Web Database for Thermodynamic Properties of Ionic Liquids." J. Chem. Eng. Data, 2007, 52(4), 1151-1159, doi: 10.1021/je700171f.

The financial support from the Estonian Research Council under the project PRG1784 „Sustainable and Effective Materials for Latent Heat Thermal Energy Storage Based on Amine Ionic Liquids" is greatly appreciated.

P 035

On the Synthesis of New $Y_{3-x-y-z}Ca_xLi_y Ce_zGa_5O_{12}$ Garnets

A. Nurpeissov[1], D. Vistorskaja[2], S. Pazylbek[2,3], D. Karoblis[2], A. Lukowiak[4], W. Strek[4], A. Laurikenas[2], T. Nurakhmetov[1], T. Raudonis[2], A. Zarkov[2], A. Kareiva[2,*]

[1] Department of Technical Physics, L.N. Gumilyov Eurasian National University, 2 Satpaeva St, Nur-Sultan ZO1A3D7, Kazakhstan

[2] Institute of Chemistry, Faculty of Chemistry and Geosciences, Vilnius University, Naugarduko 24, LT-03225 Vilnius, Lithuania

[3] Department of Mathematics and Computer Science, Tashenev University, 27 A Tokayev, Shymkent 160005, Kazakhstan

[4]Institute of Low Temperature and Structure Research, Polish Academy of Sciences, Okolna 2, PL-50422 Wroclaw, Poland

**Corresponding author, e-mail: aivaras.kareiva@chgf.vu.lt*

The main goal of this study is to investigate the preparation conditions of new high-entropy ($Y_{3-x-y-z}Ca_xLi_yCe_zGa_5O_{12}$) materials. In this paper we present a simple "chimie douce" synthetic approach to the mixed-metal $Y_{3-x-y-z}Ca_xLi_yCe_zGa_5O_{12}$ garnets using citric acid as complexing agent in the sol-gel processing. The results obtained confirm the efficiency of the suggested method for the preparation of multinary mixed-metal oxides.

The results summarized in this article demonstrate that an aqueous sol-gel processing route is suitable for the preparation of polycrystalline garnet crystal structure compounds having new chemical compositions $Y_{3-x-y-z}Ca_xLi_yCe_zGa_5O_{12}$. High-quality precursor gels were obtained using reaction of formation of coordination compounds of metal ions with citric acid. The main weight losses during thermal decomposition of gels were observed in the temperature ranges of ~30–240 °C and ~240–490 °C. The final decomposition step ended at about 850 °C. According to the XRD analysis results, the single garnet crystal structure compounds with different chemical compositions $Y_{3-x}Ca_xGa_5O_{12}$, $Y_{3-x-y}Ca_xLi_yGa_5O_{12}$, $Y_{3-x-z}Ca_xCe_zGa_5O_{12}$ and $Y_{3-x-y-z}Ca_xLi_yCe_zGa_5O_{12}$ were obtained at low substitutional level by heating of precursor gels for 5 h already at 1000 °C. With increasing amount of Ca, Li and Ce ions the cubic garnet phase was determined as the main crystalline phase, however, the impurity phases were also formed. The XRD analysis results were fully supported by FTIR spectroscopy data. The FTIR spectra recorded for the $Y_{3-x-y-z}Ca_xLi_yCe_zGa_5O_{12}$ samples were almost identical. It is well known that the FTIR spectra of the garnets usually contain several intense peaks in the range of 1000–400 cm^{-1}. The typical absorption bands for garnets in the range of 1000–400 cm^{-1} were split to the several intense peaks attributable to the stretching mode of the tetrahedral units. The surface morphology of the sol-gel derived $Y_{3-x-y-z}Ca_xLi_yCe_zGa_5O_{12}$ garnets was very similar for all samples and the volumetric grains were composed of spherical particles, with an average particles 50-120 nm in size. It could be concluded that the proposed aqueous sol-gel processing approach is appropriate for the fabrication of high-entropy garnet crystal structure compounds.

Acknowledgement. The work has been done in frame of the project TransFerr. This project has received funding from the European Union's Horizon 2020 research and innovation program under the Marie Sklodowska-Curie grant agreement no. 778070.

P 036

Molten Salt Synthesis of $REMnO_3$ (RE – Y, Er, Tm, Yb) Manganites

D. Karoblis[1,*], A. Zarkov[1], A. Kareiva[1]
[1]Institute of Chemistry, Vilnius University, Naugarduko 24, LT-03225 Vilnius, Lithuania
**Corresponding author, e-mail: Dovydas.karoblis@chgf.vu.lt*

Yttrium, erbium, thulium and ytterbium manganites ($REMnO_3$, where RE – Y, Er, Tm, Yb) belong to the hexagonal manganites family, which are known for its multiferroic properties [1]. These compounds display trimer structural distortion, which gives a rise to the polarization, bulk magnetization as well as magnetoelectric effect [2]. Traditionally, these materials are prepared by conventional solid-state method, which has various disadvantages, including several reaction steps, long reaction times, the use of high temperature, slow precursor diffusion and etc. In order to avoid these drawbacks, synthesis of these manganites can be performed in the inorganic salt medium, above its melting point. Moreover, molten salt synthesis method does not require sophisticated equipment, is cheap, easy to up-scale and formation of nanoparticles is possible [3].

In this work, we demonstrate that molten salt synthesis using nitrates and NaCl-KCl salts as reaction medium can be applied to prepare various manganites. The structural properties of the obtained specimens were characterized by X-ray diffraction analysis, and FT-IR spectroscopy, while surface morphology was investigated using scanning electron microscopy. Our study reveals that hexagonally shaped particles with hexagon side length in micrometer scale can be synthesized (Fig. 1).

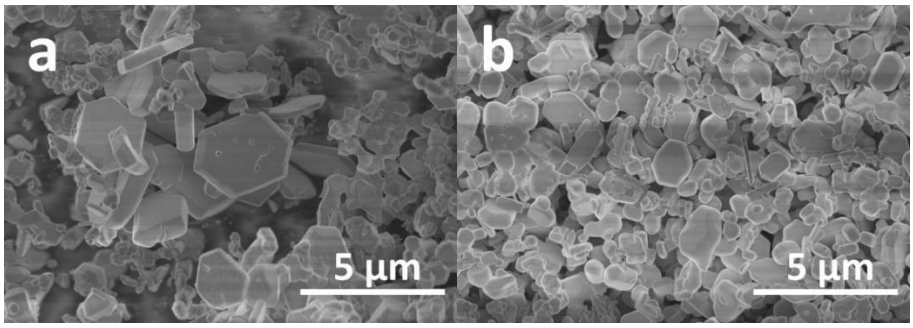

Fig. 1. SEM micrographs of $ErMnO_3$ (a) and $TmMnO_3$ (b).

Acknowledgements

This project received funding from the European Union's Horizon 2020 research and innovation programme under the Marie Skłodowska-Curie grant agreement No. 778070–TransFerr–H2020-MSCA-RISE-2017.

References

1. M. Lilienblum, T. Lottermoser, S. Manz, S.M. Selbach, A. Cano, M. Fiebig, Nat. Phys. **11** (2015) 1070-1073.
2. H. Das, A.L. Wysocki, Y. Geng, W. Wu, C.J. Fennie, Nat. Commun. **5** (2014) 1-11.
3. S.K. Gupta, Y. Mao, Prog. Mater. Sci. **125** (2021) 100734.

P 037

Investigation of Hexafluoroisopropanol-Based Aqueous Biphasic System

V. Kavaliauskas*, V. Olšauskaitė, A. Padarauskas
Vilnius university, Faculty of Chemistry and Geosciences, Naugarduko 24, 03225 Vilnius, Lithuania
**Corresponding author, e-mail: vytautas.kavaliauskas@chf.vu.lt*

Aqueous biphasic system (ABS) is a liquid-liquid fractionation technique, which has gained an interest because of great potential for the extraction and enrichment of various organic and inorganic pollutants from aqueous samples [1]. ABS formation, which is a kind of soluting-out phenomena, appears when combination of two water miscible compounds display incompatibility in aqueous media above critical concentrations [2, 3]. Typical mixtures are composed of two hydrophilic polymers or salts, or a combination of polymer and salt [4, 5]. However, since volatile organic compounds are not employed in such systems, they are hardly compatible with modern separation techniques such as chromatography with its various modes.

In this study, a novel hexafluoroisopropanol (HFIP) based ABS system was investigated and its extraction properties for the extraction of various organic compounds from aqueous solutions were tested.

In initial experiments, common polar organic solvents (acetonitrile, ethanol, isopropanol, acetone, dimethylsulfoxide, dimethylformamide and tetrahydrofuran) were tested as soluting-out agents of the HFIP phase. The ABS formation procedure was done in the following order: 5.0 mL of 0.02 mmol/L aqueous alizarin solution was placed into a glass centrifuge tube, then 3.0 mmol soluting-out agent and 0.3 mL HFIP were sequentially added. The mixture was shaken manually for 30 s, resulting in the formation of emulsion. The phases were separated by centrifugation at 3000 rpm for 5 min. Alizarin dye was added into the water solution to visualize the phase separation. Obtained results showed that only aprotic solvents act as soluting-out agent. The formed HFIP phase volumes decrease in the following order: tetrahydrofuran > acetone ≈ dimethylformamide > ACN > dimethylsufoxide. This indicates that soluting-out ability of the solvents correlates with their hydrophilicity: higher HFIP phase volumes were obtained using less hydrophilic soluting-out agents.

Next, the extraction properties of the HFIP-ACN-based ABS system were evaluated. Aromatic hydrocarbons, esters, hydroxyesters, amines, carboxylic acids, phenols and synthetic dyes were employed as model analytes. As expected, for structurally related analytes their extraction efficiency values showed good correlation with their hydrophobicity (i.e., log *P* values). For example, the extraction efficiencies of hydroxyesters (parabens) increase in the following order: methylparaben < ethylparaben < propylparaben < butylparaben. Such trend was also observed within other analyte groups studied.

Surprisingly, in contrast to conventional organic solvents, proposed ABS system exhibits significant extraction selectivity within different classes of analytes having close hydrophobicity. For selected analytes with similar log *P* values, their extraction efficiencies decrease from 98% (nicotine) to 25% (benzoic acid) in the following order: nicotine ≈ dimethylphthalate ≈ benzene > methylparaben > quercetin ≈ benzoic acid. This suggests that the ABS system exhibits significantly better extractability for basic and neutral organic compounds comparing with acidic ones.

The obtained results demonstrate that developed HFIP-ACN-based ABS system may be considered as very promising alternative extractant for various organic compounds from aqueous samples.

References

1. R.C. Assis, A.B. Mageste, L.R. de Lemos, R.M. Orlando, G.D. Rodriges, Talanta, **223** (2021) 121697.
2. R. Hatti-Kaul, Mol. Biotechnol., **19** (2001) 269-277.
3. P.E. Kee, T.C. Ng, J.C.W. Lan, H.S. Ng, Crit. Rev. Biotechnol., **40** (2020) 555-569.
4. J.A. Asenjo, B.A. Andrews, J. Chromatogr. A, **1218** (2011) 8826-8835.
5. Y.C. Chao, H.C. Shum, Chem. Soc. Rev., **49** (2020) 114-142.

P 038

Synthesis of 5-(2,4-Dihydroxyphenyl)imidazole Derivatives as Potential Hsp90 Inhibitors

P. Kaziukonytė*, V. Petraška, A. Brukštus

Vilnius University, Department of Chemistry and Geosciences, Institute of Chemistry, Naugarduko str. 24, LT-03225 Vilnius, Lithuania

**paulina.kaziukonyte@chgf.vu.lt*

Heat Shock Protein 90 (Hsp90) is an ATP-dependent molecular chaperone, responsible for the folding, correction, activation, and deactivation of its client proteins. [1] Despite Hsp90 having an important role in normal cell cycle regulation, it is also involved in the stabilization of oncogenic proteins. [2] Therefore, it is proposed that inhibiting ATP binding site with small-molecule inhibitors could lead to effective cancer therapy, with some synthetic compounds already going through clinical trials. [3]

A promising class of inhibitors is compounds containing 1,3-benzenediol moiety, based on the natural compound Radicicol. Active structures are usually composed of aromatic substitutes linked to 1,3-benzenediol by a 5-membered heterocyclic ring. Continuing our previous research on 4-(2,4-dihydroxyphenyl)-1,2,3-thiadiazoles as potential Hsp90 inhibitors [4], we decided to synthesize a series of 5-(2,4-dihydroxyphenyl)imidazoles (**2**).

Van Leusen reaction was employed to obtain imidazoles **2** from imines **1** and toluenesulfonylmethyl isocyanide (TosMIC). The reaction was held in methanol and basic conditions at room temperature for 72 hours. Additionally, an unexpected formation of compounds **3** was observed and investigated further.

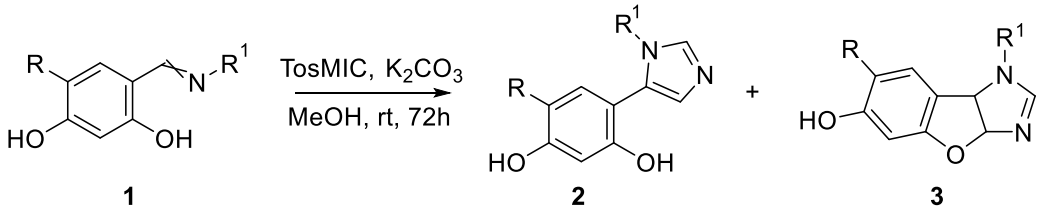

Scheme 1

References

1. J. Hahn, BMB Rep., **42(10)** (2009) 623-630.
2. Y. Miyata, H. Nakamoto, L. Neckers, Curr. Pharm. Des., **19(3)** (2013) 347-365.
3. A. Yuno, M. Lee, S. Lee, Y. Tomita, D. Rekhtman, B. Moore, J. B. Trepel, Methods Mol. Biol., **1709** (2018) 423-441.
4. E. Kazlauskas, A. Brukstus, H. Petrikas, V. Petrikaite, I. Cikotiene, D. Matulis, Anticancer Agents Med. Chem., **17(11)** (2017) 1593-1603.

P 039

Influence of Hydrothermal Synthesis Parameters on the Properties of Calcium Hydroxyapatites

G. Klydžiūtė[1,*], E. Raudonytė-Svirbutavičienė[1,2], A. Žarkov[1], A. Kareiva[1], A. Beganskienė[1]

[1]Institute of Chemistry, Faculty of Chemistry and Geosciences, Vilnius University, Naugarduko Str. 24, LT-03225 Vilnius, Lithuania

[2]Institute of Geology and Geography, Nature Research Centre, Akademijos Str. 2, LT-08412, Vilnius, Lithuania

**gabriele.klydziute@chgf.stud.vu.lt*

Because of the flexibility in the structure of calcium hydroxyapatite (Ca-HAp), various cations, such as copper, can substitute Ca^{2+} in Ca-HAp in order to improve desirable properties [1]. It is essential to develop cost-effective and efficient synthesis methods which would at the same time provide the possibility to control the properties of the products.

This study investigates the influence of hydrothermal synthesis parameters on the properties of copper-substituted hydroxyapatites. For this purpose, α-TCP was synthesized by wet precipitation method and used as a precursor of HAp [2]. Hydrolysis reactions were performed in aqueous solutions under hydrothermal conditions at 120 °C and 200 °C for 3 and 5 hours, respectively. Copper-substituted hydroxyapatites were obtained by introducing divalent cations (Cu^{2+}) to the hydrolysis aqueous solutions or by inserting it directly into the structure of the precursor during its synthesis. The concentration of the metal ions corresponded to Ca-HAp substitution level of 0.8 mol %. The phase purity and morphology of hydrolysis products was investigated with XRD and SEM, respectively.

The purity of the copper-substituted HAp phase depends on the hydrothermal synthesis parameters. Formation of HAp phase under hydrothermal conditions at 120 °C for 3 hours was less efficient and some remaining α-TCP was left after the hydrothermal treatment (Fig. 1). It is crucial to select the most optimal reaction conditions to obtain desired characteristics of the final product. Direct ions incorporation into precursors structure before the hydrolysis yields the formation of rod-like crystals as well as provides an increased surface area. The results of this study show that foreign ions could be applied as HAp morphology-controlling additives during the hydrothermal synthesis.

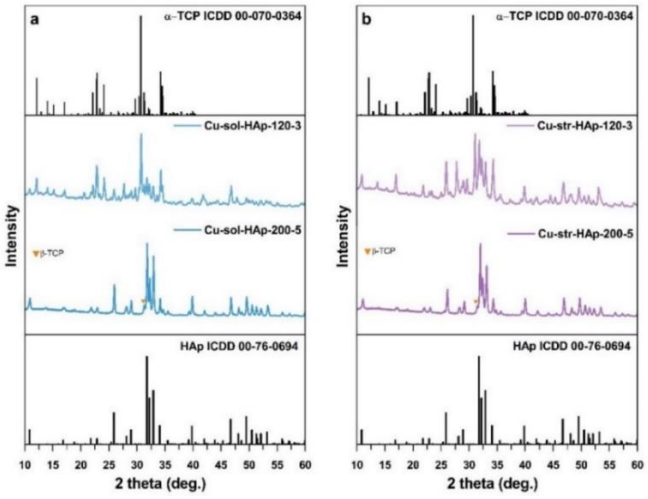

Fig. 1. XRD patterns of Cu^{2+} doped α-TCP powders after hydrolysis reactions.

References

1. S. Shanmugam, B. Gopal, Copper substituted hydroxyapatite and fluorapatite: Synthesis, characterization and antimicrobial properties, Ceramics International 40, 15655-15662 (2014).
2. L. Sinusaite, I. Grigoraviciute-Puroniene, A. Popov, K. Ishikawa, A. Kareiva, A. Zarkov, Controllable synthesis of tricalcium phosphate (TCP) polymorphs by wet precipitation: Effect of washing procedure. Ceram. Int., 45, 12423– 12428 (2019).

P 040

Garnets as Systems for Endogenous Dynamic Nuclear Polarization (DNP)

V. Klimavičius[1]*, G. Inkrataitė[2], V. Kalendra[1], A. Kareiva[2], G. Buntkowsky[3]

[1]Faculty of Physics, Vilnius University, Saulėtekio ave. 3, LT-10257 Vilnius, Lithuania

[2]Institute of Chemistry, Vilnius University, Naugarduko 24, LT-03225Vilnius, Lithuania

[3]Eduard-Zintl Institute for Inorganic and Physical Chemistry, TU- Darmstadt, Alarich-Weiss-Straße 8, DE-64287 Darmstadt Germany

**Vytautas Klimavičius, e-mail: vytautas.klimavicius@ff.vu.lt*

Dynamic Nuclear Polarization (DNP) is a hybrid solid state NMR technique which is based on strong electron polarization transfer to the nuclei of interest by introducing microwave irradiation. This allows to boost NMR sensitivity up to hundreds of times. In order to transfer strong electron polarization, the studied system has to contain unpaired electrons which is typically implemented by introducing stable radicals dissolved in an organic matrix. Nevertheless, such approach has a major drawback, namely the studied system is modified by unwanted radicals and organic solvents. To overcome this issue, recently an alternative approach was offered – endogenous DNP.[1] In this approach the system of interest is doped with paramagnetic metal ions which serve as an electron polarization source. What is more, paramagnetic metal ions such as Mn^{2+}, Fe^{3+}, Cr^{3+}, etc. are often used to tune the inorganic systems properties as luminescence, magnetic properties, biocompatibility, etc. If such paramagnetic ions could be used as polarization source for DNP, the drawback of modification of the system is overcome.

Therefore, yttrium aluminium garnets ($Y_3Al_5O_{12}$, YAGs) doped with Mn^{2+}, Fe^{3+}, Cr^{3+}, Gd^{3+} were chosen to investigate the possibility to obtain endogenous DNP effect. The doping distribution and levels were tested using SEM EDX analysis as well as EPR spectroscopy at X- and Q- bands. Further analysis was performed using ^{27}Al MAS solid state NMR spectroscopy and spin-lattice T_1 relaxation analysis. Ultimately, the DNP enhanced ^{27}Al MAS investigation was performed which showed that the signal corresponding to AlO_6 species is effectively enhanced. The magnetic field sweep experiments allowed to meet the best matching condition and the highest enhancement factor achieved is about 3 which corresponds to time saving of nearly 10. Fe^{3+} was found to be the most promising polarizing dopant in studied systems.

The ultimate goal for this research is to further tune the systems to reach the highest enhancement factors which would allow to detect ^{89}Y and ^{17}O signals. These are nearly impossible to detect using conventional solid-state NMR methods.

Funding by Vilnius University Science Promotion Foundation (MSF-JM-5/2022) is gratefully acknowledged.

References

1. T. Wolf, S. Kumar, H. Singh, T. Chakrabarty, F. Aussenac, A. I. Frenkel, D. T. Major, M. Leskes, J. Am. Chem. Soc., 141, 1 (2019) 451–462.

P 041

The Interaction of Monoammonium Phosphate with Zinc Sulphate and Starch Solutions

K. Krasauskaitė*, R. Šlinkšienė

Kaunas University of Technology, Radvilėnų pl. 19, 50254 Kaunas, Lithuania
**Corresponding author, e-mail: klaudija.krasauskaite@ktu.edu*

Monoammonium phosphate (MAP) – fully soluble in water, concentrated nitrogen-phosphorus fertilizers. Plants fertilized with these fertilizers easily absorb nutrients needed for growth and development of the plants. Next-gen, environmentally friendly, efficient and top-quality MAP fertilizers are used in agriculture for fertilizing various crops and soils. However, fertilizing becomes even more effective when complex fertilizers are used in combination with trace elements. This ensures the sustainable and stable growth of various food grains, oilseeds and legumes. Trace elements are necessary in agriculture in order to increase yields and improve the quality of agriculture production. Although these trace elements are needed in very small amounts, plants consume them for important functions [1-2]. During production, trace elements can be incorporated directly into monoammonium phosphate (MAP) or diammonium phosphate (DAP) fertilizers. This technology ensures a constant concentration of the desired trace element in each fertilizer granule and their uniform distribution in the soil [3].

In this experimental work, crystalline MAP was granulated by adding 0.495% zinc sulphate and using different amounts 2, 3, 4 and 5% of starch solution as binder. A laboratory drum granulator was used during process (Figure 1).

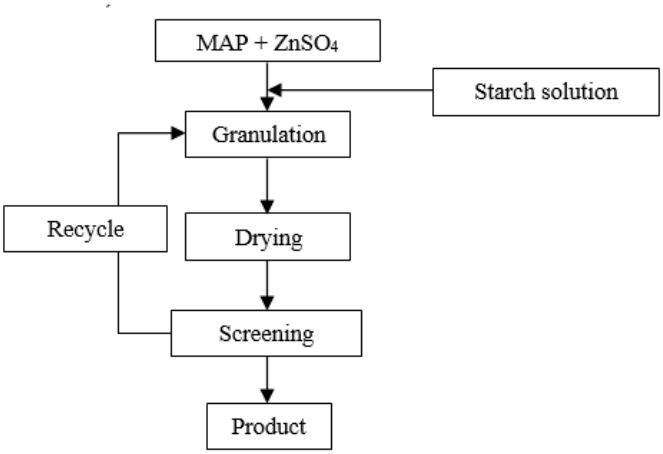

Fig. 1. MAP with zinc sulphate granulation process scheme

After screening process, marketable granular product (MAP + 0.2Zn) which size of granules is 2–4 mm was analyzed for their main properties such as granule strength, pH of 10 % solution, bulk density, hygroscopicity, etc. It was determined that the largest (30.14%) of the marketable fraction is obtained when a 2% starch solution was used, and its amount in total mass of the raw material mixture was 22.5%.

Acknowledgements. This research was supported by the project funded by LMT No. P-ST-22-118

References

1. Mordor Intelligence LLP. Global Agricultural Chelates Market, 2019.
2. X. Hu, X. Wei, J. Ling, J. Front. Plant Sci., **12** (2021) 1-24.
3. L. A. Peacock, R. Johnston, US Pat. 20150251962A1 (2015).

P 042

3,6-Diarylcarbazoles for Hole Transporting Layers of SOLAR Cells

G. Krucaite[1*], D. Tavgeniene[1], S. Grigalevicius[1], Bi. Huan[2], Z. Zhen[2], G. Kapil[2], S. Qing[2], S. Hayase[2], E. Zaleckas[3]

[1] Department of Polymer Chemistry and Technology, Kaunas University of Technology, Kaunas, Lithuania,
[2] University of Electro-Communications, 1-5-1 Chofugaoka, Chofu, Tokyo182-8585, Japan,
[3]Vytautas Magnus University, Agriculture Academy, Department of Agricultural Engineering and Safety, Studentu str. 11, LT-53361, Akademija, Kaunas distr., Lithuania
** e-mail address of presenter: gintare.krucaite@ktu.lt*

Organic photovoltaic (OPV) solar cells aim to provide an Earth-abundant and low-energy-production photovoltaic solution. This technology also has the theoretical potential to provide electricity at a lower cost than first- and second-generation solar technologies. Although numerous high-performance electron transporting layers have already been developed and deployed in state-of-the-art OPVs, reports on hole transporting layers (HTLs) remain scarce [1-3]. Herein we report two diaryl-substututed carbazoles and their application as hole-extracting interlayers in OPVs.

The synthesis of diaryl-substituted carbazoles compounds (**1-2**), was done in a multistep synthetic procedure, starting from commercially available carbazole. 9H-carbazole was alkylated, then brominated and by the means of Arbuzov reaction, aliphatic bromide was transformed into phosphonic acid ethyl ester. Dibromo atoms were changed by palladium-catalysed Suzuki reaction to yield carbazoles containing naphtalene or phenylcarbazole fragments. Finally, the cleavage of the ester utilising bromotrimethylsilane resulted in phosphonic acid containing substituted carbazole fragments as shown in Figure 1.

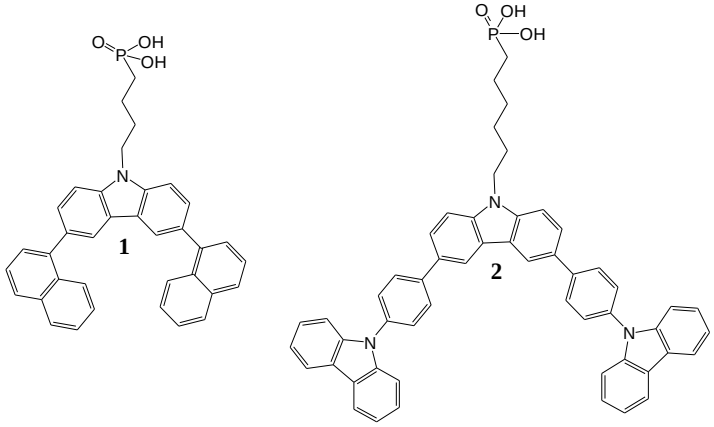

Figure 1. Structures of the diaryl-substituted carbazoles.

Tin-lead perovskite solar cells were fabricated as reported before [4]. In this work, we employed the different newly synthesized hole transporting self assembled monolayers (SAM) with phosphonic acid anchoring groups. Some of the devices yielded a maximum power conversion efficiency (PCE) higher than 5.4 %.

Acknowledgements. This work was supported by project funded by the Research Council of Lithuania (grant No. S-LJB-22-2).

References

1. Y. Lin, Y. Firdaus, F. H. Isikgor, M. I. Nugraha, E. Yengel, G. T. Harrison, R. Hallani, A. El-Labban, H. Faber, C. Ma, X. Zheng, A. Subbiah, C. T. Howells, O. M. Bakr, I. McCulloch, S. D. Wolf, L. Tsetseris, T. D. Anthopoulos. ACS Energy Letter., **5** (2020) 2935–2944.A.A. Autor, B. Autor, The Chemical Synthesis. Wiley & Sons, New York, 1999.
2. Y. Lin, B. Adilbekova, Y. Firdaus, E. Yengel, H. Faber, M. Sajjad, X. Zheng, E. Yarali, A. Seitkhan, O. M. Bakr, A. El-Labban, U. Schwingenschlogl, V. Tung, I. McCulloch, F. Laquai, T. D. Anthopoulos. ADV mat., **31** (2019) 1902965 - 1902974.
3. Z. Zheng, Q. Hu, S. Zhang, D. Zhang, J. Wang, S. Xie, R. Wang, Y. Qin, W. Li, L. Hong, N. Liang, F. Liu, Y. Zhang, Z. Wei, Z. Tang, T. P. Russell, J. Hou, H. Zhou. ADV mat., **30** (2018) 1801801-1801810.
4. G. Kapil, T. Bessho, Y. Sanehira, S.R. Sahamir, M. Chen, A. K. Baranwal, D. Liu, Y. Sono, D. Hirotani, D. Nomura, K. Nishimura, M. A. Kamarudin, Q. Shen, H. Segawa, S. Hayase. ACS Energy Let., 2022 (7), p. 966–974.

P 043

Synthesis and Characterization of Unsaturated Polyesters Modified with Malic Acid and PDMS for Tissue Engineering Applications

E. Kvietkauskas*, S. Budrienė
Department of Polymer chemistry, Vilnius University, Naugarduko 24, LT-03225 Vilnius, Lithuania
E-mail: evaldas.kvietkauskas@chgf.stud.vu.lt

Tissue engineering focuses on replacing damaged or diseased tissue by combining chemistry, engineering and biological sciences. To achieve this goal, tissue engineering must use 3D scaffold for cells to grow on and differentiate properly [1]. It is important for scaffold to be biocompatible, biodegradable and have certain mechanical properties for the tissue it needs to replace [2]. Scaffolds can be made out of metal, ceramic or polymer. Polyesters are biodegradable, biocompatible and mechanical properties can be tuned [3]. Polydimethylsiloxane (PDMS) is used in biomedical applications since it is nontoxic and transparent. But PDMS applications are limited due to hydrophobicity and poor mechanical properties [4]. These disadvantages can be decreased by modification of polyesters with PDMS and malic acid which is found in living organisms [5].

In this study, polyester was synthesized by polycondensation reaction between azelaic acid, maleic acid anhydride, diethylene glycol, PDMS and malic acid. Structure of polyester has been proven by NMR and FT-IR spectroscopy. Films from modified polyesters were produced by adding curing agents: glycidyl methacrylate, butyl methacrylate, acrylamide or bisacrylamide together with photo initiator 2,2-dimethoxy-2-phenylacetophenone and curing under UV light. Solubility and degree of swelling in three different solvents: hexane, ethanol and water were determined for all produced films. Thermal stability and degradation of films was investigated by thermogravimetric analysis. The Young's module and elongation at break of films were evaluated. The films exhibit good mechanical properties. It was obtained that the contact angle of water on films was lower and at the same the surface of films was more hydrophilic to compare with PDMS.

References

1. A. R Webb, J. Yang, G. A. Ameer, Expert Opin. Biol. Ther., 4(6) (2004) 801-812.
2. F. J. O'Brien, Mater. Today, 14(3) (2011) 88-95.
3. H. Ye, K. Zhang, D. Kai, Z. Li, X. Loh, Chem. Soc. Rev., 47 (2018) 4545-4580.
4. I. Miranda, A. Souza, P. Sousa, J. Ribeiro, E. M. S. Castanheira, R. Lima, G. Minas, J. Funct. Biomater., 13 (1) (2022) doi: 10.3390/JFB13010002.
5. D. G. Ryan, M. P. Murphy, C. Frezza, H. A. Prag, E. T. Chouchani, L. A. O'Neill, E. L. Mills, Nat. Metab. 1 (1) (2019) 16-33.

P 044

Investigation and Properties of Complexes of Anthocyanins and Cross-Linked Pectin or Sodium Alginate

D. Liudvinavičiūtė*, R. Grabauskaitė, R. Rutkaitė

Kaunas University of Technology, Radvilenu Rd. 19, LT-50524 Kaunas, Lithuania
**Corresponding author, e-mail: dovile.liudvinaviciute@ktu.lt*

Anthocyanins (ANC) are naturally occurring phenolic compounds responsible for the red, blue, and purple colors of fruits, vegetables and flowers [1]. These colorful compounds possess strong antioxidant, anti-inflammatory and antimicrobial properties, thus they could be utilized in such fields like pharmaceutics, food and active packaging. Introduction of ANC into these fields has proved to be a major challenge since ANC have low stability to environmental conditions during processing and storage [2]. ANC, due to their cationic nature could form complexes with natural or modified biopolymers having oppositely charged groups such as pectin (PCN) or sodium alginate (ALG).

The aim of present work was to obtain complexes of ANC and cross-linked PCN or ALG by using adsorption method, as well as to assess their properties.

PCN was cross-linked with epichlorohydrin to obtain insoluble low cross-linking degree PCN powder for ANC adsorption. Obtained cross-linked PCN with a cross-linking degree of 0.05 was denoted as $CPCN_{0.05}$. ALG with a M/G ratio in the interval of 0.9–1.1 was used for ANC adsorption.

For the formation of ANC and $CPCN_{0.05}$ or ALG complexes the desired amount of $CPCN_{0,05}$ or ALG powder was added to a desired amount of aqueous ANC solution and stirred for 90 min at room temperature, mixtures were centrifuged to isolate insoluble ANC and $CPCN_{0.05}$ or ANC and ALG complexes, the former was air dried at room temperature and the latter was freeze-dried afterwards. The residual concentration of ANC was determined and the amount of adsorbed ANC on $CPCN_{0.05}$ or ALG (expressed as grams of ANC per gram of $CPCN_{0.05}$ or ALG) was calculated. ANC-$CPCN_{0.05}$ and ANC-ALG complexes having 0.09 g/g and 0.1 g/g of adsorbed ANC were obtained.

Release of ANC from ANC-$CPCN_{0.05}$ (0.09 g/g) and ANC-ALG (0.1 g/g) complexes to different media, such as distilled water, 0.1 M HCl solution (simulated gastric medium), phosphate buffer solution of pH 6.8 (simulated intestinal medium) was investigated. 0.1 M HCl solution was the best medium for the release of ANC.

Antioxidant activity of ANC-$CPCN_{0.05}$ (0.09 g/g), ANC-ALG (0.1 g/g) complexes, ANC extract, ALG and $CPCN_{0.05}$ was evaluated by a modified ABTS method. ANC extract scavenged $ABTS^{\bullet+}$ instantly within the few minutes of the experiment. Neither $CPCN_{0.05}$ nor ALG alone showed antioxidant activity. Meanwhile, ANC-$CPCN_{0.05}$ (0.09 g/g) and ANC-ALG (0.1 g/g) complexes scavenged $ABTS^{\bullet+}$ gradually, which resulted in prolonged antioxidant activity.

References

1. V. P. Dia, Z. Wang, M. West, V. Singh, L. West, E. Gonzalez de Mejia, J. Agric. Food Chem., 63 (2015) 3205-3218.
2. P. Wesche-Ebeling, A. Argaiz-Jamet, In Engineering and food for the 21st century; Ed. Ch. Brennan, B. K. Tiwari, CRC Press, Boca Raton, 2002, p. 141−150.

P 045

Quantitative Analysis of Cadmium Telluride-Cadmium Sulphide Layers on Polyamide 6

M. Liudžiūtė[1*], S. Žalenkienė[1], I. Ancutienė[1]
[1]Department of Physical and Inorganic chemistry of Kaunas University of Technology, Radvilenu St. 19, 50254 Kaunas, Lithuania
migle.liudziute@ktu.edu

Photovoltaic (PV) technologies are one of the most promising aspects of clean and sustainable energy. According to the researchers second generation thin films such as amorphous silicon, cadmium telluride is among the most important materials for PV applications [1]. Therefore, the production of traditional silicon-based PV is quite complex and expensive [2]. In this case, research on cadmium telluride (CdTe) is expanding. It is an excellent substance due to its direct band gap of 1.4-1.6 eV and high absorption coefficient (~10^5 cm^{-1}). In addition, the production of CdTe for PV technology is 40 % cheaper than amorphous-Si technology and the efficiency aims to be 22.1 percent [3]. However, to increase the efficiency of these PVs, CdTe-CdS superstrates are designed. Cadmium sulphide (CdS) is used as a window layer for better optical and thermal properties [4]. In this study the preparation of thin layers composed of CdTe/CdS mixture on polyamide 6 (PA6) is investigated and the quantitative analysis of those layers is performed by atomic absorption spectroscopy (AAS) method.

Polyamide 6 films used in this study had a thickness of 500 µm, a density of 1.13 g/cm^3 and a size of 15×70 mm. One part of the PA films was boiled in distilled water for 2 h (Sample 1, S1) while the other part was treated in concentrated acetic acid at 20 °C for 0.5 h (Sample 2, S2). After that, they were modified using a two-step process. Firstly, PA 6 films were chalcogenized from 1 to 5 h at 20 °C using an acidified 0.1 mol·dm^{-3} solution of $K_2TeS_4O_6$. The salt of potassium telluropentathionate ($K_2TeS_4O_6$×1.5H_2O), was prepared according to published procedure [5]. Secondly, chalcogenized PA samples were treated with the 0.1 mol·dm^{-3} solution of cadmium acetate, $Cd(CH_3COO)_2 \cdot 2H_2O$, for 10 min at the temperatures of 70, 80, 90 °C (S1*, S2*).

Quantitative analysis of CdTe/CdS layers on PA 6 film was carried out by atomic absorption spectroscopy (AAS) method using the OPTIMA 8000 ICP-Optical Emission Spectrometer (PerkinElmer, Connecticut, USA). The solution for analysis was prepared by dissolving pieces of samples weighing 0.02-0.05 g in 5 ml of concentrated nitric acid. The resulting solution was boiled for 30 min in a water bath. During this process irreversible destruction of PA occurs and nitrogen oxides are removed. After boiling, the solution is diluted to the required volume and used for analysis.

Using the method of AAS analysis it was found that the concentrations of sulphur and tellurium in PA6 depend on the method of preparing PA6 films and different durations of chalcogenization. The influence of the treatment temperature with $Cd(CH_3COO)_2$ solution on the concentrations of sulphur and tellurium was also established. To compare the difference in concentrations the tests were carried out after the first stage and then after the second stage.

The results show that with increasing chalcogenization time, the concentration of sulphur and tellurium increases. Which ultimately leads to more $TeS_4O_6^{2-}$ ions being deposited on the PA6 surface. Increasing the temperature of $Cd(CH_3COO)_2$ solution has a positive effect, leading to higher concentrations of all elements. It can be seen from the results that the concentration of elements in samples S2 and S2* treated in concentrated acetic acid is slightly higher.

References

1. C. Qiu, H. Yang. Energy, **250** (2022), 123745.
2. R. Paul, S. Arulkumar, K. Jenifer, S. Partthiban. Journal of Electronic Materials, **52** (2023), 130-139.
3. S. K. Jain, G. Sharma, S. Vyas. Materials Today: Proceedings, 2022.
4. A. Romeo, E. Artegiani. Energies, **14** (2021), 1684.
5. O. Foss. Salts of Monotelluropentathionic Acid. Acta Chemica Scandinavica, **3** (1949), 708–716.

P 046

Properties of Starch Modified with Dodecenylsuccinic Anhydride and Acetic Anhydride

J. Luneckas*[1], L. Peciulyte[1], J. Bendoraitiene[1], R. Rutkaite[1]

[1]Department of Polymer Chemistry and Technology, Kaunas University of Technology, Radvilėnų pl. 19, 50254 Kaunas, Lithuania

As the global consumption of energy and various products grow there is an increasing need to find renewable sources to fulfill those demands. Thus, highly abundant and renewable materials are being researched to find their possible modifications that could replace current products made from non-sustainable sources. One of those highly researched materials is starch due to it being abundant, renewable, cheap and easy to modify.

The aim of this work was to get starch derivatives with different degree of substitution (DS) by modifying it with dodecenylsuccinic anhydride and acetic anhydride and evaluate the influence of such modification on hydrophobicity and thermal properties.

Starch dodecenylsuccinate with DS_{DDSA} (from 0.01 to 0.05) did not show the glass transition temperature. The same situation was with acetylated starch dodecenylsuccinate with low DS_{Ac} (up to 0.5). But the derivatives with higher DS_{Ac} showed glass transition temperature which ranged between 161 and 165 °C.

The hydrophobicity of derivatives was measured by the water contact angle with the surface of compressed material. Even with a small degree of substitution of starch dodecenylsuccinate the contact angle increased from 38.0°(native starch) to 127.8°. But additional modification of starch dodecenylsuccinate with acetic anhydride gave decrement of contact angle.

In order to assess the changes of granular structure the derivatives have been examined by scanning electron microscopy. As shown in figure 1 destruction of granules occurred during starch dodecenylsuccinate modification with acetic anhydride at higher degree of substitution.

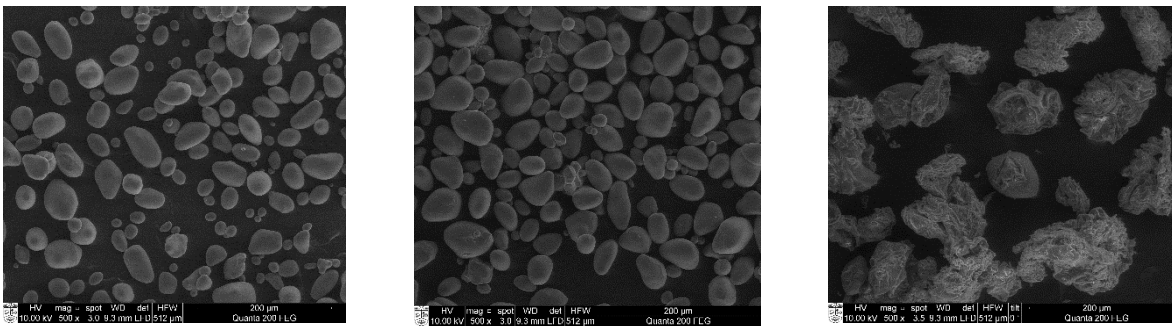

a b c

Fig. 1. Scanning electron microscope imagines (500x) of starch dodecenylsuccinate with DS_{DDSA}=0.02 (a), starch acetate dodecenylsuccinate with DS_{DDSA}=0.02, DS_{Ac}=0.38 (b) and starch acetate dodecenylsuccinate with DS_{DDSA}=0.02, DS_{Ac}=1.87 (c)

P 047

Modified 1,2-Diphenylbenzoimidazole Materials for Green And Sky-Blue Emission OLEDs

S. Macionis[1,*], J. Simokaitiene[1], J. V. Grazulevicius[1], J. H. Lee[2], C. H. Chen[2], B. Y. Lin[3], T. L. Chiu[4]

[1] Department of Polymer Chemistry and Technology, Kaunas University of Technology, Radvilenu pl. 19, LT-50254, Kaunas, Lithuania
[2]Graduate Institute of Photonics and Optoelectronics and Department of Electrical Engineering, Material Science and Engineering, and Physics, National Taiwan University, Taipei 10617, Taiwan
[3]Department of Opto-Electronic Engineering, National Dong Hwa University, Shoufeng, Hualien 974301, Taiwan.
[4]Department of Electrical Engineering, Yuan Ze University, Taiwan
**e-mail: simas.macionis@ktu.edu*

Organic light-emitting diode (OLED) technology have been steadily growing for more than two decades and have become a staple among modern lighting technologies [1]. With the discovery of thermally activated delayed fluorescence (TADF) [2] back in 2014, up to this day, the need for efficient, long-lasting and high color purity materials is ever increasing [3, 4].

In this work we present two novel 1,2-diphenylbenzoimidazole materials with cyano and di-tert-butylcarbazole substituents as host for green and sky-blue OLEDs. Materials presented were synthesized in a simple two-step synthesis process. In the first step difluoro-substituted benzimidazoles were formed via cyclization process from corresponding fluoro-substituted aromatic aldehydes and N-phenylbenzene-1,3-diamine, followed up by a second step simple and efficient nucleophilic substitution reactions to introduce electron donating 3,6-di-*tert*-butylcarbazole moieties. Thermal, electrochemical and photophysical properties of presented materials were tested and OLED devices were formed with external quantum efficiency up to 13%.

References

1. B. W. D'Andrade, S. R. Forrest, White Organic Light-Emitting Devices for Solid-State Lighting. Adv. Mater., 16: 1585-1595. (2004).
2. Zhang, Q., Li, B., Huang, S. et al. Efficient blue organic light-emitting diodes employing thermally activated delayed fluorescence. Nature Photon 8, 326–332 (2014).
3. Ha, J.M., Hur, S.H., Pathak, A. et al. Recent advances in organic luminescent materials with narrowband emission. NPG Asia Mater 13, 53 (2021).
4. Kim, H. J., Yasuda, T., Narrowband Emissive Thermally Activated Delayed Fluorescence Materials. Adv. Optical Mater. 10, 2201714, (2022).

P 048

Synthesis of Substrates for the Investigation of PmlABCDEF Monooxygenase Selectivity

G. Mačiuitytė[1,2*], V. Petkevičius[1]

[1]*Department of Molecular Microbiology and Biotechnology, Institute of Biochemistry, Life Sciences Center, Vilnius University, Lithuania*

[2]*Faculty of Chemistry and Geosciences, Vilnius University, Lithuania*

**Corresponding author, e-mail: greta.maciuityte@chgf.stud.vu.lt*

Oxygenation reactions are widely used in industry, applying various chemical methods that require various peroxides or metal catalysts. Nowadays, more environmentally friendly methods for such syntheses are needed, and as a result, more attention is shifting to the enzymes that catalyse such reactions - various oxygenases. Non-heme diiron monooxygenase PmlABCDEF possesses a broad substrate specificity and can oxidize different chemical groups, including ring heteroatoms and C=C double bonds [1]. Oxiranes, also known as epoxides, are important intermediates in organic chemistry and they bear the capacity of wide–ranging ring–opening reactions, which usually occur with predictable regioselectivity and stereospecificity [2]. *N*-oxides can be applied in the agriculture, and pharmacy industries and they have increased reactivity compared to regular *N*-heteroaromatic compounds [3].

However, it is a challenging task to selectively oxidize chemical groups of different reactivity (e. g. *N*-oxidation versus epoxidation) in a single molecule, therefore diverse synthesis strategies are employed with multiple reaction steps [4]. The aim of this study is to synthesize potential substrates for PmlABCDEF monooxygenase that have both an *N*-heteroatom and a C=C double bond.

Substrates were synthesized by attaching alkenyl substituents of different carbon chains to 3-pyridinol. The reaction products were extracted and purified by column chromatography. The obtained compounds were analysed with nuclear magnetic resonance (NMR), thin-layer chromatography (TLC), and high-performance liquid chromatography – mass spectrometry (HPLC-MS).

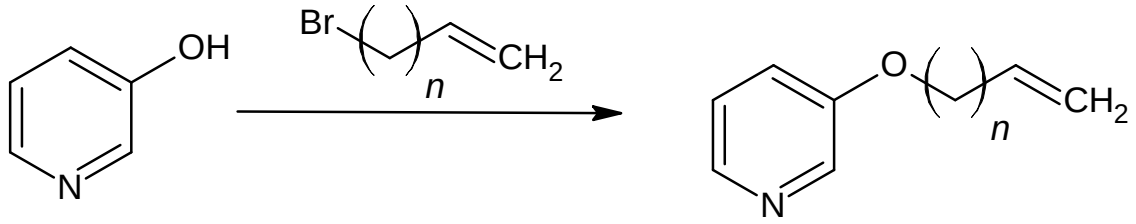

Fig. 1. Substrate synthesis scheme. Here n is from 1 to 6.

References

1. Petkevicius, V. et al. The versatility of non-heme diiron monooxygenase PmlABCDEF: a single biocatalyst for a plethora of oxygenation reactions. Catal Sci Technol 12, 7293–7307 (2022).
2. Hodgson, D. M., Stent, M. A. H., Reilly, M. K. & Gras, E. Oxiranes and Oxirenes: Fused-ring Derivatives. in Reference Module in Chemistry, Molecular Sciences and Chemical Engineering (Elsevier, 2014). doi:10.1016/B978-0-12-409547-2.11428-3.
3. Petkevičius, V., Vaitekūnas, J., Gasparavičiūtė, R., Tauraitė, D. & Meškys, R. An efficient and regioselective biocatalytic synthesis of aromatic N-oxides by using a soluble di-iron monooxygenase PmlABCDEF produced in the Pseudomonas species. Microb Biotechnol 14, 1771–1783 (2021).
4. Kocak, A., Kurbanli, S., & Malkondu S. Synthetic Access to New Pyridone Derivatives through the Alkylation Reactions of Hydroxypyridines with Epoxides, Synthetic Communications, 37:21, 3697-3708, (2007).

P 049

Optimisation of Factors Affecting the Electrospinning for Prediction of the Morphology of Biobased Poly(butylene succinate) Nanofibrous Mats

G. Masione[1, *], D. Ciuzas[1], E. Krugly[1,2], M. Tichonovas[1], D. Martuzevicius[1]

[1]Faculty of Chemical Technology, Kaunas University of Technology, Kaunas, Lithuania
[2]Bious Labs Technology, Kaunas, Lithuania
**Corresponding author: goda.masione@ktu.lt*

Introduction. Plastics have played an important role in the operation of the modern economy, combining remarkable practical properties with affordability. Plastics consumption has dramatically increased by a factor of twenty over the last fifty years and is expected to continue growing in the next 20 years. Therefore, significant attention has been directed towards biobased plastics derived from renewable resources such as plants and biomass. The adoption of biobased polymers in various applications is critical for promoting sustainability and reducing reliance on non-renewable resources. In this research, we investigated the optimisation of parameters for the fabrication of nanofibrous scaffolds made of biobased poly(butylene succinate) [1].

Methods. Biobased poly(butylene succinate) (PBS) pellets (NaturePlast, France) in the two solvent systems ($CHCl_3$/HCOOH) and ($CHCl_3$/CH_3OH) were used to fabricate nanofibrous mats by the solution electrospinning technique [2-3]. The experiment plan was designed based on D-optimal interaction model with MODDE® 10 software. The main factors that were investigated during electrospinning were polymer concentration, type of solvent, solvent ratio, and electric field intensity. The fibre morphology was characterised using scanning electron microscopy (SEM) and analysed with ImageJ software. The data collected from the experiment was fitted to partial least square regression model to obtain the response surface plots for the prediction of fibre morphology.

Results. A wide range of fibre and pore morphology of electrospun mats was obtained with an average fibre size ranging from 0.17 ± 0.05 µm to 4.54 ± 1.37 µm and a pore size between 1.12 ± 0.50 µm to 13.52 ± 6.57 µm. The polymer concentration and the solvent system appear to be the most significant two factors directly affecting the morphology of electrospun fibrous mats. The fitted model response surface plots (Fig.1) represent the prediction of the fibrous scaffold morphology depending on PBS concentration and the solvent system (ratio, parts) used in the experiment.

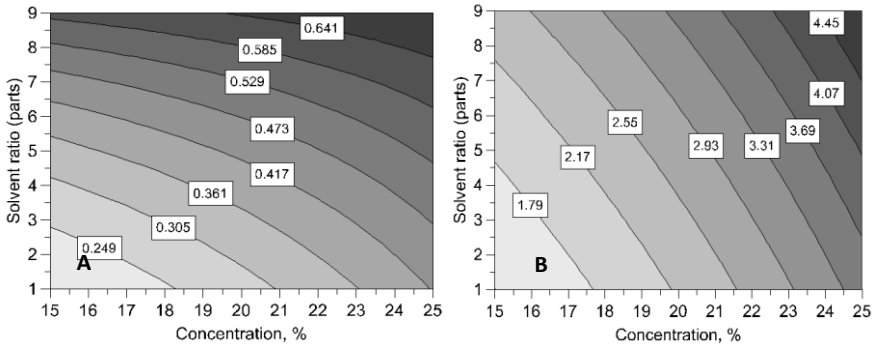

Fig. 1. Response surface plots for the prediction of PBS fibre morphology: (A) fibre diameter median, µm; (solvent system FA, electric field intensity centre point), (B) pore diameter median, µm (solvent system FA, electric field intensity centre point)

References

1. RameshKumar, S., Shaiju, P., & O'Connor, K. E. (2020). Bio-based and biodegradable polymers-State-of-the-art, challenges and emerging trends. Current Opinion in Green and Sustainable Chemistry, 21, 75-81.
2. Krugly, E., Ravikumar, P., Dabašinskaitė, L., Tichonovas, M., Ciuzas, D., Prasauskas, T., Baniukaitienė, O., Masione, G., Kauneliene, V., & Martuzevicius, D. (2022). Nanofibrous aerosol sample filter substrates: Design, fabrication, and characterization. Journal of Aerosol Science, 169, 106118.
3. Buivydiene, D., Krugly, E., Ciuzas, D., Tichonovas, M., Kliucininkas, L., and Martuzevicius, D. (2019). Formation and characterisation of air filter material printed by melt electrospinning. Journal of Aerosol Science, (2019) p. 131, 48–6.

P 050

The Surfaces of Nanodiamonds: A Modeling Perspective

Š. Masys*, V. Jonauskas

Institute of Theoretical Physics and Astronomy, Faculty of Physics, Vilnius University, LT-10257 Vilnius, Lithuania
**Corresponding author, e-mail: sarunas.masys@tfai.vu.lt*

Nanodiamonds (NDs) are carbon-based nanoparticles that have attracted significant attention due to the possible applications in a wide range of fields – from nanocomposites and tribology to quantum sensing and nanomedicine [1]. This can be attributed to their specific optical, mechanical, and chemical properties among which the versatile surface chemistry has proven to be particularly beneficial in the biomedical area [2].

In general, the surface features are the most critical factors regarding the applications of NDs [3]. Even if the cores of NDs play an important role, the interactions between them and surrounding environment are mediated by the interface at the surface, therefore the behavior of NDs in a medium is still dependent on the surface chemistry. By controlling the functional groups that NDs possess, properties such as colloidal stability, hydrophilicity, and reactivity can be tuned for the desired applications [4]. The surfaces of NDs can be covered with a variety of functional groups by applying, for example, hydrogenation, hydroxylation, amination or carboxylation procedures (see Fig. 1) [5].

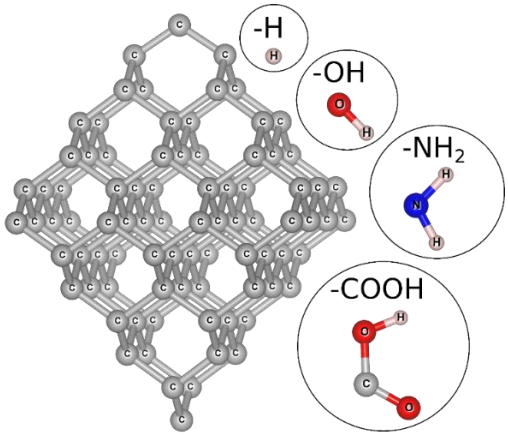

Fig. 1. Nanodiamond and its possible surface functionalization schemes.

The main aim of this work is to model NDs the surfaces of which would be fully grafted with the aforementioned functional groups. We seek to find out the optimal surface structure which would be consistent with the experimental findings and thereby could be used for the further theoretical investigation for the properties of interest. The performed quantum chemistry calculations reveal that, compared to the others, the carboxylic acid groups are harder to deal with pointing to the need for the more sophisticated modeling strategy.

References

1. S. L. Y. Chang, P. Reineck, A. Krueger, V. N. Mochalin, ACS Nano, **16** (2022) 8513.
2. D. H. Jariwala, D. Patel, S. Wairkar, Mat. Sci. Eng. C, **113** (2020) 110996.
3. N. Nunn, M. Torelli, G. McGuire, O. Shenderova, Curr. Opin. Solid State Mater. Sci., **21** (2017) 1.
4. M. B. A. Olia, P. S. Donnelly, L. C. L. Hollenberg, P. Mulvaney, D. A. Simpson, ACS Appl. Nano Mater., **4** (2021) 9985.
5. A. Krueger, D. Lang, Adv. Funct. Mater., **22** (2012) 890.

P 051

Antifrictional Effect on Dyeing of Anodic Coatings Impregnated with Fillers

T. Matijošius*, G. Bikulčius, S. Asadauskas

Center for Physical Sciences and Technology (FTMC), Saulėtekio av. 3, LT-10257 Vilnius, Lithuania

**Corresponding author, e-mail: tadas.matijosius@ftmc.lt*

Aluminum (Al) anodizing produces hard anodic Al_2O_3 coatings with vertical nanopores which improves technical features and increases the adsorption of dyes [1]. Nevertheless, wear of the colored anodic coatings remains one of the major problems due to poor tribological properties. In order to reduce friction, dyes with various fillers were tested on anodized 6082 Al alloy of 96.7% purity.

Hard anodization of Al was performed in H_2SO_4/oxalic a. (Type III) electrolyte for 70 min at 200 A/m² and 15 ºC to obtain anodic coatings of ~60 µm thickness [2]. For dyeing, the specimens were immersed into an aqueous dispersion of 1% chromium-complexed anionic azo dye Sanodal Deep Black MLW (Clariant) at 60 °C for 30 min. After rinsing in DI water the specimens were impregnated in a bath with a filler of different functional groups for 1 hour at 90 °C and suspended vertically in the oven at the same temperature for 1 hour to ensure drip-off and homogeneous distribution of the film. Pin-on-Disc Tribometer (Anton Paar TriTec SA) was used for friction tests. A bearing steel 100Cr6 of 96.5% purity or corundum ball of 99.8% purity and 6 mm OD was pressed under the 10 N, 30 N or 50 N loads and rotational motion of 1500 rpm with a track length of 31.4 mm.

Colored anodic coatings without any fillers produced only negligible tribological improvement against a steel ball. A rapid increase in friction occurred in less than 100 cycles under 10 N load and the coatings would easily break down under higher loads, see Fig. 1.

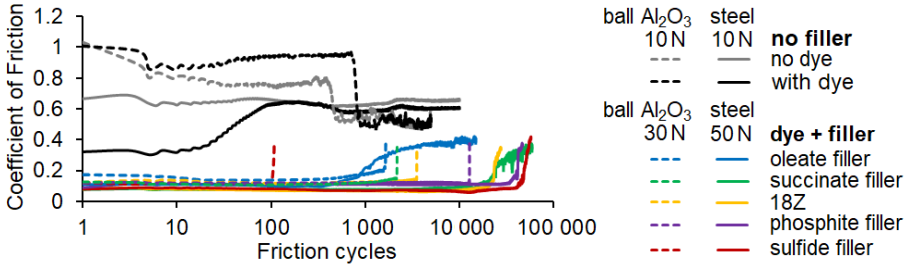

Fig. 1. Influence of impregnation of various fillers on friction tendencies of dyed anodic coatings under 10–50 N loads against steel or corundum balls.

After the impregnation, the coatings could withstand even a 50 N load against a steel ball. Most fillers are able to sustain over 10 000 friction cycles with a COF of around 0.1 except oleate filler which withstands less than 1 000 friction cycles before abrasion begins. In some cases, tribological performance can be improved significantly. The combination of dye and phosphite or sulfide functional groups, assures the most effective interaction with the electrolyte left inside the nanopores of anodic coating and sustains more than 40 000 cycles before abrasion under 50 N load against a steel ball. A chemically inert corundum ball was used to reduce the influence of counterbody-induced reactions. The load of 30 N was selected for friction tests since 50 N load completely breaks down anodic coatings just after several hundred cycles. Phosphite filler was most effective on anodic coatings and sustained more than 10 000 cycles against corundum ball. Surprisingly, sulfide filler sustains only 100 cycles against corundum by showing that tribofilm formation may be induced by the tribochemical reaction between the wear debris of steel ball, sulfide functional group and its interaction with the residual electrolyte. The tribological performance of colored anodic coatings can be dramatically improved by capitalizing on the synergistic interaction between the residual electrolyte and impregnated filler.

Acknowledgments

This work was supported by the Lithuanian federal research project [grant number 01.2.2-CPVA-K-703-03-0024].

References

1. T. Matijošius, S.J. Asadauskas, G. Bikulčius, A. Selskis, S. Jankauskas, J. Višniakov, I. Ignatjev, Color. Technol., **135** (2019) 275-282.
2. T. Matijošius, G. Stalnionis, G. Bikulčius, S. Jankauskas, L. Staišiūnas, S.J. Asadauskas, Coatings, **13** (2023) 132.

P 052

Introduction of Benzyl Substituents to Resorcinol Moiety in Search for N-Domain HSP90 Inhibitors

U. Milerytė[1*], A. Brukštus[2], I. Žutautė[2]

[1]Faculty of Medicine, Vilnius University, M. K. Čiurlionio g. 21, LT-03101, Vilnius, Lithuania
[2]Faculty of Chemistry and Geosciences, Vilnius University, Naugarduko g. 24, LT-03225, Vilnius, Lithuania
urte.mileryte@mf.stud.vu.lt

Resorcinol-based compounds comprise one subgroup of second-generation HSP90 inhibitors. [1] It is important to note that compounds in this class are typically more active in contrast to other structure chaperone inhibitors. However, for this activity and the binding to the ATP pocket of the HSP90 N-terminal domain, a second, correctly spaced aromatic ring is required. As a result, a wide range of heterocycles can be found in these analogs, which provide that distance between the rings and ensure suitable spatial conformations. [2]

Thus far, a selection of second-generation HSP90-inhibiting compounds with various heterocyclic rings and functional groups in positions 6 and 5 of the resorcinol moiety have been synthesized. However, there is not a single derivative documented in the literature that has 4-substituted resorcinol with a benzyl functional group. As a result, this research aims to synthesize new analogs, 6-(5-aryl-1,2,3-thiadiazol-4-yl)-4-arylbenzene-1,3-diols, bearing a para-substituted aromatic ring at the 4-position of the resorcinol fragment. These compounds are synthesized with the idea of utilizing the S2 subpocket of the HSP90 to boost their affinity and selectivity.

The target compounds are obtained in five steps: in the first stage, an aryl group is added to the resorcinol fragment to produce the starting materials, which are para-substituted 2,4-dihydroxybenzophenones **1**. The reduction of the acquired ketones is carried out in the second phase, which gives 4-benzylbenzene-1,3-diols **2**. In the third step, for the creation of the thiadiazole framework, p-phenylacetic acid is added to the 6-position of the reduced compounds, yielding 1-(5-benzyl-2,4-dihydroxyphenyl)-2-phenylethan-1-ones **3**. Intermediate products **4**, which are needed for the Hurd-Mori cyclization reaction, are formed in the fourth stage by exposing **3** compounds‘ p-phenylacetic acid fragments to the NH_2NHCO_2Et. The Hurd-Mori cyclization and formation of the thiadiazole rings is carried out in the last reaction, in which final products – 6-(5-aryl-1,2,3-thiadiazol-4-yl)-4-arylbenzene-1,3-diols **5** – are obtained.

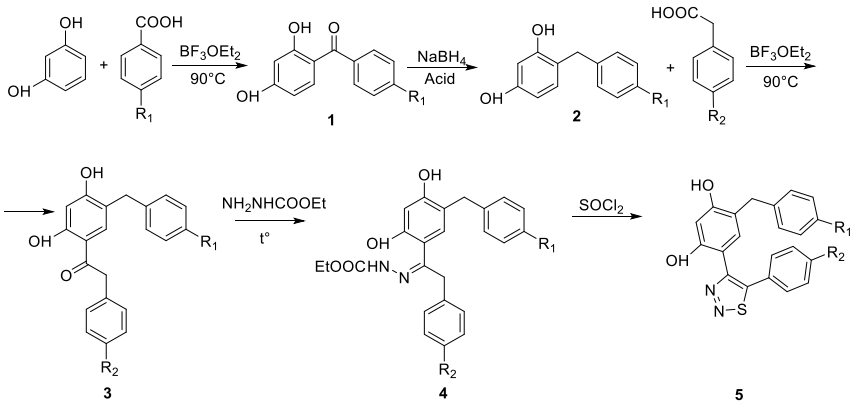

Fig. 1. General scheme of reactions

References

1. Park S, Oh Y, Park S, Oh Y, Lho Y, Jeong J, Liu K, Song J, Kim S, Ha E, Seo Y, Seo Y. Design, synthesis, and biological evaluation of a series of resorcinol-based N-benzyl benzamide derivatives as potent Hsp90 inhibitors. European Journal of Medicinal Chemistry (2018) 143 390-401.
2. Sanchez J, Carter TR, Cohen MS, Blagg BS. Old and New Approaches to Target the Hsp90 Chaperone HHS Public Access. Curr Cancer Drug Targets. 2020 m.;20(4):253–70.

P 053

Current Challenges in the Solvent-Based Multilayer Composite Waste Recycling

T. Mumladze[1*], A. Šleiniūtė[2], G. Denafas[2]
[1] *Akaki Tsereteli State University, Tamar Mepe St #59, 4600 Kutaisi, Georgia*
[2] *Kaunas University of Technology, K. Donelaičio St. 73, 44249 Kaunas, Lithuania*
**Corresponding author, e-mail:tamari.mumladze@atsu.edu.ge*

Multi-layer plastic films are commonly used in the flexible and rigid plastic packaging industry. These complex materials consist of layers of different polymers such as polyolefins and polyesters. Depending on the application, each layer is selected to provide an advantage over the main material in a particular property. Multilayer materials (laminates), as the name implies, have a multilayer structure and can consist of pure plastic film or a combination of materials (plastic, paper, metal, etc.) (Figure 1)(1, 2).

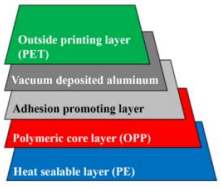

Fig. 1. Metallized film laminate with associated layers(2)

In general, recycling MCW is complicated because existing standard recycling industry technology cannot recognize, sort, and separate the different layers. These packaging materials are often disposed of in landfills or dumps in low-income countries. However, the leakage and deposition of Al in the soil are associated with significant environmental problems at large landfills (3). Solvent-based recycling is a new recycling technology for this type of waste. Various research has been conducted and many solvents have been evaluated; however, only a tiny percentage of these solvents are useful for the recycling process. A switchable hydrophilic solvent DMCHA was used for CPW recycling (4, 5), S. Favaro et al [81] used supercritical ethanol. Benzene, ethanol, xylene, toluene, hexane, and acetone have also been used in studies for the delamination of CPW (6, 7). Some substances are harmful to the polymer, causing it to dissolve. The quality and purity of the recovered materials have a significant impact on their economic value, especially in chemical processing. According to the research, the materials must be recovered, the solvents evaporated or neutralized by adding another solvent during the chemical treatment process. Solvent-based recycling still needs to be further developed from an environmental and economic point of view.

References

1. MIETH ANJA et al. Guidance for the identification of polymers in multilayer films used in food contact materials - Publications Office of the EU. *Joint Research Centre (European Commission)*. 27 April 2017. https://op.europa.eu/en/publication-detail/-/publication/12f4d00c-0203-11e6-b713-01aa75ed71a1/language-en
2. ŠČETAR, M. Multilayer Packaging Materials. In : *Packaging Materials and Processing for Food, Pharmaceuticals and Cosmetics*. John Wiley & Sons, Ltd, 2021. p. 131–144. https://onlinelibrary.wiley.com/doi/full/10.1002/9781119825081.ch6
3. GUILLARD, V. et al. The Next Generation of Sustainable Food Packaging to Preserve Our Environment in a Circular Economy Context. *Frontiers in Nutrition*. 4 December 2018. Vol. 5, p. 121. DOI 10.3389/fnut.2018.00121. https://www.frontiersin.org/article/10.3389/fnut.2018.00121/full
4. SAMORÌ, C. et al. Application of switchable hydrophilicity solvents for recycling multilayer packaging materials. *Green Chemistry*. 3 April 2017. Vol. 19, no. 7, p. 1714–1720. DOI 10.1039/c6gc03535c. https://pubs.rsc.org/en/content/articlehtml/2017/gc/c6gc03535c
5. MUMLADZE, T. et al. Sustainable approach to recycling of multilayer flexible packaging using switchable hydrophilicity solvents. *Green Chemistry*. 30 July 2018. Vol. 20, no. 15, p. 3604–3618. DOI 10.1039/c8gc01062e. https://pubs.rsc.org/en/content/articlehtml/2018/gc/c8gc01062e
6. CERVANTES-REYES, A. et al. Solvent effect in the polyethylene recovery from multilayer postconsumer aseptic packaging. *Waste Management*. 1 April 2015. Vol. 38, no. 1, p. 61–64. DOI 10.1016/j.wasman.2015.01.034.
7. ZHANG, S. et al. Interfacial separation and characterization of Al-PE composites during delamination of post-consumer Tetra Pak materials. *Journal of Chemical Technology & Biotechnology*. 1 June 2015. Vol. 90, no. 6, p. 1152–1159. DOI 10.1002/jctb.4573. http://doi.wiley.com/10.1002/jctb.4573

FUNDING – Research is carried out with EU financial support.

P 054

Transient Absorption Spectroscopy of Photochemical Reactions in Different Photoinitiators

M. Navickas[1,*], E. Skliutas[1], M. Malinauskas[1], M. Vengris[1]

[1]Vilnius University, Laser Research Center, Sauletekio av. 10, LT-10223, Lithuania
**M. Navickas, marius.navickas@ff.vu.lt*

Photopolymerization has attracted a great scientific and technological interest due to a large number of applications spanning from optoelectronics to medical areas [1,2]. This process is promoted by photoinitiators which in a very short time scale produce free radicals that trigger the cross-linking reactions [3,4]. Thus, the photopolymerization initiation becomes a significant process governing the chemical and physical nature of the final product. A large variety of different photoinitiators have been studied by various spectroscopic techniques, however, the excitation mechanisms are not fully understood. In this work, we present a comparative transient absorption (TA) spectroscopy study of photoinitiation behaviour in commercial BAPO, Irgacure 369, Irgacure 651 and TPO photoinitiators dissolved in isopropanol.

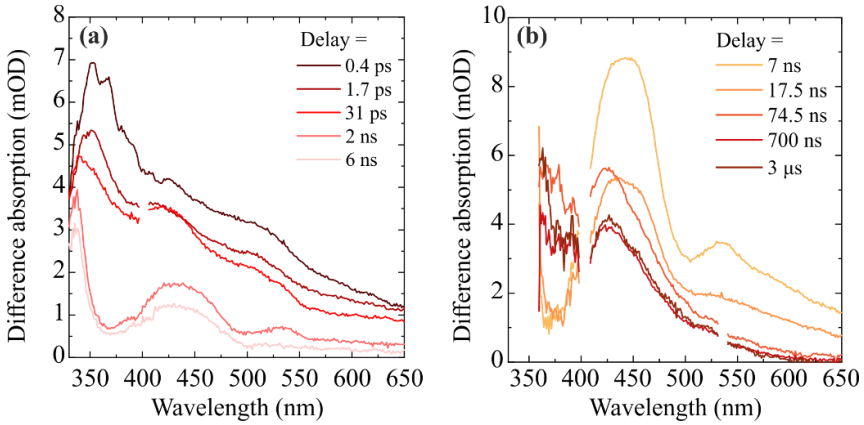

Figure 1. Transient absorption spectra of BAPO photoinitiator obtained during the (a) pump-probe and (b) laser flash photolysis experiments.

Fig 1 (a) represents the TA spectra of BAPO photoinitiator recorded during the ultrafast pump-probe experiments. This technique revealed that after one-photon excitation BAPO immediately cleaves into benzoyl, containing methyl groups, and phosphinoyl radicals. In addition, it was observed, that benzoyl radical features a significantly faster relaxation time than phosphinoyl radical. Further, we performed laser flash photolysis experiments to get a deeper knowledge of the radical relaxation timescale and formation mechanisms. The TA spectra observed by means of laser flash photolysis (Fig. 1 (b)) suggest that the latter radical relaxes in several tens of nanoseconds. These results are in a good agreement with the previously discussed photoinitiation mechanism and provide a deeper insight into the primary photoreactions of BAPO. The TA spectra of Irgacure 369, Irgacure 651 and TPO feature only two broad induced absorption (IA) bands. In case of Irgacure 369, these IA bands span around ca. 350 nm and 470 nm. The presence of transient species was confirmed by the kinetic traces. We found that the IA band of Irgacure 369 grows up in 10 ps and after 100 ps starts to decay, meanwhile the second IA band relaxes after 100 ps. In addition, the laser flash photolysis of argon-saturated Irgacure 369 solution exhibits an increase of initial Irgacure 369 relaxation time, revealing the triplet character of the radical formation.

References

1. W. Tomal, J. Ortyl, Polymers, **12** (2020) 1073.
2. K. Ikemura, K. Ichizawa, M. Yoshida S. Ito, T. Endo, Dent. Mater. J., **27** (2008) 765–774.
3. C. Decker, Polym. Int., **45** (1998) 133–141.
4. A. Alberti, M. Benaglia, D. Macciantelli, S. Rosseti, M, Scoponi, Eur. Polym. J., **44** (2008) 3022–3027.

P 055

Synthesis of Chitosan-graft-poly(N-isopropylacrylamide) Copolymers

V. Navikaite-Snipaitiene[1]*, A. Kairyte[1], M. Babelyte, L. Peciulyte[1], R. Rutkaite[1], V. Samaryk[2]

[1]Department of Polymer Chemistry and Technology, Kaunas University of Technology, Lithuania
[2]Department of Organic Chemistry, Lviv Polytechnic National University, Ukraine
**Corresponding author, e-mail: vesta.navikaite@ktu.lt*

Poly(N-isopropylacrylamide) is one of the most popular thermo-responsive synthetic polymers that exhibits dramatic and reversible phase transition behavior in water [1]. Recently, copolymers with grafted poly(N-isopropylacrylamide) side chains are highly researched, particularly, in terms of drug delivery and biomedical applications. By using such synthesis strategy thermoresponsive polymers with biocompatible polysaccharide e.g. chitosan main chain and synthetic side chains, and dual (pH and temperature) responsive properties can be obtained [2].

The aim of this study was to prepare chitosan-graft-poly(N-isopropylacrylamide) copolymers using different molar ratios of chitosan (CH) to N-isopropylacrylamide (NIPAA) (see Fig. 1). The synthesis of copolymers was carried out in aqueous solution using potassium persulfate as an initiator at 60 °C temperature under a nitrogen atmosphere. After the reaction, the products were precipitated into acetone and obtained copolymers were purified by using methanol. The molar ratio of CH to NIPAA in the polymerization mixture was varied from 1:0.25 to 1:10.

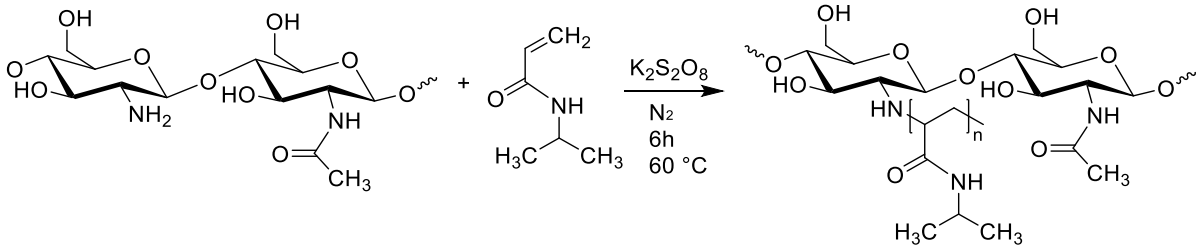

Fig. 1. Synthesis scheme of chitosan-graft-poly(N-isopropylacrylamide) copolymers.

The obtained chitosan-graft-poly(N-isopropylacrylamide) copolymers of different comonomer composition were characterized by using various techniques such as FT-IR, thermal analysis and etc. The lower critical solution temperature behaviour of prepared copolymers was assessed by dynamic light scattering and turbidimetric methods.

Acknowledgements. The financial support of the Research Council of Lithuania for the project No. S-LU-22-11 in the frame of Lithuanian–Ukrainian Cooperation Programme in the Fields of Research and Technologies is highly acknowledged.

References

1. F. Doberenz, K. Zeng, C. Willems, K. Zhang, T. Groth. J. Mater. Chem. B, 8 (2020) 607-628.
2. A. S. Patil, A. P. Gadad, R. D. Hiremath, P. M. Dandagi. J. Polym. Environ., 26 (2018) 596-606.

P 056

Life-Cycle Assessment of CO_2 Mineralization Product: Comparing Magnesia Cement and Portland Cement

E. Onokwai[1*], I. Stasiulaitiene[1]
[1]*Faculty of Chemical Technology, Kaunas University of Technology, Kaunas, Lithuania*
*elizabeth.onokwai@ktu.edu

Portland cement (PC) is the most widely used type of cement globally, with a production of 4.1 billion tons in 2022 [1]. PC is made by heating limestone and clay at high temperature in a kiln, resulting in clinker which is then mixed with gypsum. However, its high CO_2 emissions, which makes PC production one of the top three sources of anthropogenic CO_2, have led to the search for alternatives [2]. Magnesia cement is regarded as a viable alternative to PC. Produced at lower temperatures and capable of absorbing CO_2, it is made from magnesium oxide (MgO) found in magnesium silicates. The challenge in using magnesium oxide (MgO) as a raw material is the creation of cost-effective methods to separate it from silicates. A pilot project utilizing MgO from serpentinites through the Abo Akademi (ÅA) process routes is ongoing in Finland [3]. The environmental impact of such type a cement should not be forgotten as well. A study is being conducted to compare the environmental impact of both MgO cement produced through ÅA process routes and PC, using life cycle assessment based on the ISO 14040 and 14044 standards, with a functional unit (FU) of 1 ton of cement for each type. The selected system boundaries for the assessment includes all stages of production from raw material acquisition to packaging. The inventory analysis (Table 1) has been performed based on scientific literature [4-5] and own calculations. The environmental impact assessment has been performed with software SimaPro 9.0 (Pre Sustainability), Impact 2002+ method was selected for the calculations. The calculations revealed that MgO cement shows better environmental impact in terms of global warming potential and resources than PC.

Raw materials	Amount (ton) (MgO)	Amount (ton) (PC)	Energy	Amount (ton/kWh) (MgO)	Amount (ton/kWh) (PC)	Emissions	Amount (kg/m^3) (MgO)	Amount (kg/m^3) (PC)
Magnesite	2.17	-	Coal	0.27	5.53E-9	CO_2	1096.54	833.71
Water	0.01	0.53	Electricity	8.67	71.92	SO_2	4.21	0.63
Limestone	-	1.32	Diesel	0.54	9.00E-7	CO	0.021	1.96
Clay	-	0.32	Fuel oil	-	1.53E-9	NO_x)	0.01	1.79
Sand	-	0.07	Petroleum coke	-	0.10	Water vapor	0.01	-
Iron Ore	-	0.01				Magnesite/kiln dust	0.99	0.87
Gypsum	-	0.05				Particulate matter	-	0.03

Table 1. Life cycle inventory of magnesia & Portland cement based on the defined FU.

References

[1] M. Garside, "Global cement production 1995-2022," Statista, 3 February 2023.

[2] A. M. Robbie, "Global CO2 emissions from cement production," *Earth System Science Data*, vol. 10, pp. 195-217, 2018.

[3] R. Zevenhoven, M. Slotte, E. Koivisto and R. Erlund, "Serpentinite Carbonation Using the ÅBo Akademi Routes – Status Update," in *International Conference on Accelerated Carbonation for Environmental and Material Engineering (ACEME)*, 2018.

[4] S. Ruan, *Development of reactive magnesia cement-based formulations with improved performance & sustainability*, Singapore: Doctoral thesis, Nayang Technological Univeristy, 2019.

[5] J. Li, Y. Zhang, S. Shao and S. Zhang, "Comparative life cycle assessment of conventional and new fused magnesia production," *Journal of Cleaner Production*, no. 91, pp. 170-179, 2015.

P 057

Synthesis and Application Of TiO_2 Nanotube Arrays for Treatment of Pharmaceuticals in Model Wastewater

M.-A. Onoriode-Afunezie[1*], A. Sulciute[1], V. Abromaitis[2]

[1]Department of Physical and Inorganic Chemistry, Faculty of Chemical Technology, Kaunas University of Technology, Kaunas, Lithuania
[2]Department of Environmental Engineering, Faculty of Chemical Technology, Kaunas University of Technology, Kaunas, Lithuania
maria.onoriode@ktu.edu

The use of antibiotics in human medicine, livestock, and aquaculture has increased significantly [1] and the dangers posed by pharmaceuticals and their reaction products have become common knowledge resulting in increased research activities [2]. Aside from the risk of supporting microbial antibiotic resistance, antibiotic residues can harm various trophic biological levels and human health, potentially causing ecotoxicological effects [3]. Although TiO_2 has been widely applied a limited number of studies using TiO_2 nanotube arrays for photocatalytic water treatment are available [4]. This study aimed to develop and test TiO_2 nanotube arrays (NTAs) photocatalytic ozonation reactors, as one of the most effective advanced oxidation processes (AOP), to treat antibiotics in a model secondary effluent.

MATERIALS AND METHODS

TiO_2 NTAs were prepared according to the description in [5]. Wastewater was prepared with a concentration of 10mg/l of Ciprofloxacin (CIP) in demineralized water. Using six AOPs (photolysis, ozonation, ozone photolysis, photocatalytic ozonation, UV photocatalysis and catalytic ozonation), experiments were carried out ranging from 5 minutes to 60 minutes. For ozone experiments, the concentration of ozone was approximately 5mg/l.

RESULTS AND DISCUSSION

The photocatalytic ozonation process was identified as the most effective process in the removal of CIP. CIP was degraded in 7 minutes, therefore, having a 100% efficiency. The pseudo-second-order kinetics varied from 1.01 x 10^{-1} min^{-1} to 1.33 x 10^{-1} min^{-1} based on the initial concentration of CIP in the model water. Photolytic treatment and photocatalytic ozonation resulted in 51–66% and 92–100% removal efficiency of antibiotic CIP. However, in all cases where ozone was used, there was complete removal of CIP.

REFERENCES

[1] Q. G. Y. K. J. S. P. L. G. Y. L. Y. G. R. &. C. J. Yang, "Antibiotics: An overview on the environmental occurrence, toxicity, degradation, and removal methods.," Bioengineered, vol. 12, no. 1, p. 7376–7416., 2021.
[2] J. K. D. Ś. K. T. M. S. P. B.-B. A. &. D. J. Maculewicz, "Transformation products of pharmaceuticals in the environment: Their fate, (eco)toxicity and bioaccumulation potential," Science of The Total Environment, vol. 802, 2022.
[3] S. I. G. A. E. K. B. G. Ș. M. &. L. F. Polianciuc, "Antibiotics in the environment: causes and consequences.," Medicine and Pharmacy Reports, vol. 93, no. 3, p. 231, 2020.
[4] B. C. B. Z. B. S. X. Z. G. &. L. K. Liu, "Photocatalytic ozonation of offshore produced water by TiO2 nanotube arrays coupled with UV-LED irradiation.," Journal of Hazardous Materials, vol. 402, 2021.
[5] V. S. J. S. A. S. D. Z. N. M. S. T. U. I. J. D. U. M. V. S. D. R. B. K. M. D. Abromaitis, "Ozone-enhanced TiO2 nanotube arrays for the removal of COVID-19 aided antibiotic ciprofloxacin from water: Process implications and toxicological evaluation.," Journal of Environmental Management, vol. 318, 2022.

P 058

Effects of Sol-Gel Synthesis Procedure Conditions on the Stability of Polar Active Hexagonal Phase in $LuFeO_3$-$LuMnO_3$ System

A. Pakalniškis[1*], G. Niaura[2], D. Karpinsky[3], G. Rogez[4], P. Rabu[4], S. Chen[5,6], T. C-K Yang[5,6], R. Skaudžius[1], A. Kareiva[1]

[1] Institute of Chemistry, Vilnius University, Naugarduko 24, LT-03225 Vilnius, Lithuania
[2] Department of Organic Chemistry, FTMC, Sauletekio Ave. 3, LT-10257, Vilnius, Lithuania
[3]Namangan Engineering-Construction Institute, Dustlik Avenue 4, 160100 Namangan, Uzbekistan.
[4]IPCMS, 23 Rue du Loess Bâtiment 69, 67200, Strasbourg, France
[5]Precision Analysis and Materials Research Center, NTUT, Taipei, Taiwan
[6]Department of Chemical Engineering and Biotechnology, NTUT, Taipei Taiwan
andrius.pakalniskis@chgf.vu.lt

Nowadays the amount of extremely specific and niche applications is ever increasing. This is especially visible in the areas of electronic and magnetic materials. Because of this a lot of attention by scientist has been dedicated towards the invention of new materials or on the improvement of already existing ones in such a way as to adapt them for modern day requirements. One key area of research revolves around the combination different properties into a single material. While many of the different combinations have been attempted the merging of ferroic properties has attracted a lot of attention in particular. Currently compounds that exhibit at least two primary ferroic orders (elastic, magnetic or electric) are referred to as multiferroic [1].

However, the combination of both magnetic and electrical properties requires significant challenges to be overcome in order to be possible. Firstly, the classically know magnetic and electric properties arise from opposite phenomena. Since in most cases the ferroelectric properties arise from the hybridization of empty 3d orbitals and magnetic ones require them to be partially filled. In order to avoid encountering this problem other possible mechanisms for the existence of ferroelectricity were discovered. These mechanisms include lone pair, spin driven, geometric and charge ordering as they do not require empty electron shells [2]. Secondly, the coupling between the two is often weak. Lastly, at least one of the properties occurring at temperatures lower than that of room temperature. The solution to the last two problems is not as simple or clear and as in most cases is different for every material. As such the search for new multiferroic materials that would show both, ferroelectric and ferromagnetic properties with strong coupling and above room temperature is still ongoing.

Once such potential compound is hexagonal $LuFeO_3$. While undoped, $LuFeO_3$ is an orthorhombic non-polar perovskite with weak ferromagnetic properties. However, a metastable hexagonal crystal structure with $P6_3cm$ space group can be also obtained. The hexagonal variant of $LuFeO_3$ is a polar compound where ferroelectricity is caused by geometric factors, mainly the uneven displacement of Lu ions in the crystal structure [3]. The metastable structure can be stabilized by either strain during thin film preparation or by doping the $LuFeO_3$ matrix. While there are several different dopants possible their effects on magnetic properties and electrical properties are still not clear. Even the phase formation is complicated and the stability regions of the hexagonal phase are difficult to describe as they are different for each of the dopants while also being sensitive to the preparation method and even the calcination temperature [4].

As such in this work we provide insights into the stabilization of hexagonal $LuFeO_3$ by Mn doping prepared by aqueous sol-gel method. The concentration stability regions for the hexagonal phase at different calcination temperatures were described using X-ray diffraction analysis. Particle morphology was determined using SEM analysis. Lastly, we also provide additional information on the behavior of magnetic properties not only caused by the crystal structure changes, but also on the effect of Mn doping.

Acknowledgments: This project has received funding from the European Union's Horizon 2020 research and innovation programme under the Marie Skłodowska-Curie grant agreement No 778070 – TransFerr – H2020-MSCA-RISE-2017.

References

1. M. Fiebig, T. Lottermoser, D. Meier, M. Trassin, Nat. Rev. Mater. 1 (2016) 1–14.
2. M. Kumar, A. Kumar, A. Anshul, S. Sharma, Mater. Lett. 277 (2020) 128369.
3. S.M. Disseler, X. Luo, et. al., Phys. Rev. B. 92 (2015) 54435.
4. A. Pakalniškis, et.al., Materials. 15 (2022) 1048.

P 059

Effect of Deposition Cycles on the Properties of Copper Sulfide Thin Films Deposited by CBD

M. Gilić [1,2], R. Alaburdaitė[3], E. Paluckienė[3], N. Petrašauskienė[3*]

[1]*Institute of Experimental Physics, Freie Universität Berlin, 14195 Berlin, Germany*

[2]*Institute of Physics Belgrade, 11080 Belgrade, Serbia*

[3]*Department of Physical and Inorganic Chemistry, Kaunas University of Technology, Radvilenų 19, LT-50254 Kaunas, Lithuania*

**Corresponding author, e-mail: neringa.petrasauskiene@ktu.lt*

The deposition of copper sulfide as a thin layer onto the surface of the polymer is a promising approach to obtain electrically conductive films. Flexible, transparent polymer substrate coated with copper sulfide is expected to be useful in many fields, for example, as reflectors for concentrating collectors, heat mirrors, and solar control coatings [1], as conductive substrates for deposition of metal and semiconductors [1, 2], as gas sensors functioning at temperatures close to room temperature [3].

The chemical bath deposition (CBD) technique has been used for the deposition of copper sulfide thin films on polypropylene (PP) substrates. The Cu_xS thin film deposition was carried out at room temperature using a mixture of 0.05 M $CuCl_2$ and 0.05 M $Na_2S_2O_3$ solutions for 16 h. The CBD process was carried out by varying cycles (1, 2 and 3 cycles) of deposition. The formed samples were annealed at 80 ºC for 30 min.

The structure, surface morphology, and optical characterization of the deposited thin film indicated a strong relationship between the number of deposition cycles. The scanning electron microscope (SEM) showed a uniform morphology with randomly oriented nano-grains of the copper sulfide film at varying deposition cycles (Fig.1). The thin film morphology uniformly covers the PP substrate and shows a smooth surface. Additionally, the films prepared by CBD with 3 cycles were found quite dense with good crystallinity and no holes, homogenous surface, adhesion to the substrate, compact, and improved in grain size compared to copper sulfide films prepared with 2 cycles (Fig. 1.).

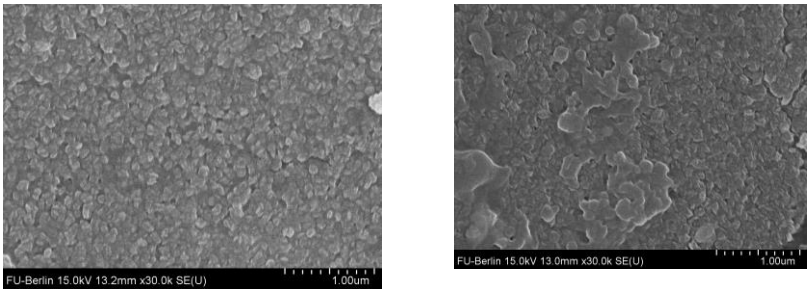

2 cycles 3 cycles

Fig. 1. Surface morphology of Cu_xS thin films prepared at different cycles

Analysis of Cu_xS thin films also was performed using X-ray diffraction analysis, ultraviolet-visible (UV-VIS) spectroscopy, and Raman after each deposition cycle. The electrical result of the thin films shows that resistivity decreases, while conductivity increases as the CBD cycle increases.

References

1. J. Cardoso et al, Semicond. Sci. Technol., **16** (2001) 123-127.
2. M. T. S. Nair and P. K. Nair, Semicond. Sci. Technol., **4** (1989) 191-199.
3. A. Galdikas et al, Sensors Actuators B Chem., **67** (2000) 76-83.

P 060

Application of Capillary Flow Porometry to Predict the Filtration Efficiency of Nanofibrous Polymer Membranes

G. Poceviciute[1,*], G. Masione[1], D. Ciuzas[1], E. Krugly[1,2], M. Tichonovas[1], D. Martuzevicius[1], V. Kauneliene[1]

[1]*Faculty of Chemical Technology, Kaunas University of Technology, Kaunas, Lithuania*

[2]*Bious Labs Technology, Kaunas, Lithuania*

**gaile.poceviciute@ktu.lt*

Introduction. Of all pollutants present in the ambient air, particulate matter (PM) is the most dangerous and has the greatest negative impact on human health. Filtration is one of the most technically and economically feasible methods for the removal of particles from air. In recent years, nanofibrous polymer membranes gain popularity due to their high filtration efficiency, which depends on fibre and pore sizes, as well as their size distribution. Capillary flow porometry (CFP) is a widely used method to measure the pore size and pore size distribution of nonwoven fibrous membranes. Here we demonstrate a systematic research of the effects of pore size distributions in nanofibrous membranes to the filtering performance.

Methods. Polybutylene succinate (PBS) fibrous mats were electrospun from the chloroform and formic acid (6:4) solution using electrospinning setup (SE-01C, Bious Labs, Lithuania). Different layers of PBS nanofibres were deposited on polypropylene spunbonded nonwoven fabric, by varying deposition duration, which corresponded to a specific weight, and in turn, pore sizes. Pore size distribution was researched using capillary flow porometer (CFP-0410, Bious Labs) and fluorinated hydrocarbon (Porofil, Anton Paar QuantaTec Inc., USA) as a wetting liquid. Scanning electron microscopy (SEM) analysis and ImageJ software were used to obtain optical morphological parameters of the same membranes. Aerosol particle filtration efficiency of fabricated membranes was research using an in-house filtration testing setup [1], where the values of filtration efficiency and pressure drop were obtained.

Results and conclusions. Filtering mats were obtained with the basis weight between and 0.88 ± 0.35 g/m^2 and 18.05 ± 0.58 g/m^2, which corresponded to mean pore sizes between 6.0 ± 0.9 µm and 0.5 ± 0.1 µm, as indicated by the CFP method (Figure 1 A). The filtration efficiency against NaCl particles varied from 31.5 to 99.5 %, while the pressure drop was in the range between 1 to 455 Pa. As expected, the efficiency and pressure drop were adversely affected by the pore size, although relationship was of different nature (Figure 1 B). Pore sizes within the interval between 0.5 and 1 um appear to be critical in terms of pressure drop, while maintaining relatively high filtration efficiency. This allows optimization of filter material in terms of the energy use for the applications of industrial filtration.

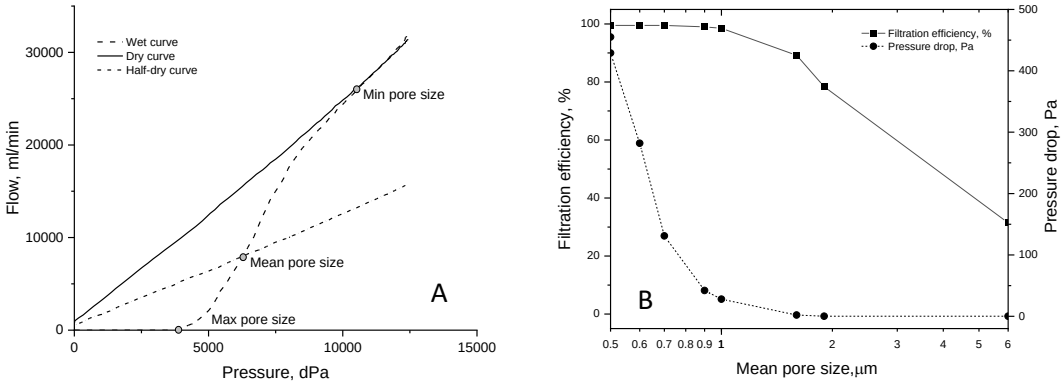

Fig. 1. Characteristic curves of CFP (A) and Relationship between mean pore size and filter pressure drop and filtration efficiency (B)

References

1. Krugly, E., Ravikumar, P., Dabašinskaitė, L., Tichonovas, M., Ciuzas, D., Prasauskas, T., Baniukaitienė, O., Masionė, G., Kaunelienė, V., & Martuzevičius, D. (2022). Nanofibrous aerosol sample filter substrates: Design, fabrication, and characterization. Journal of Aerosol Science, 169, 106118.

P 061

Polyvinyl Acetate as Binder in the Formation of Granules of Buckwheat Husk Ash

O. Pocienė*, E. Griškaitis, R. Šlinkšienė
Kaunas University of Technology, Radvilėnų st. 19, 50254 Kaunas, Lithuania
**Corresponding author, e-mail: odeta.pociene@ktu.lt*

Overall, the use of granular materials has a lot of advantages compared to powdered materials. This is also characteristic of fertilizers, because granular fertilizers don't dust, don't segregation, are better distributed in the soil, and one granule contains all the nutrients needed by plants. The granulation process is most often used in the production of fertilizers – wetting the fertilizer components with liquid (binder). The success of the process often depends on the binder selected, which wets and binds the small powder particles together. Liquid bridges appear between the wetted particles. As the number of liquid bridges increases larger particles – agglomerates [1-2].

There is presented the influence of different concentrations of polyvinyl acetate (PVA) on the granulation process and product properties of buckwheat hulls ash (Table 1).

Table 1.

No.	Moisture, %		Granulometric composition, %					pH	Density, kg/m^3	
	Raw mat.	Product	>5 mm	3–5 mm	2–3 mm	1–2 mm	<1 mm		Bulk	Tapped
10% concentration of PVA solution										
1	41.2	1.7	8.9	5.1	3.2	44.7	38.1	11.5	288.8	304.0
2	44.4	1.9	2.2	5.9	8.5	35.3	48.2	11.2	352.1	379.4
3	47.4	1.7	10.0	12.8	14.0	18.8	44.3	11.1	402.0	418.2
4	50.0	1.9	16.6	15.4	15.4	21.9	30.7	11.0	408.5	424.1
5	52.4	1.5	10.0	16.0	22.3	39.2	12.4	12.0	476.4	500.5
6	53.5	1.7	16.1	24.3	24.6	29.7	5.4	11.6	485.6	514.0
7	54.4	1.9	27.0	33.4	29.8	8.1	1.6	12.1	424.8	449.6
20% concentration of PVA solution										
8	41.2	1.9	17.8	7.9	6.6	40.7	27.1	11.1	351.9	383.0
9	44.4	1.9	21.2	9.5	7.0	24.6	37.7	10.9	393.0	412.0
10	47.4	1.9	23.7	13.5	9.0	15.2	38.7	11.1	405.0	423.0
11	50.0	1.5	26.0	15.6	10.7	17.9	29.8	11.5	432.0	466.5
12	52.4	1.7	25.0	18.4	15.0	23.6	17.9	11.4	451.0	475.0
13	53.5	1.2	23.9	19.3	16.2	21.7	18.9	11.4	417.2	441.6
14	54.4	2.0	33.7	26.2	20.3	17.8	2.1	11.9	479.5	512.0
30% concentration of PVA solution										
15	41.2	2.0	27.7	6.2	4.0	42.6	19.4	10.8	381.2	402.0
16	44.4	1.7	32.9	5.5	3.7	36.3	21.6	10.7	377.0	392.0
17	47.4	2.0	29.8	11.6	6.0	20.5	32.1	10.9	414.0	430.7
18	50.0	1.7	33.0	17.2	8.2	15.3	26.4	10.8	411.5	441.0
19	52.4	1.4	41.1	11.2	6.9	17.5	23.4	11.1	412.0	434.0
20	53.5	1.7	30.3	22.7	15.6	19.3	12.0	11.5	432.8	455.2
21	54.4	2.0	38.2	16.2	9.2	17.3	19.2	11.5	428.5	456.0

Dependence of properties of buckwheat husk ash granules on PVA concentration.

The results shows that the concentration of polyvinyl acetate has a significant effect on the granulometry of the product and the static crushing strength of the granules, but just slightly changes the properties such as pH, loose bulk and tapped density or moisture content of the granular product.

References

1. R. Paleckienė, A. Sviklas, R. Slinkšienė, V. Streimikis, Polish Journal of Environmental Studies, **19(5)** (2010) 973-979.
2. O.R. Arndt, P. Kleinebudde, Powder Technology, **337** (2018) 68-77.

P 062

Synthesis of Microcapsules Containing Polyaspartic Acid Ester within UV Curable Shell

E. Potapov, L. Pastarnokienė*, T. Kochanė, R. Makuška
Department of Polymer Chemistry, Faculty of Chemistry and Geosciences, Vilnius University
Naugarduko 24, LT-03225 Vilnius, Lithuania
**Corresponding author, e-mail: liepa.pastarnokiene@chgf.stud.vu.lt*

In recent years corrosion-resistant self-healing coatings have witnessed strong growth, and their successful laboratory design and synthesis categorises them in the family of smart/multi-functional materials. Among various approaches for achieving self-healing, microcapsule embedment through the material matrix is the main one for self-healing ability in coatings [1].

Polyaspartic coatings are based on aliphatic polyisocyanates and polyaspartic acid esters (PAAE). Reaction between those two components is extremely fast. The main advantages of polyaspartic coatings are high durability, fast return to service, UV stability, abrasion and chemical resistance. Due to high reactivity, polyisocyanates and PAAE have high potential in development of self-healing coatings. To create *two capsule* self-healing system, it is necessary to encapsulate separately both polyisocyanates and PAAE. Encapsulation of polyisocyanates like isophorone diisocyanate (IPDI) does not make any serious difficulties [2, 3]. Encapsulation of amines including PAAE is much more complicated and usually gives unsatisfactory results.

New method of encapsulation of PAAE *Desmophen NH 1220* was developed based on the use of UV-curable polyurethane acrylate resin as a shell material. 3D printing resin from *Anycubic* containing polyurethane acrylate resin, acrylate monomer and photoinitiator was used as a shell material. Formation of the microcapsules' shells was realized under UV irradiation and was very fast. Characteristics of the microcapsules were monitored by optical microscopy, scanning electron microscopy, FT-IR spectroscopy, and thermogravimetric analysis. Characteristics of the microcapsules were varied by changing processing parameters such as stirring rate, emulsifier type and concentration, and core to shell ratio. The process parameters were optimized using Taguchi experimental design method.

Changing reaction conditions and the ratio of PAAE to the solvents xylene, ethyl lactate or dichloromethane, stable microcapsules of PAAE were synthesized. The maximal amount of the encapsulated healing material PAAE was up to 64 %. Size of the microcapsules was varying in the range between 10 and 230 μm, and was controllable by the reaction conditions. Most of the microcapsules remained stable after lyophilisation and separation in powder form. Using Taguchi criteria "nominal is the better" for the microcapsule size of 50 μm, and criteria "larger is the better" for the amount of the encapsulated material, optimal conditions for encapsulation of PAAE were developed. Desirable microcapsules containing encapsulated PAAE were obtained at core to shell ratio 3:1, stirring rate 500 rpm, and a mixture of polyvinyl alcohol (1 %) and gum arabic (1.5 %) as an emulsifier.

References

1. K. Thanawala, N. Mutneja, A. Khanna, R. Raman. Development of Self-Healing Coatings Based on Linseed Oil as Autonomous Repairing Agent for Corrosion Resistance. Materials, **2014**, **7**(11) 7324–7338.
2. M. Attaei, L. M. Calado, Y. Morozov, M. G. Taryba, R. A. Shakoor, R. Kahraman, A. C. Marques, M. F. Montemor. Smart Epoxy Coating Modified with Isophorone Diisocyanate Microcapsules and Cerium Organophosphate for Multilevel Corrosion Protection of Carbon Steel. Progress in Organic Coatings, **2020**, 147, 105864.
3. M. Guo, W. Li, N. Han, J. Wang, J. Su, J. Li, X. Zhang. Novel Dual-Component Microencapsulated Hydrophobic Amine and Microencapsulated Isocyanate Used for Self-Healing Anti-Corrosion Coating. Polymers, **2018**, 10(3), 319.

P 063

Synthesis of Novel 1-(2,4-Difluorophenyl)-5-oxopyrrolidine-3-carboxylic Acid Derivatives

G. Pranaitytė[1,*], B. Grybaitė[1], E. Mickevičiūtė[2]

[1]*Department of Organic Chemistry, Kaunas University of Technology, Radvilėnų pl. 19, Kaunas, Lithuania*

[2]*Department of Information Systems, Kaunas University of Technology, Studentų g. 50, Kaunas, Lithuania*

**guoda.pranaityte@ktu.edu*

Heteroatoms complete a big part of biologically-active chemical entities – according to statistics, more than 85% of all active pharmaceutical compounds contain a heterocycle [1]. Pyrrolidine, hydrazone and benzimidazole fragments have been found to possess a number of biological activities as anticancer, antiviral, antibacterial, antihypertensive, anti-inflammatory, antitumoral, anticonvulsant and antitubercular agents in various drug molecules [2-4].

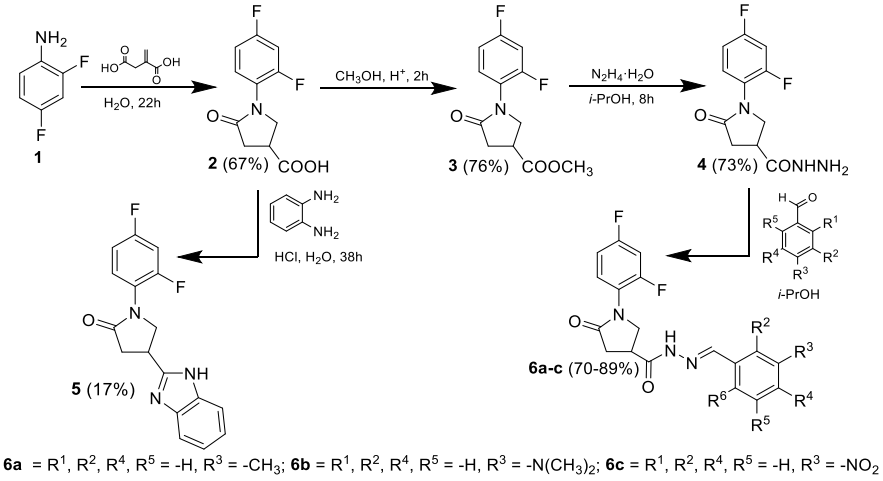

6a = R^1, R^2, R^4, R^5 = -H, R^3 = $-CH_3$; **6b** = R^1, R^2, R^4, R^5 = -H, R^3 = $-N(CH_3)_2$; **6c** = R^1, R^2, R^4, R^5 = -H, R^3 = $-NO_2$

Scheme 1. Synthesis of 1-(2,4-difluorophenyl)-5-oxopyrrolidine-3-carboxylic acid derivatives

The starting compound 1-(2,4-difluorophenyl)-5-oxopyrrolidine-3-carboxylic acid **(2)** was prepared from 2,4-difluoroaniline reaction with itaconic acid in water, at the boiling temperature of the mixture. By using Phillip's method, 4-(1*H*-benzo[*d*]imidazole-2-yl)-1-(2,4-difluorophenyl)pyrrolidine-2-one **(5)** was synthesized. 4-Acetyl-1-(2,4-difluorophenyl)pyrrolidin-2-one **(3)** was obtained from the esterification reaction using catalytic amount of sulfuric acid. In order to synthesize a compound with functional group of hydrazide, methyl ester **3** was transformed into the target product **4** by reaction with hydrazine monohydrate in refluxing 2-propanol. Functional group of hydrazide **4** easily participates in condensation reactions, for this reason interaction of the carbohydrazide **4** with various aromatic aldehydes were investigated (Scheme 1). The desired products **6a-c** were obtained by stirring compound **4** with corresponding aromatic aldehyde in the refluxing isopropanol. The structure of the compounds has been proven by ^{1}H NMR, ^{13}C NMR, FT-IR spectroscopy and elemental analysis. Further studies of the biological activity of synthesized compounds are planned.

References

1. Jampilek, J. (2019). Heterocycles in Medicinal Chemistry. Molecules 2019, Vol. 24, Page 3839, 24(21), 3839. https://doi.org/10.3390/MOLECULES24213839
2. Jeelan Basha, N., Basavarajaiah, S. M., & Shyamsunder, K. (2022). Therapeutic potential of pyrrole and pyrrolidine analogs: an update. Molecular Diversity 2022 26:5, 26(5), 2915–2937. https://doi.org/10.1007/S11030-022-10387-8A. Autor, In Organic Synthesis; Ed. B. Autor, Academic Press, Cambridge, 2009, p. 347.
3. Rollas, S., & Güniz Küçükgüzel, Ş. (2007). Biological activities of hydrazone derivatives. Molecules, 12(8), 1910-1939.).
4. Pathare, B., & Bansode, T. (2021). Review- biological active benzimidazole derivatives. Results in Chemistry, 3, 100200. https://doi.org/10.1016/J.RECHEM.2021.100200

P 064

Electrochemical SEIRAS Analysis of Imidazole Ring Functionalized Self-Assembled Monolayers

V. Pudžaitis[1*], M. Talaikis[2], G. Niaura[1,2]

[1]*Center for Physical Sciences and Technology, Sauletekio av. 3, LT-10257 Vilnius, Lithuania*

[2]*Vilnius University Life Sciences Center Institute of Biochemistry, Sauletekio av. 7 LT-10257 Vilnius, Lithuania*

**Corresponding author, e-mail: vaidas.pudzaitis@ftmc.lt*

Histidine is one of the essential amino acids, which plays an important role in the protein secondary structure and catalytic activity of enzymes. Such a biological significance is related to the histidine's side-chain imidazole ring that participates in a broad range of intermolecular interactions [1]. One of them, the hydrogen bonding interaction is highly important as it provides directionality and specificity through intra and inter-molecular interaction and is fundamental in molecular recognition [2]. Yet, it is difficult to probe H-bond interactions due to the lack of appropriate experimental methods, especially *in situ*. Here we address this issue with surface-enhanced infrared absorption spectroscopy (SEIRAS) study of imidazole ring functionalized self-assembled monolayers (SAMs) formed on the gold surface from the N-(2-(1H-imidazol-4-yl)ethyl)-6-mercaptohexanamide (IMHA) compound. SEIRAS technique coupled with density functional theory (DFT) modeling provided deeper insights into the H-bond interactions of the imidazole ring at the electrified organic layer-water interface [3].

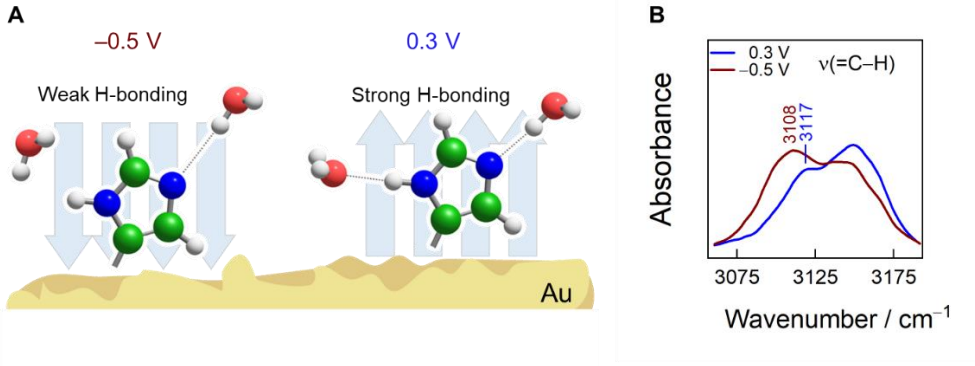

Fig. 1. (A) Schematic representation of imidazole ring interaction with water at the Au-solvent interface at different potentials (vs Ag/AgCl). (B) Fragment of SEIRAS spectrum of imidazole rings C–H stretching vibration at different potentials.

In this work we found that the optimal surface orientation of the alkane chain-nested amide groups that supports the monolayer of IMHA is adopted within 30 min, which was followed by structural changes of the terminal imidazole ring up to 60 min of incubation. It was shown, that these changes are linked with a gradual increase in H-bonding strength at the imidazole group, for which the C–H stretching vibrations at around 3110 cm^{-1} was used as a sensitive H-bond strength marker. Weakening H-bond interaction of imidazole ring with immediate water molecules is observed by a decrease of C–H stretching vibrations as the electric potential was shifted from positive values to –0.5 V.

Our findings shed some light on the interfacial behavior of the amino acid histidine, which has an essential role in protein structure and activity and will be beneficial in surface chemistry applications.

References

1. A.H. Iyer, R.N.V. Krishna Deepak, R. Sankararamakrishnan, J. Phys. Chem. B. 122 (2018) 1205–1212.
2. R. E. Hubbard, ENCYCLOPEDIA OF LIFE SCIENCES, John Wiley & Sons (2010).
3. V. Pudžaitis, M. Talaikis, R. Sadzevičienė, L. Labanauskas and G. Niaura, Materials 15(20): 7221 (2022).

P 065

Fibrous Polycaprolactone-Based 3D Scaffolds for In Vitro Cell Models

A. Pupiute[1,*], D. Ciuzas[1], D. Martuzevicius[1], and E. Krugly[1,2]
[1]Faculty of Chemical Technology, Kaunas University of Technology, Kaunas, LT50254, Lithuania
[2] Bious Labs Life, Draugystes g. 15D, Kaunas, LT51227, Lithuania
**Corresponding author, e-mail: aiste.pupiute@ktu.lt*

INTRODUCTION. Cancer is one of the major health challenges of our time, affecting millions of people around the world. It is a complex and multi-faceted disease that can affect people of all ages, genders, and ethnicities. Currently, cancer is treated with surgical resection, radiation therapy, and chemotherapy. Unfortunately, these treatments are often not successful and can cause serious side effects. In vitro scaffold adaptation is a new approach to treating cancer that could be more effective in treating the disease. This approach uses a scaffold made of inert materials such as polymers, hydrogels, etc., to provide a 3D structure that can be used to study the behavior of cancer cells. The scaffold provides a supportive environment for cancer cells, allowing them to grow and spread in a controlled manner. In addition, the scaffold can be adapted to provide a more targeted form of therapy, such as targeted drug delivery [1, 2].

METHODS. 3D fibrous polymer-based scaffolds were produced by 3D fibre printer (3Df-01C, Bious Labs, Lithuania, https://life.biouslabs.com/), which is a combination of melt electrospinning and fused deposition modelling [3]. To prevent cell migration away from the scaffold, a nanofibrous layer was added to the bottom of the scaffold via solution electrospinning. The hydrophilicity of the scaffolds was improved through low-temperature plasma treatment. The cytotoxicity of the 3D fibrous scaffolds was evaluated according to ISO 10993-5:2009 using mouse fibroblast cells L929. Additionally, the scaffolds were cultivated with human breast cell line MDA-MB-231 and glioblastoma cell line U87-MG.

RESULTS. Three different PCL scaffolds were produced with varying fiber and pore sizes, fiber width ranging between 8 and 25 µm, and pores between 35 and 155 µm (see Fig.1). After low-temperature plasma treatment, the scaffolds were more hydrophilic, with the WCA 60 ± 5°. Results of the MTT test demonstrated that the viability of the human breast cell lines MDA-MB-231 and U87-MG was equal to or higher than that of the 2D cultures during the seven-day period. Moreover, the scaffold supported the cellular growth and viability effectively. Additionally, the MDA-MB-231 cells had a more elongated shape, which was closer to their natural form.

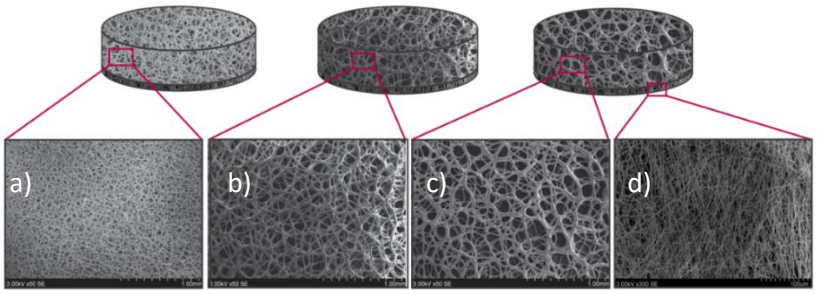

Fig. 1. 3D scaffolds morphology: a) fine fibres and small pores; b) medium size fibres; c) coarse fibres and large pores; d) nanofibrous layer for cell support

CONCLUSIONS. By employing different scaffold morphologies, it is possible to maintain cell vitality and facilitate cell proliferation. These 3D cell culture scaffolds have great potential for use in in vitro cell models for applications like drug testing, tissue engineering, and organ-on-chip simulations.

References

1. Brancato, V., Oliveira, J. M., Correlo, V.M., et.al. Biomaterials 232, 119744 (2020)
2. Nayak, B., Balachander, G.M., Manjunath, S., et.al. Colloids Surf B Biointerfaces, 180, 334-343, 31075687 (2019)
3. Ciuzas, D., Krugly E., Petrikaite V., Biochem. Eng. J. 185, 108531 (2020)

P 066

Synthesis and Investigation of Biphasic Calcium Phosphate Granules

R. Raiseliene*, G. Linkaite, A. Kareiva, I. Grigoraviciute
Faculty of Chemistry and Geosciences, Vilnius University, Naugarduko 24, LT-03225 Vilnius, Lithuania
**Corresponding author, e-mail: ruta.raiseliene@chgf.vu.lt*

Synthetic calcium phosphates (CaPs) have been widely utilized for medical and dental applications such as dental implants, alveolar bridge augmentation, orthopedics, and drug delivery systems due to their biocompatibility, and chemical and biological affinity with bone tissue [1]. These materials are vitally needed by thousands of patients every year [2]. Recently it was found that the main inorganic compounds of human hard tissue are hydroxyapatite (HAP) and magnesium whitlockite (WH) [3]. In our study, we synthesized biphasic materials consisting of various amounts of carbonated hydroxyapatite (CHA) and WH phases to obtain the one mimicking the chemical composition of the inorganic part of native bone.

References

1. Ch. Qi, S. Musetti, L.-H. Fu, Y.-J. Zhu, L. Huang, Chem. Soc. Rev., **48** (2019) 2698-2737.
2. S. Batool, U. Liaqat, B. Babar, Z. Hussain, J. Kor. Cer. Soc., **58** (2021) 530-547.
3. H. Cheng, R. Chabok, X. Guan, A. Chawla, Y. Li, A. Khademhosseini, H. L. Jang, Act. Bio., **69** (2018) 342-351.

P 067

Tunable Properties of $Ti_3C_2T_x$ MXenes 2D Structures for Applications in a Surface Enhanced Raman Spectroscopy

S. Ramanavičius[1]*, A. Popov[2], S. Adomavičiūtė-Grabusovė[3], M. Talaikis[1], V. Šablinskas[3], G. Niaura[1], A. Ramanavičius[4]

[1]Department of Organic Chemistry, State Research Institute Center for Physical Sciences and Technology (FTMC), Sauletekio av. 3, LT-10257 Vilnius, Lithuania;

[2]NanoTechnas—Center of Nanotechnology and Materials Science, Faculty of Chemistry and Geosciences, Vilnius University, Naugarduko St. 24, LT-03225 Vilnius, Lithuania

[3]Institute of Chemical Physics, Vilnius University, Sauletekio Av. 3, LT-10257 Vilnius, Lithuania

[4]Department of Physical Chemistry, Faculty of Chemistry and Geosciences, Institute of Chemistry, Vilnius University, Naugarduko 24, LT-03225 Vilnius, Lithuania

**Simonas Ramanavičius, simonas.ramanavicius@ftmc.lt:*

$Ti_3C_2T_x$ 2D titanium carbide MXenes nanostructures with unique electrical and optical properties were discovered in 2011 by Yury Gogotsi and his research group [1]. Since then, a lot has been done to find optical synthesis conditions, characterize properties and find applications for these materials. Up to date, it is reported that $Ti_3C_2T_x$ finds application in many areas, such as energy storage, photocatalysis, water purification, sensors, biosensors, SERS substrates, electrochromic devices, triboelectric nanogenerators [2,3].

This study focuses on preparing different morphology $Ti_3C_2T_x$ MXene structures and their properties evaluation. As most of the common MXenes synthesis procedures require using HF to form fine structure MXenes, here we tested the influence of HF concentration and etching time. It was found that synthesis procedures affect the structure and morphology of MXenes and determine the properties as well as the application areas. After forming a series of MXenes samples, it was found that Raman spectroscopy is a sensitive method for observing structural changes of the MXenes. Moreover, it was discovered that MXenes are suitable as SERS substrates for detecting various organic molecules and biomolecules.

This project has received funding from the Research Council of Lithuania (LMTLT), agreement No S-PD-22-155.

References

1. M. Naguib, M. Kurtoglu, V. Presser, J. Lu, J. Niu, M. Heon, L. Hultman, Y. Gogotsi, M. W. Barsoum, Advanced Materials, **23**, (2011) 4248-4253.
2. S. Ramanavicius, A. Ramanavicius, International Journal of Molecular Sciences, **21** (2020) 9224.
3. S. Adomavičiūtė-Grabusovė, S. Ramanavičius, A. Popov, V. Šablinskas, O. Gogotsi, A. Ramanavičius, Chemosensors, **9** (2021) 223.

P 068

Excited States of Chlorophyll Molecules in Light-Harvesting Antenna of PSI

G. Rankelytė[1,2,*], J. Chmeliov[1,2], A. Gelzinis[1,2], L. Valkunas[1,2]
[1]*Institute of Chemical Physics, Faculty of Physics, Vilnius University, Lithuania*
[2]*Department of Molecular Compound Physics, Centre for Physical Sciences and Technology, Vilnius, Lithuania*
[*]*gabriele.rankelyte@ff.stud.vu.lt*

Photosynthesis is one of the most important processes on Earth. The most efficient organisms that carry out photosynthesis are land plants. In thylakoid membrane of chloroplasts there are two systems that carry out photosynthesis – Photosystem I (PSI) and Photosystem II (PSII), both with their own light harvesting complexes – LHCI and LHCII. PSI is the most efficient light-to-energy conversion apparatus with quantum yield almost equal to 1 [1]. One of the conditions needed for high efficiency is very fast energy transfer between molecules in light harvesting complex. The excitation dynamics in LHCI is highly affected by the charge-transfer (CT) states that occur between two or more pigments (chlorophylls or carotenoids). Some sites in which CT states occur in LHCI are known, however, they do not completely explain the spectral properties of this antenna, such as the red-shifted peak in fluorescence spectrum.

Light-harvesting complex of PSI absorbs and emits light at the longest wavelengths compared to other pigment-protein complexes. In plants, light-harvesting antenna of PSI is composed of four species of LHCI complexes. They all have very similar structure; however, their spectral properties are different. The most red-shifted peak (at around 733 nm) is observed in the fluorescence spectrum of Lhca4 light harvesting sub-complex [2].

The structure of Lhca4 was obtained as the 4th chain of PSI supercomplex structure, freely accessible on Protein Data Bank (PDB) [3]. In order to find possible locations of the charge-transfer states in Lhca4, we examined chlorophyll dimers that have the shortest Mg-Mg distance. After performing geometry optimization of selected individual chlorophylls, they were mapped on the Lhca4 structure to form dimers (as shown in Fig. 1). We then examined the excited states properties of all selected dimers in vacuum. After analyzing the data of 12 chosen dimers and their 8 lowest excited states, 19 charge-transfer states were located.

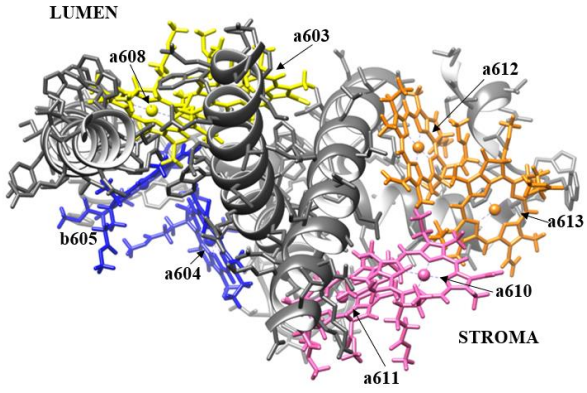

Fig. 1. Lhca4 complex. Amino acids are presented in gray, carotenoids are not in the picture. The four dimers of chlorophylls (without the phytyl tail) are indicated in the figure.

References

1. R. Croce, H. van Amerongen, Photosynth. Res., **116** (2013) 153-166.
2. T. Morosinotto, M. Mozzo, R. Bassi, R. Croce, JBC, **280** (2005) 20612-20619.
3. X. Qin, M. Suga, T. Kuang, J. R. Shen, Science, **348** (2015) 989-995.

P 069

Effect of Mn^{+2} Doping on the Formation and Properties of $BiVO_4$ Coatings

P. Rivera[1*], M. Petrulevičienė[1], I. Savickaja[1], K. Turuta[2], J. Juodkazytė[1], A. Ramanavičius[1]

[1] Center for Physical Sciences and Technology, Department of chemical engineering and technology Saulėtekio av. 3, LT-10257 Vilnius

[2] Institute of Chemistry, Faculty of Chemistry and Geosciences, Naugarduko str. 24, LT-03225 Vilnius University, Lithuania

pamela.rivera@ftmc.lt

Pharmaceuticals are among the major groups of emerging contaminants given their acute effects on living organisms even at low concentrations and the difficulty of their removal by traditional wastewater treatments. Photoelectrochemical (PEC) advanced oxidation system (AOS) for degradation of pharmaceuticals is a suitable alternative, because of sustainability and flexibility. Bismuth vanadate ($BiVO_4$) appears as a promising semiconductor for such application due its low toxicity, high photostability in neutral pH, resistance to photo-corrosion and narrow band gap [1]. However, the practical application of $BiVO_4$ is hindered by the rapid recombination of the photo-generated electron-hole pair. Doping with Mn^{+2} is an approach to prolong lifetime of charge carriers thus enhancing the photocatalytic activity of $BiVO_4$ photoanodes [2].

In the present work the influence of Mn^{2+} incorporation on the crystalline structure, morphology and the photoelectrochemical (PEC) properties of $BiVO_4$ coatings was investigated. Manganese doped $BiVO_4$ powder and thin films on fluorine doped tin oxide (FTO) substrate were synthesized via hydrothermal method. Crystalline structure and morphology of powders were analyzed using X-ray diffraction (XRD), energy dispersive X-ray (EDX) and scanning electron microscopy (SEM) analysis. The PEC properties of synthesized coatings were evaluated using cyclic voltammetry (CV) and electrochemical impedance spectroscopy (EIS). Production of reactive chlorine and reactive sulfate species will be evaluated using chronoamperometry (CA) technique.

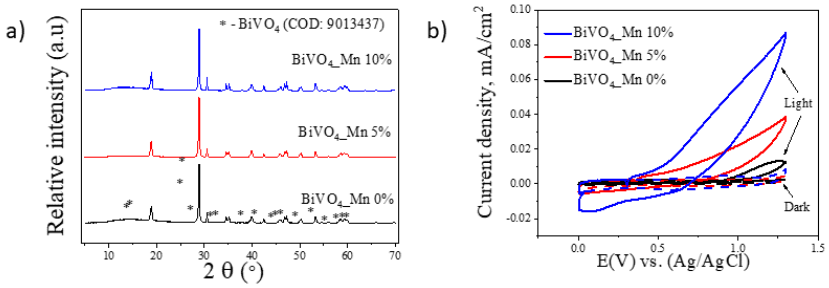

Fig. 1. a) XRD diffractograms of Mn-doped coatings; b) Cyclic voltammograms of $BiVO_4$ electrodes synthesized with different concentrations of Mn^{+2}. Experiments were performed in 0.5 M Na_2SO_4 solution; Reference electrode: Ag/AgCl; potential scan rate 50 mV/s. Light intensity 100mW/cm^2.

XRD analysis showed that all samples were fully crystalline (Fig. 1a). The results show that PEC activity is enhanced by the incorporation of increasing amounts of Mn^{+2} on the $BiVO_4$ coatings (Fig.1b). The highest photocurrent was reached ~0.08 mAcm^{-2} after doping with 10% of Mn. The results on PEC production of reactive species in the electrolytes of various composition as well as the efficiency of decomposition of organic compounds will be presented in the conference.

Acknowledgement: This project has received funding from the Research Council of Lithuania (LMTLT), agreement No S-PD-22-2.

References

1. M. A., M. J., M. Ashokkumar, and P. Arunachalam, "A review on BiVO 4 photocatalyst: Activity enhancement methods for solar photocatalytic applications," Appl Catal A Gen, vol. 555, pp. 47–74, Apr. 2018, doi: 10.1016/j.apcata.2018.02.010.
2. T. Wechprasit, T. Kansaard, A. Bootchanont, and W. Pecharapa, "Structural and Optical Properties of Mn-Incorporated $BiVO_4$ Nanoparticles Synthesized by Sonochemical Process," Integrated Ferroelectrics, vol. 222, no. 1, pp. 116–124, Jan. 2022, doi: 10.1080/10584587.2021.1961521

P 070

Role of Water Vapour Pressure in the Carbonation Process of Calcium Monosulfoaluminate 12-Hydrate

D. Rubinaite[1, *], T. Dambrauskas[1], A. Eisinas[1]

[1]Department of Silicate Technology, Kaunas University of Technology, Radvilenu pl. 19, LT–50254 Kaunas, Lithuania

**Corresponding author, email: dovile.rubinaite@ktu.lt*

Carbonation of cement hydrates is one of the crucial aspects causing the deterioration of concrete structures [1]. It is known that ambient CO_2 dissolves in the alkaline pore solution of concrete and interacts with the cementitious products causing deterioration of hydrates and formation of calcium carbonate ($CaCO_3$). This process is influenced by various environmental factors such as carbon dioxide (CO_2) concentration, relative humidity, temperature, etc. [2]. Despite numerous studies, the opinion of scientists differs on the carbonation mechanism, kinetics, and influence of external factors to date. One of the possible pathways to study carbonisation is the investigation of the behaviour of individual hydrates under different conditions [3]. Thus, this work aims to examine the influence of varying water vapour pressure (p/p_0) on the carbonation mechanism of cementitious hydrate, namely calcium monosulfoaluminate 12-hydrate (Ms12).

For the study, synthetic Ms12 was produced using a mixture of analytical grade materials (CaO, Al_2O_3, $CaSO_4 \cdot 2H_2O$), referring to ye`elimite ($Ca_4Al_6O_{12}(SO_4)$) stoichiometry. The synthesis approach consisted of the mechanochemical treatment (dry grinding at 900 rpm in a vibrating cup mill with 3 on-off cycles of 10 min) followed by the hydrothermal synthesis (for 8 h at 130 °C). After hydrothermal treatment, the suspension was decanted, rinsed with acetone, filtered, and dried in an oven at 50 °C ± 0.2 °C for 24 h. Meanwhile, for carbonation examination, prepared samples were placed in 5 desiccators with different relative water vapour pressures (p/p_0 varied from 0.355 to 1) in the presence of the room CO_2 concentration (668 ± 3 ppm). The experiment was carried out at a temperature of 21 °C ± 0.5 °C for up to 90 days.

The results indicate that the water vapour pressure conditions are an essential factor that influences the stability and carbonation rate of Ms12. It is determined that Ms12 interacting with CO_2 at p/p_0 of 0.355-0.565 gradually disintegrates into calcium carbonate, aluminium hydroxide, and calcium hemihydrate. Meanwhile, gypsum is identified at a higher p/p_0 (>0.565) instead of calcium hemihydrate. Additionally, above 0.565 p/p_0, Ms12 becomes metastable and gradually recrystallises into ettringite. Referring to the rate of carbonation, it is seen that an increase in the water vapour pressure leads to accelerated carbonation of the sample (Fig. 1.). Thermodynamic and apparent kinetic parameter calculations also were applied to verify the obtained experimental data and the theoretical hypothesis. The phase changes in the samples were confirmed by X-ray diffraction analysis and simultaneous thermal analysis methods.

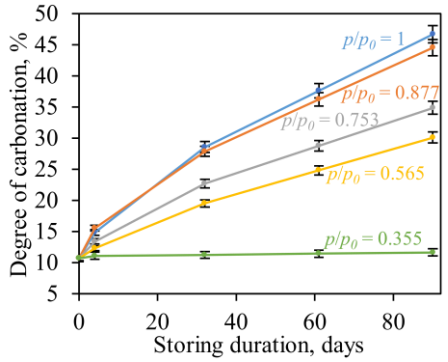

Fig. 1. Dependence of the carbonation degree of the sample on the storage duration at different p/p_0

References

1. S. von Greve-Dierfeld et al., Mat Struct., **53** (2020).
2. M. Elsalamawy, A.R. Mohamed, E.M. Kamal, Alex Eng j., **58** (2019) 1257–1264.
3. S. Steiner et al., Cem Concr Res., **135** (2020) 106-116.

P 071

Synthesis of New 1-(9-Ethylcarbazol-3-yl)-5-oxopyrrolidine-3-carbohydrazide Derivatives

E. Mieliauskaitė, B. Sapijanskaitė-Banevič*, R. Vaickelionienė, B. Grybaitė, K. Anusevičius

Kaunas University of Technology, Kaunas, Lithuania,
*birute.sapijanskaite@ktu.lt

In this work, 1-(9-ethylcarbazol-3-yl)-5-oxopyrrolidine-3-carbohydrazide **1** was used as a precursor for the synthesis of 5-oxopyrrolidine derivatives containing fragments of hydrazone, pyrrole, triazolethione, 1,2,4-triazine, and pyrrolidinone.

In the first stage of this study a series of heterocyclic compounds was prepared. For 1,3,4-oxadiazole **2**, hydrazide **1** was treated with carbon disulphide in alkaline methanolic solution. The reaction proceeded *via* an intermediate hydrazinocarbothioate whose aqueous solution was acidified with hydrochloric acid to pH 1 to obtain the target compound **2**. The condensation of hydrazide **1** with hexane-2,5-dione in propan-2-ol in the presence of a catalytic amount of acetic acid gave 2,5-dimethylpyrrole **3**.

To obtain 4-phenyl-1,2,4-triazole **5**, thiosemicarbazide **4** was first synthesized by refluxing hydrazide **1** with phenylisothiocyanate in the mixture of methanol and 1,4-dioxane for 7 h. The conversion of tiosemicarbazide **4** to triazole **5** was carried out in refluxing aqueous 2% KOH solution with the subsequent acidification of the reaction mixture with hydrochloric acid to pH 2.

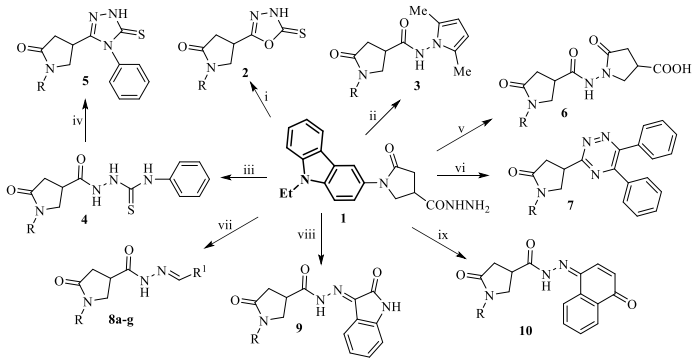

R: 9-ethylcarbazol-3-yl;
8a R^1 = 5-O_2N-2-thienyl;
8b R^1 = 2-thienyl;
8c R^1 = 4-FPh.
8d R^1 = 2,4-diFPh;
8e R^1 = 4-ClPh;
8f R^1 = 4-BrPh;
8g R^1 = 4-O_2NPh.

Reagents and reaction conditions: i CS_2, KOH, MeOH, Δ, 48 h, H_2O, HCl to pH 1; *ii* hexane-2,5-dione, propan-2-ol, AcOH, Δ, 33 h, *iii* PhNCS, MeOH:1,4-dioxane (2:1), Δ, 7 h; *iv* 2% KOH, 3 h, HCl to pH 2;
v itaconic acid, H_2O, HCl, Δ, 38 h; *vi* $(PhCO)_2$, $AcONH_4$, AcOH, Δ, 28 h, H_2O; *vii* corresponding aromatic aldehyde, propan-2-ol:1,4-dioxane (1:1), Δ, 2.5–7 h, respectively; *viii* isatin, propan-2-ol:1,4-dioxane (1:1), Δ, 2 h; *ix* 1,4-naphthoquinone, propan-2-ol:1,4-dioxane (1:1), Δ, 5 h.

The ability of the primary amines to react with itaconic acid was applied to synthesize compound **6** bearing two pyrrolidinone rings. The convenient method, namely refluxing both reagents in water afforded the desired product **6**. In this case, the reaction was catalysed with hydrochloric acid. Six-membered heterocycle triazine **7** was obtained by reacting hydrazide **1** with 1,2-diphenylethane-1,2-dione in refluxing acetic acid in the presence of 10-fold excess of ammonium acetate.
Next stage of the study was targeted to synthesize a library of hydrazone-type compounds **8–10**. Condensation of **1** with various aromatic aldehydes in 2-propanol and 1,4-dioxane mixture at reflux for 2.5−7 h resulted in hydrazones **8a–g**. 2-Oxindole derivative **9** was synthesized from **1** and isatin by refluxing them in propan-2-ol and 1,4-dioxane mixture. Furthermore, condensation of hydrazide **1** with 1,4-naphthoquinone at the same conditions provided compound **10**.

P 072

Investigation of the Changes in Structural and Optical Properties of Ag-O/PET/PVC Composites after Aging

E. Skuodaitė[1*], V. Krylova[1]
[1]*Kaunas University of Technology, Radvilenu St. 19, LT-50524 Kaunas, Lithuania*
**Corresponding author, e-mail:emilija.skuodaite@ktu.edu*

Architectural textiles (AT) are becoming increasingly important in everyday life and have attracted increased attention from the scientific community in the last decade. This interdisciplinary area of interest ranges from materials science to photovoltaic cells. The concept of textile-integrated flexible photovoltaic systems (TE-EPV) is one of the most promising forms of technology [1]. Semiconducting oxides have been used in photovoltaic (PV) technology for many years. The versatility of their properties and the simplicity of their production methods give oxides a unique place in relation to the new generation of PV. Metal oxides are stable at ambient temperature and are generally harmless to living organisms. Many metal oxides are n-type semiconductors. Silver(I) oxide belongs to p-type oxides and can form oxide p-n heterojunctions in solar cells. The optical band gap for Ag_2O ranges from 1.2 eV [2] to 3.4 eV [3] depending on the stoichiometry, structure and physical properties that result from the deposition method. Throughout the exploitation AT undergoes mechanical stress, thermal effects, chemical corrosion, etc., causing aging and functional loss of materials.

In this study, silver oxide films were synthesised by SILAR method on a 0.53 mm thick AT (SATTLER–PROTEX Austria). It was made from the polyethylene terephthalate (PET) fabric with double-sided polyvinylchloride (PVC) and lacquer coatings. Filler pigment is not specified, but from XRD analysis it was determined that the dominant inorganic filler was $CaCO_3$ and TiO_2. The main objective of this study is to elaborate the effect of thermal aging on structural and optical properties of obtained Ag-O/PET/PVC composites. Thermal aging was carried out by keeping samples in air at a temperature of 70°C and atmospheric pressure for 336 hours.

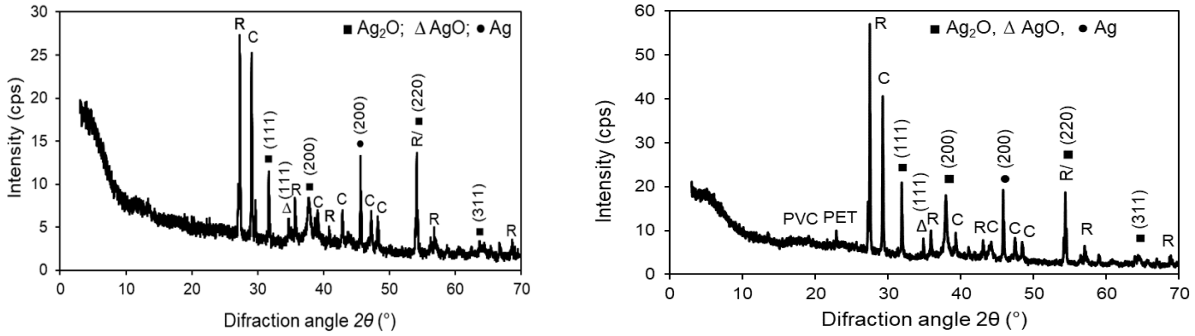

a b

Fig. 1. XRD diffractograms of the Ag-O/PET/PVC composites before (a) and after (b) thermal aging: $CaCO_3$ – C, TiO_2 – R (rutile), Ag_2O – ■, AgO – Δ, Ag – ●.

After thermal aging (Fig. 1b), in comparison with what was before it (Fig. 1a), the position of the XRD peaks did not change, and the intensity of many reflections increased, which indicates an increase in the crystallinity of the deposited films. In addition, the composition has not changed. The results obtained showed that the applied aging influenced the optical properties of the composites. Aging caused a shift in the optical bandgap (E_{bg}). After thermal aging, E_{bg} increased from 0.89 ± 0.02 eV to 1.04 ± 0.02 eV. Higher optical band gaps and refractive indices mean that Ag-O/PES/PVC composites are a good material for photovoltaic applications.

References

1. Q. Li, A. Zanelli, Renew. Sust. Energ. Rev., **139** (2021) 110678.
2. E. Fortiu, F.L. Weichman, Phys. Stat. Sol. B, **5** (1964) 515-524.
3. E. Lund, A. Galeckas, A. Azarov, E.V. Monakhov, B.G. Svensson, Thin Solid Films, **536** (2013) 156-159.

P 073

Effect of Titanium Oxide on the Formation of Hydroxyapatite under Microwave Synthesis Conditions

I. Stebryte*, K. Baltakys
Department of Silicate Technology, Kaunas University of Technology,
Radvilenu pl. 19, LT – 50270 Kaunas, Lithuania
**igne.stebryte@ktu.edu*

Titanium oxide is used in many personal care products as: toothpastes, sunscreens, pressed and loose powders, day creams and lip balms, as an inorganic UV filter/absorber or bleaching agent. Currently, the only form in which titanium oxide is used in cosmetics – titanium oxide nanoparticles [1]. Calcium phosphates have good biodegradability, compatibility, bioresorption and osteoinductivity. Calcium phosphates such as hydroxyapatite is major component of bone tissue and used in the cosmetic industry [2]. The aim of this work was to investigate the influence of titanium oxide on the formation of hydroxyapatite.

In this work, titanium oxide, calcium carbonate and ammonium hydrophosphate were used as the main raw materials in the microwave synthesis of hydroxyapatite.

The dry primary mixture of calcium carbonate and titanium dioxide was mixed with ammonium hydrophosphate, with a molar ratio of Ca/P=1,67 was mixed with distilled water to reach a solution/solid ratio of the suspension of 10:1. The microwave synthesis has been carried out in unstirred suspensions under saturated steam pressure at the temperature of 80-200 °C for 2 h. XRD, DSC, TG, and FT-IR methods were used to characterize the products of synthesis.

It was found that in the $CaCO_3$-$(NH_4)_2HPO_4$-TiO_2-H_2O system the raw materials, e.g. TiO_2 (*d*-spacing – 0.352; 0.189; 0.238 nm (PDF 00-021-1272)) and $CaCO_3$ (*d*-spacing – 0.304; 0.229; 0.210; 0.191; 0.188 nm (PDF 04-023-8700)) react poorly at a temperature of 80 °C. In the products of synthesis low intensity peaks were identified which are assigned to target product - hydroxyapatite (*d*-spacing – 0.282; 0.273; 0.278; 0.819; 0.194 (PDF 01-082-1943)). Meanwhile, it was determined that the increment of microwave synthesis temperature had a positive influence on the interaction of raw materials with intermediate synthesis compounds (Fig. 1).

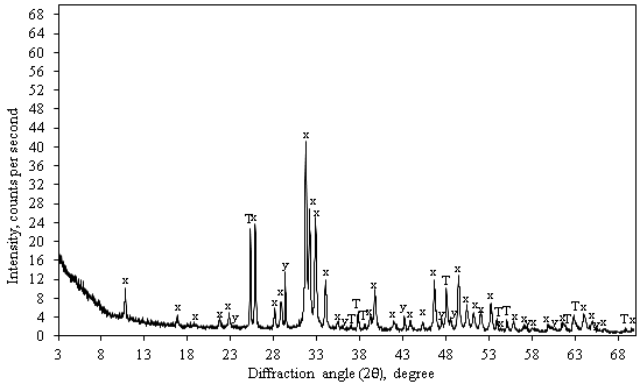

Fig. 2. XRD curves of microwave synthesis products (200 °C, 2h) in the $CaCO_3$-$(NH_4)_2HPO_4$-TiO_2 (1mol) - H_2O system. Indexes: x-hydroxyapatite; T-TiO_2; y-$CaCO_3$.

At 200 °C after 2 hours, the intensity of the main diffraction peaks of $CaCO_3$ is significantly reduced, only 3,57 % of carbonate was left unreacted in the reaction mixture. For this reason, the synthetic hydroxyapatite predominates in the synthesis products.

References

1. Dréno B., et. al. *Journal of the European Academy of Dermatology and Venereology*, **2019**, p.p. 34-36.
2. Carella F, et. al. *Materials*, **2021**

P 074

Bimetallic Nickel-Manganese/Titanium Electrocatalyst for Efficient Hydrogen Evolution Reaction

S. Barua*, A. Balčiūnaitė, J. Vaičiūnienė, L. Tamašauskaitė-Tamašiūnaitė, E. Norkus
Department of Catalysis, Center for Physical Sciences and Technology (FTMC), LT-10257 Vilnius, Lithuania
**Corresponding author: sukomol.barua@ftmc.lt*

To meet the high global energy demand and related sustainability challenging requirements, hydrogen has been promoted as a renewable, clean and green energy carrier that possess potential to replace non-renewable fossil fuels. Electrochemical water splitting is a sustainable pathway to obtain green hydrogen energy that does not contribute to CO_2 emission but the design and development of active, robust, and stable electrocatalysts for water electrolyzers with higher efficiency is the most challenging issue. In this work, we report a facile, cost-effective synthesis of catalysts consisting earth-abundant materials supported on a Ti surface (1×1 cm^2) by the electrochemical deposition method. The fabricated Ni-Mn alloy catalysts demonstrated outstanding electrocatalytic performance for hydrogen evolution reaction (HER) in alkaline media (1 M KOH) where the composition of the electrochemical bath is shown in Table 1.

Catalysts	Concentration (M)	
	Ni^{2+}	Mn^{2+}
NiMn/Ti-1	0.2	0.2
NiMn/Ti-2	0.2	0.4
NiMn/Ti-3	0.2	0.6
NiMn/Ti-4	0.2	0.8
NiMn/Ti-5	0.2	1.0

Table 1. The composition of electrochemical bath

Fabricated NiMn/Ti-5 electrocatalyst exhibits excellent HER activity with minimum overpotentials of 135 mV and 215 mV to reach a current density of 10 mA/cm^2 and 20 mA/cm^2, respectively. The corresponding NiMn/Ti-4 and NiMn/Ti-3 catalysts also have demonstrated superior lower overpotentials of 149 mV and 170 mV to drive the benchmark current density of 10 mA/cm^2 and 225 mV and 245 mV to attain a current density of 20 mA/cm^2, respectively. These catalysts have also exhibited excellent long-term stability for 10 h at the constant potential that assures their robustness and higher durability regarding alkaline water splitting.

P 075

Structural Properties of MWCNTs@PDMS-1000 Nanocomposites

I. Sulym[1,2*], O. Goncharuk[3], K. Terpiłowski[3], Z. Valdez-Nava[1]

[1]LAPLACE, Université Toulouse III - Paul Sabatier, CNRS, INPT, UPS,
118 route de Narbonne, 31062 Toulouse, France,
[2]Chuiko Institute of Surface Chemistry of NASU, General Naumov 17 str., 03164 Kyiv, Ukraine,
[3]Maria Curie-Sklodowska University, M. Curie-Sklodowska sq. 3, 20031 Lublin, Poland
**Corresponding author: iryna.sulym@laplace.univ-tlse.fr*

Multi-walled carbon nanotubes (MWCNTs) with a high degree of structural perfection exhibit great potential applications in flexible electronics, storage devices, supercapacitor, electromagnetic interference shielding, and piezoelectric sensors [1, 2]. With the addition of MWCNTs into polymer matrices, manufacturers can manipulate a material's conductivity, strength, thermal stability/flame retardancy, flexibility/flowability, etc. [3].

In this experimental work, nanomaterials based on MWCNTs and poly(dimethylsiloxane) (code name PDMS-1000, Mw ≈ 7960 g/mol) have been successfully synthesized. A series of samples was prepared by the method of physical adsorption of PDMS-1000 onto pristine carbon nanotubes (P-MWCNTs) in the amount of 5, 10, 15 and 20 wt. %. The prepared polymer nanocomposites were marked as MWCNTs@PDMS-1000(5), MWCNTs@PDMS-1000(10), MWCNTs@PDMS-1000(15) and MWCNTs@PDMS-1000(20), respectively. Raman Spectroscopy (RS) and X-ray diffraction (XRD) are valuable tools for elucidating the structure of carbon nanotubes and their polymer nanocomposites [4, 5].

The XRD data for P-MWCNTs and MWCNTs@PDMS-1000 composites are shown in Fig. 1*a*. The broad peaks at 2θ ~26°, ~43° and ~53° corresponds to (0 0 2), (1 0 0) and (0 0 4) planes of typical graphite, respectively. Also, we can observe the characteristic peak of PDMS located at 12º (Fig. 1*a*, *curve 3*) attributing to its tetragonal phase. The Raman spectra of the P-MWCNTs and polymer nanocomposites were measured (Fig. 1*b*). The characteristic bands of MWCNTs, D band (defect) at ~ 1320 cm^{-1}, G band (graphite band) at ~ 1610 cm^{-1} and G'-band (D overtone) at ~ 2630 cm^{-1} were observed. The intensity ratio of G band to D band (A_G/A_D) is used as an indicator of the amount of defects in MWCNTs. After adsorption of 20 wt. % polymer, relative intensity ratio A_G/A_D tends to decrease from 0.48 for P-MWCNTs to 0.42 for MWCNTs@PDMS-1000(20) nanocomposite, respectively. In addition, the intensity of the G'-peak for the MWCNTs@PDMS-1000(20) sample (Fig. 1*b*, *curve 5*) is significantly reduced compared to P-MWCNTs (Fig. 1*b*, *curve 1*) as it becomes less ordered (i.e., more impurities or introduced polymer).

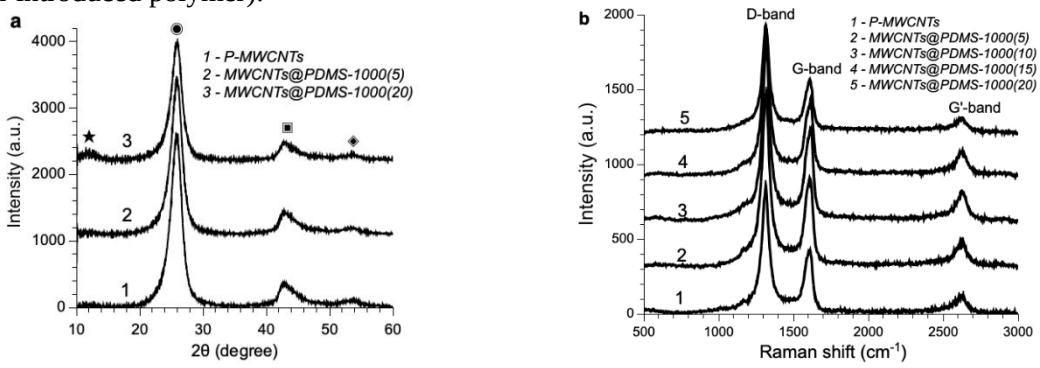

Fig. 1. XRD patterns (*a*) and Raman spectra (*b*) of P-MWCNTs and polymer nanocomposites.

Acknowledgments:
The authors are grateful for the financial support of the International Visegrad Fund (Dr. I. Sulym, Contract number 52210724; D.Sc. O. Goncharuk, Contract number 52211441; Dr.hab. K. Terpilowski, Contract numbers 52211441 and 52210724). I.S. acknowledges PAUSE Program from the College de France for the financing support.

References

1. S. Malekie, F. Ziaie, J. Polym. Eng., **37** (2017) 205–210.
2. M. Terrones, Annu. Rev. Mater. Res., **33** (2003) 419–501.
3. J. Yan, Y.G. Jeong, Appl. Phys. Lett., **105** (2014) 051907.
4. M. Dresselhaus, G. Dresselhaus, A. Jorio, J. Phys. Chem., **C 111** (2007) 17887–17893.
5. B. Emmanuel, S. Thomas, G. Raghuvaran, D. Sherwood, J. Alloys Compd., **479** (2009) 484–488.

P 076

Microwave Synthesis of Hydroxyapatite Substituted with Zn^{2+} Ions in the Temperature Range of 80 - 200°C

R. Surblyte*, K. Baltakys
Department of Silicate Technology, Kaunas University of Technology,
Radvilenu pl. 19, LT – 50270 Kaunas, Lithuania
**rugile.surblyte@ktu.edu*

Hydroxyapatite is the main inorganic component of the hard tissues of the human body, such as bones and teeth, accounting for about 70% of the skeleton and 90% of tooth enamel, therefore, it is in-demand materials for repairing bone defects, especially in the fields of dentistry, orthopedics and trauma surgery [1, 2]. Non-stoichiometric hydroxyapatite that naturally occurs in bone tissue contains small amounts of ions such as Cl^-, F^-, Zn^{2+}, K^+, Si^{2+}, Ba^{2+}, Mg^{2+} and Na^+ [3]. Hydroxyapatite doped with Zn^{2+} ions, depending on the amount of doped Zn^{2+}, is effective against gram-negative, gram-positive bacterias and fungi such as *A. niger*, *C. Albicans*. Thus, the incorporation of Zn^{2+} ions into hydroxyapatite not only improves the compatibility of the system, but also provides functional properties to the system [4, 5]. Therefore, the aim of this work was to investigate the influence of microwave synthesis temperature on the formation of hydroxyapatite substituted with Zn^{2+} ions. In this work, calcium carbonate, zinc oxide and diammonium hydrophosphate anhidride were used as raw materials for the synthesis. The synthesis of hydroxyapatite substituted with Zn^{2+} ions was based on the microwave method. The dry primary mixture of calcium carbonate, zinc oxide and diammonium hydrophosphate anhidride with a molar ratio of CaO/PO_4=1.67 was mixed with distilled water to reach a solution/solid ratio of the suspension of 10:1. The microwave synthesis has been carried out in stirred suspensions under saturated steam pressure at the temperature of 80-200 °C for 2h. XRD, DSC, TG, and FT-IR methods were used to characterize the products of synthesis. It was determined, that not only quantity of zinc additive but also temperature of synthesis influence the formation of hydroxyapatite substituted with Zn^{2+} ions and the stability of intermediate compounds. By increasing the synthesis temperature, less intermediate compounds such as calcium phosphate hydroxide hydrate, hydrogen calcium phosphate, calcium phosphate, calcium hydroxide or ammonium zinc phosphate are formed. Accordingly, larger amounts of the targeted product – hydroxyapatite substituted with Zn^{2+} ions are formed at 200 ºC (Fig.1).

Fig. 1. Results of microwave synthesis (200°C, 2h) of hydroxyapatite substituted with Zn^{2+} ions in $CaCO_3$-$(NH_4)_2HPO_4$-ZnO (1 mol)-H_2O system XRD (a) and STA(b). Indexes: h – hydroxyapatite substituted with Zn^{2+}

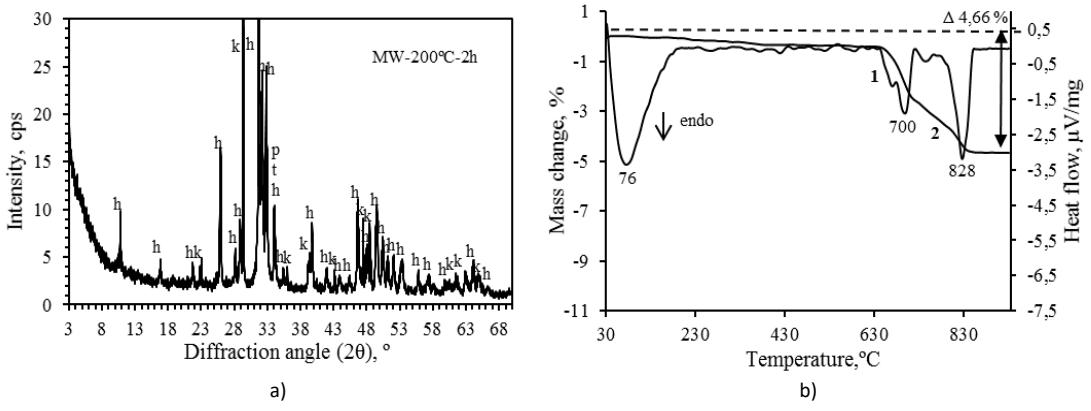

ions, k – calcium carbonate, p – calcium hydroxide, t – calcium phosphate.

References

1. M. Akram, R. Ahmed, I. Shakir, W.A.W Ibrahim, R. Hussain. J Mater Sci., **49** (2014), 1461–1475.
2. L. An, W. Li, Y.Xu, D. Zeng, Y.Cheng, G. Wang. Ceramics International, **42** (2016), 3104–3112.
3. K. Pajor, L. Pajchel, J. Kolmas. Materials, **12** (2019), 2683.
4. D.R. Behera, P. Nayak, T.R. Rautray, Journal of King Saud University – Science, **32** (2020), 848-852.
5. I. Uysal, B. Yilmaz, Z. Evis, J Aust Ceram Soc., **57** (2021), 869–897.

P 077

Adsorption of Phosphate Ions by CSH (CaO/SiO_2=1.5) Adsorbent

E. Švedaitė*, K. Baltakys, T. Dambrauskas
Department of Silicate Technology, Kaunas University of Technology,
Radvilėnu pl. 19, LT – 50270 Kaunas, Lithuania
**evelina.svedaite@ktu.edu*

An excessive amount of phosphorus in surface water is one of the leading causes of eutrophication in many lakes and rivers in the world. Therefore, phosphate recovery is necessary to reduce environmental pollution and promote the sustainable use of phosphorus resources. Various methods have been developed to reduce phosphate ions concentration in water [1]. One of the promising technologies for phosphorus removal and recovery is adsorption because it offers high flexibility. Calcium-rich materials are found to be the most promising and widely accepted sorbents for phosphorus removal [2].

This study aims to investigate the adsorption process of phosphate ions in KH_2PO_4 solution by using a hydrothermally synthesized CSH (CaO/SiO_2=1.5).

In this work, the adsorbent was synthesized in a mixture of CaO and polonite (CaO/SiO_2 molar ratio 1.5) under hydrothermal conditions (16 h, 200 °C). Adsorption experiments were carried out at 25 °C temperature in a thermostatic absorber by stirring 10 g of synthetic adsorbent in 1000 mL of KH_2PO_4 solution containing 7.8 g/dm^3 of phosphate ions. pH value of primary solution is equal to 4.5.

The results of the adsorption experiments revealed that more than 10% PO_4^{2-} ions (7.1 mg PO_4^{2-}/g) were adsorbed within first seconds (30 s). It should be noted that the adsorption proceeded intensively until 30 min because the amount of adsorbed PO_4^{2-} ions significantly increased (44.4 mg PO_4^{2-}/g) (Figure 1, b). Later, the concentration of the PO_4^{2-} ions decreases steadily in the solution (Figure 1, a). It was determined, that at the end of experiment (7 days) the amount of adsorbed phosphate ions was equal to 75.5 mg PO_4^{2-}/g, i.e. the removal efficiency of phosphates achieved 94.9%.

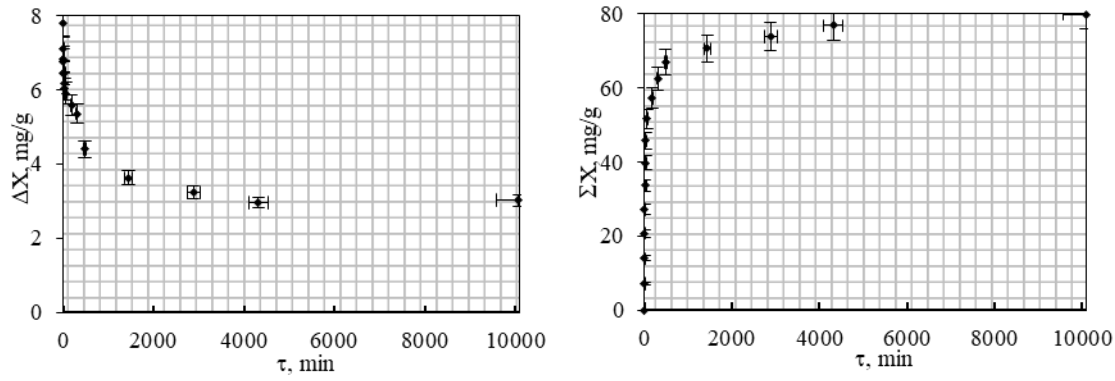

a *b*

Fig. 1. Differential (a) and integral (b) kinetic curves of PO_4^{2-} ions adsorption by hydrothermally synthesized adsorbent when the initial concentration of ions was equal to 7.8 g/dm^3.

References

1. Z. Zhang, et al. *Environmental Science: Water Research and Technology*. **2019**, 5(1), 131–139.
2. C. Li, et al. *Chemical Engineering Journal*. **2017**, 317, 844–853.

P 078

Design of 5-Substituted 2-Oxindole-hydrazone Derivatives Bearing 1,2,4-Triazole-3-thiol Moiety as Anticancer Agents

A. Šermukšnytė[1*], V. Petrikaitė[2], K. Kantminienė[3], I. Jonuškienė[1], I. Tumosienė[1]

[1]*Department of Organic Chemistry, Kaunas University of Technology, Radvilėnų pl. 19, 50254 Kaunas, Lithuania*

[2]*Institute of Cardiology, Lithuanian University of Health Sciences, Sukilėlių pr. 13, 50162 Kaunas, Lithuania*

[3]*Department of Physical and Inorganic Chemistry, Kaunas University of Technology, Radvilėnų pl. 19, 50254 Kaunas, Lithuania*

**aida.sermuksnyte@ktu.lt*

Cancer is a malignant disease characterized by rapid and uncontrolled cell proliferation. It is one of the leading causes of mortality, accounting for vast morbidity worldwide [1]. Cytotoxic drugs are among the most important treatments used for cancer; however, their permeability and efficiency are low. The search for new effective anticancer agents with superior selectivity towards cancer cells is of crucial importance. Isatin derivatives have been widely recognized in cancer therapeutics as protein kinase inhibitors. Hybrid 2-oxindole derivatives bearing the hydrazone moiety have been shown to exhibit good activity against various tumour cells (colon, leukemia, breast, and kidney) [2].

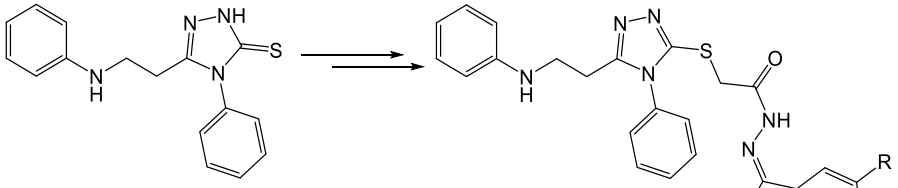

4: R = H; **5**: R = OCH_3; **6**: R = NO_2; **7**: R = F; **8**: R = OCF_3.

Scheme 1. Synthesis of 2-oxindole derivatives **4**–**8**.

Reaction of 1,2,4-triazole-5-thione **1** [3] with ethyl chloroacetate in DMF in the presence of triethylamine provided ester **2**, which subsequently was converted into 1,2,4-triazol-3-ylthioacetohydrazide **3** in the reaction with hydrazine hydrate. Reaction of **3** with the corresponding isatins provided target 2-oxindole-hydrazones **4-8** (Scheme 1) [4, 5]. The anticancer activity of **4**–**8** was tested against melanoma IGR39, triple-negative breast cancer MDA-MB-231, and pancreatic carcinoma Panc-1 cell lines. Hydrazones bearing 5-fluoro- or 5-trifluoromethoxy-2-oxindole moiety **7** and **8**, respectively, were identified as the most active against the malignant melanoma IGR39 cell line. This type of cancer is usually considered as a relatively resistant one. Tumour spheroids are one of the most simplified 3D cell models, and are characterised by hypoxia formation in their core as well as the gradient of tested substances [6]. The effects of 10 µM solutions of the hydrazones **4**, **7**, and **8** on melanoma IGR39, triple-negative breast cancer MDA-MB-231, and pancreatic carcinoma Panc-1 cell spheroid growth were evaluated. *N*'-(2-oxoindolin-3-ylidene)-2-((4-phenyl-5-(2-(phenylamino)ethyl)-4*H*-1,2,4-triazol-3-yl)thio)acetohydrazide (**4**) inhibited melanoma spheroid growth the most.

References

1. R.L. Siegel, K.D. Miller, H.E. Fuchs, A. Jemal, *CA A Cancer J. Clin.* 71 (2021) 7–33.
2. R.E. Ferraz de Paiva, E.G. Vieira, D. Rodrigues da Silva, C.A. Wegermann, A.M. Costa Ferreira, *Front. Mol. Biosci.* 7 (2021) 627272.
3. I. Tumosiene, K. Kantminiene, A. Pavilonis, Z. Mazeliene, Z.J. Beresnevicius, *Heterocycles* 78 (2009) 59–70.
4. I. Tumosienė, I. Jonuškienė, K. Kantminienė, V. Mickevičius, V. Petrikaitė, *Int. J. Mol. Sci.* 22 (2021) 7799.
5. A. Šermukšnytė, K. Kantminienė, I. Jonuškienė, I. Tumosienė, V. Petrikaitė, *Pharmaceuticals*. 15 (2022) 1026.
6. M.A.G. Barbosa, C.P.R. Xavier, R.F. Pereira, V. Petrikaitė, M.H. Vasconcelos, *Cancers* 14 (2021) 190.

P 079

Delamination of Multilayer Composite Packaging Waste by HNO_3 and Its Analysis with MODDE Software

A. Šleiniūtė [1*], T. Mumladze[2], G. Denafas[1]
[1]*Kaunas University of Technology, K. Donelaičio St. 73, 44249 Kaunas, Lithuania*
[2]*Akaki Tsereteli State University, Tamar Mepe St #59, 4600 Kutaisi, Georgia*
**Corresponding author, e-mail: agne.sleiniute@ktu.edu*

Non-recyclable packaging waste from multilayer composites is a major waste management problem. Delamination allows the polymer layers to be recycled individually, increasing their recyclability. Multilayer composite packaging (MCP), which integrates multiple materials in a layered structure, is widely used in various industries because it protects and preserves products in an economical way. The packaging polymer is layered with aluminium foil (Al), cardboard, and other polymers, with each layer serving a different purpose (1-3).

In 2020, Europe generated 80 million tonnes of packaging waste, of which plastic accounted for 19.5% (4). Also, 12% of the world's waste is plastic, including plastic packaging (5).

For the following study, 24 experiments were conducted for potato chip packaging. Nitric acid (20%, 25%, 30%) was used for delamination, the temperature was 55 ^{0}C, 65 ^{0}C, 75 ^{0}C, and the time ranged from 35 to 1350 minutes.

Modde 13.0.1 (Umetrics) was used to create a factorial design of tests. Temperature (T), concentration (C), width (a) (type: quantitative), and ultrasonic (Ult) (type: qualitative) are all elements in the overall experimental design; the response is the duration (t) (type: quantitative).

The software has determined the predicted time. Trends can be seen by evaluating the differences between the predicted and observed durations. No ultrasound was used during the experiments, so the predicted values were essentially the same as the observed values and a linear equation was formed with an R2 of 0.9749.

The trends of the linear equation are not apparent in the tests with ultrasound, and there is a significant scatter plot of points that deviate from the predicted line. However, in this fourth-degree example, the scatter plot shows a polynomial curve with R2 equal to 0.5544.

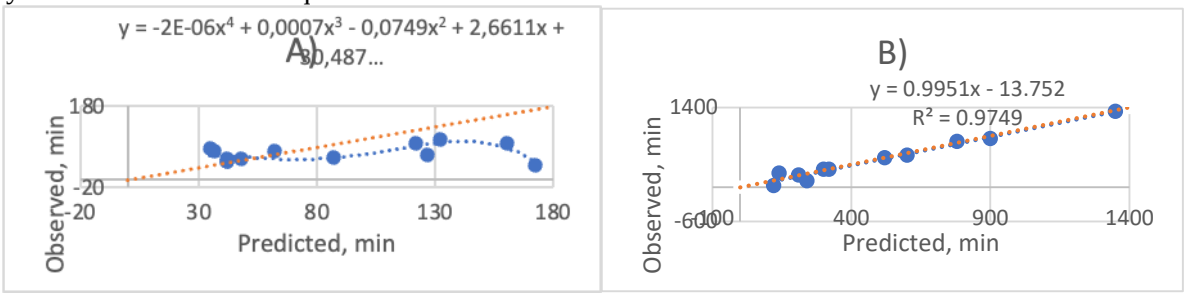

Fig. 1. The plot of the observed delamination time vs. the predicted; A - with ultrasound, B - without ultrasound. The diagonal line represents the predicted time.

References

1. MUMLADZE, T. et al. Sustainable approach to recycling of multilayer flexible packaging using switchable hydrophilicity solvents. *Green Chemistry*. 30 July 2018. Vol. 20, no. 15, p. 3604–3618. DOI 10.1039/c8gc01062e. https://pubs.rsc.org/en/content/articlehtml/2018/gc/c8gc01062e
2. YOUSEF, S. et al. Cleaner and profitable industrial technology for full recovery of metallic and non-metallic fraction of waste pharmaceutical blisters using switchable hydrophilicity solvents. *Journal of Cleaner Production*. 1 October 2018. Vol. 197, p. 379–392. DOI 10.1016/j.jclepro.2018.06.154.
3. MIETH ANJA et al. Guidance for the identification of polymers in multilayer films used in food contact materials - Publications Office of the EU. *Joint Research Centre (European Commission)*. 27 April 2017. https://op.europa.eu/en/publication-detail/-/publication/12f4d00c-0203-11e6-b713-01aa75ed71a1/language-en
4. EUROSTAT. Packaging waste Statistics. . 2023. https://ec.europa.eu/eurostat/statistics-explained/index.php?title=Main_Page
5. WORLD BANK. *Trends in Solid Waste Management*. 2023. https://datatopics.worldbank.org/what-a-waste/trends_in_solid_waste_management.html

P 080

Di(arylcarbazole) Substituted Oxetanes as Efficient Hole Transporting Materials With High Thermal and Morphological Stability for OLEDs

D. Tavgenienė[1],* B. Zhang[2], B. Achramovič[1], S. Grigalevicius[1]
[1]Kaunas University of Technology, Radvilenu plentas 19, LT50254 Kaunas, Lithuania
[2]Guangzhou University, Guangzhou 510006, China
**daiva.tavgeniene@ktu.lt*

The advantages of OLED (organic light emitting diode) based technologies as brightness, contrast ratio, production cost, viewing angle, possibility of flexible displays are not possible by liquid crystals based displays [1]. It is well known that multilayer structure devices having hole transporting layer (HTL), emitting layer and electron transporting layer should be formed for efficient light emission [2]. One method that is very widely used to improve efficiencies of the OLED devices is the insertion of effective hole transporting layers in the construction of the OLEDs [3]. The positive charge transporting materials could be of low molar mass or polymeric derivatives having electroactive chromophores attached to main polymeric chains [4].

Solution processed low molar mass derivatives containing substituted carbazole fragments are among the most studied materials for application in positive charge transporting layers due to their good chemical and environmental stability as well as high hole mobility [5]. Here, we report on oxetanes containing aryl-substituted carbazole fragments as electroactive chromophores. The synthesis of the self-assembled monolayer materials (SAMs) is presented in Figure 1.

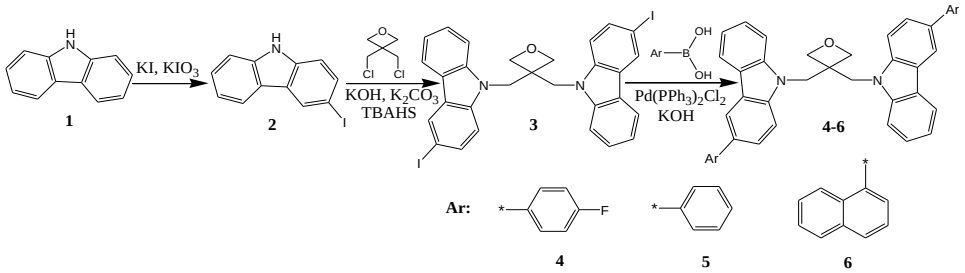

Fig. 1. New SAMs (named 3,3PrPACz, 4,3BuPACz, and 6,3HePACz)

New electro-active materials for HTL were synthesized, characterized and tested in OLED devices. The amorphous materials demonstrated very high thermal stability (371-391 °C) and high glass transition temperatures in a range of 107-142 °C due to incorporation of oxetane rings in their structures. In simple devices with Alq_3 as an emitter as well as electron transporting layer materials 5 and 6 demonstrated superior hole transporting properties than those of material 4 based device. When layer of material 5 was used in the device structure, the OLED demonstrated rather low turn-on voltage of 3.7 V, luminous efficiency of 4.2 cd/A, power efficiency of 2.6 lm/W and maximal brightness exceeding 11670 cd/m^2. HTL of 6 based device showed also exclusive OLED characteristics. The device was characterized by turn-on voltage of 3.4 V, maximum brightness of 13193 cd/m^2, luminous efficiency of 3.8 cd/A and power efficiency of 2.6 lm/W. An additional hole injecting layer of PEDOT improved considerably functions of the device with HTL of compound 4. The modified OLED using layer of derivative 4 demonstrated exclusive characteristics with turn-on voltage of 3.9 V, high luminous efficiency of 4.7 cd/A, power efficiency of 2.6 lm/W and maximal brightness exceeding 21000 cd/m^2. These observations confirmed that the tested HTL materials have a big potential in field of optoelectronics.

Acknowledgements. This work was supported by project funded by the Research Council of Lithuania (grant No. S-MIP-22-84).

References

1. R. Shinar, J. Shinar. J. Phys. Photonics., **4** (2022) 032002.
2. G. Krucaite, S. Grigalevicius, Materials., **14** (2021) 6754.
3. S. Jhulki, J.N. Moorthy, J. Mater. Chem. C., **6** (2018) 8280.
4. G. Krucaite, D. Tavgeniene, D. Blazevicius et al., Molecules., **26** (2021) 1936.
5. Z. Zhao, Y. Zhao, P. Lu et al. J. Phys. Chem. C., **111** (2007) 6883.

P 081

Perovskite Solar Cells with Monolayer Modified PTAA And Its Application to All-Perovskite Tandem Solar Cells

D. Tavgenienė[1]*, H. Bi[2], Y. Fujiwara[2], C. Ding[2], S. R. Sahamir[2], Y. Sanehira[2], A. K. Baranwal[2], K. Takeshi[2], G. Shi[2], G. Kapil[2], Z. Zhang[2], L. Wang[2], T. Bessho[3], H. Segawa[3], B. Achramovič[1], S. Grigalevicius[1], Q. Shen[2], S. Hayase[2]

[1]Kaunas University of Technology, Radvilenu plentas 19, LT50254 Kaunas, Lithuania
[2]The University of Electro-Communications, 1-5-1 Chofugaoka, Chofu, Tokyo, 182-8585, Japan
[3]The University of Tokyo, 4-6-1 Komaba, Meguro-ku, Tokyo 153-8904, Japan
**daiva.tavgeniene@ktu.lt*

Organic-inorganic perovskite solar cells (PSCs) have achieved a recorded power conversion efficiency (PCE) of 25.7%.[1] Thus, PSCs are considered to be the dominant player in the next-generation photovoltaic market.[2] So far, single-junction PSCs with narrow bandgap values have attracted attention.[3] As a member of perovskite materials, wide-bandgap perovskite (WBG-PVK) can`t be ignored because it is important for tandem solar cells due to its matchable bandgap.[4] However, low PCE and the current of WBG-PSCs limited the efficiency of the tandem solar cell. So, it is necessary to further improve the PCE of wide bandgap PSCs.

Here, we demonstrate a series of SAMs with different alkyl chain lengths as interfacial modifiers to modify the PTAA and perovskite layer for improving the optoelectronic properties of PSCs by improving the quality of perovskite films and increasing the transport and extraction of interfacial carriers. The structures of the self-assembled monolayer materials (SAMs) is presented in Figure 1.

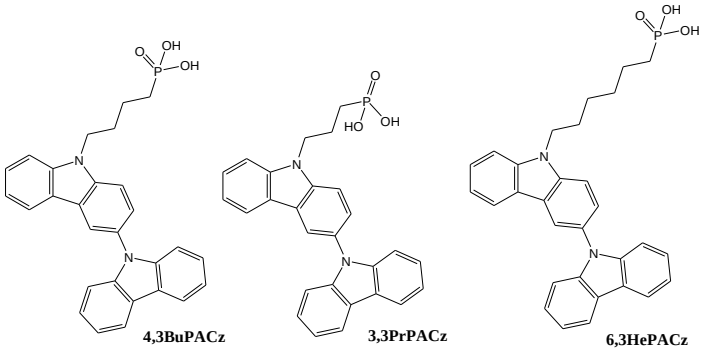

Fig. 1. New SAMs (named 3,3PrPACz, 4,3BuPACz, and 6,3HePACz)

In conclusion, several new SAMs (named 3,3PrPACz, 4,3BuPACz, and 6,3HePACz) have successfully been used to modify the interface between PTAA and WBG perovskite layer. The material with a linker group with four carbons gave the best results. The experimental results show that after the introduction of 4,3BuPACz, the quality of the perovskite thin film has significantly improved. Meanwhile, the grain size is increased, and the defects density of the films is also reduced. On the other hand, the introduction of the buffier layer can reduce the interfacial non-radiative recombination of the device and balance band offset between the perovskite and PTAA. Finally, 4,3BuPACz/PTAA-based PSCs achieved a high PCE of 16.57% with a bandgap of 1.77 eV. The target tandem solar cells gave a PCE of 25.24%, which is the highest PCE of tandem solar cells based on IZO. This work reveals a buried interface improvement mechanism with 4,3BuPACz/PTAA which can provide valuable guidance for developing effective SAMs buried layer materials.

Acknowledgements. The research was done under grant S-LJB-22-2 from Research Council of Lithuania.

References

1. Access through internet: https://www.nrel.gov/pv/cell-efficiency.html (NREL, access)
2. H. Bi, Y. Guo, M. Guo et al. Chem. Eng. J., **439** (2022) 135671.
3. S. Ma, G. Yuan, Y. Zhang et al. Energy Environ. Sci., **15** (2022) 13-55
4. K. Xiao, R. Lin, Q. Han et al. Nat. Energy., **5** (2020) 870-880.

P 082

Chemical and Electrochemical Stability of Vanadium-Based Cathodes for Aqueous Na-Ion Batteries

D.Tediashvili[1*], L. Vilčiauskas[2]

[1] *Institute of Chemistry, Faculty of Chemistry and Geosciences, Vilnius University, LT-03225,Vilnius Lithuania*

[2] *Center for Physical Sciences and Technology, Sauletekio al. 3, LT-10257 Vilnius, Lithuania*

Davit.Tediashvili@ftmc.lt

Rechargeable Li-ion batteries with organic electrolytes have been one of the main electrochemical energy storage devices for decades. They offer many attractive properties, such as high efficiency, energy density, and stability. However, for large-scale stationary applications, all these properties are overshadowed by price and safety of operation. Aqueous systems with sodium charge carriers are deemed as one of the main alternatives. Despite the advances in novel electrolyte systems, suppressing gas evolutions, and expanding operating window [1], the absence of high potential and stable cathode materials remains a bottleneck for fully utilizing this technology.

Traditionally Co and Ni-based materials have been successfully utilized as cathodes due to attractive properties such as high voltage and stability. However, with increased demand, significant effort have been made to develop rare-earth-metal-free electrodes. Mn-based materials are deemed as the most suitable alternative due to operating potential, however, unfavorable aqueous chemistry limits the application [2]. Vanadium can offer 2nd best alternative in terms of potential, as well as relative stability.

Here we report a study of NASICON-structured vanadium-based materials as aqueous Na-ion battery cathodes. Electrochemical performance of $Na_3V_2(PO_4)_3$ (NVP) and $Na_3V_2(PO_4)_2F_3$ was examined by cyclic voltammetry (CV) and galvanostatic charge-discharge (GCD) cycling. Chemical and electrochemical degradation during the operation was studied by XRD, ICP-OES, rotating ring-disc electrode, and double redox titration techniques. The results show an excellent initial performance of studied materials, however, severe chemical and electrochemical degradation is observed. The introduction of fluoride can only partially medicate these flaws.

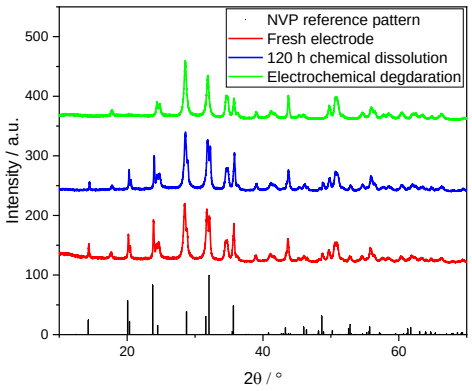

Fig 1. XRD spectroscopy of NVP electrode. From bottom up: Reference pattern, fresh (red), chemically (blue) and electrochemically (green) degraded electrode.

Acknowledgements:

This project has received funding from the European Regional Development Fund (Project No. 01.2.2-LMT-K-718-02-0005) under grant agreement with the Research Council of Lithuania (LMTLT).

References

1. L. Suo et al., "Water-in-salt" electrolyte enables high-voltage aqueous lithium-ion chemistries, Science 350, 938-943 (2015)
2. Bin ,D. et al. Progress in Aqueous Rechargeable Sodium-Ion Batteries. Advanced Energy Materials 8, 1–31 (2018).

P 083

Copper Sulfide-Based Anode Materials for Sodium-Ion Batteries

E. Ūsovienė, E. Griškonis
Kaunas University of Technology, Radvilėnų pl. 19, LT-50254 Kaunas, Lithuania
e-mail: egle.usoviene@ktu.lt

Advancements from fossil fuels to more ecologically friendly alternatives are aspirations that need to be achieved as soon as possible. For this reason, there has been a rapid production of renewable energy systems which led to the need for more electrical energy storage devices. The most prominent and widely used are lithium-ion batteries (LIB) but in recent years due to the increasing demand, they have become costly and deficient. A good alternative to LIB is sodium-ion batteries (SIB). In recent years new SIB technologies have attracted much attention for their prominent sodium abundance and low production cost. Changing battery technologies in the current market is not an easy task but when the transition from LIB to SIB happens, they need to have the same properties as their predecessor. [1]

Various SIB-negative electrode materials are being explored: carbon-based electrodes, metal alloys, metal sulfides, etc. Pure copper sulfide (CuS) is a low-cost material with high theoretical capacity and can be implemented in anode technologies when pairing them with electrically conductive materials to enhance their electrical properties. One of those materials is carbon fiber (CF), as well as graphite felt (GF) as one of the varieties of carbon fiber materials. [1-3]

CF and GF are a low-cost materials that exhibit very good mechanical properties, have a large surface area, and small density. These CF/GF properties are excellent when constructing large-dimension electrical energy-storing systems. Also, the modification capabilities of CF/GF expand its applicability. Modification is carried out using a wide range of physical and chemical methods. [4]

In this study, the following synthesis methods of CuS-based materials in presence of GF have been explored:

1. Reaction of elemental copper and sulfur;
2. Reaction of copper sulfate pentahydrate ($CuSO_4 \cdot 5H_2O$) and dimethyl sulfoxide (DMSO);
3. Reaction of elemental copper, thiourea ($(NH_2)_2CS$), dimethyl sulfoxide (DMSO), and ethyl acetate ($C_4H_8O_2$).

These samples are compared to each other using X-ray diffraction and cyclic voltammetry analysis results.

Table 1. Electrical conductivity of sample values

Sample number	Reagents							Electrical conductivity, $\Omega^{-1}m^{-1}$
	Source of copper		Source of sulfur			$C_4H_8O_2$	CF	
	Cu	$CuSO_4 \cdot 5H_2O$	S	DMSO	$(NH_2)_2CS$			
1.	+		+				+	69.96
2.		+		+			+	18.00
3.	+			+	+	+	+	22.29

References

1. J. Y. Hwang, S. T. Myung, Y. K. Sun, Sodium-ion batteries: present and future. Chem. Soc. Rev., **46** (2016) 3529-3530.
2. X. Li, X. He, C.Shi, B. Liu, Y. Zhang, S. Wu, Z. Zhu, J. Zao, Synthesis of One-Dimensional Copper Sulfide Nanorods as High-Performance Anode in Lithium Ion Batteries, Chem. Sus. Chem., **7** (2014), 3328-3333.
3. K. J. Huang, J. Z. Zhang, Y. Liu, Y. M. Liu, Synthesis of reduced graphene oxide wrapped-copper sulfide hollow spheres as electrode material for supercapacitor, **40-32** (2015), 10158-10167.
4. R. M. Kakhki, A review to recent developments in modification of carbon fiber electrodes, Arab Journal of Chemistry, **12-7** (2019), 2-3.

P 084

Study of the Quantitative Composition of the Cobalt Sulfide Layers on the Polyamide 6 Surface

K. Vaičiukynaitė[1,*] S. Žalenkienė[1], R. Ivanauskas[1]
[1]Kaunas University of Technology, Radvilenu St. 19, LT-50254 Kaunas, Lithuania
klaudija.vaiciukynaite@ktu.lt

In the face of energy degradation and global warming, there is an urgent need to develop new clean and efficient energy storage devices [1]. Transition-metal sulfides have been considered as an important material to create efficient and stable photoelectric catalysts because of their exceptional properties and distinctive structures. Over the past few years, they have been used not only in photoelectric catalysis but also in energy storage [2]. The material composition of the supercapacitor electrode has a significant influence on its capacity characteristics. In contrast with metal oxide electrode materials, transition metal sulfides have more abundant raw materials, higher theoretical capacity and low cost. Cobalt sulfide has attracted the attention of scientists due to its high specific capacity, low toxicity and simple synthesis. However, different morphologies and structures have a great impact on the performance of electrode materials [1]. Therefore, it is very important to know the quantitative and qualitative composition of the compounds obtained.

The purpose of this work was to investigate the quantitative composition of the cobalt sulfide layers obtained on the polyamide 6 (PA) surface.

At the beginning of the experiment, PA 6 films were boiled in distilled water for 2 h. Subsequently, PA 6 films were kept in pentathionic acid ($H_2S_5O_6$) for 1.0 to 5.0 h at room temperature. After interaction with acid, the samples were treated with the 0.16 mol × dm^{-3} solution of cobalt sulfate, ($CoSO_4 \cdot 7H_2O$) for 10 minutes at different temperatures – 60, 70 and 80 ºC (5 samples for each temperature).

After the formation of cobalt sulfide layers on PA 6 surfaces, films were investigated using atomic absorption spectroscopy (AAS) and electron dispersion spectroscopy (EDS). The results of the EDS analysis confirmed the presence of sulfur and cobalt elements. It was noticed that the peaks of both sulfur and cobalt elements are particularly intense in the sample that was sulfurized the longest and stored in a cobalt salt solution at the highest temperature. AAS analysis showed a clear trend of increasing cobalt concentration depending on the temperature of the solution - the higher the temperature, the higher the Co concentration.

References

1. X. Zhang, Q. Zhao, Journal of Alloys and Compounds. Elsevier, 2023.
2. B. Wang, X. Pang, Photochem., **3** (2023) 15-37.

P 085

Synthesis and Antioxidant Activity of 4-Amino-5-(2-((2-methylquinolin-6-yl)amino)ethyl)-2,4-dihydro-3*H*-1,2,4-triazole-3-thione

R. Vaitkus[1], I. Jonuškienė[1], K. Kantminienė[2*], Z. J. Beresnevičius[1], I. Tumosienė[1]

[1]*Department of Organic Chemistry, Kaunas University of Technology, Radvilėnų pl. 19, 50254 Kaunas, Lithuania*

[2]*Department of Physical and Inorganic Chemistry, Kaunas University of Technology, Radvilėnų pl. 19, 50254 Kaunas, Lithuania*

** rokas.vaitkus@ktu.edu*

Oxidative stress, induced by the generation of reactive oxygen and nitrogen species, is a major causative factor of many illnesses including cardiovascular diseases and cancer [1]. Antioxidants are involved in the defence mechanisms by slowing down or inhibiting completely the oxidation processes caused by reactive free radicals. The quinoline core is a privileged scaffold in many natural and synthetic compounds, exhibiting a broad array of biological activities such as antimicrobial, antimalarial, antitubercular, anticancer, antileishmanial, anti-inflammatory, and anti-HIV [2,3].

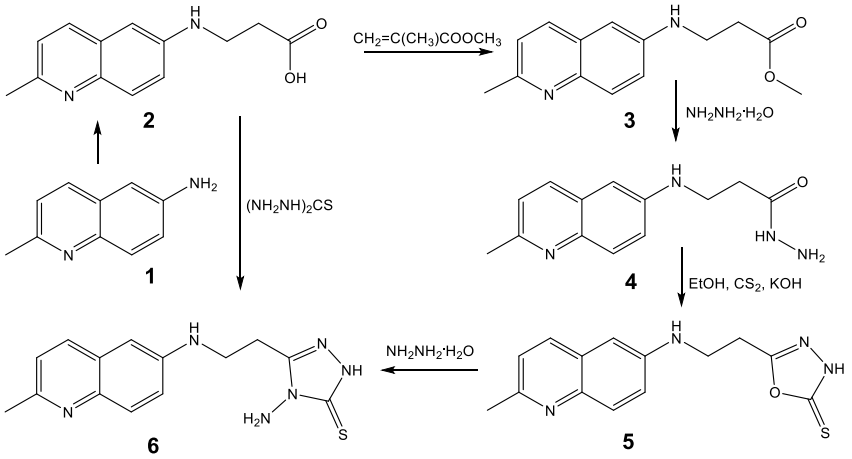

Scheme 1. Synthesis of 4-amino-1,2,4-triazole-3-thione **6**

N-(2-Methyl-6-quinolinyl)-*β*-alanine (**2**) was synthesized from 2-methylquinolin-6-amine (**1**) in reaction with acrylic acid. Acid **2** was converted to ester **3** and a subsequent reaction of **3** with hydrazine hydrate afforded hydrazide **4**. 5-[2-(Methyl-6-quinolinylamino)ethyl]-2,3-dihydro-1,3,4-oxadiazole-2-thione (**5**) was synthesized from propane hydrazide **4** via formation of intermediate potassium carbodithioate and its cyclization under treatment with concentrated sulfuric acid [4-7]. The target 4-amino-1,2,4-triazole-3-thione **6** was obtained by heating under reflux 1,3,4-oxadiazolethione **5** with hydrazine. Alternatively, **6** was also obtained directly from acid **2**. As it has been shown by the by DPPH radical scavenging assay results, 4-amino-1,2,4-triazole-3-thione **6** exhibited 2.7-fold higher antioxidant activity than that of the commercial antioxidant butylhydroxytoluene.

References

1. R.C. Seet, C.Y. Lee, E.C. Lim, J.J. Tan, A.M. Quek, W.L. Chong, W.F. Looi, S.H. Huang, H. Wang, Y.H. Chan, B. Halliwell, Free Radical Biology and Medicine, 48 (2010) 560–566.
2. T. Van de Walle, L. Cools, S. Mangelinckx, M. D'hooghe, European Journal of Medicinal Chemistry, 226 (2021) 113865.
3. S. O. Simonetti, T. S. Kaufman, E. L. Larghi, European Journal of Organic Chemistry, 23 (2022) e202200107.
4. Z.J. Beresnevicius, V. Viliunas, K. Kantminiene, Chemistry of Heterocyclic Compounds, 36-5 (2000) 569-573.
5. Z.J. Beresnevicius, V. Viliunas, K. Kantminiene, Chemistry of Heterocyclic Compounds, 36-4 (2000) 432-438.
6. I. Tumosienė, I. Jonuškienė, K. Kantminienė, Z.J. Beresnevičius, Monatsh Chem, 143 (2012) 1441–1450.
7. I. Tumosienė, Z.J. Beresnevičius, Chemija, 23-1 (2012) 48–51.

P 086

Screening and Identification of Microorganisms that Degrade Oil Products

J. Urbonavičius[1], A. Zagorskis[2], D. Vasiliauskienė, V. Valentinas[1,*]

[1]Department of Chemistry and Bioengineering, Vilnius Gediminas Technical University, Saulėtekio al. 11, 10223 Vilnius, Lithuania

[2]Research Institute of Environmental Protection, Vilnius Gediminas Technical University, Saulėtekio al. 11, 10223 Vilnius, Lithuania

[*]Vytautas Valentinas, e-mail: vytautas.valentinas@stud.vilniustech.lt

Today one of the biggest environmental problems is related to hydrocarbon pollution, which is connected to activities from the oil production industry. Accidents of oil spills can pose a danger to aquatic organisms such as fishes or zooplanktons. The oil that reaches the coastal areas can harm coastal organisms like mammals, birds and invertebrates. Nowadays to recover spilled oil from the environment several techniques such as physical, chemical, and biological methods are used. Bioremediation is a promising treatment technology for these contaminated sites because it is cost-effective and converts pollutants into minerals [1-2].

In this work, the microorganisms that could degrade wooden railway sleepers contaminated with oil hydrocarbons were investigated. The sleepers were chopped into small pieces and added into the flasks that contained either LB (Luria Bertani broth for bacteria) or ME (malt extract medium, for fungi). The flasks were incubated overnight at either 37°C for bacteria or 30°C for fungi with shaking, then the cultural medium was spread on the agarized LB or ME (for fungi) media by making serial dilutions. Several passages were performed until pure cultures were obtained and described morphologically. Then the identity of microorganisms was determined by using either bacteria-specific 16S rRNA (27F and 1492R) or fungi-specific ribosomal ITS primers (ITS1 and ITS4).

Using this approach, totally 12 microorganisms were isolated as pure cultures, 10 bacterial strains and 2 fungal strains. Among them, 7 bacterial and 1 fungal (yeast) strains were capable of oil degradation as demonstrated by measuring lipase activity using the tributyrin substrate. Further characterisation of isolated strains is currently under way.

References

1. FAQ: Microbes & Oil Spills. (2011). FAQ: Microbes & Oil Spills. https://doi.org/10.1128/AAMCOL.2-2011.

2. YANG, S. Z., JIN, H. J., WEI, Z., HE, R. X., JI, Y. J., LI, X. M., & YU, S. P. (2009). Bioremediation of Oil Spills in Cold Environments: A Review. Pedosphere, 19(3), 371–381. https://doi.org/10.1016/S1002-0160(09)60128-4.

P 087

Synthesis of *N*-Heterocycle-Fused Tetrahydro-1,4-diazepinones

M. Veikšaitė[1,2*], K. Dzedulionytė[1], V. Moravek[3], A. Žukauskaitė[3], E. Arbačiauskienė[1], A. Šačkus[1,2]

[1] *Kaunas University of Technology, Radvilėnų pl. 19, 50254 Kaunas, Lithuania*
[2] *Kaunas University of Technology, K. Baršausko g. 59, 51423 Kaunas, Lithuania*
[3] *Palacký University, Šlechtitelů 27, 78371 Olomouc, Czech Republic*
**melita.veiksaite@ktu.lt*

It is known that 1,4-diazepine heterocycles fused with nitrogen-based heterocycles exhibit diverse biological properties such as antimalarial [1], antitumor [2] and antiviral [3] activity. For example, a 1,6,7,8-tetrahydropyrazolo[3,4-*b*][1,4]diazepine derivative inhibits growth of *P. falciparum* and has potential for treating malaria [1], whereas 8,9-dihydro-7*H*-pyrimido[4,5-*b*][1,4]diazepine derivative inhibits the growth of the cell line IGROV1 responsible for ovarian cancer [2]. Another example includes 5,6,7,8-tetrahydro-4*H*-pyrazolo[1,5-*a*][1,4]diazepine-2-carboxamide derivative which inhibits the respiratory syncytial virus (RSV) polymerase complex [3].

In this work, we synthesized novel pyrazole and indole-fused tetrahydro-1,4-diazepinones. For the optimization of the reaction conditions, reactivity of 1*H*-pyrazole-5(3)-carboxylates towards alkylation with epichlorohydrin was investigated. Obtained 1-(oxiran-2-ylmethyl)-1*H*-pyrazole-5-carboxylates were further treated with ammonia resulting in oxirane ring-opening and subsequent cyclisation affording tetrahydro-4*H*-pyrazolo[1,5-*a*][1,4]diazepin-4-ones. The obtained cyclization products were further functionalized by treatment with *N*-chloro-, bromo- and iodosuccinimides to obtain 2(3)-halogenated tetrahydro-4*H*-pyrazolo[1,5-*a*][1,4]diazepin-4-ones. An analogous two-step synthesis approach was further used to expand the study and to obtain tetrahydro[1,4]diazepino[1,2-*a*]indol-1-one derivatives from corresponding indole-2-carboxylates [4].

The structures of novel heterocyclic compounds were confirmed by ^{1}H, ^{13}C, and ^{15}N-NMR spectroscopy.

References

1. B. Insuasty, et al. European Journal of Medicinal Chemistry, **93** (2015) 401-413.
2. B. Insuasty, et al. European Journal of Medicinal Chemistry, **43** (2008) 1955-1962.
3. Jiménez-Somarribas, et al. Journal of Medicinal Chemistry, **60** (2017) 2305–2325.
4. K. Dzedulionytė, et al. Molecules, **27** (2022), 8666.

P 088

4-(Cycloalkyl)-6-(1-(4-substituted)-1*H*-imidazol-5-yl)benzene-1,3-diols and 4-(Cycloalkyl)-6-(5-(4-methoxyphenyl)-1,2,3-thiadiazol-4-yl)benzene-1,3-diols Synthesis

K. Venskūnaitė[1*], A. Brukštus[1]

[1] *Faculty of Chemistry and Geosciences, Vilnius University, Naugarduko g. 24, LT-03225, Vilnius, Lithuania*

**Corresponding author, e-mail:*

kamile.venskunaite@chgf.stud.vu.lt

Heat shock protein Hsp90 is considered as a significant evolutionary preserved molecular chaperone. It is obtained in all living organisms, except archaea. Hsp90 stabilizes and folds proteins that are under stress conditions [**1**]. Molecular chaperone has hundreds protein substrates and is included in a lot of cellular processes besides protein folding. For example, DNA repair, immune system response and neurodegenerative diseases [**2**]. Furthermore, there are ongoing researches on parasitic diseases treatment using Hsp90 [**3**]. The purpose of this scientific work is to synthesize potential Hsp90 protein inhibitors and use them in biological research.

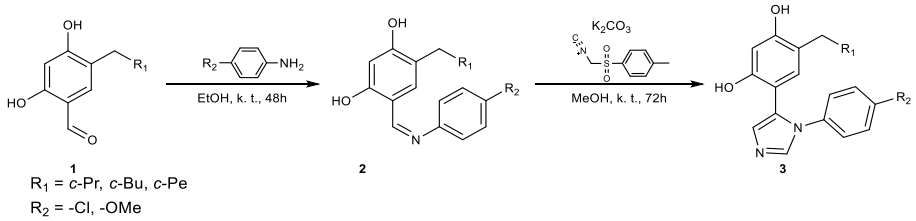

Scheme 1. Synthesis of 4-(cycloalkyl)-6-(1-(4-substituted)-1*H*-imidazol-5-yl)benzene-1,3-diols (**3**).

The reaction between aldehyde **1** and 4-substituded aniline yielded imines **2**. After, cyclization reaction was done using toluenesulfonylmethyl isocyanide (TosMIC) and previously synthesized imine **2** resulted in formation of final product **3**.

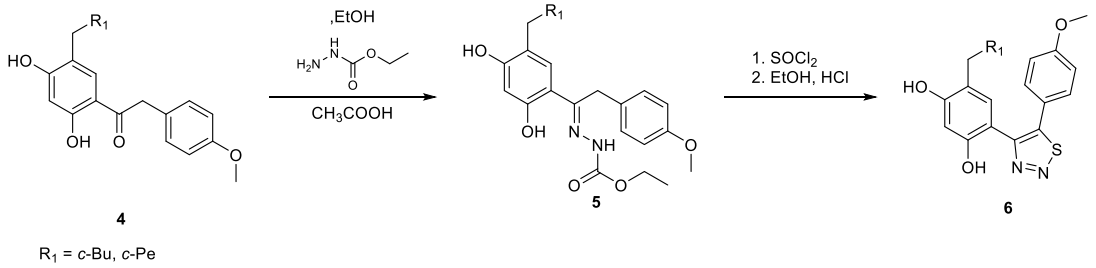

Scheme 2. Synthesis of 4-(cycloalkyl)-6-(5-(4-methoxyphenyl)-1,2,3-thiadiazol-4-yl)benzene-1,3-diols (**6**).

Compound **5** was obtained after compound **4** was submitted into reaction with ethanol and ethyl hydrazinecarboxylate. The cyclization was done by using thionyl chloride and yielded final product **6**. The synthesized compounds are currently being analyzed.

References

1. Somogyvari, M.; Khatatneh, S.; Soti, C. Hsp90: From Cellular to Organismal Proteostasis. Proteostasis. *Cells* **2022**, *11*, 2479.
2. Schopf, F. H.; Biebl, M. M.; Buchner, J. The HSP90 chaperone machinery. *Nat Rev Mol Cell Biol* **2017**, *18*(6), 345–360.
3. Faya, N.; Penkler, D. L.; Bishop, Ö. T. Human, vector and parasite Hsp90 proteins: A comparative bioinformatics analysis. *FEBS Open Bio* **2015**, *5*, 916-927.

P 089

Glucose Oxidase Inhibition-Based Hg^{2+} Ion Biosensor

P. Virbickas[1,*], G. Ziziunaite[1], A. Valiūnienė[1,*]
[1] Faculty of Chemistry and Geosciences, Vilnius University, Naugarduko st. 24, 03225, Lithuania
**Corresponding author, e-mail: povilas.virbickas@chgf.vu.lt*

Mercury and its compounds are toxic substances which can cause adverse effects on living organisms, e.g. neurological disease [1,2]. Moreover, mercury can be bioaccumulated in living organisms due to formation of organomercury derivates, thus, mercury is difficult to degrade in the environment [1,3]. Therefore, mercury-related pollution is an important public health and environmental issue [4].

Various analytical techniques can be used for determining mercury concentration, including colorimetry-based methods, mass spectrometry and electrochemical methods [2,5]. Even though electrochemical analytical techniques in general exhibit advantageous properties of high sensitivity and simple operation, electrochemical mercury determination procedures often have some drawbacks related to high price of electrodes required for analysis, an application of high potential during analysis, etc. [2].

Herein the amperometric glucose oxidase (GOx) inhibition-based Hg^{2+} ion biosensor formed by immobilising GOx on the Prussian blue-coated electrode is presented. Due to the application of Prussian blue, here described amperometric Hg^{2+} ion biosensor was able to operate at low potential of 0.2 V (*vs* Ag|AgCl,KCl_{sat}), that is lower than 0.4 V – 0.7 V (*vs* Ag|AgCl,KCl_{sat}) potentials required for operation of earlier developed amperometric GOx inhibition-based Hg^{2+} ion biosensors [6-9]. This achievement is important as low operating potential of the Hg^{2+} ion biosensor helps to avoid interfering electrochemical oxidation reactions of other compounds which might be present in the sample, e.g. alkylphenols [10]. Furthermore, the Hg^{2+} ion biosensor presented in this work does not require any expensive materials or difficult procedures for its preparation, making it convenient tool for mercury detection.

References

1. A. C. Jackson, Can. J. Sci. Neurol., 45 (2018) 620–623.
2. P. Virbickas, G. Ziziunaite, A. Ramanavicius, A. Valiūnienė, Electroanal., 34 (2022).
3. B. Gworek, W. Dmuchowski, A. H. Baczewska-Dąbrowska, Environ. Sci. Eur., 32 (2020) 1–19.
4. M. S. Bank, Sci. Total Environ., 722 (2020) 137832.
5. B. Elsebai, M. E. Ghica, M. N. Abbas, C. M. A. Brett, J. Hazard. Mater., 340 (2017) 344–350.
6. A. M. Ashrafi, M. Sýs, E. Sedláčková, A. S. Farag, V. Adam, J. Přibyl, L. Richtera, Sensors, 19 (2019) 2939.
7. C. Malitesta, M. R. Guascito, Biosens. Bioelectron., 20 (2005) 1643–1647.
8. J. Yu, H. Guan, D. Chi, J. Solid State Electrochem., 21 (2017) 1175–1183.
9. M. R. Guascito, C. Malitesta, E. Mazzotta, A. Turco, Sens. Actuators B Chem., 131 (2008) 394–402.
10. A. Chmayssem, D. Hauchard, J. Water Sci., 28 (2015) 35–40.

P 090

Sol-Gel Synthesis and Characterization of Novel Garnets with Various Stoichiometric Compositions

D. Vištorskaja[1*], A. Kareiva[1]

[1]*Institute of Chemistry, Faculty of Chemistry and Geosciences, Vilnius University, Naugarduko st. 24, LT-03225 Vilnius, Lithuania*

**diana.vistorskaja@chgf.vu.lt*

Synthetic garnets belong to a group of oxide crystals, which crystallize in the cubic lattice. Garnets doped with rare earth or transition metal are widely used in solid-state lasers [1]. The most popular synthetic garnet is the yttrium aluminium garnet ($Y_3Al_5O_{12}$, YAG). It has been recognized as one of the best phosphor host material due to its excellent chemical, optical and mechanical properties [2]. YAG materials activated with rare-earth or transition metal ions are perspective candidates for light-emitting diodes (wLEDs), cathode-ray tubes (CRTs), and scintillators. For example, YAG:Nd is well known as a lasing medium and was used in cosmetic surgery [1, 3]. Therefore, YAG-based phosphors have been widely studied in the application of displays, such as field emission display, vacuum fluorescent display, and plasma display panel [2-4]. Since numerous of these applications need materials in shape of films or powders with a high degree of purity, so several synthesis routes have been investigated. The sol-gel method is one of the most useful technique due to its advantages, such as low temperature and cost, achievement of monophasic and homogeneous multicomponent products [5].

The aim of this work was to synthesize novel $Y_{3-x}Na_xAl_5O_{12}$, $Y_{3-x}K_xAl_5O_{12}$, $Y_3Al_{5-y}V_yO_{12}$, $Y_{3-x}Na_xAl_{5-y}V_yO_{12}$ garnets with various stoichiometric compositions by a sol-gel method and to study them using X-ray diffraction (XRD) analysis, Fourier-transform infrared spectroscopy (FTIR), and scanning electron microscopy (SEM). Figure 1 shows the XRD patterns of the $Y_{3-x}Na_xAl_5O_{12}$ samples sintered at 1000 °C, with the different molar parts of sodium ($0.01 \leq x \leq 2$) in the compounds. All obtained results will be presented and discussed at the conference.

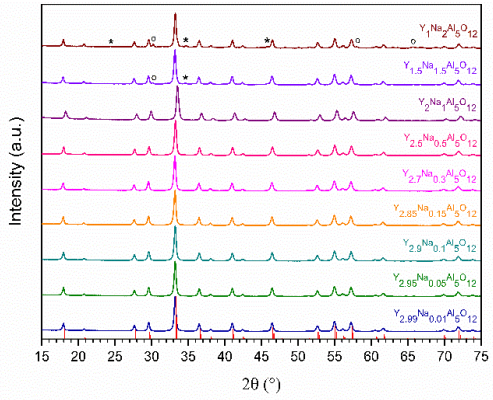

Fig. 1. XRD diffraction patterns of $Y_{3-x}Na_xAl_5O_{12}$ samples synthesized at 1000 °C. The crystalline phases are marked: vertical red lines - $Y_3Al_5O_{12}$ [PDF #96-152-9038], * - $YAlO_3$ [PDF #96-153-3070], o - Al_2O_3 [PDF #96-100-0443].

References

1. R. Skaudzius, J. Pinkas, R. Raudonis, A. Selskis, R. Juskenas, A. Kareiva, On the limitary radius of garnet structure compounds $Y_3Al_{5x}M_xO_{12}$ (M = Cr, Co, Mn, Ni, Cu) and $Y_3Fe_{5x}Co_xO_{12}$ ($0 \leq x \leq 2.75$) synthesized by sol-gel method, Mat. Chem. Phys., **135** (2012) 479-485.
2. L. G. D. Silveira, L. F. Cótica, I. A. Santos, M. P. Belançon, J. H. Rohling, M. L. Baesso, Processing and luminescence properties of Ce:$Y_3Al_5O_{12}$ and Eu:$Y_3Al_5O_{12}$ ceramics for white-light applications, Mater. Lett., **89** (2012) 86–89.
3. L. D. Thu, D. Q. Trung, T. D. Lam, T. X. Anh, Fabrication of Far Red Emission Phosphors $Y_3Al_5O_{12}$:Eu(YAG:Eu) by Co-precipitation Method, J. Electron. Mater., **45(5)** (2016) 2468–2471.
4. S. Zhou, Z. Fu, J. Zhang, S. Zhang, Spectral properties of rare-earth ions in nanocrystalline YAG:Re (Re = Ce^{3+}, Pr^{3+}, Tb^{3+}), J. Lumin., **118(2)** (2006) 179–185.
5. A. Potdevin, G. Chadeyron, D. Boyer, R. Mahiou, Sol-gel elaboration and characterization of YAG:Tb^{3+} powdered phosphors, J. Mater. Sci., **41(8)** (2006) 2201–2209.

P 091

Wastewater Treatment of Spent Dyeing Bath Using Ion Exchange and Activated Carbon Adsorbents

E. Zubrytė[1], A. Gefenienė[1], S. Jankauskas[1], R. Ragauskas[1], R. Ramanauskas[1]

[1] *State research institute Center for Physical Sciences and Technology, Public Institution. Savanorių ave. 231, LT-02300 Vilnius, Lithuania*

**Corresponding author, e-mail:edita.zubryte@ftmc.lt*

The intensely colored effluents produced as wastes during the dyeing process pose significant disposal problems. Due to increasingly strict environmental requirements, water contaminated with dyes cannot be released into the environment [1,2]. According to the International standard for the discharge of dye wastewater into the environment, the color of the wastewater should be less than 1 ppm and the pH value should be in the range of 6-9. Among biological, physical, and chemical methods, physical techniques are the most commonly used for dye removal because they are versatile, effective, and require the least amount of chemicals [3]. Although adsorption is known as a relatively simple method, its application results in a higher quality of treated colored wastewater[4]. The purpose of this study was to perform preliminary screening tests to evaluate the ability of selected adsorbents to remove color from a used dyeing bath. The influence of adsorbent properties (structure, number of functional groups and their acidity/alkalinity) on sorption capacity was investigated. Two anion exchange resins, strongly basic A500PS, and weakly basic A847, supplied by Purolite®, and commercial Norit Row 0.8 Supra granular activated carbon were selected as adsorbents to evaluate their decolorization performance.

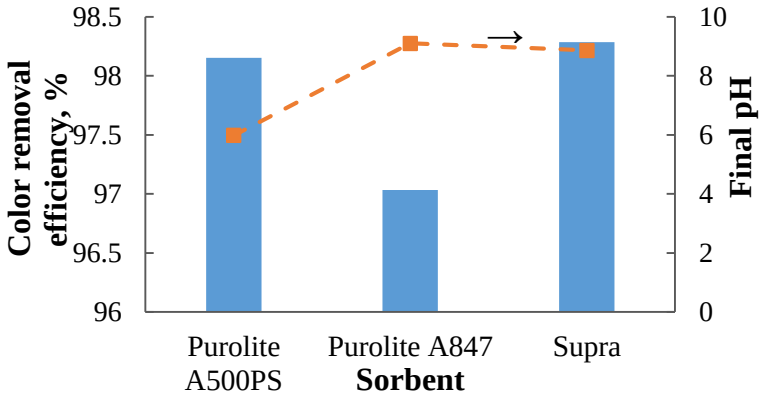

Fig. 1. Color removal efficiency and pH of treated wastewater using ion exchange and activated carbon adsorbents.

Adsorption tests were carried out in a batch configuration at ambient temperature. After reaching sorption equilibrium, the samples were filtered and analyzed with a UV/VIS spectrophotometer (Varian Cary 50) at a wavelength of 655 nm. Before treatment, the pH of the wastewater was 5.98, it was not adjusted during sorption. The pH of the treated wastewater was slightly acidic or slightly alkaline (Fig. 1). Experiments have shown that adding 100 g/L of adsorbent to the wastewater of the used dyeing bath can significantly reduce the color (Fig. 1). Anion exchange resins and basic-type activated carbon performed similarly, and color removal efficiencies in the range of 97.0-98.9% were achieved. However, the removal of color by the strongly basic macroporous styrene resin was slightly higher compared to the weakly basic anion exchanger. On the other hand, the pH-dependent nature of Purolite A847 makes it easier to desorb dyes using only an aqueous alkaline solution.

References

1. Z. Aksu, E. Balibek. J. Environ. Manage., 91(7), (2010) 1546–1555.
2. R. Al-Tohamy, S. S. Ali, F. Li, K. M. Okasha, Y. A.-G. Mahmoud, T. Elsamahy, H. Jiao, Y. Fu, J. Sun, Ecotoxicol. Environmental Saf., 231 (2022) 113160.
3. V. Katheresan, J. Kansedo, S. Yon Lau, J. Environ. Chem. Eng., 6 (4), (2018) 4676-4697.
4. B. Kassar, C. Graham, T. H. Boyer. Water Res. X, 17 (2022) 100159.

P 092

Application of Crude Animal Origin Extracts in the Aldol Reactions for the Synthesis of Chiral Bicyclic Compounds

A. Žilinskas, S. Višniakova, M. Lobanovas
Department of Organic chemistry, Vilnius university, Naugarduko 24, LT-0322, Lithuania
e-mail: albinas.zilinskas@chf.vu.lt

Bicycle[3.3.1]nonane derivatives are considered to be useful model compounds in conformational analysis and experiments aimed at obtaining optically active reaction products [1,2]. The aldol synthesis reaction with cyclohexanone and p-nitrobenzaldehyde has shown that the crude extracts of earthworms (Lumbricus terrestris) and fly larvae (Phaenicia sericata) are suitable for the synthesis of optically active chiral compounds [2]. That such extracts have better stereoselective properties than a pharmaceutical mixture of pig pancreatic enzymes (the products had 16.3% and 26.6% higher specific rotation angles of the polarized light plane $[a]^{25}_{546}$ respectively).

After analogous aldol reaction with bicyclo [3.3.1] nonane-2,6-dione and p-nitrobenzaldehyde failed to separate the optically active products by column chromatography due to the close Rf values of the synthesized compounds, but the separated product mixture showed optical activity. By measuring the rotation angles of the polarized light plane of product mixtures, formed during the reaction at different temperatures and durations, found that the most optically active products are formed after 96 hour reaction and at a temperature of 30 ºC (with crude earthworm extract the mixture of products reversed the plane of polarized light by 21.1º and with crude fly larvae extract by 18.4º). Separation of the reaction products of bicyclo [3.3.1] nonan-2,6-dione and p-nitrobenzaldehyde would make it possible to calculate the specific polarization plane angles and enantiomeric excess of the products, and this information would make it possible to find new ways to prepare crude animal origin extracts to obtain the most optically pure aldols possible.

References

1. Hönig, M., Sondermann, P., Turner, N. J., & Carreira, E. M. (2017). Enantioselective Chemo- and Biocatalysis: Partners in Retrosynthesis. *Angewandte Chemie - International Edition*, *56*(31), 8942–8973. https://doi.org/10.1002/ANIE.201612462
2. Zilinskas, A., & Sereikaite, J. (2013). Stereoselective bioreduction for the resolution of racemic mixtures of bicyclo[3.3.1]nonane-2,6-dione using vegetables. *Journal of Molecular Catalysis B: Enzymatic*, *90*, 66–69. https://doi.org/10.1016/J.MOLCATB.2013.01.022
3. Guan, Z., Chen, Y. L., Yuan, Y., Song, J., Yang, D. C., Xue, Y., & He, Y. H. (2014). Earthworm is a versatile and sustainable biocatalyst for organic synthesis. *PLoS ONE*, *9*(8). https://doi.org/10.1371/JOURNAL.PONE.0105284

P 093

Conducting Polymer Modified Laser-Induced Graphene Usage for pH Sensing

V. Žutautas[a,*], R. Trusovas[b], A. Sartanavičius[b], K. Ratautas[b], T. Rakickas[a], R. Pauliukaite[a]

[a] *Department of Nanoengineering, FTMC, Savanoriu Ave. 231, LT-02300 Vilnius, Lithuania*
[b] *Department of Laser Technologies, FTMC, Savanoriu Ave. 231, LT-02300 Vilnius, Lithuania*
**Corresponding author, e-mail: vytautas.zutautas@ftmc.lt*

Many chemical processes depend on pH. Buffer solutions usually are used to maintain constant pH; however, some processes require different pH at different steps. pH monitoring usually is performed using a pH sensor. Although the glass electrode is most widely used to detect pH, but it requires calibration and is difficult to use in minimized and flexible systems. So, the pH-dependent conductive polymer [1] was adjusted to create a flat and flexible sensor that can be easily minimised.

Laser-induced graphene (LIG) is a carbon-based nanomaterial, which is fabricated in a single step by applying laser irradiation to various carbon-containing materials [2]. The advantage of this method is that it usually does not require complex thermal management such as chemical vapour deposition or high vacuum as well as does not involve usage of hazardous chemical materials. An important peculiarity of LIG is the formation of conductive areas on insulating substrates, which leads to the production of different devices, among them is also the pH sensor [3].

Polyfolate (PFA) is a conductive polymer formed from electrochemically polymerised folate monomer. It is known that the deposition solution and its pH influence PFA quality during electrosynthesis on the electrode surface. Moreover, FA is sensitive to pH in the range between 6.0 and 10.0 [4].

In this work, a flexible pH sensor was created using LIG and PFA. For this, LIG electrode was electrochemically modified with PFA. To improve the stability of the electrode, prior to the PFA polymerisation, LIG was coated with chitosan (Chit), and the conditions of the electrode modification were optimised. The bare and modified LIG electrodes were characterised using spectroscopic and electrochemical techniques. Afterwards, PFA/Chit/LIG response to pH between 6.0 and 9.0 was tested employing potentiometry. The advantage of this pH sensor is that it requires no constant calibration.

.

References

1. U. Lange, N.V. Roznyatovskaya, V.M. Mirsky, Anal. Chim. Acta, **614** (2008) 1–26.
2. N. Dixit, S.P. Singh, ACS Omega, **7** (2022) 5112–5130.
3. R. Barber, S. Cameron, A. Devine, A. McCombe, L. Kirsty Pourshahidi, J. Cundell, S. Roy, A. Mathur, C. Casimero, P. Papakonstantinou, J. Davis, Electrochem. Commun., **123** (2021) 106914.
4. I.R. Younis, M.K. Stamatakis, P.S. Callery, P.J. Meyer-Stout, Int. J. Pharm., **367** (2009) 97–102.

P 094

Amyloid Aggregation Suppression and Carbonic Anhydrase Inhibition with Fluorinated Benzenesulfonamides

M. Žvirblis*, A. Sakalauskas, V. Dudutienė, V. Smirnovas, D. Matulis

Department of Biothermodynamics and Drug Design, Institute of Biotechnology, Life Sciences Center, Vilnius University, Vilnius, Lithuania
**Corresponding author, mantas.zvirblis@bti.stud.vu.lt*

Alzheimer's disease is one of the main causes of dementia. During its progression, amyloid beta peptides aggregate into neurotoxic aggregates that cause cognitive decline. Current treatments are ineffective at halting the disease progression[1]. Hence new potential treatment strategies are being developed to this day. One potential strategy is to halt the aggregation process with small molecule compounds that bind to the amyloid peptides and stabilize them into conformations that are then incapable of forming aggregate species[2]. Apart from strategies that directly target amyloid beta, carbonic anhydrases have emerged as a possible target as well. Fossati and colleagues discovered that inhibiting carbonic anhydrase activity mitigates neural cell damage caused by amyloid beta aggregates *in vivo*[3]. Thus, compounds that suppress amyloid aggregation and inhibit carbonic anhydrases may be viable drugs for Alzheimer's disease.

Our lab has discovered two compounds, VR16-09 and VR16-10, which are capable of inhibiting amyloidogenic protein aggregation including amyloid beta peptides[4]. Furthermore these compounds are potent carbonic anhydrase inhibitors[5]. Fluorinated benzenesulfonamides with such properties provide a viable starting point for search of potential drugs for Alzheimer's disease treatment.

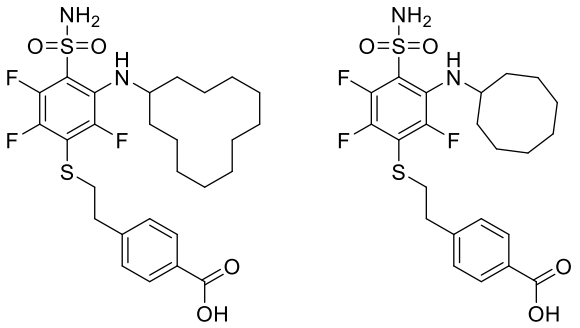

Fig. 1. Structures of biologically active fluorinated benzenesulfonamides.

References

1. Z. Breijyeh, R. Karaman, Molecules. 25 (2020) 5789. https://doi.org/10.3390/molecules25245789.
2. Q. Nie, X. Du, M. Geng, Acta Pharmacol Sin. 32 (2011) 545–551. https://doi.org/10.1038/aps.2011.14.
3. S. Fossati, P. Giannoni, M.E. Solesio, S.L. Cocklin, E. Cabrera, J. Ghiso, A. Rostagno, Neurobiology of Disease. 86 (2016) 29–40. https://doi.org/10.1016/j.nbd.2015.11.006.
4. S. Hadi Ali Janvand, L.K. Ladefoged, A. Zubrienė, A. Sakalauskas, G. Christiansen, V. Dudutienė, B. Schiøtt, D. Matulis, V. Smirnovas, D.E. Otzen, International Journal of Biological Macromolecules. 227 (2023) 590–600. https://doi.org/10.1016/j.ijbiomac.2022.12.105.
5. J. Kazokaitė, R. Niemans, V. Dudutienė, H.M. Becker, J. Leitāns, A. Zubrienė, L. Baranauskienė, G. Gondi, R. Zeidler, J. Matulienė, K. Tārs, A. Yaromina, P. Lambin, L.J. Dubois, D. Matulis, Oncotarget. 9 (2018) 26800–26816. https://doi.org/10.18632/oncotarget.25508.

P 095

Carbonated rankinite binder from JSC Akmenes cementas raw materials

R. Šiaučiūnas, E. Prichockienė, Z. Valančius*

Kaunas University of Technology, Radvilenu pl. 19, 50254 Kaunas, Lithuania;

** Raimundas Šiaučiūnas: raimundas.siauciunas@ktu.lt*

Low-calcium rankinite binder is an advanced low calcium and energy saving cement that hardens in CO_2 environment [1, 2]. JSC Akmenes cementas has been successfully producing Ordinary Portland cement (OPC) from local raw materials (Karpenai deposit limestone and Saltiskiai deposit clay) for more than 7 decades. Chemical composition of raw materials and OPC clinker is presented in Table 1. It is likely that these rocks are also suitable for the production of low-lime binder that hardens during carbonation. For comparison, we also determined the compressive strength and mineralogical composition of mortar samples formed from OPC clinker produced by JSC Akmenes cementas/sand mixture and hardened in a CO_2 environment.

Material	SiO_2	CaO	Al_2O_3	K_2O	Na_2O	MgO	Fe_2O_3	SO_3	Other	LOI
Limestone	2.02	47.95	0.71	0.17	–	3.94	1.15	0.23	0.57	43.26
Clay	45.64	10.97	14.0	3.06	0.17	4.0	7.04	–	0.22	14.9
Clinker	20.69	64.06	5.13	1.12	0.10	3.31	3.25	0.53	CaO_{free} = 1.81	

Table 1. Oxide composition of Karpenai limestone, Saltiskiai clay and OPC clinker, wt%

Two mixtures were prepared from Karpenai limestone and Saltiskiai clay with a molar ratios of CaO/SiO_2 = 1.5 (corresponds to the stoichiometry of rankinite), and 1.75 (with excess of CaO, because part of it can be combined into calcium magnesium silicates). In the mixture with CaO/SiO_2 = 1.5, after high-temperature sintering (1000–1250 °C), the predominant compound is akermanite $Ca_2Mg(Si_2O_7)$. Only negligible amounts of larnite $2CaO{\cdot}SiO_2$ and rankinite $3CaO{\cdot}2SiO_2$ are identified. Since the duration of the isothermal curing was 45 min, MgO and quartz have time to fully react already at 1100 °C temperature. The maximum firing temperature is 1200 °C, because Saltiskiai clay contains alkaline compounds (K_2O = 3.06%) and the granules begin to melt and stick together at ~1250 °C. Increasing the molar ratio of the mixture does not work – the same compounds are formed.

In order to finally make sure of the suitability of the raw materials used by JSC Akmenes cementas for the production of binding materials that harden in a CO_2 environment, the samples (Ø36×36) mm from synthesized binder and standard sand (1:3 by mass) were pressed (12.5 MPa) and cured for 24 h in atmosphere of 15 bar 99.9% CO_2, at 25 and 45 °C temperature. Analogous samples were formed and hardened under the same conditions from OPC clinker and standard sand (Table 2).

Curing temperature, °C	Synthesized binder	OPC clinker
	Compressive strength, MPa	
25	9.13	53.03
45	14.45	67.5

Table 2. The compressive strength of the samples formed from the synthesized binder or the OPC clinker mixtures with standard sand.

Since the compressive strength of the samples differs by 5–6 times, the conclusion is unequivocal – if the raw materials contain enough Mg-containing impurities (in this case, ~4% of MgO in the initial mixture), a large amount of inert akermanite is formed (~60%), and they are not suitable for the production of binders that harden in a CO_2 environment.

References

1. Zhang, H., *et al.* The usage of rankinite for carbon capture and storage and carbonation kinetics. *Energy Source Part A*, **40** (13) (2018) 1629–1646.

2. Smigelskyte, A., Siauciunas, R., Wagner, M., Urbonas, L. Synthesis of rankinite from natural Ca–Si rocks and its hardening in CO_2 atmosphere. *Rev. Rom. Mater*., **49** (1) (2019) 111–119.

INDEX

H

I

J

K

L

M

N

O

P

Q

R

S

T

U

V

W

Y

Z

CCT-2023, abstract book, 138 pages.

Vilnius University Press
9 Saulėtekio Av., III Building, LT-10222
Vilnius info@leidykla.vu.lt, www.leidykla.vu.lt/en/
www.knygynas.vu.lt, www.journals.vu.lt

CHEMISTRY &
CHEMICAL
TECHNOLOGY

CONFERENCE 2023 VILNIUS